**INSTITUTE OF SEISMOLOGY**
**UNIVERSITY OF HELSINKI**

**REPORT S-65**

# LITHOSPHERE 2016

## NINTH SYMPOSIUM ON THE STRUCTURE, COMPOSITION AND EVOLUTION OF THE LITHOSPHERE IN FENNOSCANDIA

**Geological Survey of Finland,**
**Espoo, November 9-11, 2016**

***PROGRAMME AND EXTENDED ABSTRACTS***

**edited by**

**Ilmo Kukkonen, Suvi Heinonen, Kati Oinonen, Katriina Arhe, Olav Eklund, Fredrik Karell, Elena Kozlovskaya, Arto Luttinen, Raimo Lahtinen, Juha Lunkka, Vesa Nykänen, Markku Poutanen, Eija Tanskanen and Timo Tiira**

**Helsinki 2016**

INSTITUTE OF SEISMOLOGY
UNIVERSITY OF HELSINKI
REPORT S-65

# LITHOSPHERE 2016

## NINTH SYMPOSIUM ON
## *STRUCTURE, COMPOSITION AND EVOLUTION OF THE LITHOSPHERE IN FENNOSCANDIA*

### *PROGRAMME AND EXTENDED ABSTRACTS*

**Edited by**

**Ilmo Kukkonen, Suvi Heinonen, Kati Oinonen, Katriina Arhe, Olav Eklund, Fredrik Karell, Elena Kozlovskaya, Arto Luttinen, Raimo Lahtinen, Juha Lunkka, Vesa Nykänen, Markku Poutanen, Eija Tanskanen and Timo Tiira**

**Geological Survey of Finland,
Espoo, November 9-11, 2016**

**Helsinki 2016**

Series Editor-in-Chief: Annakaisa Korja
Guest Editors: Ilmo Kukkonen, Suvi Heinonen, Kati Oinonen, Katriina Arhe, Olav Eklund, Fredrik Karell, Elena Kozlovskaya, Arto Luttinen, Raimo Lahtinen, Juha Lunkka, Vesa Nykänen, Markku Poutanen, Eija Tanskanen and Timo Tiira

Publisher: Institute of Seismology
P.O. Box 68
FI-00014 University of Helsinki
Finland
Phone: +358-294-1911 (switchboard)
http://www.helsinki.fi/geo/seismo/

ISSN 0357-3060
ISBN 978-952-10-5081-7 (Paperback)
Helsinki University Print
Helsinki 2016
ISBN 978-952-10-9282-5 (PDF)

# LITHOSPHERE 2016

**NINTH SYMPOSIUM ON
STRUCTURE, COMPOSITION AND EVOLUTION OF THE
LITHOSPHERE IN FENNOSCANDIA**

***PROGRAMME AND EXTENDED ABSTRACTS***

Geological Survey of Finland,
Espoo
November 9-11, 2016

## CONTRIBUTING ORGANIZATIONS

Finnish National Committee of the International Lithosphere Programme (ILP)
Finnish Meteorological Insititute
Geological Survey of Finland (GTK)
National Land Survey of Finland, Finnish Geospatial Research Institute (FGI)
University of Helsinki
University of Turku
University of Oulu
Åbo Akademi University

## ORGANIZING COMMITTEE AND EDITORS


| | |
|---|---|
| Ilmo Kukkonen | University of Helsinki (ilmo.kukkonen@helsinki.fi) |
| Suvi Heinonen | Geological Survey of Finland (suvi.heinonen@gtk.fi) |
| Kati Oinonen | University of Helsinki (kati.oinonen@helsinki.fi) |
| Katriina Arhe | University of Helsinki (katriina.arhe@helsinki.fi) |
| Olav Eklund | Åbo Akademi University (oleklund@abo.fi) |
| Fredrik Karell | Geological Survey of Finland (fredrik.karell@gtk.fi) |
| Elena Kozlovskaya | University of Oulu (elena.kozlovskaya@oulu.fi) |
| Arto Luttinen | University of Helsinki (arto.luttinen@helsinki.fi) |
| Raimo Lahtinen | Geological Survey of Finland (raimo.lahtinen@helsinki.fi) |
| Juha Lunkka | University of Oulu (juha.pekka.lunkka@oulu.fi) |
| Vesa Nykänen | Geological Survey of Finland (vesa.nykanen@gtk.fi) |
| Markku Poutanen | Finnish Geospatial Research Institute FGI (markku.poutanen@nls.fi) |
| Eija Tanskanen | Finnish Meteorological Insititute (eija.tanskanen@aalto.fi) |
| Timo Tiira | University of Helsinki (timo.tiira@helsinki.fi) |

**References of Lithosphere Symposia Publications**


*Pesonen, L.J., Korja, A. and Hjelt, S.-E., 2000 (Eds.).* Lithosphere 2000 - A Symposium on the Structure, Composition and Evolution of the Lithosphere in Finland. Programme and Extended Abstracts, Espoo, Finland, October 4-5, 2000. Institute of Seismology, University of Helsinki, Report S-41, 192 pages.

*Lahtinen, R., Korja, A., Arhe, K., Eklund, O., Hjelt, S.-E. and Pesonen, L.J., 2002 (Eds.).* Lithosphere 2002 – Second Symposium on the Structure, Composition and Evolution of the Lithosphere in Finland. Programme and Extended Abstracts, Espoo, Finland, November 12-13, 2002. Institute of Seismology, University of Helsinki, Report S-42, 146 pages.

*Ehlers, C., Korja A., Kruuna, A., Lahtinen, R. and Pesonen, L.J., 2004 (Eds.).* Lithosphere 2004 – Third Symposium on the Structure, Composition and Evolution of the Lithosphere in Finland. Programme and Extended Abstracts, November 10-11, 2004, Turku, Finland. Institute of Seismology, University of Helsinki, Report S-45, 131 pages.

*Kukkonen, I.T., Eklund, O., Korja, A., Korja, T., Pesonen, L.J. and Poutanen, M., 2006 (Eds.).* Lithosphere 2006 – Fourth Symposium on the Structure, Composition and Evolution of the Lithosphere in Finland. Programme and Extended Abstracts, Espoo, Finland, November 9-10, 2006. Institute of Seismology, University of Helsinki, Report S-46, 233 pages.

*Korja, T., Arhe, K., Kaikkonen, P., Korja, A., Lahtinen, R. and Lunkka, J.P., 2008 (Eds.).* Lithosphere 2008 – Fifth Symposium on the Structure, Composition and Evolution of the Lithosphere in Finland. Programme and Extended Abstracts, Oulu, Finland, November 5-6, 2008. Institute of Seismology, University of Helsinki, Report S-53, 132 pages.

*Heikkinen, P., Arhe, K., Korja, T., Lahtinen,R., Pesonen, L.J. and Rämö, T., 2010 (Eds.).* Lithosphere 2010 – Sixth Symposium on the Structure, Composition and Evolution of the Lithosphere in Finland. Programme and Extended Abstracts, Helsinki, Finland, October 27-28, 2010. Institute of Seismology, University of Helsinki, Report S-55, 154 pages.

*Kukkonen, I.T., Kosonen, E., Oinonen, K., Eklund, O., Korja, A., Korja, T., Lahtinen, R., Lunkka, J.P. and Poutanen, M., 2012 (Eds.).* Lithosphere 2012 – Seventh Symposium on the Structure, Composition and Evolution of the Lithosphere in Finland. Programme and Extended Abstracts, Espoo, Finland, November 6-8, 2012. Institute of Seismology, University of Helsinki, University of Helsinki, S-56, 116 pages.

*Eklund, O., Kukkonen, I.T., Skyttä, P., Sonck-Koota, P., Väisänen, M. and Whipp, D., 2014 (Eds.).* Lithosphere 2014 – Eighth Symposium on the Structure, Composition and Evolution of the Lithosphere in Finland. Programme and Extended Abstracts, Turku, Finland, November 4-6, 2014. Institute of Seismology, University of Helsinki, S-62, 126 pages.

*Kukkonen, I.T., Heinonen, S., Oinonen, K., Arhe, K., Eklund, O., Karell, F., Kozlovskaya, E., Luttinen, A., Lahtinen, R., Lunkka, J., Nykänen, V., Poutanen, M. and Tiira T. (Eds.), 2016.* Lithosphere 2016 – Ninth Symposium on the Structure, Composition and Evolution of the Lithosphere in Finland. Programme and Extended Abstracts, Espoo, Finland, November 9-11, 2016. Institute of Seismology, University of Helsinki, Report S-65, 166 pages.


***Keywords*** (GeoRef Thesaurus, AGI): lithosphere, crust, upper mantle, Fennoscandia, Finland, Precambrian, Baltic Shield, symposia

# TABLE OF CONTENTS

# PREFACE

The Finnish National committee of the International Lithosphere Programme (ILP) organises every second year the LITHOSPHERE symposium, which provides a forum for lithosphere researchers to present results and reviews as well as to inspire interdisciplinary discussions. The ninth symposium - LITHOSPHERE 2016 – comprises 47 presentations. The extended abstracts (in this volume) provide a good overview on current research on structure and processes of solid Earth.

The three-day symposium is hosted by the Geological Survey of Finland (GTK) and it will take place in Espoo at the Southern Finland Office of GTK in November 9-11, 2016. The participants will present their results in oral and poster sessions. Posters prepared by graduate and postgraduate students will be evaluated and the best one will be awarded. The invited talks are given by Prof. Gillian R. Foulger (University of Durham, UK) and Research director Pekka Heikkinen (Institute of Seismology, University of Helsinki).

This special volume ***"LITHOSPHERE 2016"*** contains the programme and extended abstracts of the symposium in alphabetical order.

Helsinki, October 25, 2016

Ilmo Kukkonen, Suvi Heinonen, Kati Oinonen, Katriina Arhe, Olav Eklund, Fredrik Karell, Elena Kozlovskaya, Arto Luttinen, Raimo Lahtinen, Juha Lunkka, Vesa Nykänen, Markku Poutanen, Eija Tanskanen and Timo Tiira

Lithosphere 2016 Organizing Committee

# LITHOSPHERE 2016 Symposium Programme

## Wednesday, Nov 9

09:00 - 10:00 Registration at the Geological Survey of Finland, Espoo, Sederholm Auditorium

**10:00 - 10:05 Opening: Ilmo Kukkonen**

**10:05- 11:50 Session 1: Lithosphere structure and evolution from upper crust to asthenosphere**
Chair: Ilmo Kukkonen

10:05 - 10:50 **Gillian R. Foulger [Invited]**
Plates vs. Plumes: Lithosphere vs. Asthenosphere

10:50 - 11:15 **A. Korja, M. Uski, B. Lund, S. Grigull, M. Nironen and K. Högdahl**
Intraplate Seismicity in Central Fennoscandia

11:15 - 11:40 **A.I. Slabunov, S.A. Svetov, V.S. Kulikov and A.K. Polin**
A new geological map of the SE Fennoscandian Shield as a tool for the Early Precambrian Crustal Evolution study (exemplified by the Archean)

11:40 – 12.05 **O. Eklund and D. Lindberg**
Formation of ultramafic rocks in the middle crust by partial melting of amphibolites

**12:05 - 13:00 Lunch**

**13:00-14:30 Session 2: Lithosphere structure and evolution from upper crust to asthenosphere (cont.)**
Chair: O. Eklund

13:00-13:25 **H. Huhma**
Isotope results from Utsjoki-Inari area

13:25-13:50 **R. Lahtinen, M. Sayab and S.T. Johnston**
Inari orocline – progressive or secondary orocline

13:50 – 14:15 **U. Autio, M. Smirnov, T. Korja and M. Cherevatova**
Magnetotelluric measurements centred on the Central Lapland Granitoid Complex

**14:15 - 14:45 Coffee/Tea**

**14:45-17:15 Session 3: Lithosphere evolution, structures and mineral resources**
Chair: R. Lahtinen

14:45-15:10 **I. Kukkonen and L. Lauri**
Mesoproterozoic rapakivi granite magmatism in the Fennoscandian shield and adjacent areas: Role of crustal radiogenic heating

15:10-15:35 **O.T. Rämö, J.P. Calzia, V.T. McLemore and P. Heikkilä**
Mid-Proterozoic evolution of southern Laurentian lithosphere; crustal domains and potassic magmatic suites in Mojavia and Mazatzal

15:35-16:00 **S.T. Turunen, A.V. Luttinen and J.S. Heinonen**
Defining mantle sources of large igneous provinces: insight from pristine picrites in Karoo LIP, Luenha River, Mozambique

16:00-16:25 **A. Malehmir, A. Tryggvason, C. Wijns, E. Koivisto, T. Lindqvist, P. Skyttä and M. Montonen**
Why 3D seismic data are an asset for both exploration and mine planning? Example of Kevitsa Ni-Cu-PGE, Finland

16:25-16:50 **K. Komminaho, E. Koivisto, P. J. Heikkinen, H. Tuomi, N. Junno and I. Kukkonen**
Seismic full waveform modelling of Outokumpu-type ore and processing considerations

**16:50- 17:30 Session 4: Poster introductions**
Chair: R. Lahtinen
2 min talks with two slides in the auditorium

**17:30 – 19:30 Poster viewing and networking with refreshments**

## *Posters*

**P01.** **A.J. Aalto, P.J. Heikkinen, A. Heinonen, A. Korja and S. Väkevä**
OpenFIRE – enhancing the accessibility of the Finnish Reflection Experiment data products

**P02.** **G. Gislason, S. Heinonen, M. Malinowski, E. Koivisto, L. Sito, P. Targosz, M.Wojdyla, J. Juurela, S. Juurela, T. Törmälehto and K. Vaittinen**
COGITO-MIN seismic reflection profiling in Polvijärvi: Insight into the first results

**P03.** **J. Kara, M. Väisänen, Y. Lahaye and H. O'Brien**
Post-kinematic mafic dykes in southern part of Central Svecofennia, Finland

**P04.** **I. Kukkonen, E. Koivisto and D. Whipp**
Helsinki University Kumpula Campus Drill Hole Project

**P05.** **M. Lehtinen, M. Väisänen, J. Kara, H. O'Brien and M. Lehtonen**
A shoshonitic dyke in Lohja, southern Finland

**P06.** **H. Leväniemi, R. Lahtinen, S. Mertanen and H. Säävuori**
Natural Remanent Magnetisation of Selected Rock Samples from the Finnish Bedrock: Implications for Structural Modelling of Magnetic Data

**P07.** **T. Luhta, S. Mertanen, E. Koivisto, S. Heinonen, T. Törmälehto and I. Kukkonen**
The seismic signature of the Kylylahti deposit: Initial results from new petrophysical measurements

**P08.** **J. Moreau, T. Kohout and K. Wünnemann**

Shock wave propagation in heterogeneous targets (ordinary chondrites) and in numerical setup of shock recovery experiments

**P09.** **J. Nevalainen, O. Usoltseva and E. Kozlovskaya**
Applying double-difference technique to relocate induced microseismic events in Pyhäsalmi mine, Pyhäjärvi

**P010.** **K. Nikkilä**
Effect of crustal scale shear zones to the crustal deformation during extension

**P011.** **K. Penttilä, I. Kukkonen, J.S. Heinonen, M. Räisänen and R. Valtonen**
Logging and lithology of the Kumpula Campus drill hole

**P012.** **K. Piipponen**
Modelling an Enhanced Geothermal System doublet in crystalline rock

**P013.** **M. Räisänen, I. Kukkonen, J.S. Heinonen, R. Valtonen and K. Penttilä**
Geochemical characteristics of the Kumpula campus area: drill core and outcrop data

**P014.** **T. Valjus, M. Markovaara-Koivisto and T. Tarvainen**
Aijala mine tailings area as an example of a source of secondary raw materials

**P015.** **R. Valtonen, I. Kukkonen, J.S. Heinonen, M. Räisänen and K. Penttilä**
Kumpula campus drill hole: Fracture mapping and 3D-modeling

**P016.** **V. Virtanen and E. Heilimo**: Two geochemically A-type intrusions in Central Finland Granitoid Complex: evidence of coeval mafic and felsic magmatism

## Thursday, Nov 10

09:30-11:40 **Session 5: Archaean and Proterozoic lithosphere structure and evolution**
Chair: A. Luttinen

09:30-09:55 **J.M. Salminen, R. Klein, T. Veikkolainen, L.J. Pesonen and S. Mertanen**
Mesoproterozoic Nuna supercontinent and the geomagnetic field in light of recent paleomagnetic and geochronological data from diabase dykes of Finland

09:55-10:20 **H. Silvennoinen and E. Kozlovskaya**
Comparison of the upper mantle structures beneath northern and southern Finland based on the teleseismic tomography results of POLENET/LAPNET and SVEKALAPKO seismic arrays

**10:20- 10:50 Coffee/Tea**

10:50-11:15 **E. Suikkanen and O.T. Rämö**
Metasomatic alkali-feldspar syenites within the Suomenniemi rapakivi granite complex, SE Finland

11:15-11:40 **P. Mikkola, K. Mönkäre, M. Ahven and H. Huhma**
Supracrustal rocks from the SE border of the Central Finland Granitoid Complex, something new or business as usual?

11:40-12:05 **A. Raja-Halli and H. Virtanen**
Geodynamical research with superconducting gravimeters at the Metsähovi Geodetic Research Station

**12:05-13:30 Lunch and poster viewing**

13:30-16:30 **Session 5: Crustal structures and mineral resources**
Chair: I. Kukkonen

13:30-13:55 **Emilia Koivisto, Michal Malinowski, Suvi Heinonen, Calin Cosma, Nicoleta Enescu, Sanna Juurela, Jari Juurela, Teemu Törmälehto, Katri Vaittinen and Marek Wojdyła**
New tools for deep mineral exploration: Insights from the field work stage of the COGITO-MIN project

13:55-14:20 **N. Junno, E. Koivisto, I. Kukkonen, A. Malehmir and C. Wijns**
Data mining to discover the causes of internal reflectivity within the Ni-Cu-PGE-bearing Kevitsa intrusion

**14:20- 14:50 Coffee/Tea**

14:50-15:15 **S. Heinonen, H. Leväniemi, P.Sorjonen-Ward, A.Kontinen and S.Aatos**
Integrated Interpretation of Geophysical Data for Deep Exploration in the Kylylahti Cu-Mining Area, Eastern Finland

15:15-15:40 **S. Buntin, A. Malehmir, M. Malinowski, K. Högdahl, C. Juhlin, H. Thybo and S. Buske**
Seismic reprocessing of the BABEL lines for improved interpretation of the whole crust – preliminary results

15:40 –16:30 **Pekka Heikkinen [Invited]**
Seismic lithosphere studies in Finland: glorious past, challenging future

16:30 **National Lithosphere Committee**
**Honouring Pekka Heikkinen for his work in lithospheric research**

## Friday, Nov 11

**9:30-11:15** **Session 7: Archaean and Proterozoic lithosphere evolution (cont.)**
Chair: E. Kozlovskaya

9:30-9:55 **E. Heilimo, P. Mikkola, Y. Lahaye and H. Huhma**
New evidence for crustal growth: field and geochemical data from plutonic rocks in SE corner of the Central Finland Granitoid Complex

9:55-10:20 **J.S. Heinonen, W.A. Bohrson, A.V. Luttinen, F. Molnár, M.W. Schmidt, F.J. Spera and T. Wagner**
Start of project PALIN – Partial melting processes in the contact zones of layered intrusions

**10:20- 10:50 Coffee/Tea**

**10:50 – 14:10 Session 8: Neotectonics, recent seismicity, short communications**
Chair: Suvi Heinonen

10:50-11:15 **T. Kohout and ASPECT team**
Exploration of asteroids using small satellites – case study ASPECT

11:15-11:40 **J. Mattila, A.Ojala, R. Sutinen, J-P. Palmu and T. Ruskeeniemi**
Digging deeper with LiDAR: vertical slip profiles of post-glacial faults

11:40-12:05 **N. Afonin, E. Kozlovskaya, I. Kukkonen and DAFNE/FINLAND Working Group**
Structure of Suasselkä Postglacial Fault in northern Finland obtained by analysis of local events and ambient seismic noise

**12:05-13:05 Lunch**

13:05-13.30 **T. Elminen, H. Zwingmann and A. Kaakinen**
Neoproterozoic faulting and sedimentation documented in a railway tunnel, Vantaa, southern Finland

13:30-13:55 **T. Veikkolainen, I.T. Kukkonen and T. Tiira**
Applying seismic cutoff depth in thermal modelling of the Fennoscandian Shield

13:55-14:10 **A. Korja, T.A.Vuorinen and FIN-EPOS**
FIN-EPOS – Finnish national initiative of the European Plate Observing System

14:10-14:30 Final discussion
14:30- 14:45 Poster Award

**Closing of symposium**

# EXTENDED ABSTRACTS

For color versions of figures, see the web version of the publication,
http://www.seismo.helsinki.fi/ilp/lito2016/

# OpenFIRE – enhancing the accessibility of the Finnish Reflection Experiment data products

A.J. Aalto[1], P.J. Heikkinen[1], A. Heinonen[1], A. Korja[1], and S. Väkevä[1]

[1]Insitute of Seismology, Gustaf Hällströmin katu 2B, 00014, University of Helsinki
E-mail: aku.heinonen@helsinki.fi

OpenFIRE is an open science project acting within the Finnish Open Science and Research Initiative (ATT) by the Ministry of Education and Culture of Finland, which will produce a revised data archive and a new intuitive map-based user interface for the seismic reflection data of the Finnish Reflection Experiment (FIRE). All FIRE data and related products will be freely available for anyone to browse and download through the AVAA open research data portal. The OpenFIRE platform and user interface are produced as open source resources and proposed to act as a reference realisation of a web service for reflection seismic data in the scope of the European Plate Observing System (EPOS).

**Keywords:** deep seismic sounding, seismic reflection data, open science, continental lithosphere, Fennoscandian Shield

## 1. Motivation

The Finnish Reflection Experiment (FIRE) is a reflection seismic experiment that was conducted in collaboration with the Universities of Oulu and Helsinki, Geological Survey of Finland (GTK), and the Russian company SpetsGeofysika in the early 2000s. The field measurements were carried out during four field seasons in 2001–2004 and the data were originally processed and published in 2005–2009. The dataset comprises over 2100 kilometres of high-resolution seismic reflection profiles that transect all the major Precambrian geological formations of the Finnish bedrock (Figure 1).

Regardless of the fact that the FIRE dataset is considered to be one of the best of its kind in the world it has been relatively underused up to date. The main academic output on most of the FIRE profiles was compiled already in 2006 and published as a preliminary report (Kukkonen and Lahtinen, 2006). The material and datasets have all been freely available for anyone interested but their accessibility has been rather poor, which has led to relatively low usage and academic output.

## 2. The OpenFIRE project

The OpenFIRE project that was launched in the beginning of the year 2016 is a Ministry of Education and Culture of Finland -funded endeavour that is aimed at increasing the visibility and accessibility of the FIRE data and lowering their user initiation threshold. The project has been conducted in the context of the Finnish Open Science and Research Initiative (ATT) at the Institute of Seismology, University of Helsinki in collaboration with the AVAA-team of the ATT-initiative and GTK. The finished materials will be hosted by the IDA service and the online interface will run on the AVAA open research data portal platform (Figure 2). One of the principal aims of the OpenFIRE has been to produce an EPOS (European Plate Observation System) -compatible web service for reflection seismic data (EPOS-IP WP6 & WP7 Teams, 2015).

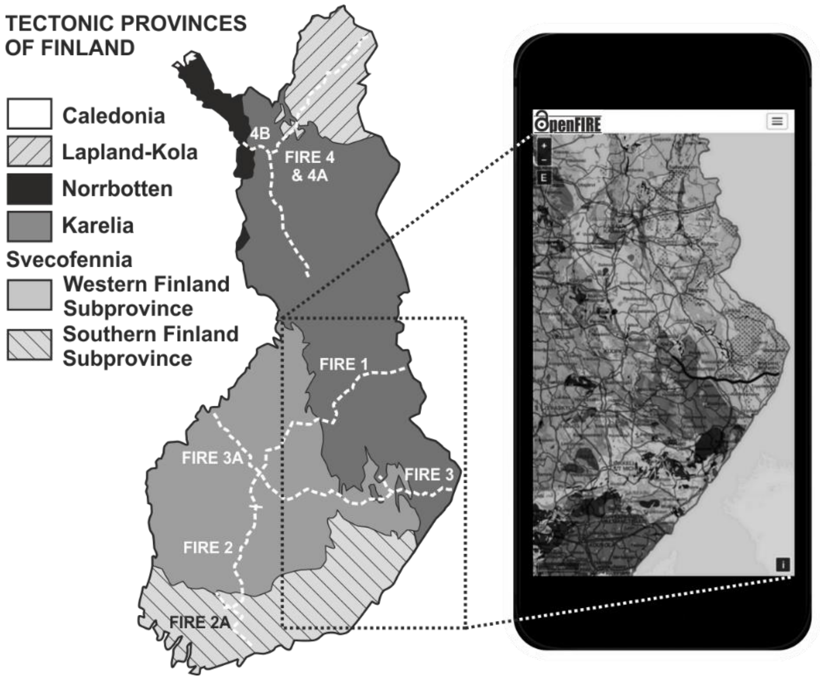


**Figure 1.** Locations of the FIRE transects on the tectonic province map of Finland (left) and an example view of the OpenFIRE map interface for FIRE 3 profile on a mobile device (right).

**3. Verification, documentation, and re-processing of the FIRE data**

The first goal of the project has been to produce and store a coherent database of all FIRE-related raw data, materials, and data products. Unlike other web-services that offer open reflection seismic data, OpenFIRE works on all levels of "data taxonomy" (Jefferey et al., 2015) from raw data (level 0) to intermediate data products (level 1; e.g., stacks and statically corrected data), interpreted materials (level 2; e.g., geological models), and integrated community-based materials (level 3; e.g., research catalogues).

OpenFIRE assembles material from all the major processing steps and thus makes the entire workflow visible to the end-user. In the online database, the files have been grouped into data classes (e.g., "Field records", "Shot gathers", "Observer's notes", "Pole coordinates", "DMO stacks") to facilitate subsequent filtering procedures. Each file has been assigned a unique URN (Uniform Resource Name) by which it can be identified. The persistency and uniqueness of the identifiers is ensured by the National Library of Finland.

OpenFIRE is conducted with a strict focus on quality. A comprehensive errata is available for all profiles, and quality-controlled versions of shot gathers have been prepared for the entire FIRE project at the Institute of Seismology. Typical errors in the original data include missing coordinates, duplicate traces, and false numeric values. Occasionally even the observer's notes themselves have been lost.

The shot gathers have been repackaged into SEG-Y (Society of Exploration Geophysicists Y-format) files that each contain at maximum around 100 shots (10 kilometres). Where shot points have been skipped, the file size is accordingly smaller. All relevant SEG-Y headers, including the textual and binary header, are set. Both NMO (normal moveout) and DMO (dip moveout) stacks are distributed as un-migrated, migrated, and depth-converted versions and all modifications are strictly documented.

## 4. OpenFIRE online user interface

The second goal of the project has been to build an online map-based interface for browsing, accessing, and downloading the archived material, which would be capable of catering to the needs of a diverse set of user segments. The visual map- and section-based interfaces and geological descriptions have especially been designed to orientate the geologist end-users, who have a high user potential but may require a more familiar context to utilize the service due to the rather technical nature of the available materials. Information on the surface geology and existing interpretations of deep crust structures along the FIRE profiles is organized into description entities that can be accessed through a series of dedicated web pages. The geological descriptions include comprehensive lists of pertaining scientific references and additional sources of information.

Parsing the header information into a relational database enables the possibility for database queries matching information in the dataset to other logical models describing the geology of the Fennoscandian Shield. With this approach the GTK open data repositories have been linked to the seismic records. Procedural methods are used to generate an agnostic visualisation of reflectors in the dataset correlating to bedrock units mapped from the surface. In another visualisation view the user can see an expert opinion on the bedrock structure as viewed by the geoscientific community accompanied by proper academic citations.

The "seismologist's interface" is separate from the section-based interface, and is aimed to allow the easy downloading of shot gathers and exploring the related metadata. The application relies on download models, i.e., the download orders made in the section-based and shot-gather-based interface are by default customised by the expected type of use. OpenFIRE also provides a filtering-table approach for accessing the entire FIRE data at once.

The infrastructure of the web service is compliant with the EPOS ICS-TCS Level 2 Integration Guideline (EPOS-IP WP6 & WP7 Teams, 2015). The service is built over microservices, some of which are externally produced by Finnish government organisations (i.e., GTK and the National Land Survey of Finland – NLS). External services include geological, general, and topographic maps and the data download API (Application Programming Interface). Georeferenced images of stacked data and geographical data describing source point and common depth point locations will be provided over OGC (Open Geospatial Consortium) APIs. CERIF (Common European Research Information Format) compatible metadata describing the project will be stored in a metadata catalogue. Guidelines for initializing a computing environment will be provided. The infrastructure of the service is suitable for scaling up the amount of data in the service and its modularity makes it possible to change a single microservice to another depending on requirements and resources.

The user interface and the visualisation methods used in the map view are suitable for visualising other types of data as well. The authors are not aware of other similar EPOS compliant services and thus propose the results of the OpenFIRE project to be used as a reference realisation in the field of reflection seismic data.

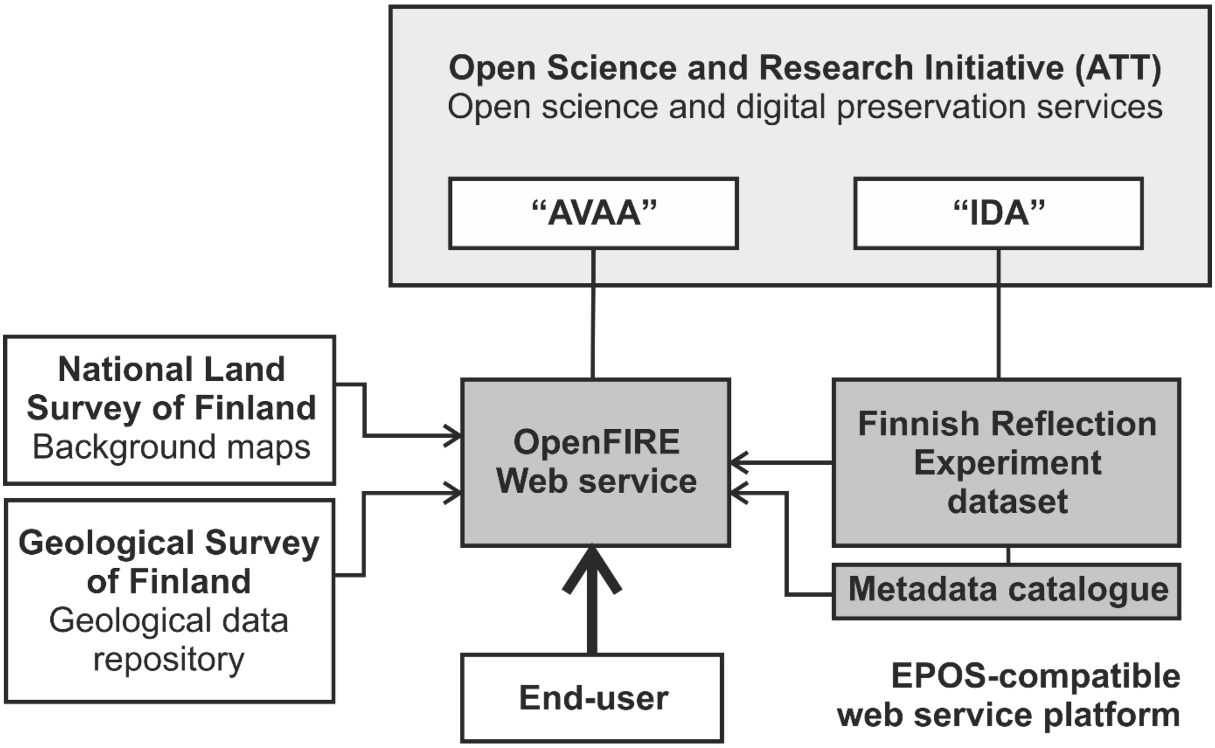


**Figure 2.** A schematic diagram of the interdependencies and relationships between different entities related to the services produced by the OpenFIRE project. The end-user can browse the desired FIRE database materials through the web service and place a data product order that will be fulfilled by a dedicated e-mail service.

**5. Beta test and community engagement**

By November 2016 the OpenFIRE project has entered open beta testing with first-order functionality and a limited dataset that encompasses the FIRE 3 profile. The product will be honed and developed based on user feedback and the final launch with full datasets and functionality will happen in early 2017. The entire Finnish lithosphere research community is invited to take part in the beta and to provide feedback on the contents and usability of the service. OpenFIRE usage statistics will be logged and together with user feedback reports will be compiled for the scientific community.

The OpenFIRE service can be accessed through the project portal at:
www.seismo.helsinki.fi/openfire

**References:**

EPOS-IP WP6 & WP7 Teams, 2015. ICS-TCS integration guidelines - Handbook for TCS integration: Level-2. Zenodo. http://doi.org/10.5281/zenodo.34666

Jefferey, K.G., Bailo, D., Euteneuer, F., Ulbricht, D., 2015. Report on EPOS e-infrastructure prototype. Zenodo. http://doi:10.5281/zenodo.19175

Kukkonen, I., Lahtinen, R., 2006 (Eds.). Finnish Reflection Experiment FIRE 2001–2005, Geological Survey of Finland Special Paper 43, 247 pages.

# Structure of Suasselkä Postglacial Fault in northern Finland obtained by analysis of local events and ambient seismic noise

N. Afonin[1], E. Kozlovskaya[2,3], I. Kukkonen [4] and DAFNE/FINLAND Working Group

[1]Federal Centre for Integrated Arctic Research RAS, Arkhangelsk, Russia
[2]Oulu Mining School, POB-3000, FIN-90014, University of Oulu, Finland
[3]Geological Survey of Finland, P.O. Box 96, FI-02151, Espoo, Finland
E-mail: afoninnikita@inbox.ru

In our study we investigate seismicity and inner structure of Suasselka post-glacial fault in northern Fennoscandian Shield using analysis of local seismic events and ambient seismic noise recorded by the temporary DAFNE/FINLAND array. As a result of experiment and data interpretation, we found a number of natural seismic events originating from the fault area, which proves that the fault is still seismically active. In addition, analysis of ambient seismic noise recorded by the array demonstrated that that the area of the SPGF corresponds to a narrow region of low S-wave velocities surrounded by rocks with high S-wave velocities. We interpret this low velocity region as a non-healed mechanically weak fault damage zone (FDZ) that remained after the last major earthquake that occurred after the last glaciation.

**Keywords:** Post-glacial faults, intraplate seismicity, ambient noise, empirical Green’s functions, fault damage zone

## 1. Introduction

For understanding mechanisms of intraplate seismicity studying of seismogenic faults structure and properties is of particular importance. Traditionally, this studies concentrate on mapping the seismic source using recordings of seismic events (fault plane and centroid moment tensor solutions, distribution of events locations). The inner structure of fault zones can be also studied using structural geology, palaeoseismology, seismic reflection and refraction experiments and geodetic measurements. In our study we investigate the inner structure of the Suasselkä post-glacial fault (SPGF) using distribution of hypocentres of local seismic events and analysis of ambient seismic noise recorded by the temporary DAFNE/FINLAND array (Afonin et al., 2016). The project was performed by several organizations in Finland (Geological Survey of Finland, Sodankylä Geophysical Observatory of the University of Oulu and Institute of Seismology of the University of Helsinki). The DAFNE/FINLAND array comprised the area of about 20 to 100 km and consisted of 8 short-period and 4 broad-band 3-component autonomous seismic stations installed in the close vicinity of the fault area. The array recorded continuous seismic data during September, 2011-May, 2013.

## 2. Detection and location of seismic events

One of the problems for studying of natural seismicity in northern Finland is a huge number of production and development blasts originating from numerous mines and quarries. The DAFNE array recorded up to 100 of such blasts per day from northern Sweden, Russia and Finland. Due to this, it was not possible to use automatic event detection and manual data analysis was used. As a result of this analysis, we distinguished two types of events originating from our target area, but having different waveforms:

1) Blasts originating from the Kittilä mine;
2) Events originating from the SPGF area and its surrounding that could be of natural origin.

From them we found and relocated about 40 events that could be of natural origin. Hypocentres of events originating from the SPGF zone have depths up to 8.5 km and epicentres show good spatial correlation with the fault. This is indication that the fault zone is still seismically active.

## 3. Ambient seismic noise analysis

Analysis of azimuthal distribution of ambient noise sources during the experiment showed that this distribution is uniform during the time period considered. This was a necessary precondition for estimation of Empirical Green's Functions (EGF) by stacking of ambient noise. In our study we use the procedure described in Poli et al. (2012, 2013) in order to calculate EGF from continuous recordings of vertical component of all stations of the DAFNE array. The functions were then used to estimate surface wave dispersion curves which, in turn, were inverted in order to obtain seismic velocities in the uppermost crust of the SPGF area. Analysis of distribution of dispersion curves demonstrated that it is generally bi-modal and the set of all curves can be splitted into two groups. The first group (Group 1) is composed of the pairs in which stations are installed on different sides of the fault or on top of fault and the second group (Group 2) is composed of the pairs of stations installed on the same side of the fault or if one of station installed on top of fault. We calculated separately averaged dispersion curves for EGFs corresponding to two groups of pairs of stations and inverted them using the Geopsy software (http://www.geopsy.org). The inversion revealed significant (about 1000 m/s) difference in seismic velocities inside the fault zone and outside the fault zone.

## 4. Results

Two major results obtained in our study can be formulated as follows:
1) Suasselkä Post-Glacial Fault zone is still seismically active, as shown by distribution of hypocentres of local earthquakes from the fault area detected by the DAFNE array;
2) Analysis and inversion of averaged dispersion curves obtained from EGFs for two groups of seismic stations pairs (e.g. the pairs in which stations are located on opposite sides of the fault and the pairs in which stations are located outside the fault) revealed significant low S-wave velocity zone inside the SPGF area. We interpret this feature as a non-healed mechanically weak fault damage zone (FDZ) that remained after the last major earthquake that occurred after the last glaciation. This suggests that the SPGF has the potential for future reactivation.

## 5. References

Afonin, N., Kozlovskaya, E., Kukkonen, I. and DAFNE/FINLAND Working Group, 2016. Structure of Suasselkä Postglacial Fault in northern Finland obtained by analysis of local events and ambient seismic noise. Solid Earth Discuss. doi:10.5194/se-2016-90-SC1.

Poli, P., Pedersen, H. A., Campillo, M. and the POLENET/LAPNET Working Group, 2012. Emergence of body waves from cross-correlation of short period seismic noise. Geoph. J. Int. 188, 2, 549-588.

Poli, P., Campillo, M., Pedersen, H. and the POLENET/LAPNET Working Group, 2013. Noise directivity and group velocity tomography in a region with small velocity contrasts: the northern Baltic shield application to the northern Baltic Shield. Geoph. J. Int., 192, 1, 413-424, DOI: 10.1093/gji/ggs034

# Magnetotelluric measurements centred on the Central Lapland Granitoid Complex

U. Autio[1], M. Smirnov[2], T. Korja[2] and M. Cherevatova[3]

[1]Oulu Mining School, University of Oulu, Finland
[2]Department of Civil, Environmental and Natural Resources Engineering, Luleå University of Technology, Sweden
[3]Applied Geophysics Group, University of Münster, Germany
E-mail: uula.autio@oulu.fi

Magnetotellurics (MT) is an electromagnetic geophysical method where temporal variations of the natural electromagnetic field of the Earth are measured on its surface. The measurements contain information about the electrical conductivity structure of the subsurface down to hundred kilometres and more. We analyse MT data collected within the Magnetotellurics in Scandes (MaSca) -project. In the Summer 2014 we measured total of 79 MT sites in Northern Finland. The site array is centred on the Central Lapland Granitoid Complex and covers parts from the Peräpohja Belt and the Central Lapland Area. This is the first time extensive MT studies are being conducted in the area. With site spacing of 10–40 km and a period range of 0.001–10000 s, the data set contains information about the large scale conductivity structures of the crust and upper mantle below the site array. The complex geological setting requires three-dimensional (3-D) inversion to infer the conductivity variations in the most realistic manner. We will discuss the foremost features of the MT data set and present the first steps towards geologic implications.

**Keywords:** electromagnetic, magnetotellurics, array measurements, central lapland granitoid complex

## 1. Description of the 2014 MT data set

During April–June 2014 in total 79 broadband (BMT) and long period (LMT) MT sites, supported with vertical magnetic field measurement at each site, were installed (Fig. 1a, black symbols). Site spacing is ca. 10–20 km for BMT and 20--40 km for LMT. Most of the measurements were conducted with the MTU2000 system developed in the University of Uppsala (Smirnov et al., 2008a). The installed electric line lengths ranged between 70--100 m, depending on site conditions. The BMT sites were occupied for 20--48 hours (with exceptions towards longer times), whereas the LMT sites were occupied approximately for 3–4 weeks. Data from total of 56 BMT and 23 LMT sites are available. In all installations, the horizontal EM fields were measured in the geomagnetic N-S and E-W directions as obtained from handheld compass. In 2014, magnetic declination ranged between 10–12 degrees in the measurement area, growing towards East.

From the raw electric and magnetic field time series, transfer functions (impedance tensor and tipper) were derived using a robust remote-reference processing code (Smirnov, 2003; Smirnov & Pedersen, 2009). Good quality transfer functions were obtained with period ranges approximately of 0.003–1000 s and 10–10000 s for BMT and LMT data, respectively. All transfer functions have been rotated to geographic coordinates for further analysis. The transfer functions allow us to infer the regional conductivity structures in crustal and lithospheric scales. We have also extended the limits of the array with MT data from EMMA 2007 (Smirnov et al. 2008b) and MaSca 2013 (Cherevatova et al. 2015), see Figure 1.

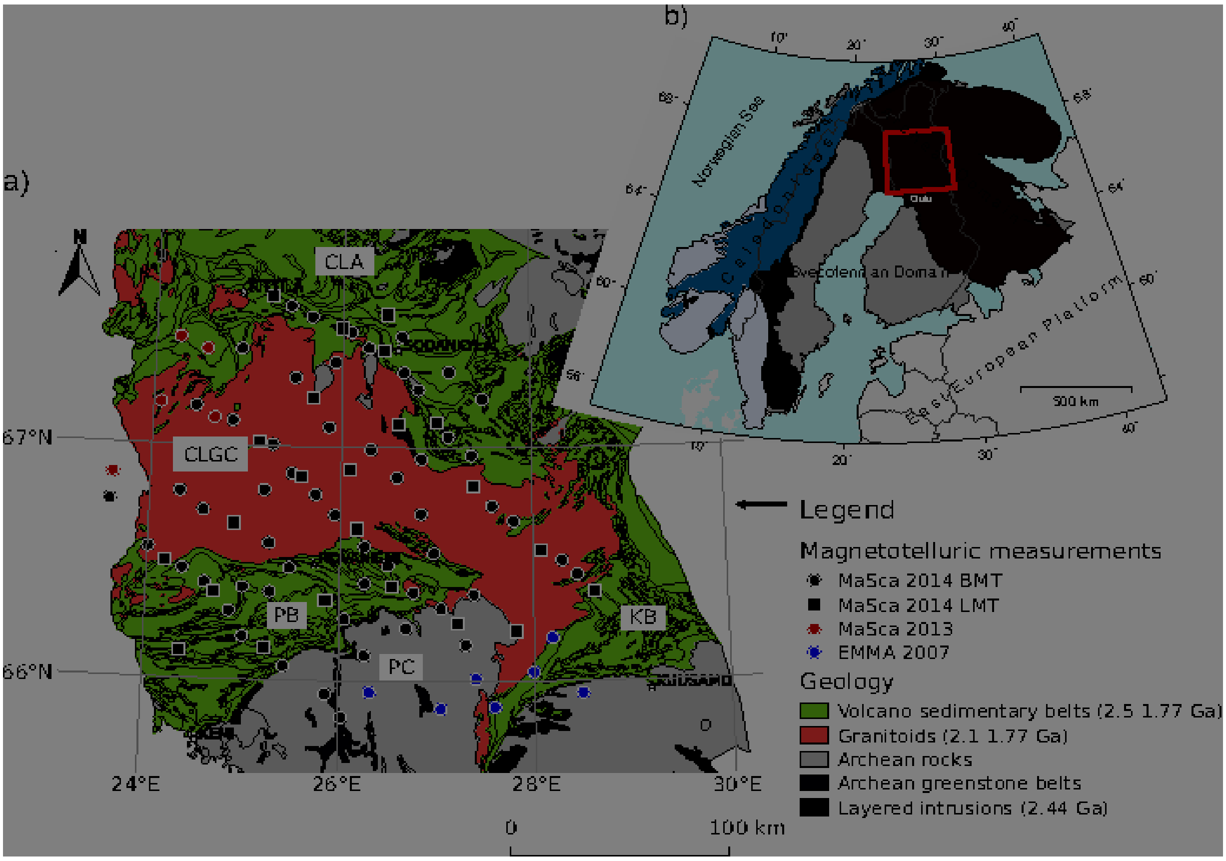


**Figure 1.** Location map. a) Magnetotelluric sites on a simplified geologic map (Korsman et al. 1997). b) Large scale geologic domains. The red rectangle shows approximately the measurement area extent. CLA=Central Lapland Area, CLGC=Central Lapland Granitoid Complex, KB=Kuusamo Belt, PB=Peräpohja Belt, PC=Pudasjärvi Complex

## 2. Results

Preliminary analysis reveals a complex data set requiring 3-D inversion codes. Most complex data responses are found in the belt areas of Peräpohja Belt (PB) and Central Lapland Area (CLA). These are due to strong near-surface and deeper crustal conductors. Most part the Central Lapland Granitoid Complex (CLGC) is implied as a resistive structure crossing the array all the way from East to West and extending deep in to the mantle. The data set also hints existence of a deep conductor (~200 km), possibly the lithosphere-asthenosphere boundary. These tentative interpretations need more analysis for further implications and confirmation.

## References:

Cherevatova, M., Smirnov, M. Y., Jones, A., Pedersen, L., & MaSca Working Group, 2015. Magnetotelluric array data analysis from north-west Fennoscandia, Tectonophysics, 653, 1–19.

Korsman, K., Koistinen, T., Kohonen, J., Wennerström, M., Ekdahl, E., Honkamo, M., Idman, H., & Pekkala, Y., 1997. Geological map of Finland 1:1000 000 , Geological Survey of Finland.

Smirnov, M., 2003. Magnetotelluric data processing with a robust statistical procedure having a high breakdown point, Geophys. J. Int., 152(1), 1–7.

Smirnov, M., Korja, T., and Pedersen L.B., 2008. Electrical conductivity of the Archean lithosphere in Fennoscandia from two mini arrays (EMMA project). Extended Abstract, 19th EMIW, Beijing, China

Smirnov, M., Korja, T., Dynesius, L., Pedersen, L. B., & Laukkanen, E., 2008a. Broadband magnetotelluric instruments for near-surface and lithospheric studies of electrical conductivity: a Fennoscandian pool of magnetotelluric instruments, Geophysica, 44(1-2), 31–44.

Smirnov, M. & Pedersen, L., 2009. Magnetotelluric measurements across the Sorgenfrei-Tornquist Zone in southern Sweden and Denmark, Geophysical Journal International , 176, 443–456(14).

# Seismic reprocessing of the BABEL lines for improved interpretation of the whole crust – preliminary results

S. Buntin[1], A. Malehmir[1], M. Malinowski[2], K. Högdahl[1], C. Juhlin[1], H. Thybo[3] and S. Buske[4]

[1]Uppsala University, Department of Earth Sciences, Uppsala, Sweden
[2]Institute of Geophysics, Polish Academy of Sciences, Warsaw, Poland
[3]University of Copenhagen, Department of Geography and Geology, Copenhagen, Denmark
[4]TU Bergakademie Freiberg, Institute of Geophysics and Geoinformatics, Freiberg, Germany
E-mail: sebastian.buntin@geo.uu.se

This on-going study focuses on the reprocessing of the historical BABEL (Baltic and Bothnian Echoes from the Lithosphere, 1989) seismic lines in the Bay of Bothnia in preparation for the acquisition of a 400 km long onshore reflection and refraction profile in central part of Sweden. The main aim of the project is to increase the understanding of the tectonic evolution of the mineral-rich Bergslagen region both offshore and onshore. The seismic data have been recovered and currently being reprocessed using up-to-date processing methods and preliminary results show promising outcome from this work.

**Keywords:** BABEL, Bergslagen, crust, Moho, seismic imaging, reprocessing

## 1. Introduction

In September and October 1989, over 2200 km of offshore seismic lines were acquired in the Baltic and Bothnian Sea (BABEL Working Group, 1990). These data were fundamental on some of the understanding of the Paleoproterozoic plate tectonic, a matter of debate remained, but also several major crustal-scale structures observed from the upper crust all the way to great depths and likely some reaching the Moho. To improve and revaluate imaging capability of the BABEL data and hence the whole crust in the Bergslagen region in central Sweden, lines 1, 6 and 7 (Figure 1) have been chosen for now. A particular focus will be given to the northern boundary of the Bergslagen in order to study its nature and geological implications.

Sponsored by the Swedish Research Council (VR), the reprocessing results will serve as a basis for the preparation of a proposed onshore refraction and reflection profile in central Sweden, parallel to lines 1 and 6, planned to be acquired in early 2017.

## 2. Preliminary result

Up to now, only seismic data along line 7 have carefully been processed up to prestack level (Figure 2). This included spherical divergence correction, FK-filtering, deconvolution, velocity analysis and NMO corrections. This line has a total length of 174 km and consists of 2322 shot points (Table 1) with air guns as the seismic source (BABEL Working Group, 1993). Given the earlier success with DMO correction (Shahrokhi et al., 2012), we hope additional processing steps such as DMO corrections combined with residual statics, and coherency enhancement methods and migration will significantly improve the imaging results near the surface and likely ready for the time we present these results.

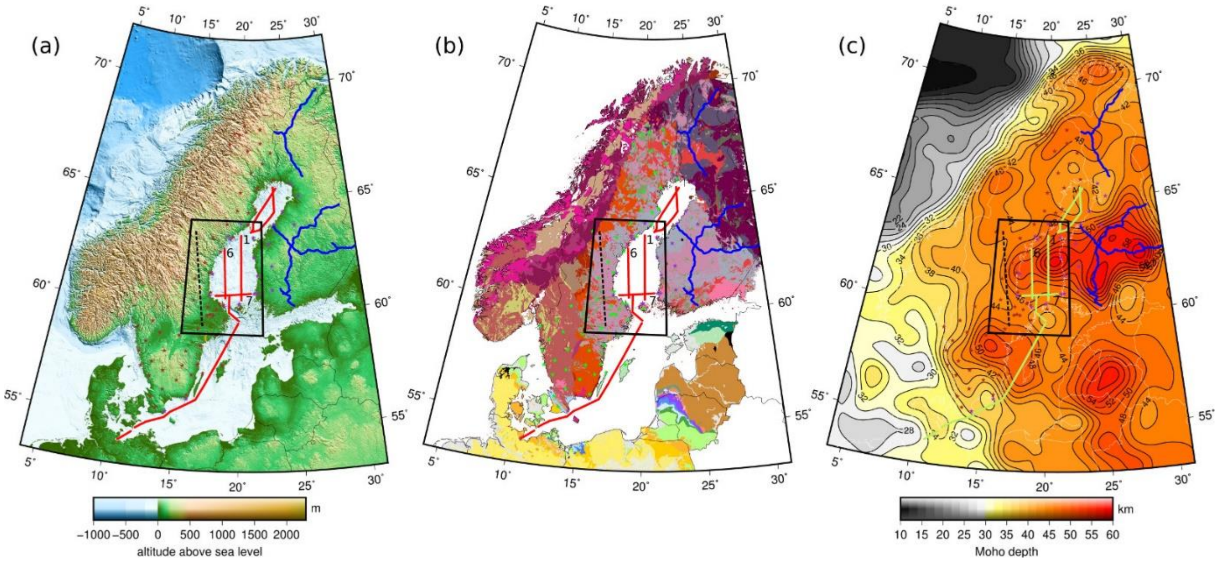


**Figure 1.** (a) Topography and bathymetry, (b) geological and (c) Moho depth maps of the areas around BABEL seismic lines. FIRE seismic profiles (blue line), seismological stations (stars) and the proposed onshore seismic profile (dashed line) are also shown. Moho depth map is plotted based on the data from Grad et al. (2009).

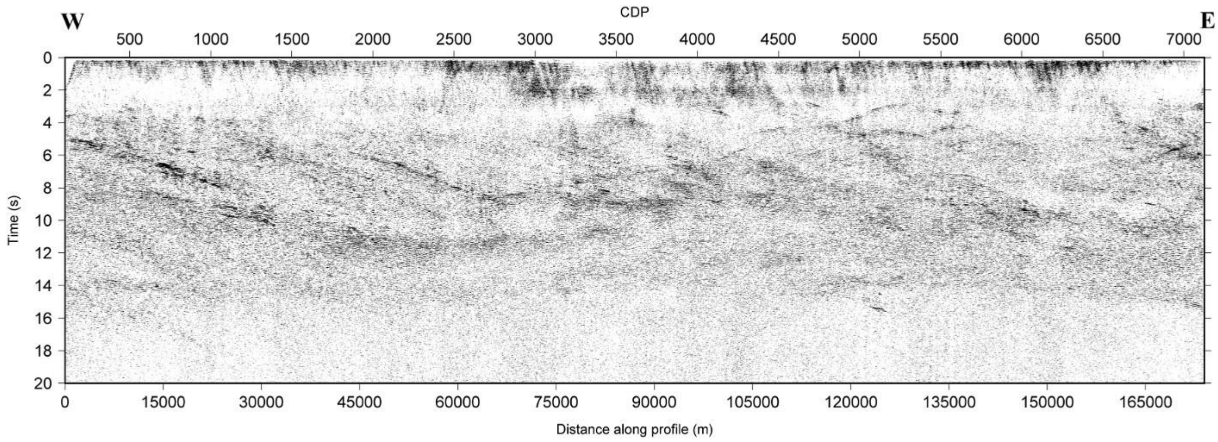


**Figure 2.** Preliminary stacked section of BABEL line 7 reprocessed in this study.

## 3. Outlook

BABEL seismic data are not only historical but also contain valuable and unique information about the overall tectonic structures of the Baltic Shield. BABEL lines 6 and 1 will be reprocessed to provide continuity from one line to another and consistent interpretation of the results in the northern boundary of Bergslagen region. One of the aims of the reprocessing is to image reflections that are hidden in the source-generated noise in the shallow subsurface (< 3 km depth) to be able to better link the deeper reflections to near surface information.

**Table 1.** Acquisition parameters of BABEL survey (BABEL Working Group, 1993).

| **Line** | **1** | **6** | **7** |
|---|---|---|---|
| No. of shots | 4283 | 3979 | 2322 |
| Shot interval (m) | 75 | 62.5 | 75 |
| Profile length (km) | ~ 321 | ~ 249 | ~ 174 |
| Receiver group interval (m) | 50 | 50 | 50 |
| Receiver cable length (m) | 3000 | 3000 | 3000 |
| Record length (s) | 25 | 23 | 25 |
| Sampling rate (ms) | 4 | 4 | 4 |

## Acknowledgments
This study is sponsored by the Swedish Research Council (VR, project 2015 – 05177) for which we are grateful. We also thank Michael Stephens (Geological Survey of Sweden, SGU) for the initiation of the project.

## References:
BABEL Working Group, 1990. Evidence for early Proterozoic plate tectonics from seismic reflection profiles in the Baltic Shield, Nature, 348 (6296), 34–38

BABEL Working Group, 1993. Integrated seismic studies of the Baltic shield using data in the Gulf of Bothnia region, Geophysical Journal International, 112(3), 305-324.

Grad, M., Tiira, T. and ESC Working Group, 2009. The Moho depth map of the European Plate, Geophysical Journal International, 176, 279–292.

Shahrokhi, H., Malehmir, A., and Sopher, D., 2012. New insights on shallow and deep crustal geological structures of BABEL line 7 marine reflection seismic data revealed from reprocessing, In EGU General Assembly Conference Abstracts, Vol. 14, 4236.

# Formation of ultramafic rocks in the middle crust by partial melting of amphibolites

O. Eklund[1] and D. Lindberg[2]

[1]Åbo Akademi University, Geology and mineralogy, Geohouse, Akademigatan 1, FI-20500 Åbo, Finland
[2]Åbo Akademi University, Process Chemistry Centre c/o Combustion and Materials Chemistry
Biskopsgatan 8, FI-20500 Åbo, Finland
E-mail: olav.eklund@abo.fi

Ultramafic rocks in the middle crust do not necessarily have to be of igneous origin. In the granulite area of southwestern Finland, an outcrop contains an ultramafic rock with orthopyroxene ($En_{65}$), amphibole (tschermakite), interstitial plagioclase ($An_{90}$) and some biotite (Mg# = 75). Veins and melt sinks of a coarse-grained rock with graphic intergrowths of plagioclase ($An_{31}$) and tourmaline (dravite, Mg# = 0.66) appear in the ultramafic rock. The outcrop was investigated with both petrological and experimental methods. The result of the study was that the amphibole-orthopyroxene-plagioclase rock represents the melanosome after fluid-induced partial melting of the surrounding amphibolite. Laboratory experiments indicated that boron did not have an influence on the petrological processes.

**Keywords:** lithosphere, middle crust, partial melting, amphibolites

## 1. General

The metamorphic peak in the granulites in southwestern Finland has been determined to 5-7 kbar and above 800 °C at 1.84–1.82 Ga (Väisänen & Hölttä, 1999). In these conditions metapelites melt by dehydration melting, but metavolcanites (amphibolites) need temperatures higher than 850 °C before dehydration melting can start. However, melting of amphibolites can be seen in the Turku granulite area. Usually the melting is identified as tonalitic leucosomes with clinopyroxene and orthopyroxene, and a melanosome of amphibole, clinopyroxene and orthopyroxene.

An ultramafic body is found in a metavolcanite in the Late Svecofennian granite–migmatite zone of southern Finland (Ehlers et al., 1993). The best outcrop is by Café Piikkiö by the Turku–Helsinki highway.

The ultramafic rock is coarse-grained and consists of sub- to euhedral-shaped amphiboles (tschermakite and cummingtonite), corroded orthopyroxene (En65) mantled with cummingtonite, some biotite (Mg# = 75) and plagioclase. The plagioclase (An90) appears as interstitial films or irregular crystals. The opx are corroded with reaction rims of cummingtonite. In the ultramafic rock, veins and melt sinks with plagioclase (An31), quartz and tourmaline (dravite)—often as graphic intergrowths—appear. Sometimes the tourmalines are up to 10 cm in size.

In granitic systems, boron may decrease the solidus temperature with more than 100 °C (Pichavant, 1987; Holtz & Johannes, 1991; Dingwell et al., 1996). According to Kriegsman (1999), the outcrop was formed either by infiltration of granitic melts in a partially melted mafic rock**,** or by infiltration of boron rich fluids that initiated partial melting in the amphibolites. However, the effect of boron in anatexis of metabasites is unknown.

The high amounts of tourmaline in the rock indicate a high boron activity when these rocks were formed. Since temperatures around 850 °C (about 50 °C above the metamorphic temperature in the area) are needed before dehydration melting is initiated in amphibolites, we wanted to test a hypothesis that high boron activity may have decreased the solidus temperature of the amphibolite, and thereby initiated the partial melting.

**2. Experiments**

To test the hypothesis, a series of experiments were done at the laboratory of the Department of Geology, Tromsø University, Norway.

As starting material for the experiments, an amphibolite from Torsholma (Åland Island) was selected. The modal composition of the amphibolite was magnesiohornblende 50.6 %, plagioclase (labradorite) 39.9 %, quartz 8.5 %, biotite 0.6 % and opaque 0.4%.

In the experiments, an end-loaded piston cylinder apparatus with a NaCl-MgO-C-cell with a diameter of 1.27 cm was used. Gold capsules were filled with 50 mg amphibolite rock powder with grain size 10–20 µm and varying amounts of $H_3BO_3$ and distilled water. Experiments were made at a pressure of 5 kbar and 750, 800 and 850 ºC. Running time for the experiments was between 114 and 535 hours.

**3. Results of the experiments**

The general formula for the melting reaction of the amphibolite was:

*plagioclase + quartz + hornblende1 + fluid = melt + hornblende2 ± clinopyroxene*

Water was the most important agent that depolymerised the initial plagioclases and quartz, whereupon a water-rich tonalitic melt was formed. The restitic plagioclase had a high An-content. Since water stabilizes hornblende, a second generation was formed instead of pyroxenes.

The results of the experiments show that boron did not affect the melting process significantly. On the contrary, the experiments with the highest boron content produced the smallest melt fraction at 850 °C. The melt fraction at 850 °C with 0–0.25 % $B_2O_3$ was 40–45%, and with 0.5–1 % $B_2O_3$ 30–35 %.

**4. Comparison to the studied outcrop**

The studied outcrop contains only a few % melt, the interstitial plagioclase is An90, and the mineralogy of the ultramafic rock contains tschermakite, cummingtonite and biotite. This indicates that the melting of the amphibolite took place in an open system where external fluids decreased its solidus and generated melting. The melt sink structures, the low leucosome content in the rock and the high An content in the restitic plagioclases indicate that the outcrop is melt-depleted. The tourmaline-bearing leucosomes are interpreted as differentiated melts that did not leave the system.

**5. Discussion**

Usually mafic rocks contain very low contents of boron (2–35 ppm), but the amphibolites at Piikkiö contain 50 ppm B. This indicates that the boron must be external, originating most probably from the surrounding S-type granites and pelitic migmatites.

A scenario may be that boron rich fluids escaped from the granites during the retrograde stage of the metamorphism. The fluids invaded the amphibolites and decreased their solidus until partial melting was initiated. The hydrous mineral assemblage in the ultramafic rock indicates a high fluid content in the process. Despite the partial melting, the following reactions support influx of fluids from an external source:

*Orthopyroxene +* $H_2O$ *=> cummingtonite*

*Cummingtonite + plagioclase +* $H_2O$ *=> tschermakite*

## 6. Conclusions

This study shows that during the 1.83 Ga metamorphic event, fluids from metapelites invaded metabasalts, reduced their solidus temperature and initiated partial melting. This resulted in tonalitic magmas and restites comprising amphiboles, pyroxenes and anorthite, showing that all tonalites are not pre- or synorogenic, and all ultramafic rocks are not from the mantle.

## 7. References:

Dingwell, D. B., Pichavant, M. & Holtz, F., 1996. Experimental studies of boron in granitic melts. In: Grew, E. S. & Anovitz, L. M. (ed.). Boron: mineralogy, petrology and geochemistry. Reviews in mineralogy vol. 33, Mineralogical society of America.

Ehlers, C., Lindroos, A. & Selonen, O., 1993. The Late Svecofennian granite–migmatite zone of southern Finland—a belt of transpressive deformation and granite emplacement. Precambrian Research 64, 296-309.

Eklund, O (ed.), 2000. A NorFA sponsored Nordic Network on the transition from orogenic to anorogenic magmatism in the Fennoscandian shield, Geocenter informerar, rapport nr 17, 66 p.

Holtz, F. & Johannes, W.,1991. Effect of tourmaline on melt fraction and composition of first melts in quartzofeldspathic gneiss. European Journal of Mineralogy 3, 527-536.

Hölttä, P., 1986. Observations on the metamorphic reactions and PT conditions in the Turku granulite area. Geological Survey of Finland, Bulletin 339, 43-58.

Kriegsman, L. M., 1999. Field Guide for the ESF Exploratory Workshop ”Restite- melt and solid-vapour reactions: Implications for petrology, tectonics and ore-forming-processes”, Turku, 23-25 August 1999.

Lindberg, D., 2002. Effekten av bor i smältningsstudier av metabasiter - en jämförelse med fältförhållanden i Pikis, sydvästra Finland. M.Sci. thesis Åbo Akademi, Geologi och mineralogi.

Pichavant, M., 1987. Effects of B and H2O on liquidus phase relations in the haplogranite system at 1 kbar. American Mineralogist 72, 1056-1070.

Väisänen, M., & Hölttä, P., 1999. Structural and metamorphic evolution of the Turku migmatite complex, southwestern Finland. Bulletin of the Geological Society of Finland 71, 177–218.

# Neoproterozoic faulting and sedimentation documented in a railway tunnel, Vantaa, southern Finland

T. Elminen[1], H. Zwingmann[2] and A. Kaakinen[3]

[1]Geological Survey of Finland GTK, P.O.Box 96, FI-02151 Espoo, Finland
[2]Department of Geology and Mineralogy, Graduate School of Science, Kitashirakawa Oiwakecho, Sakyo-ku, Kyoto University, Kyoto, 606-8502, Japan
[3]Department of Geosciences and Geography, P.O.Box 64, 00014 University of Helsinki, Finland
Email: tuija.elminen@gtk.fi

K-Ar dating was performed on a fresh clay that was filling a crevasse in Savio railway tunnel, Myras, Vantaa. The ages for different grain sizes vary from c. 967 to 697 Ma. The original faulting is assumed to have taken place before 967 Ma related to the collapse of Sveconorwegian orogeny in the west. Sedimentation in a shallow marine intracratonic basin and neocrystallization of illite followed at c. 967 Ma. Continental break-up caused reactivation in the fault and the smaller autigenic illite crystals were formed during the movements in c.679 Ma.

Keywords: clay, K-Ar dating, Neoproterozoic, Finland

## 1. Introduction

The bedrock in southern Finland is mainly of Paleoproterozoic origin. The last event that had a major effect on the basement was the 1650 Ma rapakivi magmatism. In late stages of the event brittle strike-slip and normal faults were formed in transcurrent conditions (Elminen et al. 2008). Other, more well-known brittle structures are the grabens in Satakunta and Muhos that have formed before 1270 Ma and 1400 Ma, based on the diabases crosscutting the sedimentary rocks in Satakunta (Suominen, 1991) and on the K-Ar and Rb-Sr-dating of sediments in Muhos (Simonen 1980), respectively.

However, numerous brittle faults and joints that crosscut the basement have not been dated because of the lacking fresh exposure. The weathering of faults near the surface excludes the possibility of K-Ar dating of illite that is common in fault gouges. Recently, K-Ar ages of 1006.2 ± 20.5 Ma and 885 ± 18.3 Ma from gouges in drill cores were obtained in Olkiluoto (Viola et al. 2013).

A discovery of a clay-filled fault at Savio railway tunnel constructions at Myras, Vantaa provided a unique opportunity to investigate faulting, tectonics and sedimentation. Illite from fresh clay samples was dated by K-Ar method.

## 2. The fault and dating approach

The clay deposit was discovered underground while a railway tunnel was excavated at Myras, in 60 m depth, and was examined both in the tunnel and two drill cores. The deposit forms a steep NNE-trending 30-70 cm thick clay-filled crevasse, associated with a 5-cm-thick arenite. The homogenous greenish gray clay consists mainly of illite with some quartz, K-feldspar and chlorite. In addition steep slicken-lines were observed in the tunnel. A decanted coarse fraction of the clay consists of well-rounded quartz grains supporting the sedimentary origin of the clay instead of mechanically crushed gouge, which is a common clayish material in faults. The arenite is mature containing well-rounded quartz grains and calcite cement. Some feldspar, muscovite, illite grains and glauconite both as a grain and cement are also present.

Transmission Electron Microscopy (TEM) images reveal fibrous, hexagonal and prismatic morphologies for the fine grained illite, suggesting in situ neocrystallization (Clauer and Chaudhuri, 1995). The illite fractions < 0.1 to 2-6 μm were used for dating. The clay fraction yield Neoproterozoic ages from 697.3 ± 14.1 (Cryogenian) to 967.6 ± 19.7 Ma

(Tonian). A classical consistent decrease in age with decreasing grain size can be observed. A total age span of 270 My is recorded within the clay fractions ranging from the Cryogenian for the finer <0.1 and <0.4 µm fraction to the Tonian for the coarser <2 and 2-6 µm fractions.

### 3. Discussion

The authigenic illite was formed after the sedimentation. Thus the fault has been opened before 967 Ma. The relative textural and compositional maturity of the sand fraction and glauconite appear to be compatible with the continental shallow marine depositional setting, likely in an intracratonic basin. The Neoproterozoic age estimation of c. 970 Ma provides evidence for deposition within a time interval where sedimentary records from Fennoscandian shield are scarce, and geochronological data almost non-existing.

The fault geometry suggests extensional conditions and the age is consistent with the collapse of Sveconorwegian orogeny in the west, estimated to have commenced after 970 Ma (Bingen et al. 2006). The smaller 697 Ma illite fraction is probably attributable to reactivation of the fault, likely related to continental break-up that started around 800-700 Ma in the west (Kumpulainen & Nystuen 1985). These and congruent ages from Olkiluoto suggest that at least some of the brittle structures in the Paleoproterozoic bedrock in southern Finland have been formed in Tonian and Cryogenian times reflecting these collapse and break-up events in the edge of the Fennoscandian shield.

### References

Bingen, B., Stein, H.J., Bogaerts, M., Bolle, O., Mansfeld, J. 2006, Molybdenite Re–Os dating constrains gravitational collapse of the Sveconorwegian orogen, SW Scandinavia. Lithos, 87, 328–346

Clauer, N. and Chaudhuri, S. 1995, Clays and Crustal Cycles, Springer, Heidelberg, Germany.

Elminen, T., Airo, M.-L., Niemelä, R., Pajunen, M, Vaarma, M., Wasenius, P. and Wennerström, M. 2008. Fault structures in the Helsinki area, Southern Finland. In Pajunen, M. (ed.) Tectonic evolution of the Svecofennian crust in southern Finland - a basis for characterizing bedrock technical properties. Geological Survey of Finland, Special Paper 47, 185-213

Kumpulainen, R. and Nystuen, J.P., 1985. Late Proterozoic basin evolution and sedimentation in the westernmost part of Baltoscandia. In: D.G. Gee and B.A. Sturt (Editors), The Caledonide Orogen--Scandinavia and Related Area. Wiley, Chichester, 213-232.

Simonen, A., 1980. The Precambrian in Finland. Geological Survey of Finland, Bulletin 304, 58 p.

Suominen, V. 1991. The chronostratigraphy of southwestern Finland with special reference to Postjotnian and Subjotnian diabases. Geological Survey of Finland, Bulletin 356. 100 p.

Viola, G., Zwingmann, H., Mattila, J., & Käpyaho, A., (2013). K-Ar illite age constraints on the Proterozoic formation and reactivation history of a brittle fault in Fennoscandia. Terra Nova, 25, 236-244.

# Plates vs. Plumes: Lithosphere vs. Asthenosphere

G.R. Foulger

Dept. Earth Sciences, Durham University, Durham DH1 3LE, U.K.
E-mail: g.r.foulger@durham.ac.uk

There is an ongoing debate regarding whether processes intrinsic to the lithosphere ("Plate") or the convecting mantle ("Plume") give rise to currently active volcanic provinces. The Plume hypothesis has the disadvantages that its predictions often are not verified by observation, but that at the same time the hypothesis is intrinsically unfalsifiable. A Plate-based model for the Yellowstone volcanic province, USA, is described and compared with the Proterozoic Musgrave volcanic province, Australia. Some outstanding potential questions that could be addressed with lithospheric studies are introduced.

**Keywords:** lithosphere, plates, plumes, testing hypotheses, Yellowstone

## 1. The Plates vs. Plumes controversy

The Plume hypothesis envisages a large, thermal diapir that rises from the core-mantle boundary, actively penetrates the lithosphere, and causes surface volcanism. It forms independently of shallow structures and processes, and is driven by thermal energy from Earth's core.

The Plate hypothesis is the conceptual inverse. It envisages magmatism to be driven by shallow processes driven ultimately by plate tectonics (Foulger, 2010; Foulger & Jurdy, 2007; Foulger *et al.*, 2005; http://www.mantleplumes.org/). In this model, magmatism is a passive reaction to lithospheric extension and its quantity and chemistry reflect source fusibility and composition. Thus magmatism is expected to occur preferentially near extensional plate boundaries, *e.g,*, the mid-Atlantic ridge, and in continental rift zones, *e.g.*, the East African Rift. The mere existence of melt in the mantle is not sufficient to explain surface eruptions. Lithospheric extension is required to release it. Where volumes are large, the chemical fingerprints of high source fusibility are expected.

The Plates vs. Plumes controversy basically amounts to a shallow-lithosphere vs. deep-mantle controversy. Much of the work done to address this controversy uses seismic tomography of the mantle, and the geochemistry of erupted lavas. However, not only are these techniques almost powerless to inform us about the lithosphere, which critically involved, but they are intrinsically unable to deliver the information needed to solve the controversy. Thus, much work looks in the wrong place and uses the wrong tools.

The Plate hypothesis can only be tested by studying the lithosphere. Predictions of the Plume hypothesis related to the lithosphere include:

- kilometer-scale domal uplift occurs some millions of years prior to the eruption of flood basalts associated with the arrival of a plume head,
- large volumes of melt can only form if the lithosphere is thinned prior to eruption, so sufficient decompression melting can occur, and
- ongoing "plume tail" volcanism forms a time-progressive trail on a moving plate.

Predictions of the Plate hypothesis related to the lithosphere include:

- magmatism is accompanied by extension,
- the pattern of vertical motions reflects the process at work, *e.g.*, continental rifting or lithosphere delamination, and
- ongoing volcanism, if it occurs, follows the locus of ongoing extension. This may become extinct rapidly, persist at the same locality, or migrate.

**2. A currently active example: Yellowstone**

An example of a currently active volcanic province is the Yellowstone system (Figure 1). It comprises the ca. 17 Ma Columbia River flood-basalts, a time-progressive chain of rhyolitic calderas blanketed with non-time-progressive basalts (the Eastern Snake River Plain), and the currently active Yellowstone volcano. The Plume hypothesis postulates that these eruptives correspond to an arriving plume head followed by time-progressive “plume-tail” volcanism.

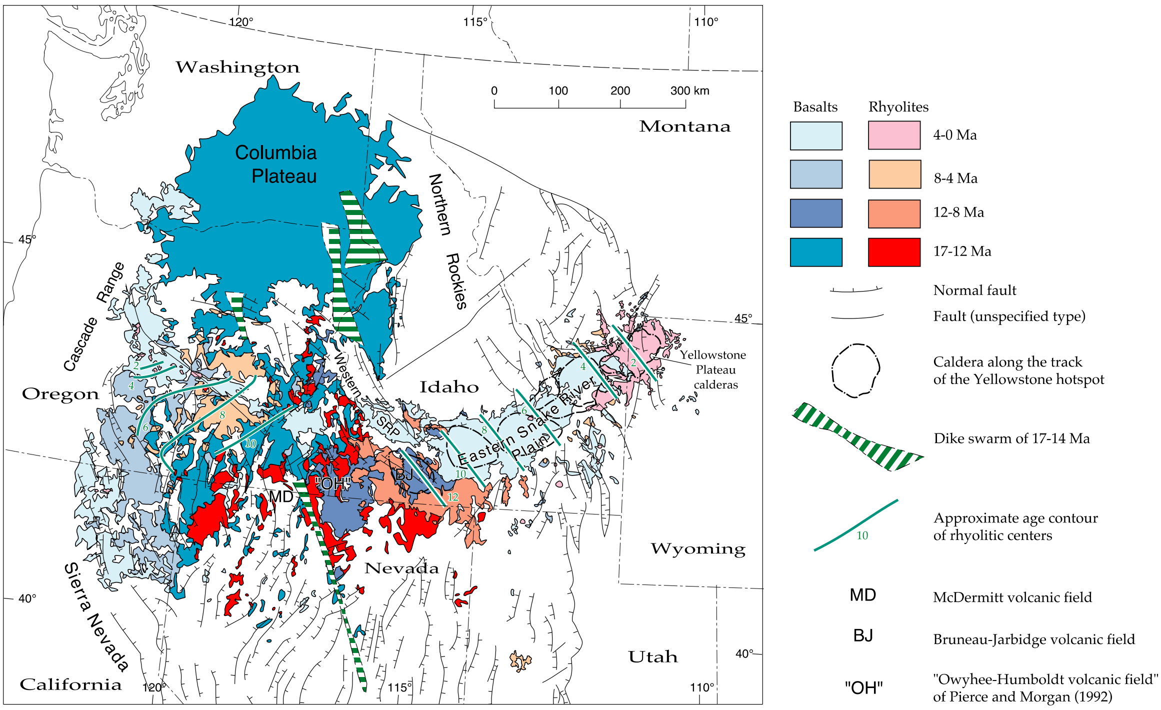


**Figure 1.** Map of the northwestern United States showing basin-range faults, and basalts and rhyolites of 17 Ma and younger. Approximate age contours of rhyolitic volcanic centers (~12, 10, 8, 6, 4, and 2 Ma) across the northeast-trending Eastern Snake River Plain are shown. A contemporaneous trend of oppositely propagating rhyolitic volcanism that trends northwest across central Oregon is indicated by similar contours (from Christiansen et al., 2002).

There are, however, numerous geological mismatches and logical flaws in this model. Mismatches include lack of uplift precursory to the eruption of the Columbia River Basalts, spatial mismatches between the predicted and observed sites of subsequent “plume tail” volcanism, volcanic activity along the Eastern Snake River Plain prior to the predicted plume-tail arrival time, persistent, scattered basaltic volcanism there, and mirror-image backward-propagating volcanism in the High Lava Plains region to the west (the “Newberry trend”). Logical flaws include citing high-$^{3}He/^{4}He$ isotope ratios and the time-progressive trail of silicic calderas along the Eastern Snake River Plain as evidence for a "shallow-mantle plume". In the plume model, high- high-$^3He/^4He$ isotope ratios require an origin at the core-mantle-boundary. Also, the Plume hypothesis requires that the melt locus is fixed relative to Hawaii. This, in turn, requires plumes to be rooted in the deep mantle where they cannot be displaced by the vigorous shallow convection associated with plate tectonics. A model that postulates a plume rooted in the shallow mantle, but appeals to arguments that require a core-mantle-boundary origin, is internally inconsistent. Furthermore, no seismic tomography has imaged a deep-mantle plume beneath Yellowstone, despite numerous published studies.

The Plate hypothesis predicts that time-progressive migration of volcanism results from time-progressive migration of lithospheric extension (Foulger et al., 2015). Such migration of extension in the region is well-documented. Lithospheric extension and thinning is associated with the adjacent basin-range region. Superimposed on this, the most intense extension occurred in a northerly trending zone ~ 125 km wide that migrated systematically from the central basin-range region to its present position at the eastern edge of the province over the last ~ 17 Ma. Bimodal rhyolite-basalt volcanism followed migration of this locus of intense extension.

## 3. A Proterozoic example: The Musgrave province

Yellowstone is an extraordinarily large and spectacular volcano and as a natural phenomenon it is extreme. However, it is not unique. Long Valley caldera in California is a somewhat smaller but similar bimodal volcano that erupted ~ 600 $km^3$ of material at ~ 0.76 Ma (~ 25% of the great Huckleberry Tuff at Yellowstone). A Proterozoic example is the 1090 – 1040 Ma Musgrave volcanic province in central Australia. This event added mantle-derived melt to the crust including one of the largest mafic intrusions ever produced and the Warakurna large igneous province which extends over and area of $\sim 1.5 \times 10^6$ $km^2$. It also included huge volumes of felsic emplacements, one of the world's longest-lived rhyolitic centres, and the Talbot "supervolcano". Magmatism there lasted more than 50 Ma and persisted in the same region with no discernible age-progressive spatial trend.

High lithospheric temperatures are thought to have existed at this locality for ~ 100 Ma prior to magmatism. The main magmatic phase may have onset when the region was deformed by a shear zone that separated the Musgrave Province from the extending Capricorn Orogen (Smithies *et al.*, 2015b). The province was described by Smithies et al. (2015a) as "analogous to compressing or superimposing the entire regional (>600 km) felsic magma track of the Miocene Snake River Plain-Yellowstone Plateau of North America…into a single volcanic centre".

Both Long Valley caldera and the Musgrave volcanic province are likely consequences of extension occurring where lithospheric structure is locally disjoint and, I suggest, is the Yellowstone system also.

## 4. Some potential problems

As the above observations highlight, and as Prof. Ilmo Kukkonen pointed out in a private communication, the controversy regarding litho-centric vs. a convecting-mantle-centric initiating processes for shallow magmatism can aid, and be aided by, studies of Proterozoic lithosphere. Some outstanding potential questions are:

1. Is there evidence for melt reservoirs at the base of the lithosphere, that may be rapidly drained to form surface flood basalts?
2. Can observed variations in lithosphere temperature be explained by radiogenic decay, or are temperature anomalies in the convecting mantle required?

3. What is the evidence for lithospheric thinning, resulting either from delaminations or thermal upwellings?
4. Can extinct magmatic provinces be used to test the Plate and Plume hypotheses?
5. What is the composition of mantle lithosphere? Can it explain the geochemical signatures observed in Phanerozoic flood basalts and volcanic provinces or are exotic mantle compositions and/or ancient subducted crust required?

*Ad hoc* application of the Plume hypothesis can explain all volcanism, and fundamentally cannot be disproved. Thus, attributing all magmatism to mantle plumes offers little potential for improving our understanding underlying processes. On the other hand, testing the Plate hypothesis has the potential to contribute significantly, including addressing questions such as when plate tectonics started.

**References:**

Christiansen, R. L., G. R. Foulger, and J. R. Evans (2002), Upper mantle origin of the Yellowstone hotspot, Bull. Geol. Soc. Am., 114, 1245-1256.

Foulger, G. R. (2010), Plates vs Plumes: A Geological Controversy, Wiley-Blackwell, Chichester, U.K., xii+328 pp.

Foulger, G. R., and D. M. Jurdy (2007), Plates, Plumes, and Planetary Processes, Geological Society of America, Special Paper 430, 997+ix pp.

Foulger, G. R., R. L. Christiansen, and D. L. Anderson (Eds.) (2015), The Yellowstone "hot spot" track results from migrating basin-range extension, Geological Society of America, Boulder, CO.

Foulger, G. R., J. H. Natland, D. C. Presnall, and D. L. Anderson (2005), Plates, Plumes, and Paradigms, Geological Society of America, Special Paper 388, 881+xi pp.

Smithies, R. H., H. M. Howard, C. L. Kirkland, F. J. Korhonen, C. C. Medlin, W. D. Maier, R. Quentin de Gromard, and M. T. D. Wingate (2015a), Piggy-back Supervolcanoes–Long-lived voluminous, juvenile rhyolite volcanism in Mesoproterozoic central Australia, J. Pet., 56, 735-763.

Smithies, R. H., C. L. Kirkland, F. J. Korhonen, A. R. A. Aitken, H. M. Howard, W. D. Maier, M.T.D.Wingate, R. Q. d. Gromard, and K. Gessner (2015b), The Mesoproterozoic thermal evolution of the Musgrave Province in central Australia — Plume vs. the geological record, Gondwana Research, 27, 1419-1429.

# COGITO-MIN seismic reflection study in Polvijärvi: Insight into the first results

G. Gislason[1], S. Heinonen[1], M. Malinowski[2], E. Koivisto[3], L. Sito[4], P. Targosz[4], M. Wojdyla[4], J. Juurela[5], S. Juurela[5], T. Törmälehto[5] and K. Vaittinen[5]

[1]Geological Survey of Finland, P.O. Box 96, FI-02151 Espoo, Finland
[2]Institute of Geophysics, Polish Academy of Sciences, Ksiecia Janusza 64, 01-452 Warsaw, Poland
[3]Department of Geosciences and Geography, P.O. Box 64, FI-00014 University of Helsinki
[4]Geopartner Ltd., Skosna 39B, 30-383 Krakow, Poland
[5]Boliden Kylylahti Oy., Kaivostie 9, FIN-83700, Polvijärvi, Finland
E-mail: gardar.gislason@gtk.fi and suvi.heinonen@gtk.fi

New 2D seismic reflection data have been acquired in Polvijärvi, Finland during autumn 2016 as a part of the COGITO-MIN project that aims to develop cost-effective mineral exploration methods with special focus on seismic techniques. Both vibroseis and explosive sources were used in the survey, and preliminary observations about the subsurface reflectivity are encouraging the hypothesis that upper crustal structures are imaged with these data.

**Keywords:** seismic reflection profiling, upper crust, mineral exploration, Outokumpu

## 1. Introduction

Seismic reflection surveying has been the preferred tool of exploration within the petroleum industry for over 80 years. Despite their commercial success in the petroleum industry, reflection seismic methods are yet to make a similar, commercial breakthrough in hardrock environments and have mainly been used for research purposes. The primary reasons for the difficulties in hardrock terrains are related to the complexity of geological structures and subtle contrasts in the acoustic impedance between the target and its surrounding rock. Furthermore, the lithological variation in hardrock environments is often much greater than in sedimentary basins. However, results of petrophysical studies (e.g. Luhta et al., this volume) are encouraging the use of seismic reflection methods in hardrock terrain. Technological developments have increased the S/N ratio of the seismic data acquisition, and processing schemes tailored for hardrock conditions have further improved the results achieved in crystalline bedrock environments. The COGITO-MIN project – coordinated by the University of Helsinki – is developing cost-effective geophysical mineral exploration techniques, with main emphasis on seismic methods (Koivisto et al., this volume). Project partners from Poland and Finland, representing both academia and industry, are working together in the project with the aim to develop new data acquisition, processing and interpretation techniques. Locally, the goal is to achieve a better understanding of the subsurface structures in the vicinity of the Kylylahti mine, in Polvijärvi, Eastern Finland. As part of this project, new 2D reflection seismic data have been acquired.

Kylylahti mine is located in Polvijärvi, within the north-eastern extension of the famous Outokumpu mining and exploration district in Eastern Finland. Kylylahti Cu-Au-Zn mine started production in 2012 and is currently owned and operated by Boliden Kylylahti. Mining is currently taking place at about 700 m depth, and the known ore reserves will last until 2020. Main rock type of the Kylylahti area is mica gneiss and copper ore of the Kylylahti is hosted by so called Outokumpu assemblage rocks (serpentinites with carbonate, skarn and quartzrocks) enveloped in sulphide bearing black schists. Because of their high conductivity, the black schists mask the response of the metallic ore deposits and pose a challenge to traditionally used electromagnetic exploration methods. One of the aims of the COGITO-MIN project is to image the continuation of the ore-hosting rock sequence with seismic data and indicate new deep drilling targets that can lead to new discoveries, thus leading to extend of the mine's life.

## 2. Field work

The seismic data in the Kylylahti area were acquired along two, almost parallel ca. 6 km long profiles. Geopartner, an industrial partner of the COGITO-MIN project, provided the wireless recording system and vibroseis sources used in the project (Figure 1a). Acquisition of the high resolution 2D seismic profiles (Figure 1b) was done within two weeks in August-September 2016. A total of 577 receivers with 10 meter spacing were deployed for line A and 574 receivers for line B. With a total of 456 total source points, two types of sources were used; 125 or 250 g dynamite charges and two INOVA UniVib 9.5-ton trucks. Explosive sources were drilled to about 2 m depth. In each vibroseis source points, two Univib vibroseis sources (Figure 1a) produced three 16 s long, linear sweeps from 4 to 220 Hz in a tail-to-nose configuration. Nominal source spacing was 20 m.

Explosives were used in areas not accessible for vibroseis trucks, in order to achieve as uniform source spacing along the profiles as possible. Vibroseis source points were located on the roads while most of the explosive source points were located along small forest paths, resulting in a crooked line geometry presented in Figure 1b on a geological map. Both survey

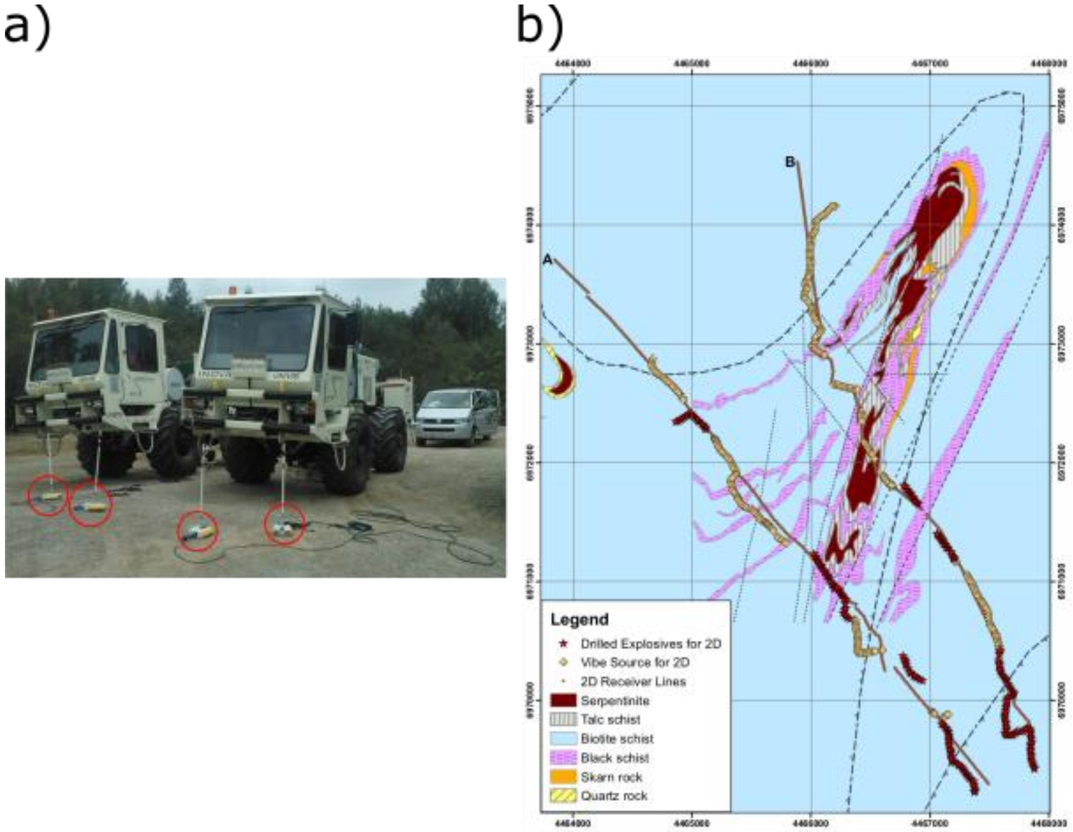


**Figure 1.** a) Kylylahti seismic reflection data were acquired with wireless receivers and Univib-vibroseis sources owned by Geopartner, industrial partner of the COGITO-MIN project. Photo: Suvi Heinonen. b) Location of receivers and sources of the COGITO-MIN seismic 2D profiles in the Kylylahti area in 2016. Light crosses and dark stars represent vibroseis and dynamite sources, respectively.

lines cross the Kylylahti formation, and are expected to image the north-western and south-eastern extent of the Kylylahti formation. Previous studies have indicated that the Kylylahti formation is located on a hinge of an overthrusted Outokumpu nappe (Figure 1b), and these newly acquired seismic data will possibly shed light to the dip of the earlier interpreted thrust zones. Kylylahti mine is located in the middle part of the profile B and the densely drilled mine area will provide good geological reference data for seismic interpretation.

**3. Comparison of vibroseis and explosive sources**

Both dynamite and vibroseis shot gathers were collected at six source locations to compare the two source types and also to aid parameter selection in data processing. Figure 2 shows a comparison of the vibroseis and explosive shot records. It is apparent from the data that the vibroseis record has a better signal-to-noise ratio when compared to the explosive shot gather. This is attributed to the fact that a vibroseis record is actually stack of three records allowing efficient suppression of noise. Both shot gathers show clear first breaks, indicating good quality of the data along the whole length of 6 km geophone spread. In both records, the same channels are contaminated by noise, suggesting uniform data acquisition circumstances. The shot gather acquired using an explosive source shows clearly a more prominent source induced ground roll (velocity 2300 m/s), that is supressed in the vibroseis records because of stacking. Reflections at 1800-2500 ms are especially apparent in the vibroseis shot gather. These reflections visible already in the unprocessed data are encouraging for future processing efforts.

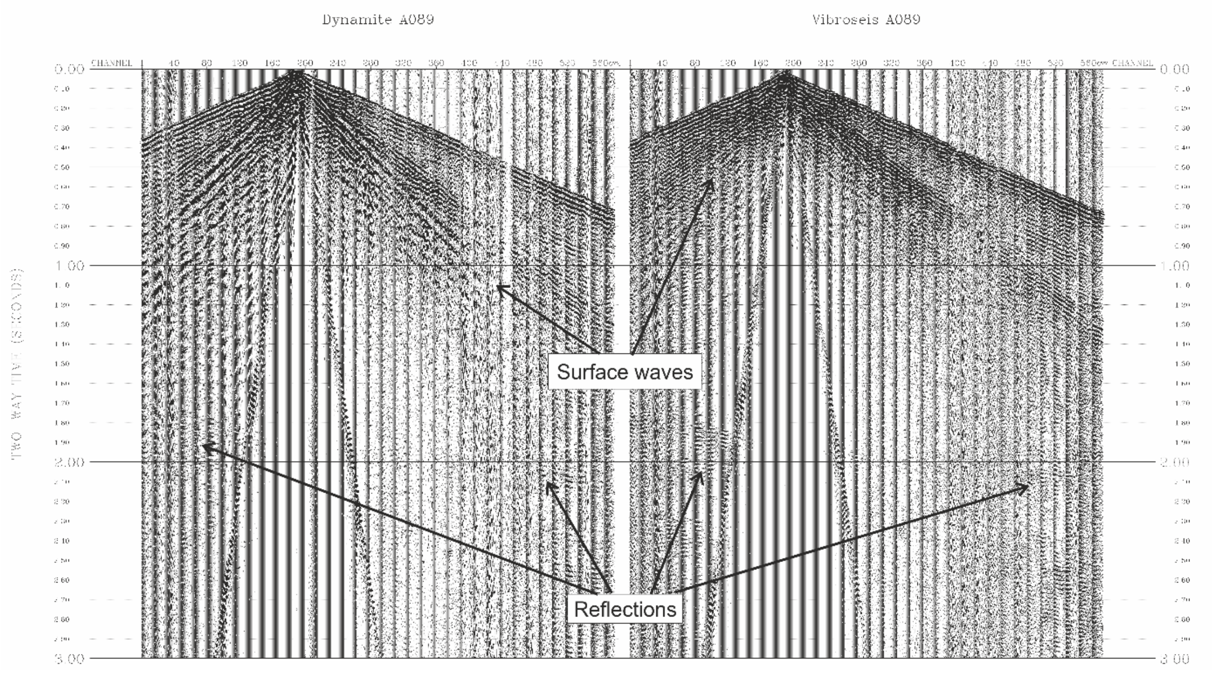


**Figure 2.** Comparison of a vibroseis source and a dynamite source shot gather on peg location A089. On the vibroseis gather, S/N ratio is increased by stacking three shot gathers measured at the same location together.

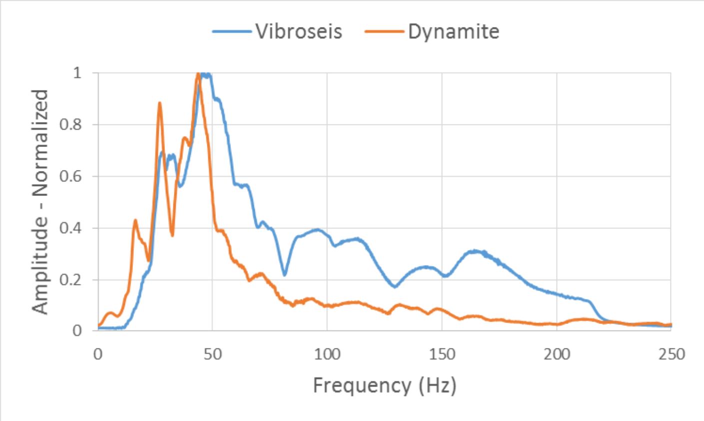


**Figure 3.** Spectral comparison of the vibroseis and dynamite shot gathers from Figure 4.

Figure 3 shows comparison of amplitude spectrum of vibroseis and dynamite records presented in Figure 2. In both records highest amplitudes are recorded at 25-60 Hz, and it is apparent that high frequencies need to be enhanced in the future seismic processing.

## 4. Conclusions and future work

Preliminary insight to the 2D reflection seismic data acquired as a part of COGITO-MIN project shows that energy from both vibroseis and explosive sources penetrates down to depths of several kilometres, with reflections observed even in unprocessed seismic data. First breaks are clear along the whole spread enabling future refraction static model building and calculation of near-surface velocity model. Comparison of the vibroseis and explosive shot records acquired at the same location show that similar reflectivity is observed with both sources but prior to processing vibroseis records are less noisy due to stacking.

## 5. Acknowledgements

The COGITO-MIN project has been funded through the ERA-MIN network. At the national level, the funding comes from Tekes in Finland and the NCBR in Poland. Leica Geosystems Oy is thanked for providing their SmartNet for the project use.

## References:

Koivisto, E., Malinowski, M., Heinonen, S., Cosma, C., Enescu, N., Juurela, S., Juurela, J., Törmälehto, T., Vaittinen, K. and Wojdyła, M., 2016. New tools for deep mineral exploration: Insights from the field work stage of the COGITO-MIN project *in* this volume.

Luhta, T., Mertanen, S., Koivisto, E., Törmälehto, T., Heinonen, S. and Kukkonen, I., 2016. The seismic signature of the Kylylahti deposit: Initial results from new petrophysical measurements *in* this volume

# New evidence for crustal growth: field and geochemical data from plutonic rocks in SE corner of the Central Finland Granitoid Complex

E. Heilimo[1], P. Mikkola[1], Y. Lahaye[2] & H. Huhma[2]

[1]Geological Survey of Finland, P.O. Box 1237, 70211 Kuopio, Finland
[2]Geological Survey of Finland, P.O. Box 96, 02151 Espoo, Finland
E-mail: esa.heilimo@gtk.fi

We represent new geochemical and isotopic data from the Jyväskylä-Kangasniemi area of southeast Central Finland Granitoid Complex (CFGC). The plutonic rocks represent mainly intermediate calc-alkaline rocks formed between ca. 1895 and ca. 1875 Ma. They are coeval with the supracrustal Makkola suite that likely represents continuum of classic Tampere group rocks. The plutonic rocks can be separated into several suites based on field relationships, geochemical composition and isotope data. Our new findings will further refine the earlier interpretations of relationships between these groups in space and time. Updated interpretations will contribute to our understanding of the central part of the Svecofennian orogeny.

**Keywords:** Paleoproterozoic, Svecofennia, Fennoscandia, granitoid, age determinations, Hf-isotopes

## 1. General

The Svecofennian bedrock grew by sequential accretion of arcs and thus its geological history is composed of episodic collision events. During crustal growth, uplifting, folding, and variable stages of deformation affected the still ductile crust. Our study area concentrates in the SE corner of the synorogenic Central Finland Granitoid Complex (CFGC) (Fig. 1). The area is located at the boundary between CFGC and Pirkanmaa migmatite and intrusive suites. This boundary coincides in most places with two geological features trending northeast A) Leivonmäki shear zone crosscutting the geological units and B) Makkola suite volcanic rocks occurring as discontinuous belt in the area.

## 2. Intrusive units

Southeast of the Leivonmäki shear zone the bedrock consist mainly of plutonic rocks belonging to the Pirkanmaa intrusive suite (mainly granodiorites and tonalites) and Lammuste quartz diorite lithodeme, which is the plutonic member of the Makkola suite. Rocks of both these units are ca. 1895 Ma in age and thus 10 Ma older than the main magmatic phase of the CFGC (1885–1880 Ma; Nikkilä et al. 2016, Rämö et al. 2001). Porphyrite dykes belonging to the Makkola suite and crosscutting, both Lammuste quartz diorites and Pirkanmaa intrusive suite as well as the volcanic units indicate that all of these units formed a geological entity at ca 1895 Ma.

The main magmatic phase of the GFGC that formed most of the crust northeast of the Leivonmäki shear zone, relates to the peak of the collisional phase in the area. This phase is slightly younger than the dominant volcanic activity within the Makkola suite, but partly overlaps with it. Plutonic rocks belonging to this phase have been divided into Muurame and Vaajakoski lithodemes. The previous includes the foliated K-feldspar porphyritic granitoids, making up the bulk of the CFGC and the latter contains quartz diorites and diorites. These coeval calc-alkaline plutonic rocks in our study area, and in other parts of the CFGC as well, Rämö et al. 2001, Nikkilä et al. 2016) were emplaced as numerous magma pulses with varying compositions.

The bimodal Saarijärvi suite (1885–1875 Ma, Rämö et al. 2001 also called as postkinematic) partly overlaps in age with the Jyväskylä suite. It contain K-feldspar porphyritic quartz montzonites and granites as variably sized intrusions as well smaller gabbro and diorite intrusions. The bimodality of this suite manifests it at both areal and outcrop scale, mafic intrusions commonly occur in contact with the granitoids and on outcrops different magma mingling structures are common. Compositionally the granitoids share A-type geochemical affinity. The magmas derived from relatively deep sources were able to descent via large scale faults providing sufficient pathways.

Oittila suite consisting of granites and granodiorites and yielding ages of ca 1875 Ma are of the same as the as the youngest members of the Saarijärvi suite, although represent different types of magmas. Their often leucocratic composition hints to small degree of partial melting of pre-existing crust in the area. In field the Oittila suite forms crosscutting dykes and small intrusions, often intruding into relatively brittle structures.

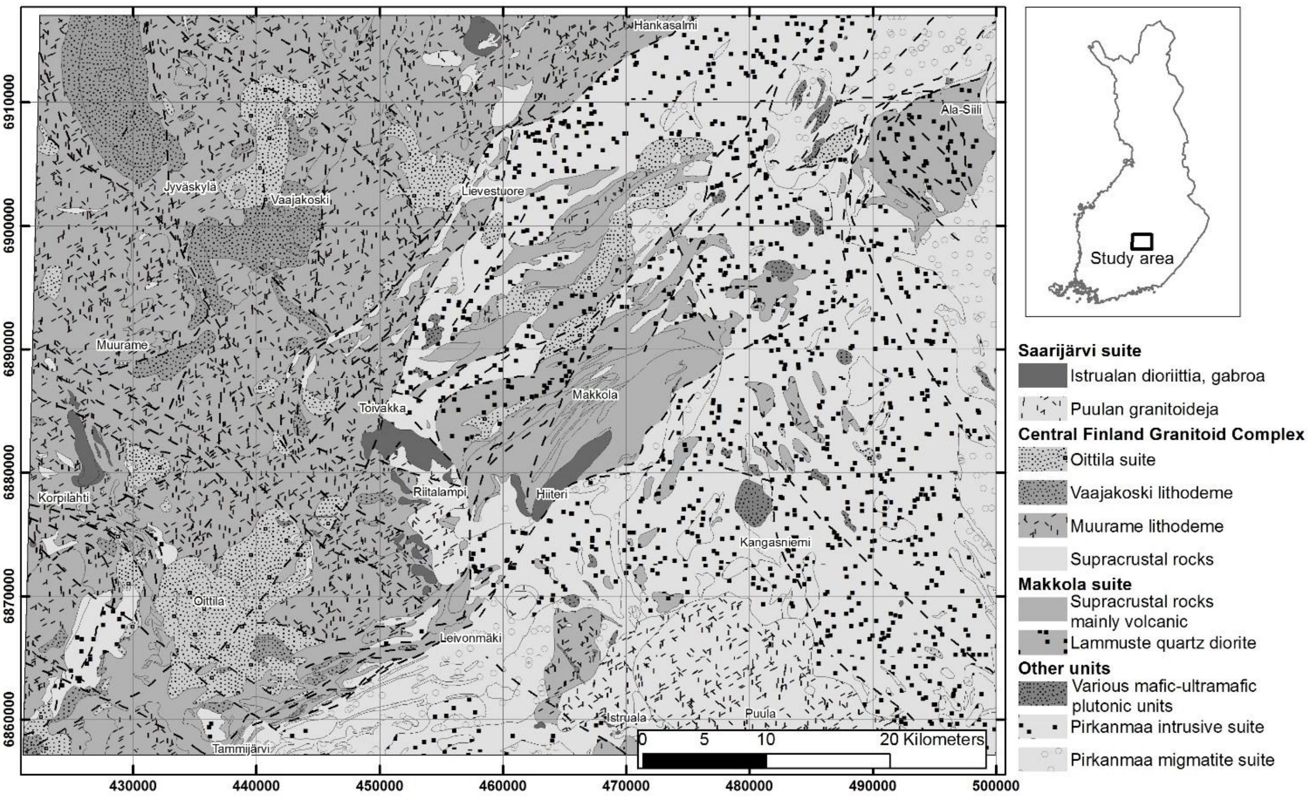


Figure 1. Geological map of the study area, northeast – southwest trending Leivonmäki shear zone divides the study area together with the Makkola suite forming discontinuous belt into Central Finland Granitoid complex (CFGC) and Pirkanmaa migmatite and intrusive suites (Mikkola et al., in review).

## 4. Isotopic results

The rapid growth of the crust in the area, mere 20 Ma from ca. 1895 to ca. 1875 Ma, supports the previous scenarios for quick process of the crustal growth. To trace down possible involvement of significantly older crustal material in the genesis of the igneous rocks related to collision of arc material with the Archean crust during Svecofennian orogeny we have carried out a Lu-Hf study on zircons. The analysis were done from single crystal with ablation multicollector inductively coupled mass spectrometer (LAM-ICPMS). The average initial $^{176}Hf/^{177}Hf$ values range in preliminary studied plutonic samples from 0.28151 to 0.28170 ($\varepsilon_{Hf}$ = − 2.0 to 4.2: 2s ≤ 1.1), do not necessarily require the significant involvement of ca 2.1 Ga component i.e. Keitele microcontinent of Lahtinen et al. (2005) in the development of the plutonic suites in the study area. But do not completely rule such involvement out either.

## References:

Mikkola, P., Heilimo, E., Aatos, S., Ahven, M., Eskelinen, J., Halonen, S., Hartikainen, A., Kallio, V., Kousa, J., Luukas, J., Makkonen, H., Mönkäre, K., Niemi, S., Nousianen, M., Romu, I. and Solismaa, S. (in review) Jyväskylän seudun kallioperä. Geologian tutkimuskeskus, tutkimusraportti.

Lahtinen, R., Korja, A. and Nironen, M. 2005. Paleoproterozoic tectonic evolution. In Lehtinen, M., Nurmi, P., Rämö, O.T. Precambrian geology of Finland key to the evolution of the Fennoscandian shield. Developments in Precambrian Reseach, 14, 479–531.

Nironen 1997. The Svecofennian Orogen: a tectonic model. Precambrian Reseach 86, 21–44.

Nikkilä, K., Mänttäri, I., Nironen, M., Eklund, O. and Korja, A., 2016. Three stages to form a large batholith after terrane accreation – An example from the Svecofennian orogen. Precambrian Research 281, 618–638.

Rämö, O.T., Vaasjoki, M., Mänttäri, I., Elliot, B.A. and Nironen, M. 2001. Petrogenesis of the Post-kinematic Magmatism of the Central Finland Granitoid Complex I; Radiogenic Isotope Constraints and Implications for Crustal Evolution. Journal of Petrology 41, 1971–1993.

# Start of project PALIN – Partial melting processes in the contact zones of layered intrusions

J.S. Heinonen[1], W.A. Bohrson[2], A.V. Luttinen[3], F. Molnár[4], M.W. Schmidt[5], F.J. Spera[6] and T. Wagner[1]

[1]Department of Geosciences and Geography, P.O. Box 64, 00014 University of Helsinki, Finland
[2]Department of Geological Sciences, Central Washington University, Ellensburg, WA 98926-7418, USA
[3]Finnish Museum of Natural History, P.O. Box 44, 00014 University of Helsinki, Finland
[4]Geological Survey of Finland, P.O. Box 96, 02151 Espoo, Finland
[5]Department of Earth Sciences, ETH Zürich, Clausiusstrasse 25, 8092 Zürich, Switzerland
[6]Department of Earth Science, University of California, Santa Barbara, CA 93106, USA

E-mail: jussi.s.heinonen@helsinki.fi

Magma-wallrock interaction in crustal magma chambers (a process known as crustal assimilation) is critical to the evolution of a magmatic system and formation of many of the most economically important base and precious metal deposits. Although such generalized model is largely accepted, details on how these interactions take place are relatively poorly characterized. One of the major issues has been the lack of models that integrate mass and energy exchange, thermodynamics and geochemistry. We propose to explore magma-wallrock interaction at three major intrusive complexes in Antarctica, USA, and Finland in a multidisciplinary study that includes state-of-the-art computational modeling with recently developed energy-constrained equations. The modeling will be tested against existing and potentially new geochemical data and wallrock partial melting experiments that provide new insight into generation of layered intrusions and associates ore deposits.

**Keywords:** magma chamber, assimilation, thermodynamics, geochemistry, experimental petrology, modeling

## 1. Introduction

There is considerable evidence that mafic intrusions vigorously react with the surrounding wall rocks during their emplacement (e.g., Johnson et al., 2003). Such interactions have notable effects on phase relations of the whole magmatic system, and thus also on the precipitation of base and precious metals in these systems (e.g., Benkó et al., 2013). The so-called AFC (assimilation-fractional crystallization) model (DePaolo, 1981) is a classical and the most widely used chemical assimilation model in geoscientific research. However, it does not provide any hint on whether its results are thermodynamically feasible or not. Instead, it mixes a compositionally fixed bulk contaminant into a magma body and does not allow progressive melting of crustal wallrock. Such limitations may significantly impact the mass balance of crustal and magma sources in the models of magmatic systems.

The improvements in computational capacity have enabled ever more complex and larger dataset to be handled using personal computers and new tools to address how magma and wallrock interact have emerged over the last 15 years. First energy-constrained assimilation-fractional crystallization (EC-AFC) equations that account for mass and energy conservation in a magmatic system were developed by Spera and Bohrson (2001). Their latest contribution, Magma Chamber Simulator, (MCS; Bohrson et al., 2014) builds on these equations by adding thermodynamic constraints for a multicomponent + multiphase magma body that crystallizes in contact with a crustal wallrock and is recharged with batches of fresh magma (Figure 1).

We propose to explore the petrologic and geochemical impact of magma-wallrock interaction at three major intrusive complexes in Antarctica, USA, and Finland (two of which are economically important) in a multidisciplinary study that includes computational modeling using existing and potentially new geochemical data and wallrock partial melting experiments. EC-AFC and MCS models have mostly been used to study the evolution of volcanic systems so far; the proposed research will concentrate on layered intrusions and dive directly into the magma chambers, in which all of the aforementioned action takes place – the study will be the first of its kind. The research is funded by the Academy of Finland and will be conducted 2016–2021.

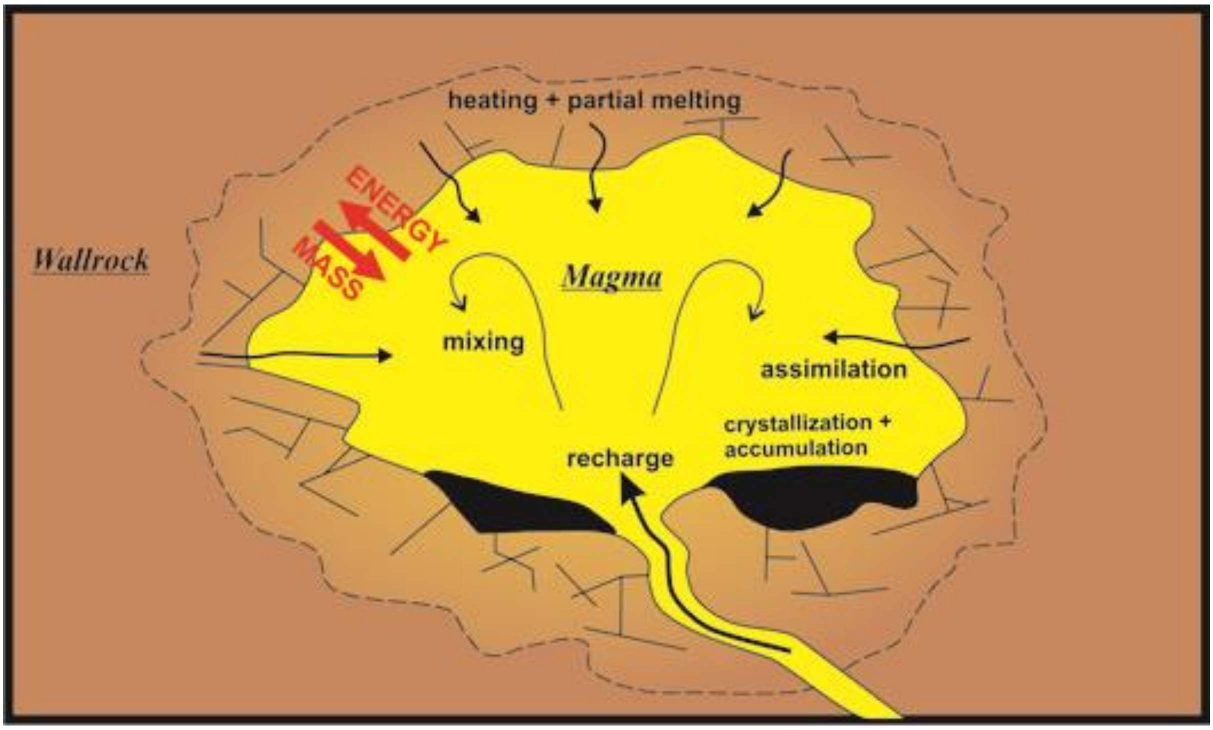


**Figure 1.** Crustal magma chamber processes that are taken account in our research.

**2. Case studies**

The ~180-million-year old Utpostane and Muren gabbroic intrusions are the first case study and are found in contact with continental flood basalts that belong to the Jurassic Karoo large igneous province in Antarctica. Geochemical evidence suggests that the magmas were contaminated in a two-stage process, first one involving the contamination of the magma with the underlying Precambrian basement, and the second one involving contamination with the surrounding flood basalts (see Vuori, 2004; Luttinen et al., 2015). The combination of these processes resulted in the gabbros becoming less radiogenic (in terms of Nd and Sr isotopes) towards the contacts with the present wallrock (hydrothermally altered basalt). To our knowledge, such compositional gradation has not been described before.

The 1100-million-year old Duluth Igneous Complex is the second case study and is one of the largest magmatic Cu-Ni- and PGE-hosting intrusive complexes in the world. It is part of the Mid-continent rift and covers 5700 $km^2$ west of Lake Superior. Interaction between footwall and mafic intrusion is regarded as one of the most important factors in the formation of the basal mineralization zones (e.g., Ripley and Al-Jassar, 1987; Benkó et al., 2015), but modeling of the interaction of partial melts from the Archean footwall with the mafic-ultramafic melts has not been performed. Furthermore, important source for the sulfur has been suggested to be the sulfide-rich metasedimentary formations also found in the contact of the igneous complex (e.g., Ripley and Al-Jassar, 1987; Queffurus and Barnes, 2014).

The Paleoproterozoic (~2440-million-year old) layered intrusions as part of the Fennoscandian large igneous province are found as a roughly E-W trending, 300-km-long belt in northern Finland and are the third case study. These intrusions are known to host all mineralization types characteristic of layered intrusions globally, including magmatic Cu-Ni sulphide, and PGE deposits similar to those found in Duluth (Iljina and Hanski, 2005). The contact zones with the footwall Archaean rocks are important hosts for magmatic sulphide ores and show modification in composition due to various degrees of magma-country rock interaction. Importantly, the highest known primary PGE concentrations in Fennoscandia are connected to these zones and related areas in the country rocks (Andersen et al., 2006).

**3. Approach**

Applying MCS (Bohrson et al., 2014) for the different (and possibly additional) case studies is the most important activity for our research. The MCS constraints that are usually the most difficult to estimate, are the trace element partition coefficients and partial melting behavior of the wallrock, however. The planned partial melting experiments can be assessed using the wallrock melting function in MCS. That is, we can directly compare the partial melt compositions from the experiments to those predicted by MCS. This “cross-checking” has not been done for MCS, and will have impact on our understanding of how MCS does in melting certain kinds of wallrock. To achieve this aim, melting experiments on representative wallrock samples will be performed at crustal pressures. The goal is to melt the wall rock alone, and to melt the wall rock together with the resident magma. The latter approach has never been done before either and the peritectic reactions involved may lead to a very different mineralogy that may further improve our understanding of assimilation mechanisms. The resulting glass (and residual mineral phases) will be analyzed for major and trace elements.

Samples for the experiments will be collected from already existing field samples (Antarctica) and drill core archives (USA, Finland) of the case-study intrusions. Considerable amount of geochemical data already exists for all the localities, but additional geochemical analyses will also be performed, if necessary.

**4. Outcome of the project**

The expected results should be of great interest to both academic and non-academic institutions and mineral exploration and mining companies. Combining new methods of experimental petrology with MCS modeling and testing hypotheses in layered intrusions is expected to result in significant advancements in the field of petrology and ore geology. For example, mappings of “thermodynamically feasible” magma-wallrock pairs can potentially lead to new discoveries of base and precious metal deposits in the future. We emphasize that our research is not bound to the presented case studies and it is possible to include additional magmatic systems in the modeling. We therefore encourage collaboration between national and international teams who are working with different magmatic systems and their thermodynamic and chemical evolution.

**References:**

Andersen, J.C.O., Thalhammer, O.A.R., Schoenberg, R., 2006. Platinum-group element and Re-Os isotope variations of the high-grade Kilvenjärvi Platinum.ground elelemnt deposit, Portimo layered igneous complex, Finland. Econ. Geol., 101, 159-177.

Benkó, Z., Mogessie, A., Molnár, F., Severson, M.J., Hauck, S.A., Raič, S., 2015. Partial Melting Processes and Cu-Ni-PGE Mineralization in the Footwall of the South Kawishiwi Intrusion at the Spruce Road Deposit, Duluth Complex, Minnesota. Econ. Geol., 110, 1269-1293.

Bohrson, W.A., Spera, F.J., Ghiorso, M.S., Brown, G.A., Creamer, J.B., Mayfield, A., 2014. Thermodynamic Model for Energy-Constrained Open-System Evolution of Crustal Magma Bodies Undergoing

Simultaneous Recharge, Assimilation and Crystallization: the Magma Chamber Simulator. J. Petrol., 55, 1685-1717.

DePaolo, D.J., 1981. Trace element and isotopic effects of combined wallrock assimilation and fractional crystallization. Earth Planet. Sci. Lett., 53, 189-202.

Iljina, M., Hanski, E., 2005. Layered mafic intrusions of the Tornio–Näränkävaara belt. In: Lehtinen, M., Nurmi, P.A., Rämö, O.T. (Eds.), Precambrian Geology of Finland – Key to the Evolution of the Fennoscandian Shield. Elsevier B.V., Amsterdam, 101-138.

Johnson, T.E., Gibson, R.L., Brown, M., Buick, I.S., Cartwright, I., 2003 Partial Melting of Metapelitic Rocks Beneath the Bushveld Complex, South Africa. J. Petrol., 44, 789-813.

Luttinen, A.V., Heinonen, J.S., Kurhila, M., Jourdan, F., Mänttäri, I., Vuori, S., Huhma, H., 2015. Depleted mantle-sourced CFB magmatism in the Jurassic Africa-Antarctica rift: petrology and $^{40}Ar/^{39}Ar$ and U/Pb chronology of the Vestfjella dyke swarm, Dronning Maud Land, Antarctica. J Petrol., 56, 919-952.

Queffurus, M., Barnes, S.-J., 2014. Selenium and sulfur concentrations in country rocks from the Duluth complex, Minnesota, USA: implications for formation of the Cu-Ni-PGE sulfides. Econ. Geol., 109, 785-794.

Ripley, E.M., Al-Jassar, T.J., 1987. Sulfur and oxygen isotope studies of melt-country rock interaction, Babbitt Cu-Ni deposit, Duluth Complex, Minnesota. Econ. Geol., 82, 87-107.

Spera, F.J., Bohrson, W.A., 2001. Energy-constrained open-system magmatic processes I: General model and energy-constrained assimilation and fractional crystallization (EC-AFC) formulation. J. Petrol., 42, 999-1018.

Vuori, S.K., 2004. Petrogenesis of the Jurassic gabbroic intrusions of Vestfjella, Dronning Maud Land, Antarctica. Academic Dissertation, University of Helsinki, Gummerus, Saarijärvi, 25 pages.

# Integrated Interpretation of Geophysical Data for Deep Exploration in the Kylylahti Cu-Mining Area, Eastern Finland

S. Heinonen[1], H. Leväniemi[1], P. Sorjonen-Ward[2], A. Kontinen[2] and S. Aatos[2]

[1]Geological Survey of Finland, PL 96, 02151 Espoo, Finland
[2]Geological Survey of Finland, PL 1237, 70211 Kuopio, Finland
E-mail: suvi.heinonen@gtk.fi

The Kylylahti Cu-Au-Zn mine is located in the historical Outokumpu ore district in eastern Finland. We used high resolution reflection seismic profiles imaging the subsurface structures down to depth of 5 km to study the deep exploration potential of the Kylylahti area. A regional interpretation of the seismic data suggest that the peridotite body of Kylylahti has substantial down-plunge extent towards the south. We have interpolated the densities measured in laboratory from drill-core samples to create a 3D-subsurface density distribution grid and compared it with the seismic reflection data and also with the near surface velocity model that was derived from the first arrival times of the seismic data. These data are used to discuss the deep exploration potential of the Kylylahti area.

**Keywords:** seismic reflection, velocity model, reflectivity, density, Kylylahti, Polvijärvi,

## 1. Introduction

In this study, we are investigating the potential for deeply buried extensions of the Outokumpu type Kylylahti copper deposit in eastern Finland (Peltonen et al., 2008), based on high resolution seismic reflection profiles, gravity data and density measurements from drill core samples. The study was conducted as a part of project "Developing Mine Camp Exploration Concepts and Technologies –Brownfield Exploration" (Aatos, 2016 and reference therein). Kylylahti is an ideal test case for geophysical deep exploration, as it has no surface exposure and because of its discovery as a result of structural geology and geophysical exploration targeting (Rekola and Hattula, 1995). Gravity data and seismic reflection profiles provide a regional outline of the Kylylahti formation while the combination of interpolated density distribution and seismic data are used to characterize the subsurface around the Kylylahti deposit.

## 2. Geological background

The Outokumpu Cu-Co-Zn-Ni ore district lies within an extensive tectonostratigraphically distinct package that can be traced for nearly 300 km through eastern Finland and covers an area of about 5400 km$^2$ (Huhma and Huhma, 1970). The Outokumpu ores occur within a rock assemblage comprising serpentinites, gabbros, talc-carbonate schists, Cr-bearing calc-silicate rocks, dolomite and quartz rock; this so-called Outokumpu assemblage is typically distinguishable from the surrounding mica gneisses by geophysical methods because of its distinct and highly variable petrophysical properties.

A network of seismic reflection profiles (Figure 1) was acquired in the Outokumpu area during the HIRE-project (High Resolution Reflection Seismics for Ore Exploration 2007-2010) by Spetsgeofysika for the Geological Survey of Finland. The applied data acquisition, processing and interpretation procedures are presented in Kukkonen et al. (2012). This study mainly utilizes the profile E1 crossing the Kylylahti mine area. These data were collected using explosive sources at 25 or 50 m intervals and receiver group spacing of 12.5 m. Other seismic profiles were collected with vibroseismic source and are used to illustrate the regional structural framework of the Kylylahti deposit.

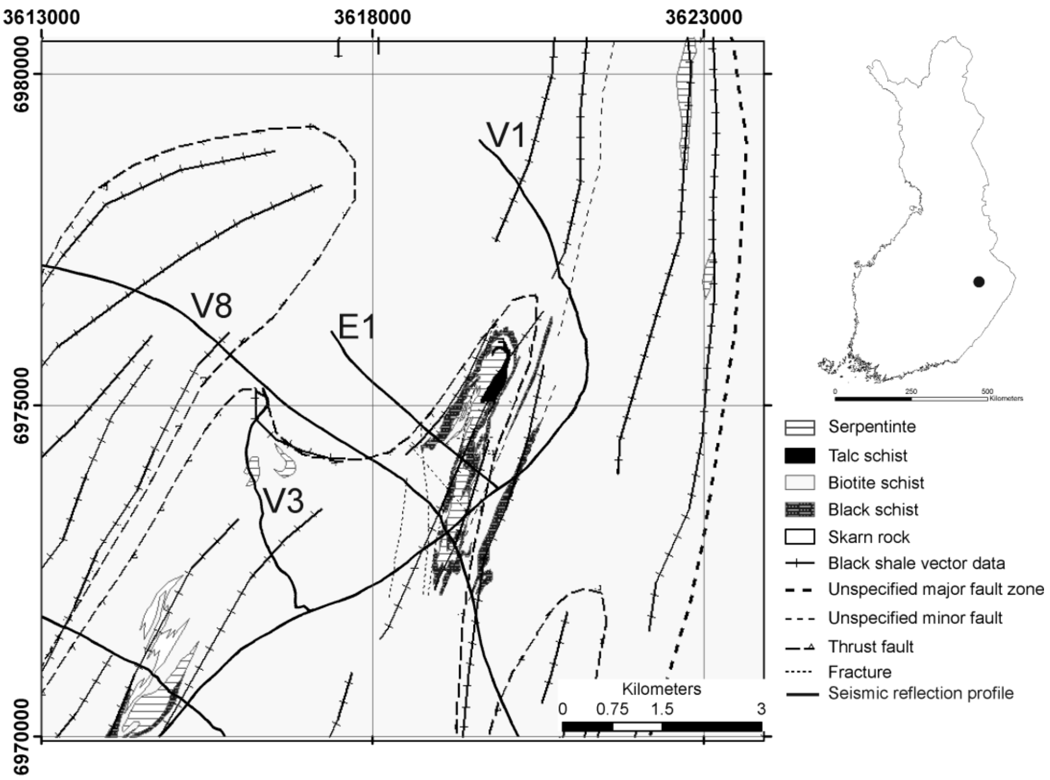


**Figure 4**.HIRE-seismic reflection profiles on a geological map of Polvijärvi area.Map modified from Bedrock map: Digital Bedrock Map Database of Finland (Bedrock of Finland − DigiKP).

In addition to the deep penetrating seismic data, this study utilizes the laboratory density measurements of 12859 drill core samples from the Kylylahti mining camp. The subsurface location of each sample is known and densities were interpolated inside of a 3D grid covering the study volume. The density measurements are also used to constrain the inversion of the gravity data measured in the area.

**3. Data interpretation**

Based on the seismic data and previous geological observations, Kylylahti can be modelled as a part of a wedge shaped body of originally dominantly mantle peridotites thrust and folded within a package of metasediments and bound by curved faults. The Kylylahti body is characterized with prominent but discontinuous reflectivity and it is internally faulted, as suggested for example by Saalman and Laine (2014). Seismic images suggest that the Kylylahti body has substantial down plunge extent towards the south and below the current mine. However, on the seismic profile E1 the inversion of the ground gravity data constrained with the densities measured from drill-core samples does not indicate existence of considerable masses below the depth extent of the current drilling. Inversion results become more ambiguous towards the south-west of the known deposit because of lack of drill hole constraints but results indicate existence of high density rock masses underneath the intersection between seismic profiles V8 and V1. This predicted extension of Kylylahti body should have continued sulphide potential due to the apparent continuation of favourable reflective rock types and deep penetrating faults that could have controlled mobilization of sulfides during the final stages of the ore formation process.

First breaks of the seismic reflection data were used to create a refraction seismic model of the subsurface velocity distribution along the profile E1 in the vicinity of the Kylylahti mine area. The model consisted of two layers, the first corresponding to the overburden and the second to the uppermost, weathered and fractured bedrock, beneath which the velocities represent fresh bedrock. Seismic velocities were allowed to vary laterally within the layers and were iterated simultaneously with layer thickness.

We used the densities measured in laboratory from drill-core samples to create a 3D-subsurface density distribution grid (cell size 50 x 50 x 10 m). Interpolation was done inside an ellipsoidal volume with dimensions 15 0x 150 x 50 m, dip direction of 90° and dip of 30°. These parameters were chosen based on the general direction of reflectivity.

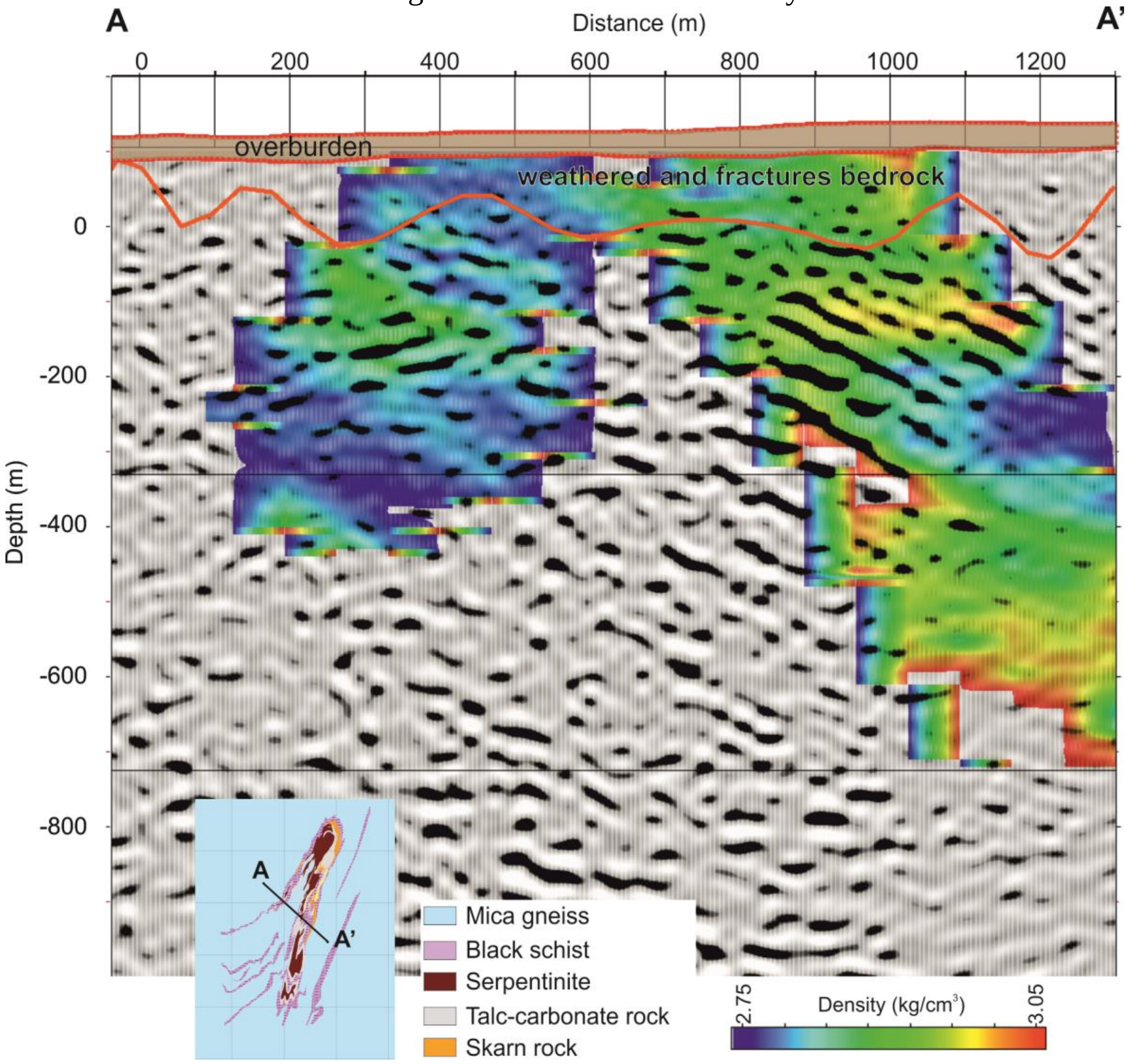


**Figure 2.** Comparison of the near surface velocity model, interpolated density distribution and seismic reflectivity along the seismic profile E1 in the vicinity of the Kylylahti mine.

Comparison of the resolved layer shapes from the refraction seismic model with the reflection profile shows that similar trends are observable from the reflections and the base of the layer representing weathered and fractured bedrock (Figure 3). Moreover, the interpolated density distribution is also compatible with the shape of the base of the weathered rock layer. High density values correlate particularly well with high amplitude reflections at 100-500 m depth and density is uniformly low (< 2.85 g/cm$^3$) in the areas where high amplitude reflections disappear,. These observations are consistent with the overall properties of the Outokumpu assemblage hosting the ore in the region: the overall density is higher than that of the surrounding mica schists, and the assemblage is internally highly heterogeneous and thus strongly reflective (Kukkonen et al., 2012).

**4. Discussion and conclusions**

Based on the interpretation of seismic reflection data presented, the serpentinized peridotite-dominated unit hosting the Kylylahti massive sulphide deposit appears to continue to several kilometres depth in the south of the current mine. Strong discontinuous reflections are present at the deeper levels (~500 m) of the eastern part of the Kylylahti body and thus it is likely that the prospective Kylylahti rock types extend in these areas underneath the mica gneiss cover. High density zones interpolated from the drill hole data coincide with strong reflectors, while areas of uniformly low density are characterized by lack of reflectivity. The integrated interpretation of different geophysical data presented here encourages the future deep exploration efforts in the area.

**Acknowledgements**

Boliden Kylylahti Oy is thanked for permission to publish these data. Members of the working group of "Developing Mine Camp Exploration Concepts and Technologies – Brownfield Exploration" –project from Geological Survey of Finland, University of Helsinki and industrial partners are thanked for their contribution during the project. This project has received funding from TEKES.

**References**

Aatos, S. (ed.) 2016. Developing Mining Camp Exploration Concepts and Technologies – Brownfield Exploration Project 2013–2016. Geological Survey of Finland, Special Paper 59, 214 pages, 141 figures, 16 tables. In press.Huhma, A. and Huhma, M., 1970. Contribution to the geology and geochemistry of the Outokumpu region. Bulletin of Geological Society of Finland 42, 57-88.

Kukkonen, I.T., Heinonen, S., Heikkinen, P.J. and Sorjonen-Ward, P., 2012. Delineating ophiolite-derived host rocks of massive sulfide Cu-Co-Zn deposits with 2D high-resolution seismic reflection data in Outokumpu, Finland. Geophysics, 77, p. WC213-WC222.

Peltonen, P., Kontinen, A., Huhma, H., and Kuronen, U., 2008. Outokumpu revisited: New mineral deposit model for the mantle peridotite-associated Cu-Co-Zn-Ni-Ag-Au sulphide deposits. Ore Geology Reviews 33, 559-617.

Rekola, T. and Hattula, A., 1995. Geophysical surveys for strata-bound Outokumpu-type Cu-Co-Zn deposits at Kylylahti, Eastern Finland. Exploration Geophysics 26, p. 60-65.

Saalmann, K. and Laine, E.L., 2014. Structure of the Outokumpu ore district and ophiolite-hosted Cu-Co-Zn-Ni-Ag-Au sulfide deposit revealed from 3D modeling and 2D high-resolution seismic reflection data. Ore Geology Reviews 62, p. 156-180.

# Isotope results from Utsjoki-Inari area

H. Huhma

Geological Survey of Finland. P.O.Box 96, FI-02151 Espoo, Finland
E-mail: hannu.huhma@gtk.fi

Abundant isotopic data have been obtained from the Inari-Utsjoki area since 1970's. Many old age results have been recently confirmed by spot analyses. These together with Sm-Nd and geochemical data suggest that new juvenile crust with arc affinities was formed in the Utsjoki area ca. 1.91-1.94 Ga ago. The results on the Archaean Lake Inari area show strong metamorphic effects at ca. 1.9 Ga.

**Keywords:** Finland, Lapland-Kola Province, juvenile crust, U-Pb, Sm-Nd, Pb-Pb

## 1. Introduction

The understanding of the geological evolution of the Lapland-Kola Province in Finland is largely based on the comprehensive isotopic studies (U-Pb, Pb-Pb and Rb-Sr) performed at the GTK in early seventies. Main results were reported by Meriläinen (1976), but no isotopic data were included in the paper. Recent studies using U-Pb spot analyses on zircon have largely confirmed the old findings but together with Sm-Nd results also introduced new views on the topic. Relevant results from the Lapland granulite belt were published by Tuisku & Huhma (2006) and Tuisku et al. (2012), but data from other areas have remained unpublished.

## 2. Old results

The results obtained 40 years ago using U-Pb on zircon, titanite and monazite include:

- The Archaean Inari gneisses have zircon age estimates 2.5-2.7 Ga, whereas titanites in these samples are ca. 1.9 Ga. This is exceptional within the Archaean granitoids in Finland and suggests a strong 1.9 Ga thermal overprinting on the Archaean crust NE of the granulite belt. In contrast, titanite in an Archaean rock on the southern side of the granulite belt is Archaean.
- Quartz dioritic gneisses in Utsjoki, east of the granulite belt (Kuorboaivi belt) provide zircon age estimates of ca. 1.93 Ga (mostly one discordant analysis/ sample). No indications of Archaean ages are found within this area.
- In the Lapland granulite belt meta-igneous rocks of have zircon ages of 1.91-1.93 Ga, whereas meta-sedimentary rocks provided heterogeneous zircon populations with Pb/Pb ages of 2.0-2.15 Ga; monazites are ca. 1.91 Ga.

The Pb-Pb data on whole rocks and K-feldspar suggested that:

- The whole rock Pb-Pb age on the Archaean gneisses is ca. 2.6 Ga, whereas K-feldspars in these rocks register Palaeoproterozoic Pb isotopic compositions (Figure 1). The K-feldspar analyses provide a trend on Pb-Pb diagram with a slope of 0.301. If T2 is 1.9 Ga (age of resetting) the slope yields T1=2.6 Ga (primary age). Individual K-feldspar whole rock pairs give ages of ca. 1.9 Ga. These results suggest a strong 1.9 Ga thermal influence on the Archaean crust.
- The whole rock K-feldspar age estimate for the "1.93 Ga" (Kuorboaivi) rocks is 1.96 ± 0.14 Ga. The initial Pb isotopic composition suggests a juvenile Proterozoic source.

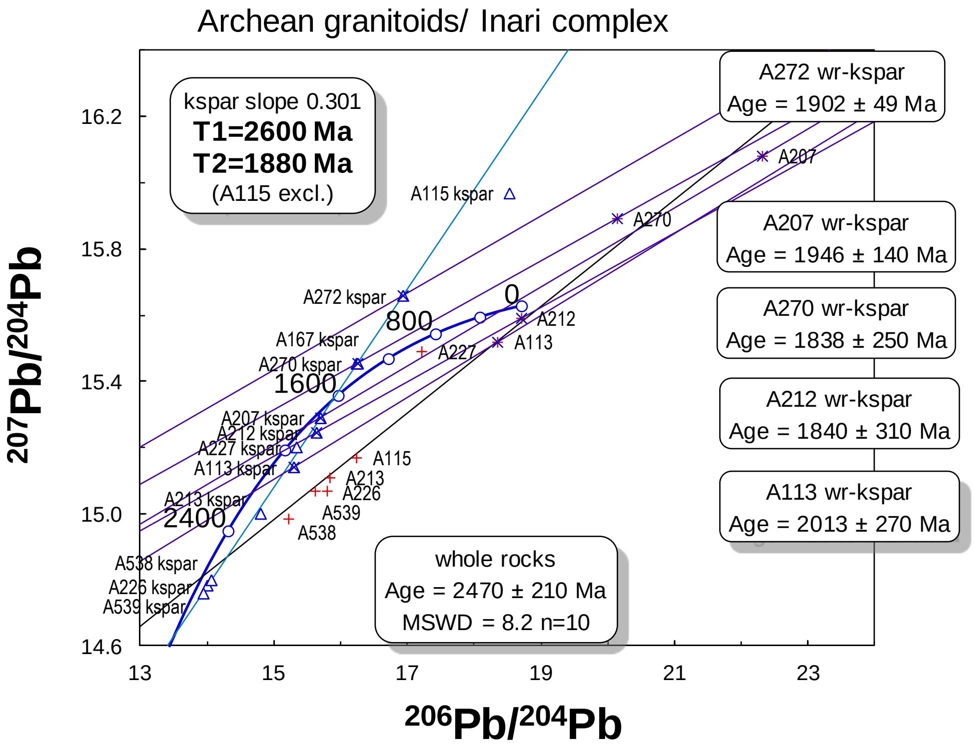


Figure 1. Pb-Pb isotope results from the Archaean gneisses in the Lake Inari area.

**3. Updated results**

The old TIMS ages of 1.91-1.93 Ga from the meta-igneous rocks of the Lapland granulite belt have been confirmed by SIMS analyses. The results from migmatitic granulites showed that detrital zircons were mostly derived from 1.94-2.1 Ga sources (Tuisku and Huhma 2006; Tuisku et al. 2012). Few Archaean grains were also obtained and as a whole the detrital population shares similarities with the Svecofennian and Upper Kalevian metasediments (e.g. Huhma et al. 1991, Lahtinen et al. 2009, 2010). Constraints for the metamorphic evolution are provided by ca. 1.91 Ga monazite, ca. 1.90-1.88 Ga zircon and 1.89-1.88 Ga Sm-Nd garnet-whole rock ages.

Recent U-Pb spot analyses on zircon using LA-ICPMS have confirmed ages of 1.94-1.91 Ga for several granitoids in Utsjoki, east of granulite belt ("Kuorboaivi belt", Figure 2), as well as Archaean ages for some gneisses in the lake Inari area. Few samples between these two domains seem to contain zircons with ages of ca. 2.5 Ga. Interestingly, such ages using LA-ICPMS have also been obtained from the S-SW side of the granulite belt.

The Sm-Nd analyses on ca. 70 whole rock samples from the Lapland-Kola Province provide information of crustal sources. Together with geochemical data they show that the 1.91-1.94 Ga magmatism east of the granulite belt in Utsjoki is largely juvenile with arc affinities (Figures 3, 4), thus confirming the early speculations (Huhma 1996, Svekalapko workshop, Lammi, Finland; Barling, Marker and Brewer, 1996, Proterozoic Evolution in the North Atlantic Realm, Goose Bay conference; Daly et al. 2006).

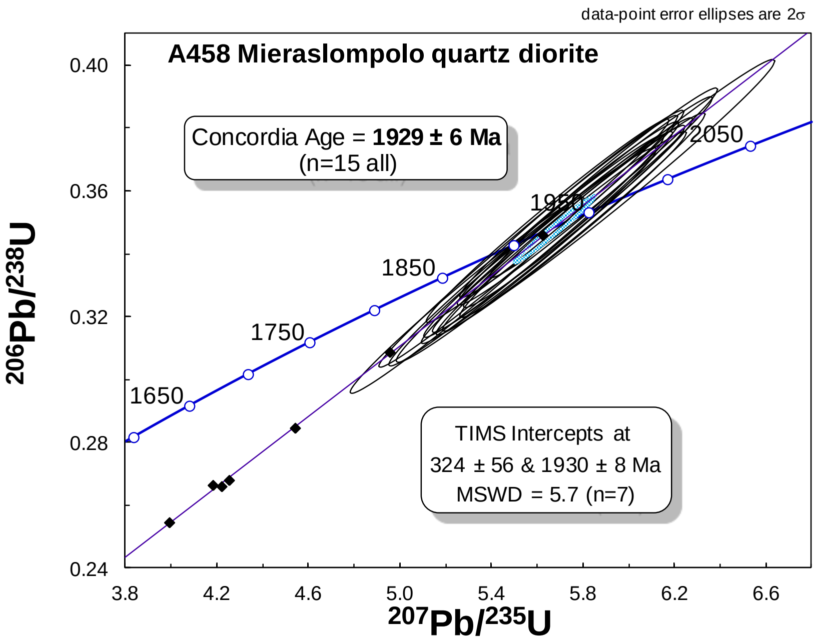


Figure 2. Concordia diagram showing U-Pb analyses on zircon by TIMS (dots) and LA-MCICPMS (error ellipses).

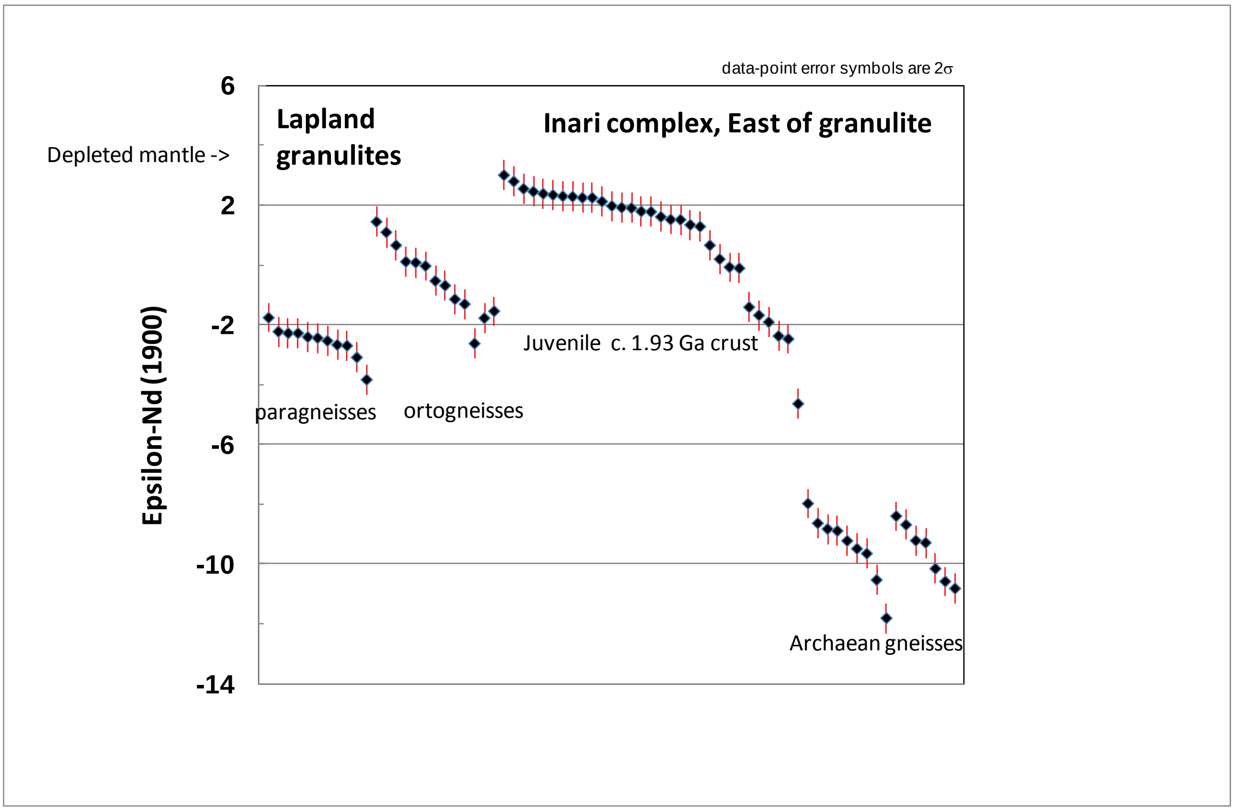


Figure 3. Epsilon-Nd (1900) for whole rock samples from the Utsjoki-Inari area.

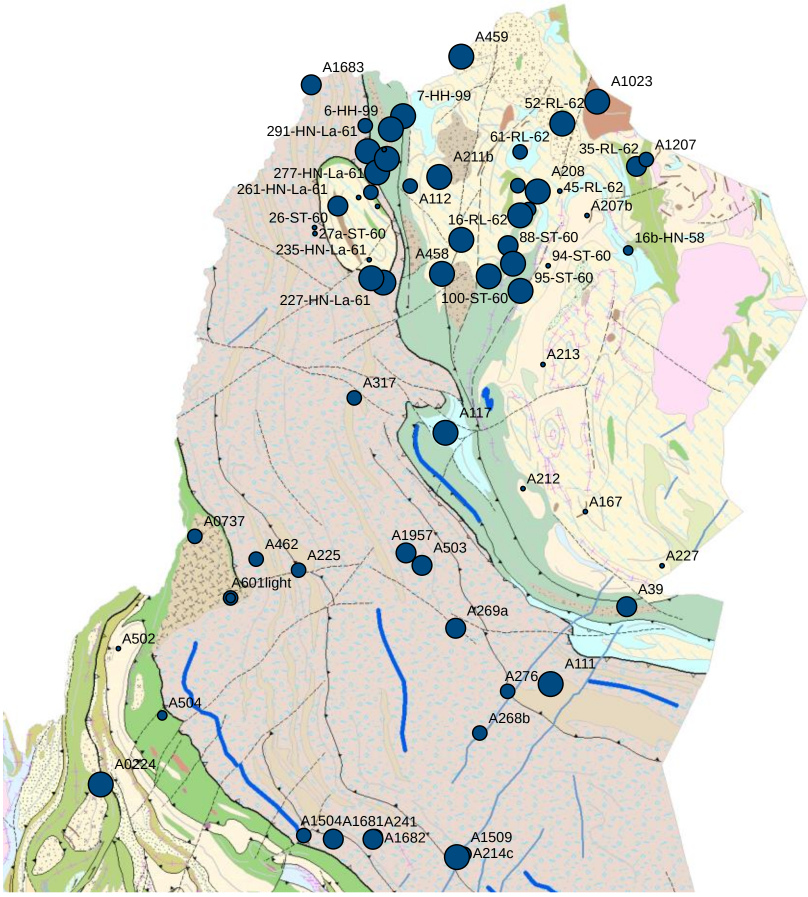


Figure 4. Geological map showing epsilon-Nd (1900) in five categories: largest symbols €-Nd>+0.6, smallest symbol (dot) €-Nd<-7.9.

## 3. References


Daly, J.S., Balagansky, V.V., Timmerman, M.J. and Whitehouse, M.J. 2006. The Lapland-Kola Orogen; Palaeoproterozoic collision and accretion of the northern Fennoscandian lithosphere. In: European lithosphere dynamics. Edited by D.G. Gee and R.A. Stephenson. Memoirs of the Geological Society of London, 32, pp. 579-598.

Huhma, H.; Claesson, S.; Kinny, P. D.; Williams, I. S. 1991. The growth of Early Proterozoic crust: new evidence from Svecofennian detrital zircons. Terra nova 3 (2), 175-178.

Lahtinen, R., Huhma, H., Kähkönen, Y. and Mänttäri, I., 2009. Paleoproterozoic sediment recycling during multiphase orogenic evolution in Fennoscandia, the Tampere and Pirkanmaa belts, Finland. Precambrian Research 174, 310-336.

Lahtinen, R., Huhma, H., Kohonen, J., Kontinen, A. & Sorjonen-Ward, P., 2010. New constraints for the source characteristics, deposition and age of the 2.1-1.9 Ga metasedimentary cover at the western margin of the Karelian Province. Precambrian Research 176, 77–93.

Meriläinen, K., 1976. The granulite complex and adjacent rocks in Lapland, northern Finland. Geological Survey of Finland, Bulletin 281, 1-129.

Tuisku, P. and Huhma, H., 2006. Evolution of Migmatitic Granulite Complexes: Implications from Lapland Granulite Belt, Part II: Isotopic dating. Bulletin of the Geological Society of Finland, 78, 143-175.

Tuisku, P., Huhma, H. & Whitehouse, M. 2012. Geochronology and geochemistry of the enderbite series in the Lapland Granulite Belt: generation, tectonic setting and correlation of the belt. Canadian Journal of Earth Sciences, 49, 1297-1315.

# Data mining to discover the causes of internal reflectivity within the Ni-Cu-PGE-bearing Kevitsa intrusion

N. Junno[1], E. Koivisto[1], I. Kukkonen[2], A. Malehmir[3] and C. Wijns[4]

[1]Department of Geosciences and Geography, University of Helsinki
[2]Department of Physics, University of Helsinki
[3]Department of Earth Sciences, Uppsala University
[4]First Quantum Minerals Ltd.
E-mail: niina.junno@helsinki.fi

The Kevitsa Ni-Cu-PGE disseminated sulphide deposit is hosted by the Kevitsa mafic to ultramafic intrusion, located within the Central Lapland Greenstone Belt in northern Finland. A 3D seismic reflection survey was conducted in Kevitsa in 2010 for mine planning and deep mineral exploration purposes. Within the Kevitsa resource area, the 3D seismic data are characterized by laterally continuous reflections. Here we use data mining, namely Self-Organizing Map (SOM), analysis to better understand the possible causes of reflectivity within the Kevitsa intrusion. The results show that the mineralized zones within the intrusion could be potential causes of reflectivity, and hence could set potential exploration targets in the area.

**Keywords:** data mining, reflection seismic data, exploration, self-organizing maps (SOM)

## 1. Introduction

Data mining approaches, such as Self-Organizing Maps (SOM), can be used for objective analysis of the complex and sparse geophysical and geological data sets typical for mining camps, to better understand the underlying linear and non-linear relationships between the different data. The SOM analysis (Kohonen, 2001) is based on vector quantization and measures of vector similarity. It is unsupervised, so no prior knowledge is required on the nature or number of clusters within the data. The underlying statistical relationships between different data are visualized with 2D maps that make the interpretation of the multidimensional, complex data possible. The main objective of this study was to use the SOM analysis to better understand the potential causes of observed internal reflectivity in the 3D seismic reflection data within the Kevitsa intrusion, and its relationship to the disseminated Ni-Cu-PGE-bearing sulphide mineralization.

## 2. Background and motivation of the study

The Kevitsa Ni-Cu-PGE deposit is hosted by the Kevitsa mafic-ultramafic intrusion located within the Central Lapland Greenstone Belt in northern Finland (Figure 1). The Kevitsa open-pit mine started in 2012 and is currently operated by Boliden. The mine was operated by First Quantum Minerals Ltd. until June 2016. It has been suggested (e.g. Standing et al., 2009) that the extent of economic mineralization is controlled by the extent of smaller-scale, laterally discontinuous and internally differentiated magma pulses that represent a spectrum of olivine pyroxenites consisting of plagioclase and orthopyroxenite rich tops that gradationally change into more olivine and clinopyroxenite rich bottoms. The mineralogical change within an individual pulse is gradational, meaning that no internal boundaries exist within a pulse, but the base of one pulse will grade relatively sharply into the top of another pulse. The mineralization is more strongly associated with the bases of these individual magma pulses.

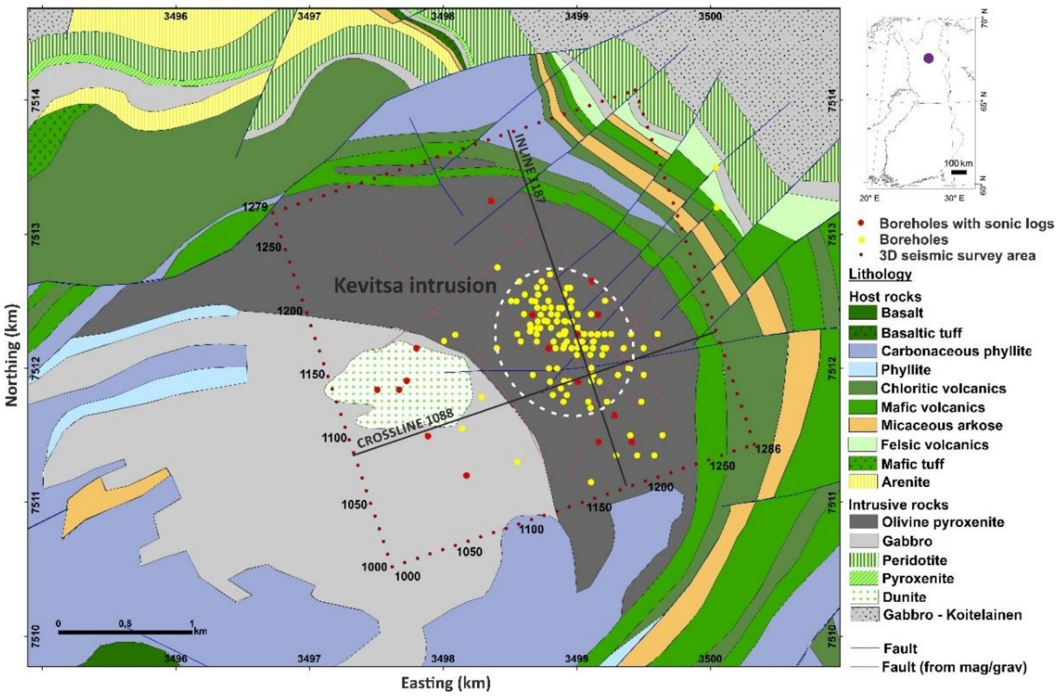


**Figure 1.** Geological map of the Kevitsa area. Location of the open-pit in dashed white line.

A 3D seismic reflection survey was conducted in Kevitsa in 2010 for mine planning and deep mineral exploration purposes (Malehmir et al., 2012; 2014). The 3D seismic survey area, corresponding to about 9 km$^2$, is located over the Kevitsa resource area (Figure 1). In earlier studies (Malehmir et al., 2012; 2014; Koivisto et al., 2015), laterally continuous reflections were observed in the 3D seismic data within a constrained area inside the Kevitsa intrusion (Figure 2). It was suggested that this internal reflectivity originates from the contacts between the tops and bottoms of the individual magma pulses controlling the extent of the main economic mineralization. On average, the physical properties of the olivine pyroxenite variants constituting the tops and bottoms of these magma pulses differ enough to produce detectable reflections (e.g., Koivisto et al., 2015). However, the interpretation is not fully supported by the borehole data and therefore, requires further research.

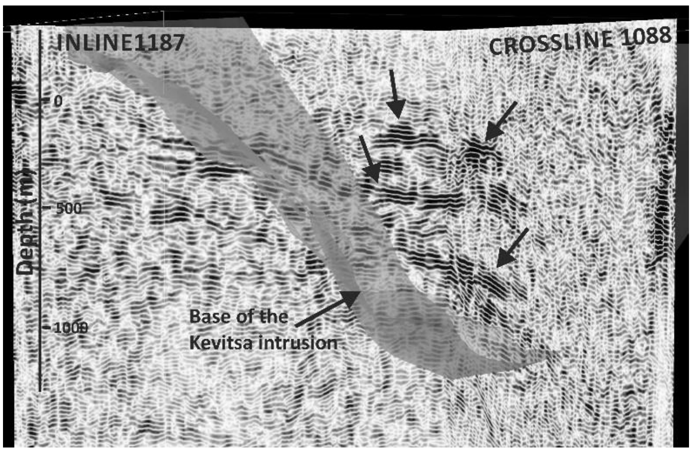


**Figure 2.** Observed internal reflectivity in the 3D seismic reflection data (Malehmir et al., 2012) within the Kevitsa intrusion. See location of inline 1187 and crossline 1088 from Figure 1. Sections viewed from northwest.

**3. Method**

In this study, data mining, namely the SOM analysis with SiroSOM (Kohonen, 2001; *SiroSOM*: Fraser and Dickson, 2007), is used to better understand the origin of internal reflectivity observed in the 3D seismic reflection data within the Kevitsa intrusion and its relationship to the Kevitsa Ni-Cu-PGE deposit. At this stage, only borehole data was used to conduct the analyses. In the SOM, the clustering of the complex multidimensional (nD) input data is represented by node vectors that are trained in an unsupervised learning process, based on vector quantization and the measures of vector similarity. Regression is used to map these node vectors from nD to 2D maps. This process preserves the topology of the node vectors. The underlying statistical relationships between different data are visualized with the help of these 2D maps that make the interpretation of the complex multidimensional data possible.

**4. Results**

The results show that the contacts between the tops and bottoms of the suggested magma pulses do not alone fully explain the observed internal reflectivity within the Kevitsa 3D seismic reflection data (Figures 2 and 3). This is partly because in the Kevitsa borehole data there are not enough samples of the plagioclase and orthopyroxenite rich olivine pyroxenite variant to comprehensively determine the physical properties of the tops of the suggested magma pulses, and map the overall extent. This could partially be attributed to the possible dunitic magma contamination that has resulted in more olivine and clinopyroxenite rich magmas, thus overprinting the extent of the plagioclase and orthopyroxenite rich variants. Most interesting finding in the SOM results is the division of olivine pyroxenite into a lower and higher seismic velocity group (Figure 3), which seem to differ enough to produce detectable reflections (Figures 4). It seems that the mineralization associated with the olivine pyroxenite lowers the seismic velocity, while densities remain about the same, resulting in necessary acoustic impedance difference. The main ore-bearing sulphide minerals in Kevitsa are pyrrhotite, pentlandite and chalcopyrite that tend to lower the seismic velocities of the hosting silicate rocks.

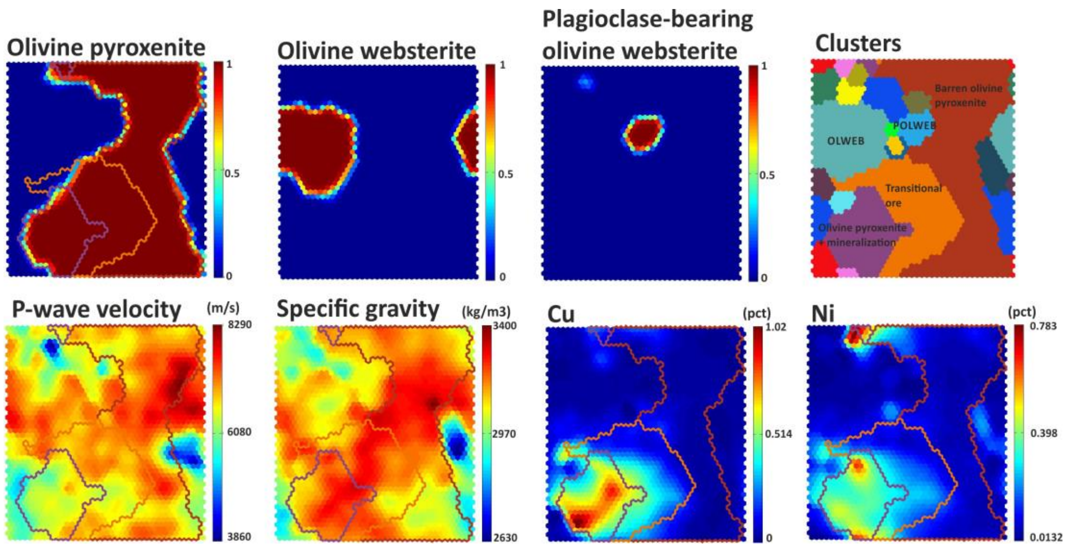


**Figure 3.** Component plots showing possible causes of reflectivity within the Kevitsa intrusion. The most interesting finding is the lower seismic velocity area that exists within the olivine pyroxenite unit associated with the mineralization (highest Cu and Ni) that makes the olivine pyroxenite itself internally reflective.

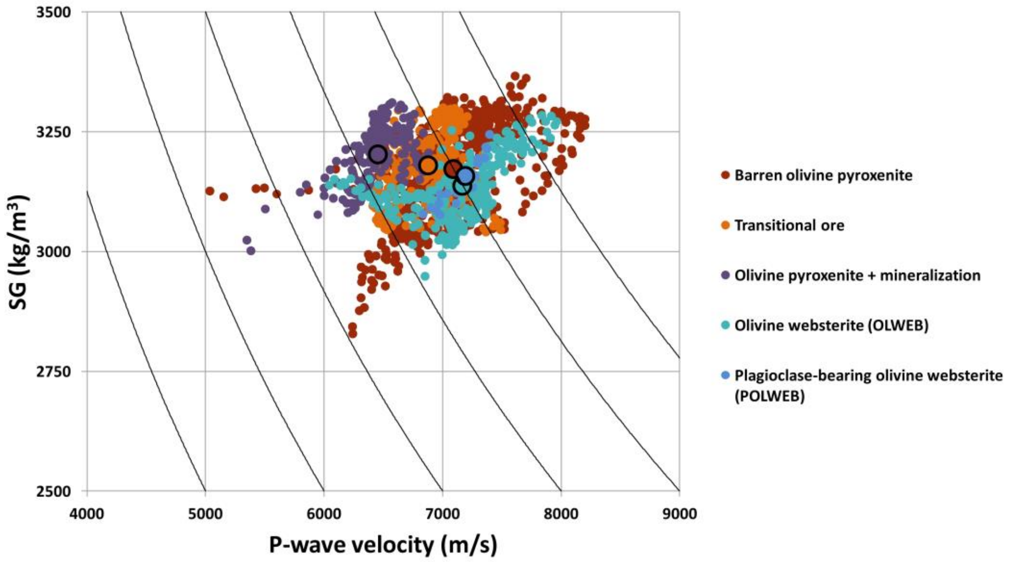


**Figure 4.** P-wave velocity versus specific gravity (SG) plot for different clusters showing that on average (larger black circled dots) the barren olivine pyroxenite group (maroon) has higher seismic velocity than the olivine pyroxenite group with mineralization (purple). Density does not seem to differ much at all (similar range of densities defines all the groups) resulting in acoustic impedance difference that is enough to produce a detectable reflection.

## 5. Conclusions

The contacts between the tops and bottoms of the suggested magma pulses do not alone fully explain the observed internal reflectivity in the 3D seismic data within the Kevitsa intrusion. The mineralized zones within the intrusion could be potential causes of the observed internal reflectivity, and hence could set potential exploration targets in the area.

## 6. Acknowledgements

This work has been funded through a grant from the K. H. Renlund's Foundation. First Quantum Minerals Ltd. provided the seismic and borehole data used in this study.

## References:

Fraser, S. and Dickson, B.L. 2007. A New Method for Data Integration and Integrated Data Interpretation: Self-Organizing Maps. In *Proceedings of Exploration 07: 5th Decennial International Conference on Mineral Exploration* (ed. Milkereit, B.), p. 907-910.

Kohonen, T. 2001. Self-Organizing Maps, 3rd Edition. *Series in Information Sciences* 30, 501 pp. Springer, New York.

Koivisto, E., Malehmir, A., Hellqvist, N., Voipio, T. and Wijns, C. 2015. Building a 3D model of lithological contacts and near-mine structures in the Kevitsa mining and exploration site, northern Finland. *Geophysical Prospecting* 63, p. 754–773.

Malehmir, A., Juhlin, C., Wijns, C., Urosevic, M., Valasti, P. and Koivisto, E. 2012. 3D reflection seismic imaging for open-pit mine planning and deep exploration in the Kevitsa Ni-Cu- PGE deposit, northern Finland. *Geophysics* 77 (5), p. WC95-WC108.

Malehmir, A., Koivisto, E., Manzi, M., Cheraghi, S., Durrheim, R.J., Bellefleur, G., Wijns, C., Hein, K.A.A. and King, N. 2014. A review of reflection seismic investigations in three major metallogenic regions: The Kevitsa Ni-Cu-PGE (Finland), Witwatersrand goldfields (South Africa), and the Bathurst Mining Camp (Canada). *Ore Geology Reviews* 56, p. 423-441.

Standing, J., De Luca, K., Outwhite, M., Lappalainen, M., Wijns, C., Jones, S. et al. 2009. Report and Recommendations from the Kevitsa Campaign, Finland. *Confidential Report to First Quantum Minerals Ltd.*, pp. 125. Jigsaw Geosciences Pty Ltd., West Perth, Australia.

# Post-kinematic mafic dykes in southern part of Central Svecofennia, Finland

J. Kara[1], M. Väisänen[1], Y. Lahaye[2] and H. O'Brien[2]

[1] Department of Geography and Geology, University of Turku, FI-20014 Turku, Finland
[2] Geological Survey of Finland, P.O. Box 96, FI-02151 Espoo, Finland
E-mail: jkmkar@utu.fi

The geochemical composition of seven post-kinematic mafic dykes in southern part of Central Svecofennia have been studied. Two dykes have been selected for in situ zircon U-Pb geochronology and one for in situ zircon Lu-Hf isotope analysis. These c. 1.86 Ga dykes can be divided into two subgroups by their geochemical characteristics: i) an enriched type with Nb contents up to 42 ppm, high contents of certain fluid mobile elements such as F, Ba, Sr, $K_2O$ and LREE and elevated contents of $Fe_2O_3$, $Ti_2O$ and $P_2O_5$, and ii) a primitive type with high MgO and Cr content. The primitive dyke exhibit positive, average c. +3, initial εHf values. The geochemical data combined with the petrological and the field observations suggest that the dykes are juvenile and derived from a subduction-enriched mantle source in a within-plate environment during the post-kinematic stage of the Svecofennian orogeny.

**Keywords:** Svecofennian orogeny, Lu-Hf, U-Pb, geochemistry, mafic dykes

## 1. Introduction

The Svecofennian orogen in southern Finland is proposed to consist of two terranes: Central Svecofennia (CS) in the north and Southern Svecofennia (SS) in the south (Korsman et al. 1997; Figure 1a). Central Svecofennia is characterized by the large Central Finland Granitoid Complex (CFGC) in the north, followed by the volcanic arc-type Tampere schist belt (TSB) on its southern fringe (Kähkönen 2005). South of the TSB is the Pirkanmaa migmatite belt (PB), metamorphosed at c. 1.88 Ga (Mouri et al. 1999). Southern Svecofennia consists of two separate volcanic arc-type belts, the Häme (HB) and Uusimaa (UB) belts (Kähkönen 2005; Figure 1b). Southern Svecofennia is characterised by the late-Svecofennian high heat flow and production of granites and migmatites, which formed the Late Svecofennian Granite Migmatite zone (LSGM) at c. 1.84-1.81 Ga (Ehlers et al. 1993, Väisänen et al. 2002, Mouri et al. 2005).

The age difference in metamorphic processes between Central Svecofennia and Southern Svecofennia is evident indicating different tectonic processes within a short distance. In this study, we present petrological, geochemical, zircon U-Pb and Lu-Hf isotope data from mafic dykes cross-cutting the Pirkanmaa migmatites, a few kilometres north of the proposed terrane boundary, in order to evaluate their petrogenesis and tectonic significance. We also compare these dykes with a dyke of the same age in Southern Svecofennia.

## 2. Geological setting

The study area straddles the proposed terrane boundary between Central Svecofennia and Southern Svecofennia (Figure 1b). The northern part of the study area, belonging to Central Svecofennia, consists of the PB high-grade sedimentary rocks (Mouri et al. 1999, Kähkönen 2005; Figure 1b). The PB is characterised by migmatized psammitic supracrustal rocks and gneisses of a turbiditic origin (Kähkönen 2005) but it also includes some mafic to ultramafic volcanic rocks with MORB to WPL affinities (Peltonen 1995) and various synorogenic granitoids (Mouri et al. 1999). It has been interpreted to represent the forearc sediments of a volcanic arc complex (Lahtinen 1996, Kähkönen 2005).

The southern part of the study area consists of the c. 1.88 Ga HB comprising mafic, intermediate and felsic volcanic and plutonic rocks (Vaasjoki 1994, Nironen 1999, Kähkönen 2005, Saalmann et al. 2009). The volcanics are well-preserved and have been metamorphosed at amphibolite facies. The HB is considered to have formed in a subduction-related volcanic arc setting and the volcanic rocks show mature volcanic arc affinities (Hakkarainen 1994, Lahtinen 1996, Kähkönen 2005).

In between the terranes is a proposed terrane boundary that is not straightforwardly observable in the field (Korsman et al. 1997, Sipilä et al. 2011). Within the study area the boundary is demarcated by various syn to post-kinematic granitoids and an E-W trending shear zone.

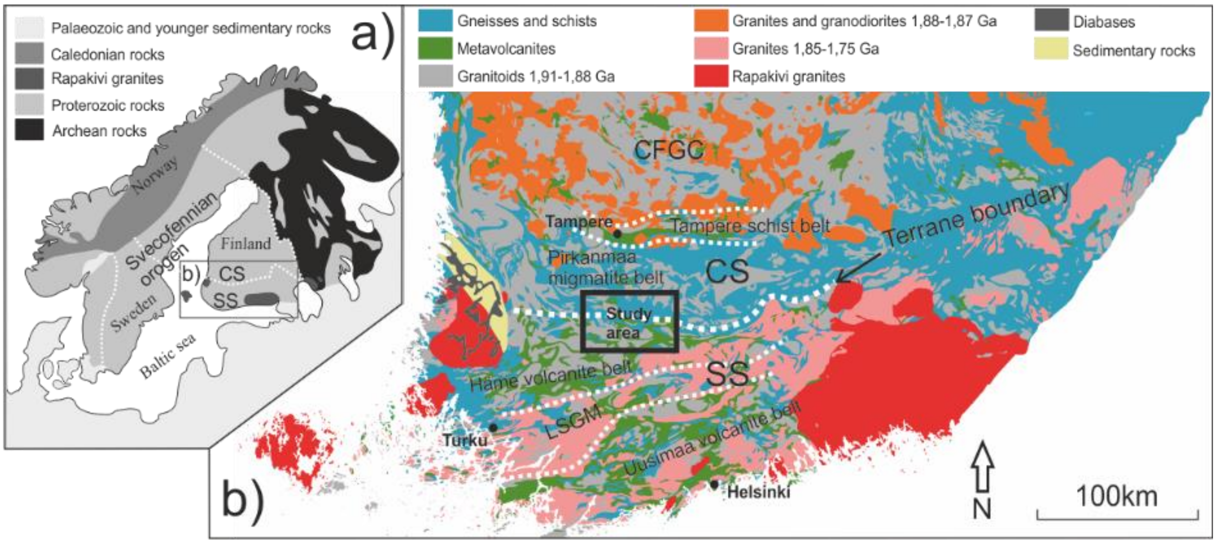


**Figure 5.** a) Geological overview of the Fennoscandian shield, modified after Koistinen et al. (2001). b) Lithological map of southern Finland, modified after Kallioperä - Bedrock of Finland 1:200 000. The study area is indicated by a black rectangle. See text for abbreviations.

## 3. Petrology and geochemistry of the mafic dykes

The dykes occur as elongated intrusions a few to tens of metres wide and tens to hundreds of metres long which cut the migmatisized metasedimentary country rocks in the NWW-SEE direction with an apparent gentle NNE dip. The country rock is partially melted on the upper contact of the mafic dyke and the veins of tonalitic leucosome cut the dykes in places. Otherwise the dykes are undeformed and exhibit an ophitic to subophitic texture of plagioclase laths and intergranular hornblende and primary and secondary biotite (Figure 2b and c). Prismatic apatite is the most common accessory phase (Figure 2d) with minor pyroxene. The grain size ranges from a rapidly cooled fine-grained contact zones (Figure 2b) to slowly cooled medium-grained interiors (Figure 2c).

Geochemically the dykes can be divided into two subgroups, although they share some common features. The first group is characterized by Nb, F, Ba, Sr and LREE enrichment, and show elevated $Fe_2O_3$, $K_2O$, $P_2O_5$ and $Ti_2O$ contents. In the TAS diagram this group is classified as monzogabbro and the $K_2O$ content shows a shoshonitic composition. The second group, a gabbro in the TAS diagram, is calc-alkaline and exhibits a more primitive nature by higher MgO and Cr contents but also shows slightly elevated $Ti_2O$, and F values. Both groups show distinct subduction zone characteristics with LILE enrichment and Nb and Ta depletion in the NMORB normalized multielement diagram. However, the overall trace element concentrations are higher in the enriched type, especially the Nb and Ta contents.

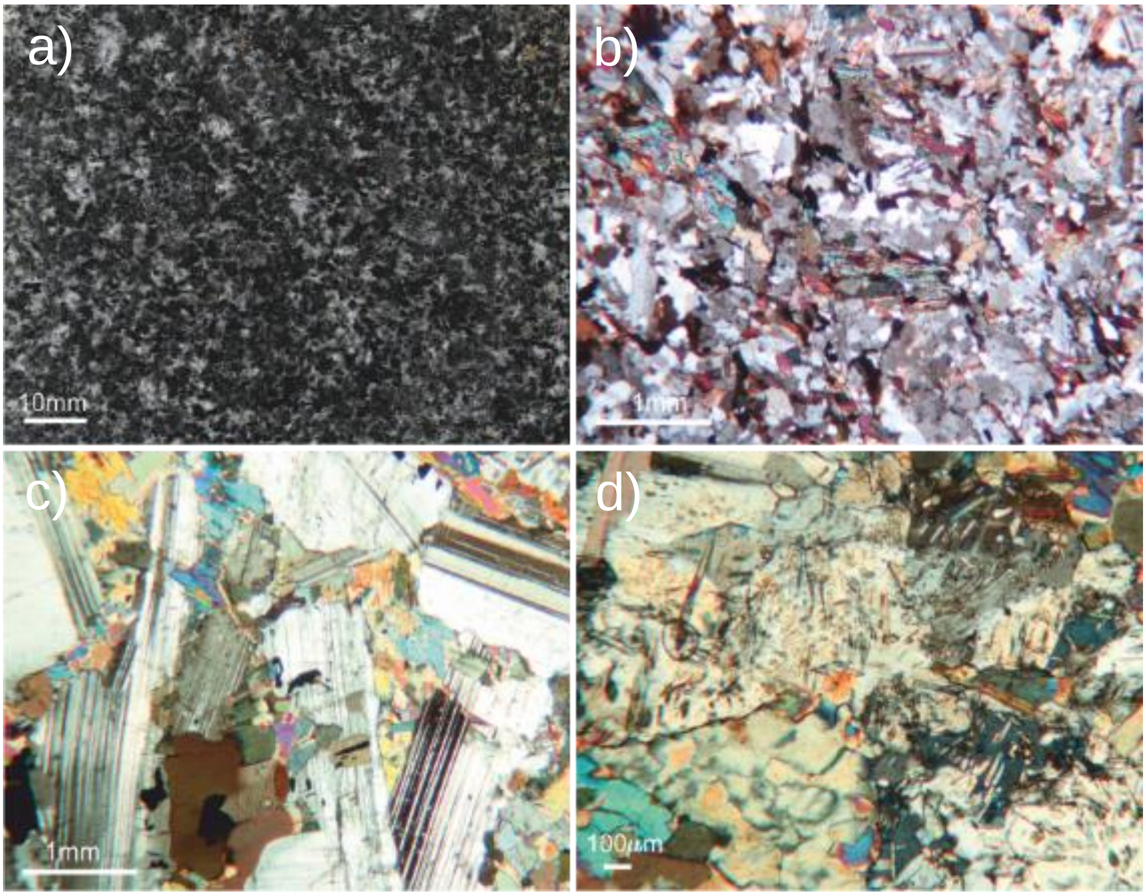


**Figure 6.** a) A photograph from a cut surface of a medium-grained dyke. Photomicrographs of a thin section from a fine-grained variety (b), medium-grained dyke (c) and apatite inclusions in plagioclase (d).

**4. Isotope characteristics**

The zircon U-Pb ages of two of the dykes, one of each type, were determined by the laser ablation inductively coupled mass spectrometry (LA-ICP-MS) in the Finnish Geoscience Research Laboratory at GTK, Espoo, Finland. A concordia age of c. 1.86 Ga was obtained for both of the dykes. The Lu-Hf isotope composition was determined for one of the primitive dykes on the previously dated zircons using the same LA-ICP-MS facility. 36 analyses on 29 zircons show an average initial $\varepsilon Hf_{(1.86\ Ga)}$ of c. +3.

**5. Discussion and conclusion**

Nevalainen et al. (2014) have described c. 1.86 Ga intra-orogenic enriched monzogabbros from Southern Svecofennia which are deformed in the late Svecofennian stage at c. 1.83 Ga. The mafic dykes of the same age in this study show many similar geochemical features, e.g. LILE, LREE, F, $K_2O$ and $P_2O_5$ enrichment, but lack signs of structural deformation.

Both dyke types in this study show WPL affinities (e.g., Pearce 1982; Schandl and Gorton 2002). However, the magmas have been enriched by a subduction-related metasomatism. According to the Hf isotopes the primitive type is juvenile, although it displays a large variation in initial εHf values. Although the initial eHf values are scattered, its average value indicates a dominantly mantle derived primitive source for these dykes. Whether the dyke types are derived from the same magma source is still unknown.

The field observations, the emplacement age and the geochemical signature support the post-kinematic nature of the dykes. This suggests that cratonization had already started in Central Svecofennia at 1.86 Ga and that the tectonic regime had changed from an active continental margin to a within-plate environment.

**Acknowledgements**
This study was funded by the Finnish Cultural Foundation, the Turku University Foundation and the Finnish Society of Sciences and Letters.

**References:**

Ehlers, C., Lindroos, A., and Selonen, O. 1993. The late Svecofennian granite-migmatite zone of southern Finland—a belt of transpressive deformation and granite emplacement. *Precambrian Research*, *64*, 295-309.

Hakkarainen, G., 1994. Geology and geochemistry of the Hämeenlinna-Somero volcanic belt, southwestern Finland: a Paleoproterozoic island arc. *Geological Survey of Finland, Special Paper 19*, 85-100.

Kallioperä - Bedrock of Finland 1:200 000 [Electronic resource]. *Geological Survey of Finland, Espoo, Finland*. Version 1.0 [Referred 20.9.2016]

Koistinen, T., Stephens, M.B., Bogatchev, V., Nordgulen, Ø., Wennerström, M. and Korhonen, J., 2001. Geological map of the Fennoscandian Shield, scale 1:2 000 000. *Geological Surveys of Finland, Norway and Sweden and the North-West Department of Natural Resources of Russia.*

Korsman, K., Koistinen, T., Kohonen, J., Wennerström, M., Ekdahl, E., Honkamo, M., Idman, H. and Pekkala, Y., 1997. Bedrock map of Finland 1: 1 000 000. *Geological Survey of Finland, Espoo, Finland*.

Kähkönen, Y., 2005. Svecofennian supracrustal rocks. *Developments in Precambrian Geology*, *14*, 343-405.Lahtinen, R., 1996. Geochemistry of Palaeoproterozoic supracrustal and plutonic rocks in the Tampere-Hameenlinna area, southern Finland. *Geological Survey of Finland, 389*, 113 p.

Lahtinen, R., Korja, A. and Nironen, M., 2005. Paleoproterozoic tectonic evolution. In: Lehtinen, M., Nurmi, P.A. and Rämö, O.T. (Eds.), Precambrian Geology of Finland – Key to the Evolution of the Fennoscandian Shield. Elsevier Science B.V., Amsterdam, pp. 481–532.

Mouri, H., Korsman, K. and Huhma, H., 1999. Tectono-metamorphic evolution and timing of the melting processes in the Svecofennian Tonalite-Trondhjemite Migmatite Belt: an example from Luopioinen, Tampere area, southern Finland. *Bulletin of the Geological Society of Finland*, *71,* 31-56.

Mouri, H., Väisänen, M., Huhma, H. and Korsman, K., 2005. Sm-Nd garnet and U-Pb monazite dating of high-grade metamorphism and crustal melting in the West Uusimaa area, southern Finland. *GFF*, *127*, 123-128.

Nevalainen, J., Väisänen, M., Lahaye, Y., Heilimo, E. and Fröjdö, S., 2014. Svecofennian intra-orogenic gabbroic magmatism: a case study from Turku, southwestern Finland. *Bulletin of the Geological Society of Finland*, *86*, 93–112.

Nironen, M., 1999. Structural and magmatic evolution in the Loimaa area, southwestern Finland. *Bulletin of the Geological Society of Finland 71*, 57-71.

Pearce, J.A., 1982. Trace element characteristics of lavas from destructive plate boundaries. *Andesites*, *8*, 525-548.

Peltonen, P., 1995. Petrogenesis of ultramafic rocks in the Vammala Nickel Belt: implications for crustal evolution of the early Proterozoic Svecofennian arc terrane. *Lithos*, *34,* 253-274.

Saalmann, K., Mänttäri, I., Ruffet, G. and Whitehouse, M.J., 2009. Age and tectonic framework of structurally controlled Palaeoproterozoic gold mineralization in the Häme belt of southern Finland. *Precambrian Research*, *174,* 53-77.

Schandl, E.S. and Gorton, M.P., 2002. Application of high field strength elements to discriminate tectonic settings in VMS environments. *Economic Geology*, *97,* 629-642.

Sipilä, P., Mattila, J. and Tianen, M., 2011. Pirkanmaan vyöhykkeen ja Hämeen vyöhykkeen välinen terraanirajatulkinta. Geologian tutkimuskeskus, raportti 2/2011, 27 s.

Vaasjoki, M., 1994. Valijärven hapan vulkaniitti: minimi Hämeen liuskejakson iäksi. Summary: Radiometric age of a meta-andesite at Valijärvi, Häme schist zone, southern Finland. *Geologi*, *46,* 91-92.

Väisänen, M., Mänttäri, I. and Hölttä, P., 2002. Svecofennian magmatic and metamorphic evolution in southwestern Finland as revealed by U-Pb zircon SIMS geochronology. *Precambrian Research*, *116,* 111-127.

# Exploration of asteroids using small satellites – case study ASPECT

T. Kohout[1,2] and ASPECT team[3]

[1]Department of Physics, University of Helsinki, Finland
[2]Institute of Geology, Academy of Sciences of the Czech Republic.
[3] A, Näsilä, T, Tikka, M, Granvik, A. Kestilä, A. Penttilä, K. Muinonen
E-mail: Tomas.Kohout@helsinki.fi

Aspect is a miniaturized satellite designed to investigate Didymos binary asteroid as a part of AIDA mission. Its scientific objectives include spectral and compositional characterization of Didymos system and investigation of space weathering and shock effects.

**Keywords:** asteroid, exploration, Didymos, AIDA, ASPECT

## 1. AIDA mission

The joint ESA/NASA AIDA (Asteroid Impact & Deflection Assessment) mission to binary asteroid Didymos consists of AIM (Asteroid Impact Mission, ESA) and DART (Double Asteroid Redirection Test, NASA) spacecrafts. DART is targeted to impact Didymos secondary component (Didymoon) and serve as a kinetic impactor to demonstrate deflection of potentially hazardous asteroids (Figure 1). AIM will serve as an observational spacecraft to evaluate the effects of the impact and resulting changes in the Didymos dynamic parameters.

## 2. ASPECT CubeSat

The AIM mission will also carry two CubeSat miniaturized satellites, released in Didymoon proximity. This arrangement opens up a possibility for secondary scientific experiments. ASPECT (Asteroid Spectral Imaging Mission) is one of the CubeSat proposals (Figure 1).

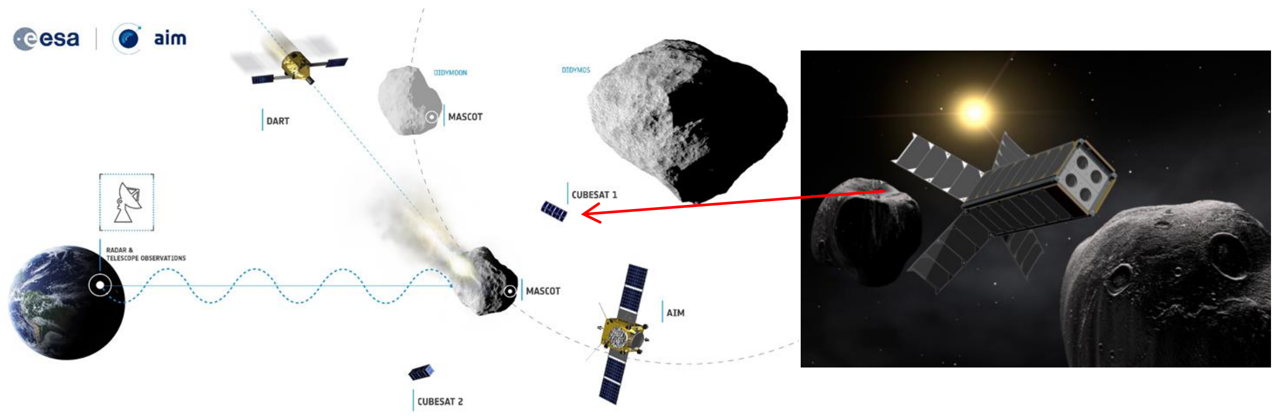


**Figure 1.** AIDA mission scenario (left) and illustration of ASPECT satellite (right).

## 3. ASPECT configuration and payload

ASPECT is 3U (3 unit) CubeSat with avionics, propulsion, and scientific payload occupying one unit each. ASPECT design builds on Aalto-1 and Aalto-2 CubeSat heritage. Scientific payload consists of visual – near infrared (VIS-NIR) spectrometer build at VTT. The spectrometer parameters are as follows:

- 3 measurement channels
  - VIS (500–900 nm) spectral imager (614 x 614 pixels)
  - NIR (900–1600 nm) spectral imager (256 x 256 pixels)
  - SWIR (1600–2500 nm) spectrometer (1 pixel)
- 45 nm spectral resolution
- Better than 2 m spatial resolution (pixel size) from 4 km orbit

**4. ASPECT science objectives**

| | **ASPECT scientific objectives and results** |
|---|---|
| AS1 | Map the surface composition of the Didymos system |
| Result | **Composition and homogeneity of the Didymos asteroid, changes as a result of DART impact** |
| Result | **Information on the origin and evolution of the Didymos binary system** |
| AS2 | Photometric observations and modeling of the Didymos system under varying phase angle and distance |
| Result | **Surface particle size distribution and composition for Didymoon and Didymain (simultaneous modeling of photometry and spectroscopy)** |
| AS3 | Evaluate space weathering effects on Didymoon by comparing mature and freshly exposed material |
| Result | **Information on the surface processes on airless bodies due to their exposure to the interplanetary environment** |
| AS4 | Identify local shock effects on Didymoon based on spectral properties of crater interior |
| Result | **Information on the processes related to impacts on small Solar System bodies** |
| AS5 | Observations of the plume produced by the DART impact |
| Result | **Evolution and composition of the DART impact plume** |
| AS6 | Map global fallback ejecta on Didymoon and Didymain |
| Result | **Detailed global mapping of fallback ejecta on both Didymain and Didymoon** |

**5. Conclusions**

ASPECT is a CubeSat mission with a VIS-NIR imaging spectrometer. Main science objectives are to characterize Didymos surface and its changes after DART impact and to significantly improve understanding of space weathering and shock processes. ASPECT will be first CubeSat operation autonomously in a vicinity of an asteroid.

**6. Acknowledgments**

The project is done under ESA SysNova Sys-Nova R&D Studies Competition for Innovation contract and is partly supported by Academy of Finland and ERC.

# New tools for deep mineral exploration: Insights from the field work stage of the COGITO-MIN project

Emilia Koivisto[1], Michal Malinowski[2], Suvi Heinonen[3], Calin Cosma[4], Nicoleta Enescu[4], Sanna Juurela[5], Jari Juurela[5], Teemu Törmälehto[5], Katri Vaittinen[5] and Marek Wojdyła[6]

[1]Department of Geosciences and Geography, P.O. Box 64, FI-00014 University of Helsinki
[2]Institute of Geophysics, Polish Academy of Sciences, Ksiecia Janusza 64, 01-452 Warsaw, Poland
[3]Geological Survey of Finland, P.O. Box 96, FI-02151 Espoo, Finland
[4]Vibrometric Oy, 127 Taipaleentie, 01860 Perttula
[5]Boliden Kylylahti Oy, Kaivostie 9, 83700 Polvijärvi, Finland
[6]Geopartner Ltd., Skosna 39B, 30-383 Krakow, Poland
E-mail: emilia.koivisto@helsinki.fi

The collaborative COGITO-MIN project between six partners from Finland and Poland aims to develop cost-effective, novel, geophysical deep mineral exploration techniques, with particular emphasis on seismic imaging. The three-year-long project was launched in January 2016, with the data acquisition stage ending in late September 2016. The purpose of this presentation is to provide insights to the data acquisition stage, and to the future directions of the COGITO-MIN project.

**Keywords:** seismic imaging, deep mineral exploration, exploration targeting

## 1. COGITO-MIN project 2016-2018

University of Helsinki, Geological Survey of Finland (GTK), Institute of Geophysics, Polish Academy of Sciences (IG PAS), Boliden Kylylahti, Vibrometric and Geopartner, research institutions and industry partners from Finland and Poland, are collaborating on the project COGITO-MIN (COst-effective Geophysical Imaging Techniques for supporting Ongoing MINeral exploration in Europe). COGITO-MIN aims to develop cost-effective, novel, geophysical deep mineral exploration techniques, with particular emphasis on seismic imaging. Seismic imaging is attractive for deep mineral exploration (e.g., Malehmir et al., 2012; 2014) because of superior depth penetration and resolution when compared to other geophysical imaging techniques. The project equally addresses data acquisition, processing and interpretation aspects of seismic reflection methods, with the overall goal to develop integrated geophysical-geological approaches for mine planning and exploration targeting. COGITO-MIN has been funded through ERA-MIN, which is a network of European organisations owning and/or managing research programs on raw materials. The funding for the Finnish COGITO-MIN project partners comes from Tekes and for the Polish project partners from the NCBR (the National Centre for Research and Development). The overall budget of the three-year-long project, launched in January 2016, is about 2 million euros.

## 2. New tools for deep mineral exploration: insights from the GOCITO-MIN field work

The data acquisition stage of the COGITO-MIN project took place from early August to late September 2016 in the vicinity of the Kylylahti Cu-Zn-Au mine in Polvijärvi, eastern Finland. The Kylylahti mine is operated by Boliden and is located within the famous Outokumpu brownfield area. The long history of geological and geophysical studies in the Outokumpu area, also including earlier seismic reflection profiles (e.g., Heinonen et al., 2011; Kukkonen et al., 2012), makes the site ideal for testing new concepts.

On the surface, the executed experiments include, 1) a novel 3D passive seismic interferometry experiment (e.g., Cheraghi et al., 2015) in which 1000 seismic receivers in a 3.5 x 3 km grid were left to record ambient noise sources for 4.5 weeks, with the aim to develop a cost-effective method for mapping the continuity of ore-bearing rock units in the initial stages of exploration targeting, 2) two approximately 6-km long high-resolution seismic reflection 2D profiles tailored to accommodate full-waveform inversion for improved seismic velocity model building and exploration targeting, and 3) a seismic reflection 3D survey utilizing the passive seismic grid and a “random” distribution of active seismic sources instead of more expensive, regular source line geometry typical for seismic reflection 3D surveys.

Inside the Kylylahti mine, the experiments include, 1) a multi-azimuth three-component VSP (Vertical Seismic Profiling) survey in three, approximately 500 m long, boreholes, with sources in the mine tunnels and on the surface, and 2) a VSP survey, as well as passive ambient noise measurements, in one borehole utilizing a new distributed acoustic sensing (DAS) technology (e.g., Parker et al., 2014) with the ability to take measurements at any point along the fibre optic cable used as a seismic sensor in the borehole (Figure 1A). The aim of these experiments is to develop methods for high-resolution resource evaluation and near-mine exploration.


**Figure 1.** A) Fibre optic cable installed to act as a seismic sensor in a borehole in the Kylylahti mine. B) New postdoctoral researcher of the COGITO-MIN project at the University of Helsinki, Marko Riedel, participating in the VSP data acquisition work. Marko`s postdoctoral research work will focus on the development of processing and interpretation methods for the acquired VSP data sets, in collaboration with Vibrometric.

All the project partners participated in all the components of the field work, with different partners in charge of different components. Boliden Kylylahti was in charge of laborious permitting and site-related matters. The GTK was in charge of the passive seismic interferometry experiment. Massive surveying work was done by the GTK from June to September 2016, and they also handled all the explosive surface sources of the overall experiment. Geopartner, a geophysical company from Poland, provided equipment and executed 2D data acquisition, with the IG PAS in charge of the active-source imaging component of the surface work. Vibrometric, a Finnish company specializing in borehole seismic measurements, was in charge of the VSP work inside the Kylylahti mine (Figure 1). Additionally, NovaSeis, a geophysical company from Poland that provided the 1000 wireless recorders for passive seismic interferometry experiment, and Silixa, a company from the UK specializing in the DAS measurements (Figure 1A), acted as contractors. The University of Helsinki acts as the overall coordinator of the COGITO-MIN project.

After the extensive data acquisition stage, the next stage of the project will start, i.e., development of the data processing and interpretation methods; including, for example, development of techniques for processing the passive seismic data and for combining the active source surface and borehole data in a fashion that provides a larger range of illumination angles of the targets. Multiple researchers are participating from each partnering organization, and the project is expected to produce several Doctoral and Master`s theses. For example, in collaboration between the GTK and the University of Helsinki, petrophysical characterization of the Kylylahti deposit is currently underway as a Master`s thesis work (see Luhta et al., this volume) and a doctoral student has already started his work at the IG PAS on the passive seismic 3D data.

## 3. Conclusions

The collaborative COGITO-MIN project between six research institutions and industry partners from Finland and Poland aims to develop cost-effective, novel, geophysical deep mineral exploration techniques, with particular emphasis on seismic imaging. The three-year-long project was launched in January 2016, and the data acquisition stage of the COGITO-MIN project was successfully finished at the end of September 2016. The purpose of this presentation is to provide insights to the data acquisition stage, and to the future directions of the COGITO-MIN project.

## 4. Acknowledgements

The COGITO-MIN project has been funded through the ERA-MIN network. At the national level, the funding comes from Tekes in Finland and the NCBR in Poland. Leica Geosystems Oy is thanked for providing their SmartNet for the project use.

## References:

Cheraghi, S., Craven, J.A. and Bellefleur, G., 2015, Feasibility of virtual source reflection seismology using interferometry for mineral exploration: A test study in the Lalor Lake volcanogenic massive sulphide mining area, Manitoba, Canada. Geophysical Prospecting, 2015, 63, 833–848 doi: 10.1111/1365-2478.12244.

Heinonen, S., Kukkonen, I. T., Heikkinen, P. J., & Schmitt, D. R. (2011). High resolution reflection seismics integrated with deep drill hole data in Outokumpu, Finland. Geol.Sur.Finl., Special Paper, 51, 105-118.

Kukkonen, I.T., Heinonen, S., Heikkinen, P.J., and Sorjonen-Ward, P., 2012, Delineating ophiolite-derived host rocks of massive sulphide Cu-Co-Zn deposits with 2D high-resolution seismic reflection data in Outokumpu, Finland. Geophysics. 77, p. WC213-WC222.

Malehmir, A., Durrheim, R., Bellefleur, G., Urosevic, M., Juhlin, C., White, D. J., et al., 2012. Seismic methods in mineral exploration and mine planning: A general overview of past and present case histories and a look into the future. Geophysics, 77(5), WC173-WC190. doi:10.1190/GEO2012-0028.1

Malehmir, A., Koivisto, E., Manzi, M., Cheraghi, S., Durrheim, R., Bellefleur, G., Wijns, C., Hein, K. and King, N., 2014, A review of reflection seismic investigations in three major metallogenic regions: the Kevitsa Ni-Cu-PGE district (Finland), Witwatersrand goldfields (South Africa), and the Bathurst Mining Camp (Canada). Ore Geology Reviews, 56, 423-441.

Parker, T., Shatalin, S., and Farhadiroushan, M., 2014, Distributed Acoustic Sensing – a new tool for seismic applications. First Break, Volume 32, 61-69.

# Seismic full waveform modelling of Outokumpu-type ore and processing considerations

K. Komminaho[1], E. Koivisto[2], P. J. Heikkinen[1], H. Tuomi[1], N. Junno[1] and I. Kukkonen[3]

[1]University of Helsinki, Department of Geosciences and Geography, Institute of Seismology, P.O. Box 68, FI-00014 University of Helsinki, Finland
[2]University of Helsinki, Department of Geosciences and Geography, Division of Geology and Geochemistry, P.O. Box 64, FI-00014 University of Helsinki, Finland
[3]University of Helsinki, Department of Physics, Division of Materials Physics, P.O. Box 64, FI-00014 University of Helsinki, Finland
E-mail: kari.komminaho@helsinki.fi

**Keywords:** seismic, reflection, 3D modelling, full waveform, Outokumpu

## 1. Introduction

The Seismic forward modelling can be used to understand better the seismic signatures of ore deposits and ore-bearing formations (e.g., Bohlen et al. 2003; Ahmadi et al. 2013). First, seismic forward modelling can be used to predict the seismic signature that would be recorded given an assumed ore body and host formation within the crust. Then, the model is compared to real reflection seismic data. For forward seismic modelling, a preliminary 3D geological model, or alternative models, of the subsurface is needed, along with density and seismic velocity structure of the medium where the seismic waves are travelling. Based on the forward modelling results, the 3D geological model can be verified or further improved, and with the acquired understanding of the seismic response at the deposit scale, real data can be analyzed for potential direct indications of new ore deposits. In addition, forward modelling can also be used for testing of optimal acquisition geometries and processing schemes for ore exploration.

Before obtaining the seismic images of the subsurface, the reflection seismic data need to go through extensive data processing. During data processing, development of target-specific processing schemes has been in a key position to adapt the seismic reflection methods for hard rock ore exploration (e.g., Eaton et al. 2003; Malehmir et al. 2012). Specific processing problems arise for example from the typically used crooked-line survey geometries, and highly variable near-surface layer thickness and seismic wave velocity that cause time shifts to the reflected signals (e.g., Schmelzbach et al. 2007). However, previous studies (e.g., Milkereit et al. 2000; Salisbury et al. 2003; Adam et al. 2003) have shown that the scattering response of massive sulphide deposits can be preserved with careful acquisition and target-specific processing of the data, provided that the response is not obscured by scattering response of the heterogeneous background typical to hard rock environments (e.g., L`Heureux et al. 2009).

## 2. Seismic forward modelling

Crystalline bedrock is a challenging environment for seismic forward modelling at a mining camp scale. That is because the structures usually have very complex geometry and heterogeneous petrophysical properties due to their complicated geological history, and the dimensions of the ore bodies are typically comparable to seismic wavelengths. This means that approximative methods cannot be used accurately because they do not handle diffractions and scattering of seismic waves from heterogeneous formations and small objects. For example, results by Bohlen et al. (2003) show that massive sulphide ore bodies produce strong and complex scattering response that depends on the composition, size and shape of the scatterer.

The response is characterized by strong dependence on azimuth and offset, as well as phase reversals.

Approximative modelling methods include for example seismic ray tracing and Born approximation. Ray tracing is valid only when the model structure is varying smoothly compared to the seismic wavelengths (Červeny 2005). Born approximation gives the theoretical elastic-wave scattering response of a 3D geological model in a weakly inhomogeneous medium (Eaton 1997). While these methods are computationally fast and can be used for quick modelling at a regional scale, especially at a deposit scale fully elastic algorithm is required for accurate forward modelling. Full waveform modelling of complicated structures is possible only by finite element or finite difference methods, out of which the finite-difference (FD) technique provides good balance between accuracy and computational efficiency (e.g., Moczo et al. 2014).

Sofi2D/3D used in this study is massively parallel finite difference code which implements 2D/3D full waveform viscoelastic wave equations (Bohlen 2002). It uses higher-order FD operators, staggered-grid formulation and numerically optimized Holberg coefficients for enhanced accuracy and computational efficiency. Parallelization is based on domain decomposition. Global model grid is decomposed into sub-grids which each are computed by a different processor. By using the portable message passing interface standard (MPI) for the communication between processors, running times can be reduced and grid sizes increased significantly (Bohlen 2002). Furthermore, the code shows good performance on massively parallel supercomputers, which makes the computation of large grids feasible.

**3. Seismic signature of the Outokumpu assemblage along OKU1**

Kukkonen et al. (2012) have suggested that most of the reflectivity within the uppermost 2 km of high-resolution seismic reflection sections OKU1, OKU2 and OKU3 could be due to bodies of the potentially ore-bearing Outokumpu assemblage rocks, i.e., serpentinites, and carbonate, skarn and quartz rocks enveloped by black schists and enclosed within quite homogeneous mica schists. This conclusion is based on the known surface geological features and drill-hole data, in particular the 2.5-km-deep Outokumpu Deep Drill Hole.

The near surface structures of our 3D geological model, used for seismic forward modelling, are based on the geological cross-sections by Koistinen (1981). The model has been continued to greater depths by creating a model of the deeper units from the seismic reflection data, based on the rock units observed in the Outokumpu Deep Drill Hole.

Seismic forward modelling was carried out with the real survey geometry of OKU1. The modelled shot gathers were processed with the same processing sequence as used for obtaining the stacked section of the real OKU1, as applicable (adding the CMP geometry, muting of air waves and first arrivals, NMO corrections and stacking). The main features of real OKU1 profile are visible in the synthetic data, confirming that the Outokumpu assemblage rocks can be identified from the seismic sections as internally strongly reflective packages. However, the real observed reflectivity patterns have not been completely reproduced in the synthetic section. This naturally means that the our geological model used for seismic forward modelling is not 100% correct.

**4. Seismic signature of the Outokumpu-type sulphide deposits**

To examine the seismic response of the Outokumpu-type, typically semi-massive to massive sulphide ore bodies within the Outokumpu assemblage, we added hypothetical ore bodies to our geological model. The Outokumpu-type sulphide deposits typically form thin, narrow and sharply bounded sheets or lenses of semi-massive to massive sulphides, located along or close to the interfaces between black schists and quartz–carbonate rocks.

Our hypothetical ore bodies are 12–16-m-thick and 75–120-m-wide lenses, with a length spanning the whole length of the 3D geological model (about 1 km) perpendicular to the cross-section.

From the residual response of the ore bodies only (derived by subtracting the stack obtained without the hypothetical ore bodies from the stack obtained with the ore bodies added), diffractions are produced from all the hypothetical ore bodies. The strongest response is from the ore body placed in contact between serpentinite and quartz rocks, as expected based on the acoustic impedance contrasts. Comparison of the stacks indicates that the diffractions produced by the ore bodies are not easily recognised from the other reflective contacts within the Outokumpu assemblage.

**5. Crooked-line processing**

To test the effect of the crooked-line survey geometry and processing on the visibility of the ore bodies, seismic forward modelling was done for shot gathers with the real crooked-line survey geometry of OKU1, as well as for shot gathers along a straight survey line approximating the survey geometry of OKU1. The modelled shot gathers were processed with the same processing sequence as used to obtain the stacked section of the real OKU1, as applicable for the synthetic data. Diffractions from the hypothetical ore bodies are visible in both stacked sections, for straight survey geometry and for crooked-line survey geometry. This indicates that the seismic signature of the ore bodies is preserved in the crooked-line processing.

However, it should be noted that the diffractions for the crooked-line survey geometry are smeared and less clear when compared to the diffractions for the straight survey geometry, and that especially the shallow parts of the geological model (Outokumpu assemblage rocks near the surface based on the cross-sections by Koistinen (1981)) produce a more detailed response with the straight survey geometry. Furthermore, the crooked-line survey geometry and/or processing produces features that are not present in the stacks obtained for the straight survey geometry.

**7. Conclusions**

The Outokumpu assemblage rocks, and black schist enveloping them, form internally strongly reflective packages within the mica schist, typically characterized by numerous diffraction hyperbolas in the stacked sections. The reflectivity characteristics can be used to identify the Outokumpu assemblage rocks at depth.

Based on the results of this study, it seems possible that the Outokumpu-type sulphide mineralizations could even be directly observed as high-amplitude anomalies in the seismic reflection sections, if the dimensions and orientation are optimal. A careful crooked-line data processing sequence enables the preservation of direct signals, if they are present in the data, except for very shallow signals that are more likely to be distorted by the crooked-line effects. The crooked-line effects can also potentially produce high-amplitude anomalies, and care is required when interpreting the high-amplitude anomalies.

**Acknowledgments**

CSC – The Finnish IT Center for Science is acknowledged for providing computing resources.

## References:

Adam, E., Perron, G., Arnold, G., Matthews, L., & Milkereit, B. (2003). 3D seismic imaging for VMS deposit exploration, Matagami, Quebec. Hardrock Seismic Exploration: SEG, 229-246.

Ahmadi, O., Juhlin, C., Malehmir, A., & Munck, M. (2013). High-resolution 2D seismic imaging and forward modeling of a polymetallic sulphide deposit at Garpenberg, central Sweden. Geophysics, 78(6), B339-B350.

Bohlen, T. (2002). Parallel 3-D viscoelastic finite difference seismic modelling. Computers & Geosciences, 28(8), 887-899.

Bohlen, T., Müller, C., & Milkereit, B. (2003). Elastic seismic-wave scattering from massive sulphide orebodies: On the role of composition and shape, in B. Milkereit, D. Eaton, and M. Salisbury, eds., Hardrock seismic exploration: SEG, 70-89.

Červeny, V. (2005). Seismic ray theory. Cambridge university press.

Eaton, D. W., Milkereit, B., & Salisbury, M. (2003). Seismic methods for deep mineral exploration: Mature technologies adapted to new targets. The Leading Edge, 22(6), 580-585.

Eaton, D. (1997). BMOD3D: A program for three-dimensional seismic modelling using the Born approximation. Open File, 3357

Koistinen, T. (1981). Structural evolution of an early Proterozoic strata-bound Cu-Co-Zn deposit, Outokumpu, Finland. Unpublished, University of Helsinki, Helsinki.

Kukkonen, I. T., Heinonen, S., Heikkinen, P., & Sorjonen-Ward, P. (2012). Delineating ophiolite-derived host rocks of massive sulphide Cu-Co-Zn deposits with 2D high-resolution seismic reflection data in Outokumpu, Finland. Geophysics, 77(5), WC213-WC222. doi:10.1190/GEO2012-0029.1

L'Heureux, E., Milkereit, B., & Vasudevan, K. (2009). Heterogeneity and seismic scattering in exploration environments. Tectonophysics, 472(1), 264-272.

Malehmir, A., Durrheim, R., Bellefleur, G., Urosevic, M., Juhlin, C., White, D. J., et al. (2012). Seismic methods in mineral exploration and mine planning: A general overview of past and present case histories and a look into the future. Geophysics, 77(5), WC173-WC190. doi:10.1190/GEO2012-0028.1

Milkereit, B., Berrer, E., King, A. R., Watts, A. H., Roberts, B., Adam, E., et al. (2000). Development of 3-D seismic exploration technology for deep nickel-copper deposits-A case history from the Sudbury Basin, Canada. Geophysics, 65(6), 1890-1899.

Moczo, P., Kristek, J., & Gális, M. (2014). The finite-difference modelling of earthquake motions: Waves and ruptures. Cambridge University Press.

Salisbury, M. H., Harvey, C., & Matthews, L. (2003). The acoustic properties of ores and host rocks in hardrock terranes. Hardrock Seismic Exploration, (10), 9-19.

Schmelzbach, C., Juhlin, C., Carbonell, R., & Simancas, J. F. (2007). Prestack and poststack migration of crooked-line seismic reflection data: A case study from the south Portuguese zone fold belt, southwestern Iberia. Geophysics, 72(2), B9-B18.

# Intraplate Seismicity in Central Fennoscandia

Korja, A.[1], Uski, M.[1], Lund, B.[2], Grigull, S.[3], Nironen, M.[4], E., Högdahl, K.[2]

[1]University of Helsinki, Institute of Seismology, Helsinki, Finland
[2]University of Uppsala, Uppsala, Sweden
[3]Geological Survey of Sweden, Uppsala, Sweden
[4]Geological Survey of Finland, Espoo, Finland
E-mail: annakaisa.korja[at]helsinki.fi

In this paper we describe intraplate seismicity of the Fennoscandian Shield and try to analyse the fault movement potential of the existing shear zones in the current stress field.

**Keywords:** seismicity, intraplate, Fennoscandia, Moho, crust

## 1. General

Fennoscandian Shield (Fig. 1) is situated in a continental intraplate setting in northern Europe. The latest plate tectonic event, which affected the study area, is the opening and spreading of the Atlantic Ocean that initiated 60 Ma ago. This ongoing event has subjected the area to a long-standing tectonic stress-field oriented in a WNW–ESE direction. During the Pleistocene glaciations, the area has been subjected to repeated glacial cycles and associated loading and unloading events. The area is still rebounding.

Current seismicity in the Fennoscandian Shield is generally low and it has been attributed to a complex interplay of intraplate and plate margin processes; the opening of the northern Atlantic Ocean, glacial isostatic adjustment (GIA) and local stress caused by mass deficit or excess in the area. An up-to-date estimate of the intraplate seismicity in the Central part of the Fennoscandian Shield and its sources is needed in seismic hazard estimates of nuclear power plant sites. Fennovoima Oy nuclear power company commissioned a seismotectonic study from the Universities of Helsinki and Oulu and from the Geological Surveys of Finland and Sweden. Original data, interpretations and references can be found in Korja and Kosonen, 2014.

## 2. Seismicity

The seismicity in the Fennoscandian intraplate area is clustered along NE–SW-trending zones that are parallel to the Norwegian margin and the Mid-Atlantic ridge. A slight change in the general pattern takes place across an N–S-trending zone running east of the Finnish-Swedish national border (Pajala shear zone). East of this zone, the seismicity rates are lower and the NE–SW trend is less obvious. The NE-SW trending earthquake clusters in northern Sweden and Finland are associated with PGF zones and western flank of the Gulf of Bothnia. The most active NE–SW-trending zone in Finland is the Kuusamo-Kandalaksa zone.

Based on a subset of the most recent earthquake data (2000-2012) most of the earthquakes (80%) occur in the upper crust down to 17 km in depth, a minority (19%) in the middle crust (17-31 km) and only a few in the lower crust 31-45 km (1%) The seismogenic layer is less than 30 km in depth.

## 3. Orientation of structures in the current stress field

The current strain rates in Fennoscandian Shield are rather low and thus cannot produce new structures but rather reactivate old structures, joints and extension fractures, where stress overcomes fault friction. The potential of reactivation of the pre-existing deformation zones and faults depend on the directions and relative magnitudes of the principal stresses, and the stress state, as well as the orientation of the pre-existing structures. The orientation of the overall maximum horizontal stress field in northern Europe is WNW–ESE to NW–SE. Pre-existing deformation zones that are optimally oriented in the present stress field can potentially be reactivated.

The deformation zones were analysed for their length and azimuth and they were assigned a potential reactivation type (reverse, normal or strike slip) based solely on their azimuth. The earthquakes in the seismically most active area, close to Skellefteå, Sweden along the western coast of the Gulf of Bothnia and its north-easterly continuation, appear to cluster around the shoreline and along post-glacial faults, which are mostly oriented optimally for reverse or strike slip faulting. The seismically active Kuusamo area in Finland is transacted by wealth of deformation zones all trending in directions optimal for reactivation.

The seismically active areas are located in areas where the crust is less than 50 km thick. Where the crustal thickness gradient trends in a NE–SW direction, e.g. along the faulted western margin of the Bothnian Sea and along the Auho-Kandalaksha fault zone in the Kuusamo area, the gradient seems to be associated with a zone of increased seismicity. In these areas, the crustal thickness gradients are optimally oriented for reactivation.

## 4. Glacial isostatic adjustment

It is noted that the zones of increased seismicity in the western flank of the Gulf of Bothnia as well as the currently seismically active “postglacial faults” are parallel and along the long axes of the ellipsoidal GIA anomaly. The direction of the long axis of the ellipsoid is orthogonal to and the short axis is parallel to the maximum horizontal stress in Fennoscandia stemming from the opening of the Atlantic. Neither the seismicity nor faulting are following the isosurfaces of the ellipsoid.

## 5. Conclusions

In the Fennoscandian intraplate area has low seismicity. Most of the earthquakes (99%) occur in the upper to middle crust down to 31 km in depth and the seismogenic layer is around 30 km in depth. The seismically most active zones appear to be optimally oriented for reverse or strike slip faulting stemming from the opening of the Atlantic.

## 5. References

Korja, A. and Kosonen, E. (eds), 2015. Seismotectonic framework and seismic source area models in Fennoscandia, northern Europe. Univ. Helsinki, Instit. Seismology, Report S-63. 284 p. http://www.seismo.helsinki.fi/pdf/Seismotectonic_S63_Korja_Kosonen.pdf

# FIN-EPOS – Finnish national initiative of the European Plate Observing System

A. Korja, T.A.Vuorinen and FIN-EPOS

University of Helsinki, Institute of Seismology, Helsinki, Finland
E-mail: annakaisa.korja[at]helsinki.fi, fin-epos[at]helsinki.fi

FIN-EPOS-consortium consists of the national geoscientific RI's involved in EPOS. The main objective of the FIN-EPOS research infrastructure is standardize and harmonize the Finnish national data set so that they will be interoperable with the EPOS Thematic Core Services/ Thematic data centers. The consortium will develop a Finnish-language login page on which users are identified and their user rights for EPOS resources are defined.

**Keywords:** EPOS, database, measurements, observatory, laboratory, time series, geophysics, geology, seismology, geodesy, geomagnetism, petrophysics, distributed, data management system

## 1. General

The European Plate Observation System – EPOS - is a single, Pan-European, sustainable and distributed research infrastructure (RI) (http://www.epos-eu.org/) and it is the sole RI for solid Earth Science in ESFRI. EPOS will be an open-access infrastructure, aiming to be the principal source of data and tools in geosciences. EPOS will simplify and speed-up the process of combining information from different fields of geophysics. EPOS opens a wealth of new possibilities for cross-cutting and innovative research in Earth Sciences, their applications in society as well as in raw material and energy exploration. EPOS will also stimulate and support geographically distributed multidisciplinary studies. At the moment the Research Infrastructure Database for EPOS - RIDE ( http://www.epos-eu.org/ride/) includes metadata of the NRI's participating in EPOS. RIDE is constantly being updated.

In addition to the significant scientific benefits gained through membership in EPOS, students and researchers will have an opportunity to gain valuable hands-on experience using a modern, integrated RI and data portal. One of the major challenges that educators and researchers face is providing students and other researchers with access to and experience using modern geoscientific data and analysis tools to adequately prepare them for a fruitful geoscience career. EPOS is planning in-house training courses in data usage, summer schools for geophysical tools applicable to EPOS data sets and instrumentation.

At the moment 23 countries are involved and 19 countries have signed LOI, with more pending. EPOS is collaborating with other ESFRI's and other RI'S globally. EPOS comprises of solid Earth observatory and laboratory facilities that are already linked with European and Global data centers and science programs in their own fields (e.g. ORFEUS, EMSC, GEOFON, GGOS, EUREF, TOPMOD, GEOSS, OneGeology and EuroGeoSurveys, ERA-MIN, EUDAT, EURAMET, TOPOEUROPE etc.).

EPOS is essentially an e-science facility summarized at http://www.epos-eu.org/dataproducts/ict-architecture.html. During IP-project EPOS faces two challenges: (1) Integration of highly heterogeneous observational and experimental multidisciplinary data and (2) development of e-infrastructures and e-science to support the construction of collaborative data platforms.

EPOS-PP preparatory phase (2010-2014) is finished and EPOS has entered Implementation Phase in October 2015 with the help of 18 M€ H2020 Intra-Dev3 grant agreement (Fig. 4). Finland is actively taking part in 4 Working Packages of EPOS-IP: WP3 National harmonization (UH), WP4 Governance and Legal (UH), WP 13 Geomagnetic observations (FMI), WP14 Anthropogenic Hazard (UO; Fig. 6). In Governance and Legal Working group UH is involved in drafting the setting up governance structures of TCS and ICS and drafting the service contracts between EPOS-ICS and the various TCS and ICS-D. In WP 13 FMI is involved in the designing the Geomagnetic observatory metadata within Geomagnetic observations TCS. In WP14, university of Oulu is setting up a national HUB for the human induced seismic events in Finland. In addition, the Finnish RI's will be transmitting data to the several other TCS (WP 8 Seismology, WP10 Geodesy, WP 15 Geological information, WP 16 Multiscale laboratories, WP17 Geoenergy testbeds). For this purpose the NRI will describe their metadata and accommodating their data flow to EPOS data standards.

**2. FIN-EPOS - a FINnish national initiative of the EPOS**

The FIN-EPOS - FINnish national initiative of the EPOS is a research infrastructure consortium. The partners of the consortium are: the University of Helsinki, the University of and Oulu, Finnish Geospatial Research Institute, FGI, of the National Land Survey (NLS), Finnish Meteorological Institute, Geological Survey of Finland, CSC – IT Center for Science, MIKES Metrology at VTT Technical Research Centre of Finland Ltd. The consortium partners own and operate the geophysical and geodetic RIs that are distributed across Finland.

Each partner collects different types of data with different geophysical instruments and utilizing different standards for data formatting, archiving and sharing. IT solutions for interoperability require certain level of standardization. The EPOS will set standards for data formatting and archiving that each partner is obliged to follow and harmonize their data and metadata accordingly. The harmonization of data formats and metadata will take place in EPOS-IP project. This will impose a severe workload in 2016-2019 on all the NRI. Part of this work is funded through the Academy of Finland's FIRI2015 funding.

FIN-EPOS has a joint council that will meet twice a year for decision making and strategic brainstorming. The council will be assisted by the coordinator, who will be prepare meetings and documents, correspond with EPOS-ECO, co-ordinate the metadata cataloging and data formatting (harmonization), helping in outlining/updating the FIN-EPOS web pages and national entry portal. The consortium is hosted by the Institute of Seismology, University Helsinki (ISUH) where the national co-ordination office is placed at (email: fin-epos[at]helsinki.fi, URL: http://www.helsinki.fi/geo/). The consortium chair is RD Annakaisa Korja, vice-chair is prof. Markku Poutanen from the FGI and the coordinator is Tommi Vuorinen.

The short-term goal of the council is to ensure that each partner is committed to applying EPOS metadata catalogues and data format standards to their own data sets, to build and design of national entry portal/ Finnish interface.

The longterm goal of the council is ensure that Finland benefits from joining EPOS-ERIC as a country. For this purpose, the FIN-EPOS council discusses the long-term scientific goals of EPOS and FIN-EPOS communities and build a solid Earth sciences RI plan to support the scientific goals. The discussions are also the basis for Nordic RI collaboration and for joint Nordic participation in EPOS-ERIC advisory committees.

# Mesoproterozoic rapakivi granite magmatism in the Fennoscandian shield and adjacent areas: Role of crustal radiogenic heating

I.T. Kukkonen[1] and L. Lauri[2]

[1]Department of Physics, University of Helsinki, Finland
[2]Geological Survey of Finland, Rovaniemi, Finland
E-mail: ilmo.kukkonen @helsinki.fi

Mesoproterozoic rapakivi granite and associated gabbro-anorthosite magmatism are considered to be anorogenic, i.e., to have no causal relationship with the hosting Paleoproterozoic orogenic rocks. In the Fennoscandian shield and adjacent sediment-covered areas, the 1.65–1.47 Ga rapakivi granite magmatism is mainly felsic in composition and represented by both large batholiths >100 km in diameter as well as smaller stocks. The rapakivi granite and associated mafic magmatism have been attributed to partial melting of lower crustal or upper mantle sources, but the heat source of the magmatism has remained unresolved. We propose that the most plausible heat source for Fennoscandian rapakivi granite magmatism was provided by the radiogenic heat production of the crust initially thickened in the Paleoproterozoic late Svecofennian orogeny at ca. 1.86 Ga. The seemingly anorogenic magmatism may actually be post-orogenic with a link to the long-term thermal evolution of the host rocks.

**Keywords:** Rapakivi granite, thermal models, crustal thickening, radiogenic heat, Fennoscandian Shield

## 1. Introduction

The Fennoscandian shield and adjacent sediment-covered areas are characterized by extensive Mesoproterozoic rapakivi granite and minor gabbro-anorthosite intrusions. Comparable Mesoproterozoic anorogenic bimodal magmatism is common also in other areas and continents with varying proportions of felsic and mafic components (Rämö and Haapala, 1995; Dörr et al., 2002; Vigneresse, 2005, and references therein).

The rapakivi magmatism in the Fennoscandian Shield has been considered as anorogenic in nature, commonly due to magmatic activity of the mantle resulting in magmatic underplating and partial melting of the lower crust (e.g., Rämö and Haapala, 1995; Elo and Korja, 1993).

We present a model for the genesis of the rapakivi granite and related mafic magmatism based on thermal evolution of crust collision-thickened during late Svecofennian time (~1.86 Ga). Collision-thickened crust warms up by conductive heat transfer due to radiogenic heat from U, Th and K. This crust-derived heat affects not only the crust, but inevitably also the upper mantle by gradually increasing the lithospheric temperatures and eventually generating melts in the crust and even in the upper mantle.

## 2. Thermal effects of crustal thickening

We apply here a conductive heat transfer model of Svecofennian collisional crustal thickening adapted from Kukkonen and Lauri (2009). In our model the crust is thickened instantaneously at 1860 Ma from 30 km to 70 km by tectonic stacking of layers of metasedimentary and volcanic rocks. Conductive heating of the crust is due to radiogenic heat production from decay of U, Th and K. In about 30 Ma time the thickened crust is already heated sufficiently for partial melting at 30-50 km depth, and the melts are emplaced in the middle-upper crust boundary as late-orogenic granites at the magmatic and metamorphic peak of the orogeny. The heating, however, does not stop with the late-orogenic granitoid formation, because the crust remains (and remains even today) very thick. Without erosion of the stack, the temperatures would become excessively high. Removal of heat sources by erosion and the simultaneous downward movement of the surface level (temperature at 5°C) result in typical counterclockwise loops in the metamorphic P-T diagrams.

The conductive heating in the thick crust continued steadily after 1.8 Ga, because the crust remained thick keeping its total radiogenic heat sources at an elevated level. Slowly the heating affected also the upper mantle and straightened the geotherm. Simultaneously the heating progressed upward in the crust and finally, about 200-250 Ma after the Svecofennian collision and tectonic stacking, a new phase of melting was initiated in the middle crust. Dehydration melting of biotite in fertile layers started at 800-850ºC and continued until about 900 ºC when all biotite was consumed. Melting was possible in our model at 30 km from about 1.7 Ga. Correspondingly, the lowermost crust at 40-50 km would have exceeded 1000 ºC at times <1.7 Ga. The heating of the collision thickened crust did not affect solely the crust but also the upper mantle, and temperatures beneath the crust were also elevated by several hundred degrees. This heating could provide a mechanism for generating coeval mafic magmas by partial melting of the mantle (or mafic rocks in the lower crust to make anorthosites).

## 3. Conclusions

Our interpretation is that the Mesoproterozoic thermal evolution was controlled by the crustal thickening of the Svecofennian orogenic front at ~1.86 Ga and subsequent post-orogenic heating. Conductive heating of lower crust and uppermost mantle in the 'anorogenic' time provided the conditions required for the generation of the bimodal rapakivi granite suite. Crustal radiogenic heat generation was the most important heat source for the rapakivi granite magmatism. The long delay between the Svecofennian orogenic peak and the onset of rapakivi magmatism is attributed to slowness of conductive heat transfer in a thick crust. Due to the causal relationship with the Svecofennian orogeny, rapakivi granites should not be considered anorogenic but post-orogenic.

## References:


Dörr, W., Belka, Z., Marheine, D., Schastok, J.,Valverde-Vaquero, P., Wiszniewska, J., 2002, U-Pb and Ar-Ar geochronology of anorogenic granite magmatism of the Mazury complex, NE Poland: Precambrian Research, v. 119 , p. 101-120.

Elo, S. and Korja, A., 1993, Geophysical interpretation of the crustal and upper mantle structure in the Wiborg rapakivi granite area, southeastern Finland: Precambrian Research, v. 64, p. 273-288.

Kukkonen, I. T. and Lauri, L. S., 2009. Modelling the thermal evolution of a collisional Precambrian orogen: high heat production migmatitic granites of southern Finland. Precambrian Research 168 (3-4), 233-246.

Rämö, O.T., Haapala, I., 1995, One hundred years of rapakivi granite: Mineralogy and Petrology, v. 52, p. 129-185.

Vigneresse, J.L., 2005, The specific case of Mid-Proterozoic rapakivi granites and associated suite within the context of the Columbia supercontinent: Precambrian Research, v. 137, p. 1-34.

# Helsinki University Kumpula campus drill hole project

I.T. Kukkonen[1], E. Koivisto[2] and D. Whipp[2]

[1] Department of Physics, University of Helsinki, P.O. Box 64, FI-00014 University of Helsinki;
[2]Department of Geosciences and Geography, University of Helsinki, P.O. Box 68, FI-00014 University of Helsinki
E-mail: ilmo.kukkonen@helsinki.fi

The Kumpula Campus Drill Hole Project comprises a fully cored diamond drill hole in the Kumpula campus of the University of Helsinki and a representative suite of wire-line logs. The main purpose of the drill hole is in undegraduate education in borehole geophysics, wireline logging, petrophysics and geological logging of the core as well as 3D modeling of downhole and surface structures.

**Keywords:** Drill holes, core samples, wireline logs, crystalline rocks, Kumpula campus, Helsinki, Finland

## 1. Summary

A 370 m deep drill hole with continuous coring was drilled in the southern part of the Kumpula campus of University of Helsinki in late 2015. In addition to the drilling, a number of wireline logs were measured as a contracted service for a full characterization of the geology and geophysics of the hole. The main use of the drill hole will be in undegraduate education in borehole geophysics, wireline logging, petrophysics and geological logging of the core as well as 3D modeling of downhole and surface structures. The Precambrian bedrock in the Kumpula campus is steeply dipping hornblende gneiss, amphibolite, tonalite and granite. The drilling site is on a hilltop on an extensive 1 ha size outcrop. The hole diameter is 76 mm and the hole is oriented to NE with a dip of 70°. The campus drill hole is an important component in the university infrastructure for the education and research of geosciences. The presentation reviews the drilling and logging operations on a densely built campus area and the planned post-drilling use of the hole and the core.

Three related posters present the first results of three Master thesis projects based on the campus hole materials. Penttilä et al. (this volume) study the lithology of the drill core, Valtonen et al. (this volume) investigate the fracturing of the campus bedrock as revealed by the drill core and the outcrops, and Räisänen et al. (this volume) present the first geochemical results of the drill core and outcrops using a portable XRF analyzer.

## References:

Penttilä, K., Kukkonen, I., Heinonen, J.S., Räisänen, M. and Valtonen, R. (this volume). Logging and lithology of the Kumpula Campus drill hole. In: *Kukkonen et al. (Eds.),* Lithosphere 2016 – Ninth Symposium on the Structure, Composition and Evolution of the Lithosphere in Finland. Programme and Extended Abstracts, Espoo, Finland, November 9-11, 2016. Institute of Seismology, University of Helsinki, Report S-65, 166 pages.

Räisänen, M., Kukkonen, I., Heinonen, J.S., Valtonen, R. and Penttilä, K. (this volume). Geochemical characteristics of the Kumpula campus area: drill core and outcrop data. In: *Kukkonen et al. (Eds.),* Lithosphere 2016 – Ninth Symposium on the Structure, Composition and Evolution of the Lithosphere in Finland. Programme and Extended Abstracts, Espoo, Finland, November 9-11, 2016. Institute of Seismology, University of Helsinki, Report S-65, 166 pages.

Valtonen, R., Kukkonen, I., Heinonen, J.S., Räisänen, M. and Penttilä, K. (this volume). Kumpula campus drill hole: Fracture mapping and 3D-modeling. *Kukkonen et al. (Eds.),* Lithosphere 2016 – Ninth Symposium on the Structure, Composition and Evolution of the Lithosphere in Finland. Programme and Extended Abstracts, Espoo, Finland, November 9-11, 2016. Institute of Seismology, University of Helsinki, Report S-65, 166 pages.

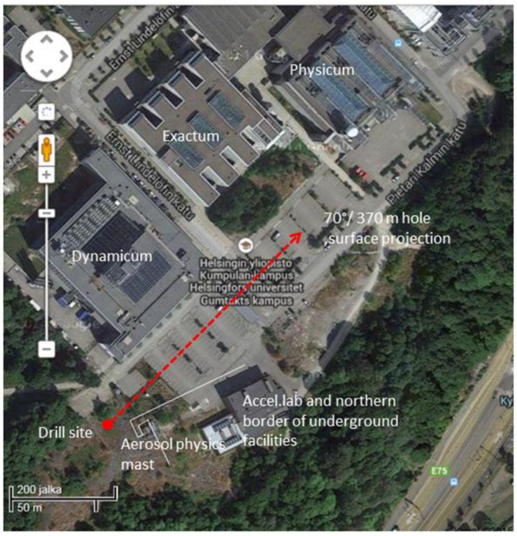


**Figure 1.** Drill site and surface projection of the Kumpula campus hole.

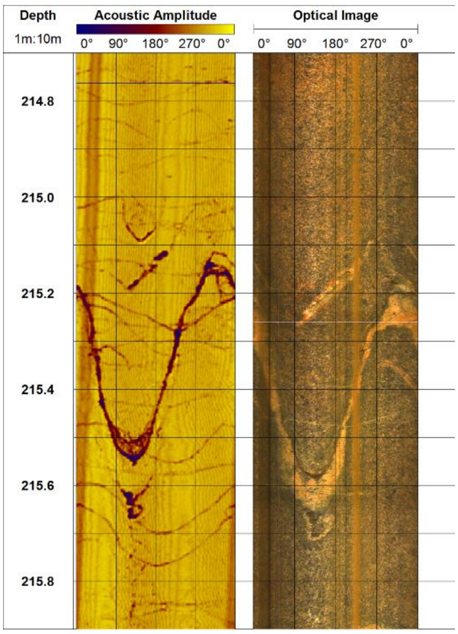


**Figure 2.** Open and closed fractures and neosome veins in gneiss at 215 m.

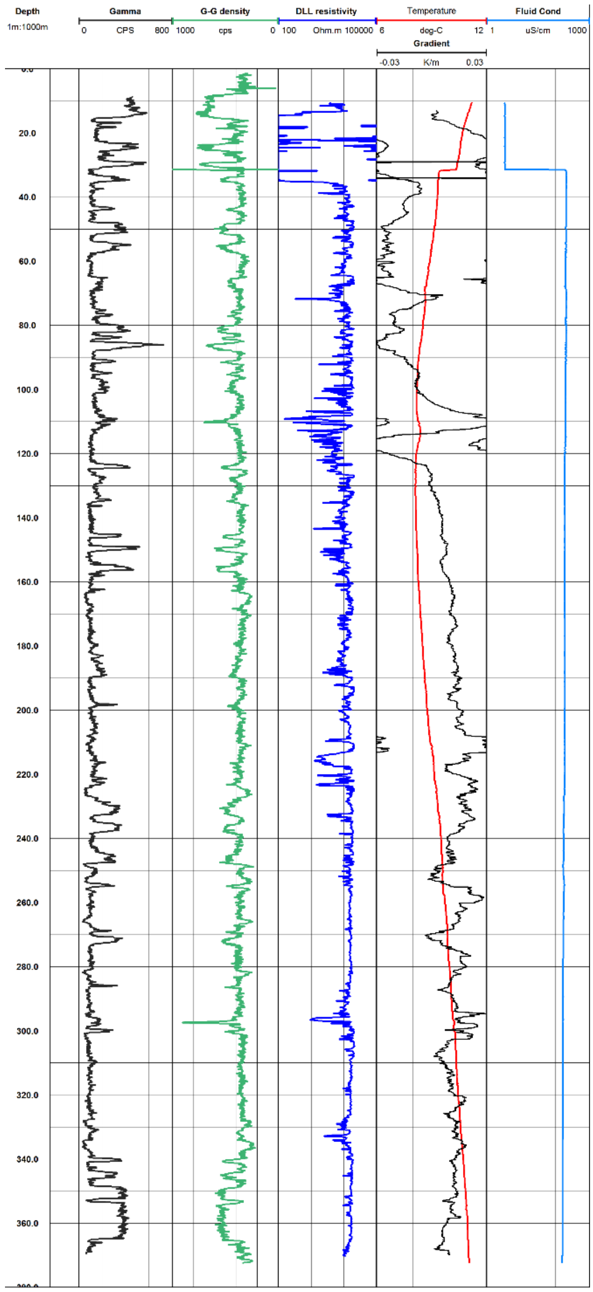


**Figure 3.** A selection of downhole logs

# Inari orocline – progressive or secondary orocline

R. Lahtinen[1], M. Sayab[1] and S.T. Johnston[2]

[1] PL 96 (Betonimiehenkuja 4), 02151Espoo, Finland
[2] A1-26 Earth Sciences Building, University of Alberta, Edmonton, Alberta, Canada T6G 2E3
E-mail: raimo.lahtinen@gtk.if

Inari orocline is a collage of Lapland granulite belt (LGB) and the Tana (TB) and Karasjok (KB) belts. The arcuate shape geometry of the Inari orocline has been traditionally interpreted to have formed coevally with SW directed thrusting. We propose, based on preliminary data and interpretations, that the Inari orocline is instead a secondary orocline, characterized by radial fractures and conical folds, formed during buckling about a vertical axis of rotation. Also the formation of Au mineralizations can be tentatively linked to the buckling stage.

**Keywords:** orocline, orogen, lithosphere, crust, Fennoscandia

## 1. Introduction

Oroclines or curvatures of previously linear arcs (or belts) are tectonic structures that bridge manufacturing of arcs and formation of stable, equant continental blocks. Oroclines are well documented and spatially distributed on a global scale and form curved mountain belts of varying degree both in young and ancient orogens (Johnston et al., 2013). We have recently demonstrated that the Precambrian terranes offer excellent exposures, representing windows into deep levels of orogens, to study the crustal roots of oroclines by taking the Bothnian oroclines of Fennoscandia as an example (see Fig. 1; Lahtinen et al., 2014). Johnston et al. (2013) recognized two distinct types of oroclines: progressive and secondary. Progressive oroclines are thin-skinned (thrust sheet/thrust belt) and develop during thrusting in response to the same orogen-perpendicular stress responsible for thrust sheet emplacement. Secondary oroclines occur at the scale of an orogen, are plate-scale features that affect crust and lithospheric mantle, and form in response to an orogen parallel principal shortening direction.

## 2. Inari Orocline

Inari orocline (Fig. 1) is a collage of the Lapland granulite (LGB), Tana (TB) and Karasjok (KB) belts. The TB and KB are located south-southwest and northwest of the LGB, respectively (not shown in the map). The LGB is correlated with the Umba granulite belt (UB in Fig. 1) suggesting continuation of the Inari orocline to the southeast. The bending of the Belomorian rocks (marked with ? in Fig. 1) is probably also related to the formation of the Inari orocline. The evolution of the LGB in Finland has been studied for decades by Finnish (Tuisku and Huhma, 2006 and Tuisku et al., 2006 and references therein) and French geologists (Cagnard et al., 2011 and references therein) and most of them agreed that the lithological package (LGB+TB+KB) developed between 1.91-1.87 Ga during SW directed thrusting and shortening. The arcuate shape geometry of the LGB has been considered coeval with thrusting (e.g., Gaál et al., 1989) suggesting that the Inari orocline constitutes a progressive orocline.

## 3. Secondary orocline hypothesis

Existing studies (see above) indicate that the peak metamorphic conditions of the Inari orocline were attained just before or syn- thrusting followed by decompression. Coeval basal thrusting and early normal-sense shear-zones have been considered important in the exhumation history (Cagnard et al., 2011). Based on existing studies and our preliminary field data we propose following stages for the LGB evolution: 1) extension/thrusting and intrusion of enderbites at ≥1.91 Ga leading to peak metamorphic conditions; 2) main thrusting phase at ≤1.91 Ga (Fig.

1); 3) extension and decompression melting at 1.90-1.88 Ga; 4) renewed shortening with relatively low angle to stage 2 thrusting at 1.88-1.87 Ga; 5) buckling at ≤1.87 Ga.

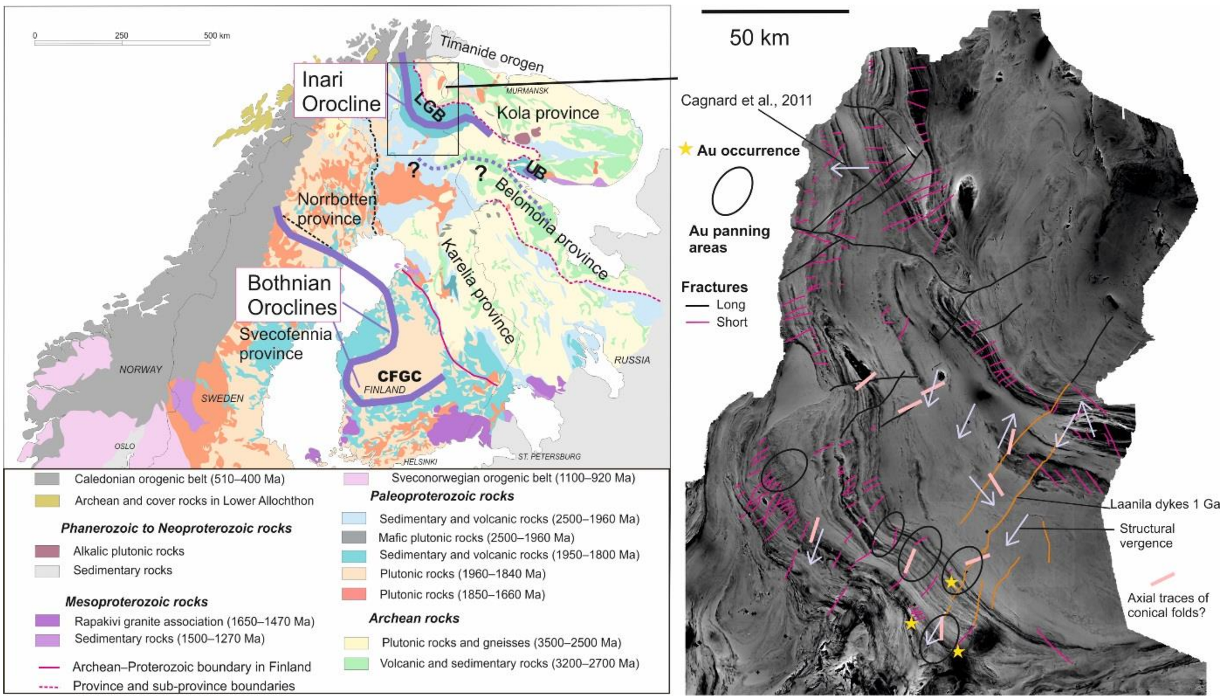


**Figure 1.** Left: A geological map of Fennoscandia. CFGC – Central Finland Granitoid Complex; LGB – Lapland granulite belt; UB – Umba granulite belt. Right: Aeromagnetic map of the inset area. Fractures interpreted from the aeromagnetic map and structural vergence directions and axial traces are based on preliminary data. Map data from GTK.

We propose that layer specific short fractures and conical folds in the Inari Orocline (Fig. 1) are radial features and have formed during large-scale buckling about a vertical axis of rotation in response to an orogen parallel principal compressive stress. Gold mineralization can be tentatively linked to the buckling stage.

## References:

Cagnard, F., Barbey, P., Gapais, D., 2011. Transition between “Archaean-type” and “modern-type” tectonics: Insights from the Finnish Lapland Garnulite Belt. Precambrian Research 187, 127-142.

Gaál, G., Berthelsen, A., Gorbatschev, R., Kesola, R., Lehtonen, M.I., Marker, M., Raase, P., 1989. Structure and composition of the Precambrian crust along the POLAR Profile in the northern Baltic Shield. Tectonophysics 162, 1–25.

Johnston, S.T., Weil, A.B., Gutiérrez-Alonso, G., 2013. Oroclines: Thick and thin. Geological Society of America Bulletin 125, 643–663.

Lahtinen R., Johnston S.T., Nironen M., 2014. The Bothnian coupled oroclines of the Svecofennian Orogen: a Palaeoproterozoic terrane wreck. Terra Nova 26, 330-335.

Tuisku, P., Huhma, H., 2006. Evolution of migmatitic granulite complexes: implications from Lapland Granulite Belt, part II: Isotopic dating. Bulletin Geological Society Finland 78, 143–175.

Tuisku, P., Mikkola, P., Huhma, H., 2006. Evolution of migmatitic granulite complexes: implications from Lapland Granulite Belt, part I: metamorphic petrology. Bulletin Geological Society Finland 78, 71–105.

# A shoshonitic dyke in Lohja, southern Finland

Marek Lehtinen[1], Markku Väisänen[1], Jaakko Kara[1], Hugh O'Brien[2] and Marja Lehtonen[2]

[1]Department of Geography and Geology, 20014 University of Turku, Finland
[2]Geological Survey of Finland, 02151 Espoo, Finland
E-mail: mmtleh@utu.fi

We describe here a newly discovered cross-cutting mafic dyke in the vicinity of Lohja, southern Finland. The dyke is E-W trending and about 6 m in width. Only a few zircons were recovered from the dyke despite the high Zr contents and they all were inherited. Therefore, the crystallisation age remains uncertain. The dyke is shoshonitic in composition and the closest analogues are the Åva lamprophyre dykes in SW Finland.

**Keywords:** postorogenic, dyke, enriched mantle, Fennoscandia, Lohja

## 1. Introduction

Post-tectonic mafic dykes of different ages and compositional groups cross-cut sharply the Svecofennian bedrock in central and southern Finland and Russian Karelia (Figure 1). The main groups from oldest to youngest are:

a) 1.84-1.83 Ga lamprophyre dykes of eastern Finland (Neuvonen et al. 1981, Laukkanen 1983, O'Brien et al. 2005)
b) 1.79-1.78 Ga lamprophyre dykes of SW Finland and Russian Karelia (Eklund et al. 1998, Andersson et al. 2006, Woodard et al. 2014)
c) 1.65-1.54 Ga diabase dykes related to rapakivi granite magmatism (Rämö and Haapala 2005)
d) 1.26 Ga diabase dykes of the Satakunta area (Suominen 1991, Kohonen and Rämö 2005)

In Uusimaa, southern Finland, several diabase dykes cut the Svecofennian host rock (Figure 1). To the west of the 1.65 Ga Bodom and Obbnäs rapakivi granite intrusions is the Lohja diabase swarm, where the largest estimated dyke is 30 km long and 10 m wide (Vaasjoki 1977, Laitala 1987, 1994).

A newly discovered dyke from the Lohja area apparently belongs to the Lohja swarm. We compare the geochemistry of this dyke with data from the above-mentioned main groups to estimate whether it belongs to some of them. We also present a preliminary U/Pb age dating of the dyke.

## 2. The Lohja dyke

The studied mafic dyke is located about 25 km NW from the town of Lohja in a road cut of the E18 Turku-Helsinki motorway (Figure 1). The dyke is E-W-trending, 5-6 m in width and sharply cross-cuts the surrounding Svecofennian migmatitic garnet-cordierite mica gneiss. The inner parts of the dyke are fine to medium-grained and show an ophitic texture, whereas the contact to the country rock shows a chilled margin with aphanitic, almost glassy texture. On a fresh surface the rock is dark grey, and it contains rounded xenoliths of varying colour and size. The main minerals are plagioclase, hornblende, brown mica with secondary carbonate and chlorite. The EDS-analyses with FE-SEM also identified rutile, titanite, galena, sphalerite, apatite, baryte, epidote, allanite and bastnäsite in the same heavy mineral fraction that contained the zircons. The reddish xenoliths are less than 5 mm wide and the light-coloured are larger, ~ 20 mm wide. There are also ~ 5 mm wide amygdales, filled with carbonate and chlorite (Figure 2).

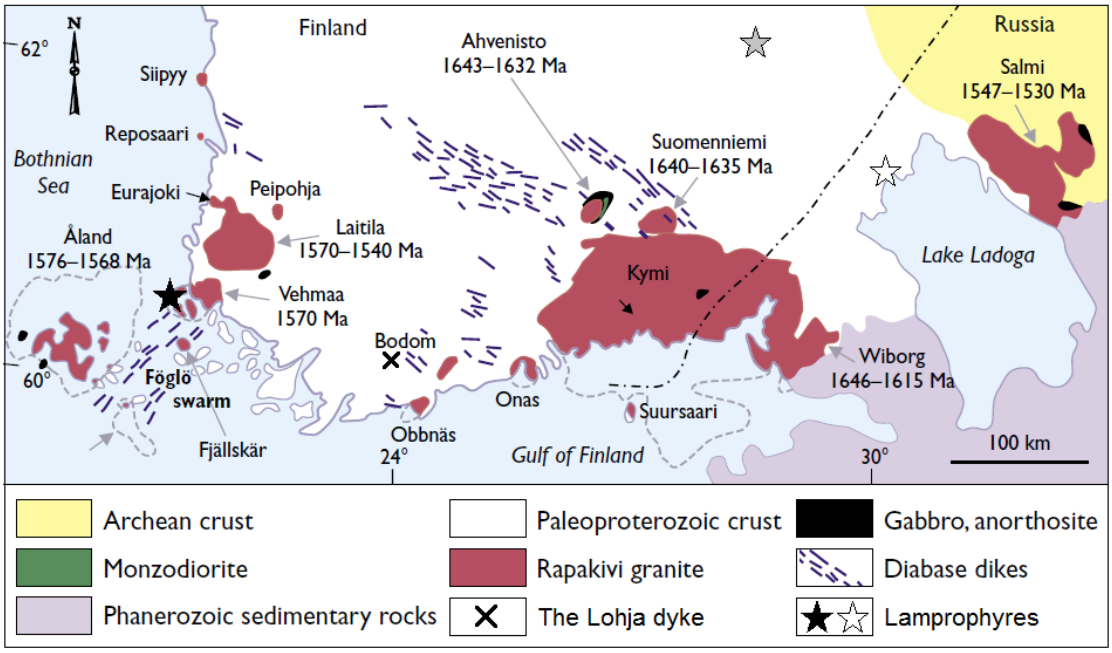


**Figure 1.** Geological map of southern Finland focusing on diabase dykes and rapakivi granites. Stars indicate lamprophyres: black for Åva (Andersson et al. 2006), grey for eastern Finland (Laukkanen 1983) and white for Russian Karelia (Woodard et al. 2014). Cross indicates the Lohja dyke (modified after Rämö and Haapala 2005).

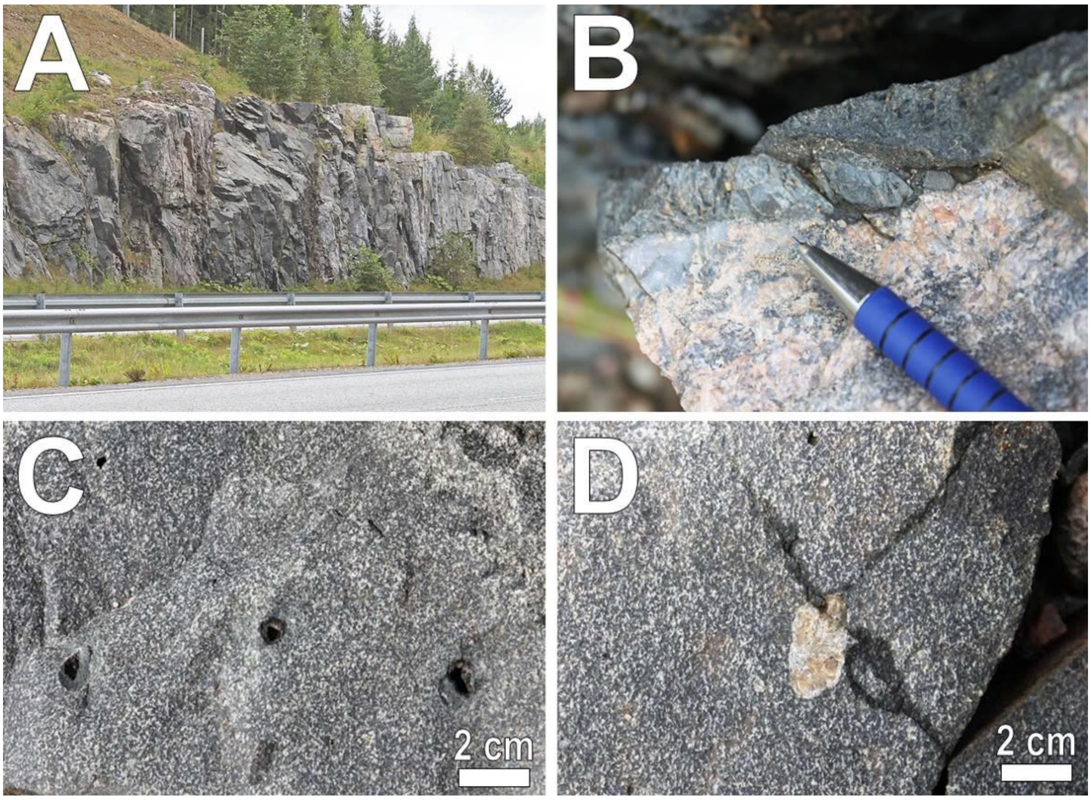


**Figure 2.** Outcrop photographs of the Lohja dyke. (A) Road cut of the E18 motorway showing the 5.5 m wide cross-cutting mafic dyke. (B) Sharp contact with a chilled margin. (C) Carbonate- and chlorite-filled amygdales. (D) Light-coloured felsic xenolith. Ophitic texture is visible in the mafic dyke.

**3. U/Pb age dating and geochemistry**

From quite a big sample (~ 6 kg), only 10 zircons were recovered after the standard heavy mineral separation process. The BSE-imaging and isotopic analyses were performed in the Finnish Geosciences Research Laboratory (GTK, Espoo, Finland) using the FE-SEM and LA-SC-ICPMS for imaging and isotope analyses, respectively. The U/Pb analyses were performed in two steps. Firstly, one spot was placed on each zircon. These showed a range of $^{207}Pb/^{206}Pb$ ages between 1.52-1.86 Ga. Therefore, the two youngest zircons were selected for additional analyses. All combined the results show three groups: (i) 20 analyses with ages between 1.80-1.86 Ga, (ii) a cluster of 7 analyses with a concordia age of c. 1.78 Ga and (iii) a cluster of 5 analyses with a concordia age of c. 1.68 Ga. We also tested U-Pb dating on rutile and titanite. The rutile was devoid of radiogenic Pb and was discarded. The titanite contained some radiogenic Pb but 30 analyses nevertheless showed too low contents of radiogenic Pb and gave geologically meaningless results.

Three samples were collected for geochemical analyses; two from the centre of the dyke and one from the chilled margin. They all have very similar compositions and form a tight cluster in most diagrams. The dyke shows high content of $Fe_2O_3$ but very low MgO, CaO and Mg-number along with low ferromagnesian trace element contents (Ni, Cr, Co). The dyke is enriched in Rb, Ba, Y and especially in Zr, and shows a fractionated REE pattern. High $K_2O$ content, $K_2O/Na_2O$ and Ce/Yb vs. Ta/Yb ratios show that the composition is shoshonitic.

**4. Discussion and conclusions**

Despite the high Zr content, very few zircons were recovered and their U/Pb analyses showed that they were inherited from older rocks. Zircons either did not crystallize from such a melt or they were too small and were lost during the separation. Many of the zircons had been heterogeneously affected by some later geological event. The 1.78 Ga age might readily correlate with the well-documented post-orogenic magmatism which includes lamprophyre dykes. The 1.68 Ga age is unclear as no such a geological event is known in southern Finland. Those ages might represent incomplete resetting during the 1.65 Ga magmatic pulse represented by the Bodom and Obbnäs rapakivi plutons. In summary, the crystallisation age of the Lohja dyke remains uncertain.

The composition of the dyke is more enriched than the rapakivi-related dykes or the 1.26 Ga dykes, but less enriched than the lamprophyre dykes in the reference data set (Savolahti 1964, Laitakari 1969, Laukkanen 1983, Rämö 1990, 1991, Suominen 1991, Lindberg and Bergman 1993, Väisänen 2004, Luttinen and Kosunen 2006, Woodard et al. 2014). The closest analogue is the Åva lamprophyre dykes with partially overlapping geochemical characteristics (Hollsten 1997, Eklund et al. 1998, Andersson et al. 2006). However, the Åva data is more enriched, e.g., in LREE, Ba, Sr and F. Therefore, we prefer to call the Lohja dyke a shoshonitic dyke rather than a lamprophyre dyke.

**5. Acknowledgements**

This study was funded by the Finnish Cultural Foundation, Varsinais-Suomi Regional Fund and the Turku University Foundation.

**References:**

Andersson, U. B., Eklund, O., Fröjdö, S. and Konopelko, D. 2006. 1.8 Ga magmatism in the Fennoscandian Shield; lateral variations in subcontinental mantle enrichment. Lithos 86, 110–136.

Eklund, O., Konopelko, D., Rutanen, H., Fröjdö, S. and Shebanov, A. D. 1998. 1.8 Ga Svecofennian post-collisional shoshonitic magmatism in the Fennoscandian shield. Lithos, 45, 87–108.

Hollsten, S. 1997. Lamprofyrernas klassificering och petrologi med tillämpning på Åvamassivets lamprofyrgångar i sydvästra Finland. Master's Thesis, Department of Geology, Åbo Akademi University, Finland, 67 p.

Kohonen, J., and Rämö, O. T. 2005. Sedimentary rocks, diabases, and late cratonic evolution. In: Lehtinen, M., Nurmi, P.A., and Rämö, O. T. (Eds.), Precambrian Geology of Finland – Key to the Evolution of the Fennoscandian Shield. Elsevier Science B. V., Amsterdam, 563–604.

Laitakari, I. 1969. On the Set of Olivine Diabase Dikes in Häme, Finland. Bulletin de la Commission geologique de Finlande 241, 66 p.

Laitala, M. 1987. Diabase dykes in the coastal area of the Uusimaa province. In: Aro, K., and Laitakari, I. (Eds.), Diabases and Other Mafic Dyke Rocks in Finland. Geological Survey of Finland, Report of Investigation 76, 129–131.

Laitala, M. 1994. Lohja. Bedrock map 1:100 000 – Maps of Pre-Quaternary Rocks, Sheet 2041, Geological Survey of Finland.

Laukkanen, J. 1983. Itä-Suomen lamprofyyrit ja lamprofyyriproblematiikka. Master's Thesis, Department of Geology and Geography, University of Turku, Finland, 108 p.

Lindberg, B., and Bergman, L. 1993. Pre-Quaternary rocks of the Vehmaa map-sheet area. Geological map of Finland 1: 100 000, Explanation to the maps of Pre-Quaternary rocks, Sheet 1042, Geological Survey of Finland, 56 p.

Luttinen, A. V. and Kosunen, P. J. 2006. The Kopparnäs dyke swarm in Inkoo, southern Finland: New evidence for Jotnian magmatism in the SE Fennoscandian Shield. In: Hanski, E., Mertanen, S., Rämö, T., and Vuollo, J. (Eds.), Dyke Swarms—Time Markers of Crustal Evolution. Balkema, London, 85–97.

Neuvonen, K. J., Korsman, K., Kouvo, O., and Paavola, J. 1981. Paleomagnetism and age relations of the rocks in the main sulphide ore belt in central Finland. Geological Society of Finland Bulletin 53, 109–133.

O'Brien, H.E., Peltonen, P., and Vartiainen, H., 2005. Kimberlites, carbonatites, and alkaline rocks. In: Lehtinen, M., Nurmi, P.A., and Rämö, O. T. (Eds.), Precambrian Geology of Finland – Key to the Evolution of the Fennoscandian Shield. Elsevier Science B. V., Amsterdam, 605–644.

Rämö, O. T., 1990. Diabase dyke swarms and silicic magmatism - Evidence from the Proterozoic of Finland. In Parker, A. J., Rickwood, P. C., and Tucker, D. H. (Eds.), Mafic dykes and emplacement mechanisms. Balkema A. A., Rotterdam, Brookfield, 185–199.

Rämö, O. T. 1991. Petrogenesis of the Proterozoic rapakivi granites and related basic rocks of southeastern Fennoscandia: Nd and Pb isotopic and general geochemical constraints. Geological Survey of Finland Bulletin 355, 165 p.

Rämö, O. T. and Haapala, I., 2005. Rapakivi granites. In: Lehtinen, M., Nurmi, P. A., and Rämö, O. T. (Eds.), Precambrian Geology of Finland – Key to the Evolution of the Fennoscandian Shield. Elsevier Science B. V., Amsterdam, 533–562.

Savolahti, A. 1964. Olivine diabase dike of Ansio in Padasjoki, Finland. Bulletin de la Commission geologique de Finlande 215, 99–111.

Suominen, V. 1991. The chronostratigraphy of southwestern Finland: with special reference to Postjotnian and Subjotnian diabases. Geological Survey of Finland Bulletin 356, 110 p.

Vaasjoki, M. 1977. Rapakivi granites and other postorogenic rocks in Finland: their age and the lead isotopic composition of certain associated galena mineralizations. Geological Survey of Finland Bulletin 294, 64 p.

Väisänen, M. 2004. Mynämäen karttalehden 1044 kallioperäkartoituksen loppuraportti. Geological Survey of Finland, Report File 4898, 22 p.

Woodard, J., Kietäväinen, R. and Eklund, O. 2014. Svecofennian post-collisional shoshonitic lamprophyres at the margin of the Karelia Craton: Implications for mantle metasomatism. Lithos 205, 379–393.

# Natural Remanent Magnetisation of Selected Rock Samples from the Finnish Bedrock: Implications for Structural Modelling of Magnetic Data

H. Leväniemi[1], R. Lahtinen[1], S. Mertanen[1] and H. Säävuori[1]

[1] Geological Survey of Finland, P.O. Box 96, 02151 Espoo
E-mail: hanna.levaniemi@gtk.fi

High intensity of natural remanent magnetisation in rock formations complicates their modelling based on magnetic survey data, especially in cases where the direction of remanence is unknown. In this paper we present a dataset of samples with high natural remanent magnetisation intensities collected throughout the Finnish bedrock and discuss some preliminary observations on the data characteristics and their implications on modelling.

**Keywords:** natural remanent magnetisation, magnetic modelling, Finland

## 1. Introduction

The local variation in the properties and distribution of magnetic minerals (most notably magnetite and pyrrhotite) in the crust result in anomalies observed on any magnetic survey map. The local anomaly shape and amplitude is affected by the type and characteristics of the magnetisation of the minerals: the total magnetisation $\mathbf{M_{total}}$ of rock is a sum of two components, namely the induced magnetisation $\mathbf{M_i}$ and remanent magnetisation $\mathbf{M_r}$:

$$\mathbf{M_{total}} = \mathbf{M_i} + \mathbf{M_r} = k\mathbf{H} + \mathbf{M_r} \quad (1)$$

where $k$ is magnetic susceptibility and $\mathbf{H}$ the Earth's magnetic field intensity. Magnetic susceptibility is a parameter readily measurable with either field or laboratory equipment. Thus, as the direction of the $\mathbf{M_i}$ is aligned with the Earth's field, the induced magnetisation vector can typically be estimated with some confidence for magnetic anomaly modelling purposes. However, applying the permanent remanent magnetisation component $\mathbf{M_r}$ to modelling is more complex as the direction as well as the magnitude of the component vector need to be determined; this requires oriented sampling and laboratory measurements. Hence the remanent component is often neglected in the modelling workflow.

Ferromagnetic minerals are composed of 'magnetic domains'. In the single domain (SD) type the grain size is very small and all magnetic moments within the grain point to the same direction. SD minerals can carry a strong remanent magnetisation which can retain its original direction for billions of years. In rocks with coarse grained ferromagnetic minerals, multi-domain (MD) type dominates, and the magnetic moments within the grain point to varying directions. So called viscose remanence (VRM) can be easily formed in such grains, when the remanent magnetisation gradually aligns to the direction of the external magnetic field. Small-grained pyrrhotite and magnetite typically contain SD grains, whereas large-grained ferromagnetic minerals are typically of MD type (e.g. Butler 1992).

When modelling of bedrock features based on magnetic survey data, we are interested in the current *in-situ* remanent magnetisation of the rock, i.e. the natural remanent magnetisation (NRM) prevailing in the rock at the time of the magnetic survey. The magnitude of NRM can be measured for any rock sample, and the Königsberger ratio (Q) denotes the significance of NRM as a magnetic anomaly source in comparison to induced magnetisation:

$$Q = |\mathbf{M_r}| / |\mathbf{M_i}| \quad (2)$$

For rocks with Q > 1, remanent magnetisation dominates over the induced component. In case the direction of a NRM with high Q value is unknown, magnetic modelling of bedrock structures becomes an ambiguous process (even more so than geophysical modelling in general) as there are simply too many degrees of freedom to solve the modelling problem reliably. The issue of NRM in modelling is yet more complicated than merely obtaining reliable parameter values: in deformed bedrock the NRM directions within a formation are typically dispersed in case the deformation takes place after the rock has gained a stable remanent magnetisation (e.g. Mertanen and Karell, 2015, and the references therein). Thus the directions of NRM also indicate tectonic and metamorphic events when observed locally. In general, Q values < 1 are typical of the Finnish bedrock, but especially for pyrrhotite-bearing schists higher values are common (Airo & Säävuori, 2013).

In this study we use samples with high intensity of remanent magnetisation selected from the Rock Geochemical Database of Finland (RGDB) (Rasilainen et al., 2007) of the Geological Survey of Finland (GTK) to display and discuss some NRM characteristics in the Finnish bedrock.

## 2. The NRM Dataset

The Rock Geochemical Database of Finland (Rasilainen et al., 2007), collected in 1990-1995, contains a total of 6,544 bedrock samples throughout Finland. The main purpose of the database is to represent a consistent, high-quality overview of the geochemical properties of the Finnish bedrock. Although not published, petrophysical laboratory measurements were also conducted for the sample dataset. These petrophysical data comprise determination of density, P-wave velocity, porosity, magnetic susceptibility and remanent magnetisation intensity and direction. The north directed samples were taken with a portable mini-drill and the N direction, measured with hand compass, can be estimated to be accurate within ±10º. Typically the drilling was performed vertically with an estimated variation of ±10º for inclination but on steeper outcrop surfaces this might have been higher.

The remanent magnetisation parameters were determined with the GTK in-house fluxgate equipment R2 (Puranen & Sulkanen, 1985), most optimal for samples with a volume of 200 $cm^3$ (Airo and Säävuori, 2013). With the RGDB samples with a diameter of 2.5 cm, the sample size proved to be too small to be measured with the fluxgate magnetometer for samples with weak to moderate remanence intensity. Duplicate measurements with sensitive SQUID magnetometer showed that only samples with NRM intensity ≥ 1000 mA/m had reliable precision in the fluxgate measurements. Thus in this study we have only included these samples in our inspection; the total number of samples in the subset is 357.

It should be noted that albeit we can only make use of a fraction of the RGBD sample dataset and the data is not representative for the overall distribution of the remanent magnetisation or Q value parameters in the Finnish bedrock, this is still (to our knowledge) the largest coherent national database of the NRM directions, as the GTK petrophysical sample database (Säävuori and Hänninen, 1997) with over 130,000 samples only contains the intensity of the NRM but not the direction.

## 3. The NRM Directions and Magnitudes in the Dataset

The NRM directions and the related Q values with a histogram of all samples are presented in Figure 1. For samples with a NRM direction close to the current Earth's magnetic field direction (declination D = 10 ± 20° and inclination I = 75 ± 20°; a total of 21 samples), the Q values largely remain below value 1, suggesting that in these samples the remanent magnetisation is aligned in the direction of the current inducing field, the NRM being viscose remanence.

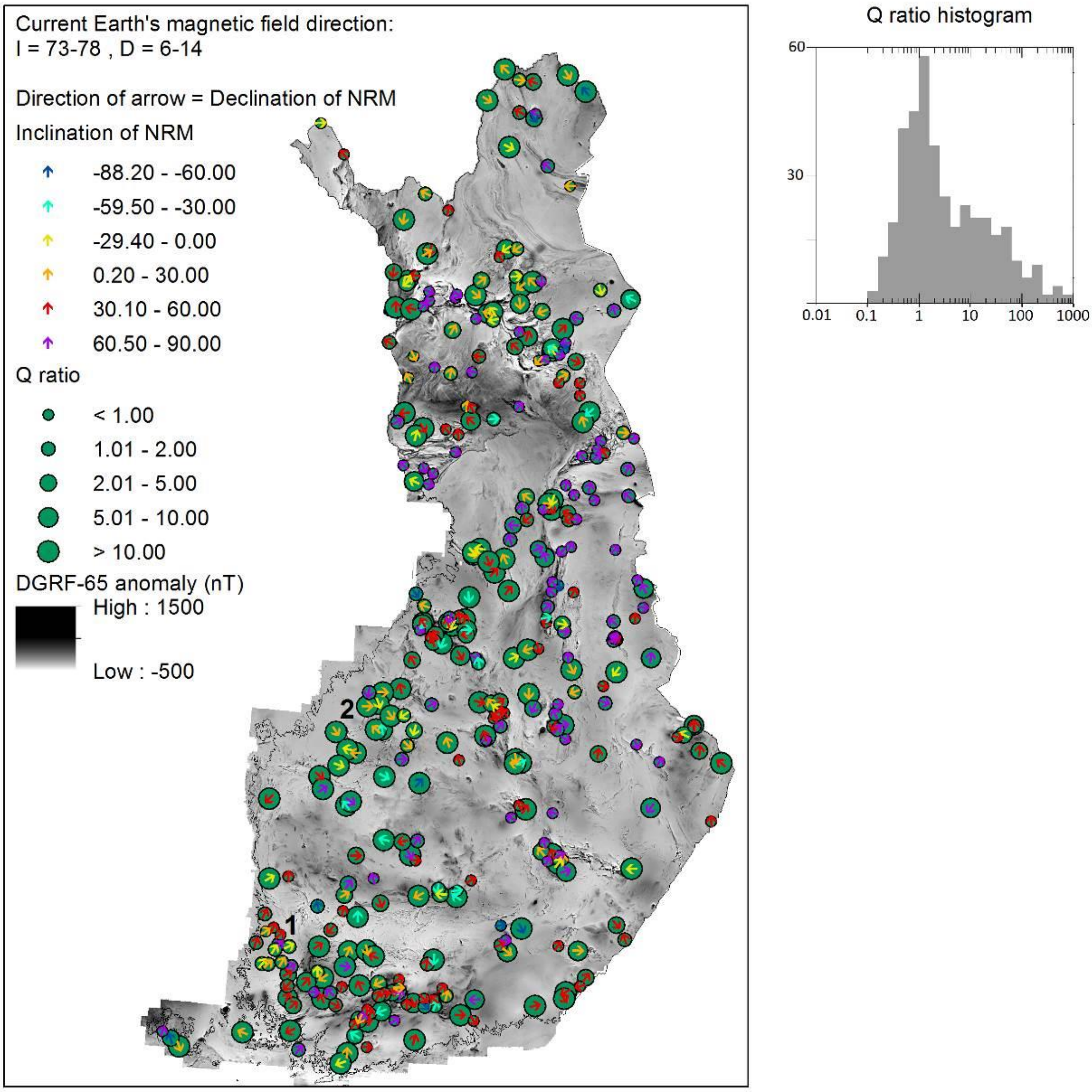


**Figure 1.** The NRM directions and Q ratios for the RGDB samples with intensity of NRM ≥ 1000 mA/m. Numbered regions: 1 = Satakunta, 2 = Pohjanmaa. Background map: GTK airborne magnetic data.

The majority of the data does not conform to the current direction of the Earth's magnetic field. We are planning to do more detailed study on the regional NRM variation, but based on visual inspection, two examples of NRM 'domains' are presented here. In the undeformed Satakunta dolerites the remanence directions have low NE pointing directions, which are in agreement with paleomagnetic studies of Neuvonen (1965), although there's more variance in the inclination directions. In the Pohjanmaa region the population of samples with Q > 10 are mainly related to pyrrhotite-rich volcanic and sedimentary rocks; the variation in the declination directions of these supracrustal rocks seem to correlate with structural vergence directions and later folding. Accordingly, when dealing with pyrrhotite, a factor to be taken into account is the strong intrinsic magnetocrystalline anisotropy caused by the lattice structure of the mineral (Dunlop & Özdemir 1997). Due to the anisotropy the remanent magnetization may be deflected from the direction of the ambient geomagnetic field. The remanence direction is then controlled by the geological structures and does not correctly reflect the external magnetic field (e.g. Thomson et al. 1991).

## 4. Discussion

The dataset presented in this paper highlights some of the complex factors that need to be taken into consideration when using the NRM data in the context of modelling of bedrock structures from magnetic data. In case of prominent remanent magnetisation, excluding the information of remanence from modelling can lead to misinterpretation of bedrock structures. Hence, the NRM of the target region should be at least considered and preferably measured before the modelling takes place. In case the deformation events postdate the blocking of remanent magnetisation, including the NRM direction reliably in any model is a challenging task that requires knowledge on the structural characteristics of the region. However, variation in the NRM directions itself is an indication of deformation.

## References:

Airo, M.-L., Säävuori, H., 2013. Petrophysical characteristics of Finnish bedrock – Concise handbook on the physical parameters of bedrock. Geological Survey of Finland, Report of Investigation 203, 33 pages.

Butler, R. F., 1992. Paleomagnetism: Magnetic Domains to Geological Terranes. Boston: Blackwell Scientific, 319 pages.

Dunlop, D. J., Özdemir, Ö., 1997. Rock Magnetism: Fundamentals and Frontiers, Cambridge Studies in Magnetism. Cambridge: Cambridge University Press, 573 pages.

Mertanen, S., Karell, F., 2015. Petrophysical and rock magnetic studies to aid Au exploration – case studies from the Häme belt, southern Finland. In: Airo, M.-L. (ed.) Geophysical signatures of mineral deposit types in Finland. Geological Survey of Finland, Special Paper 58, 89-106.

Neuvonen, K. J., 1965. Paleomagnetism of the dike systems in Finland, I. Remanent magnetisation of Jotnian olivine dolerites in southwestern Finland. Comptes Rendus de la Société géologique de Finlande 37, 153-168.

Puranen, R., Sulkanen, K., 1985. Technical description of microcomputer-controlled petrophysical laboratory. Geological Survey of Finland, unpublished report Q15/27/85/1, 257 pages.

Rasilainen, K., Lahtinen, R., Bornhurst, T. J., 2007. The Rock Geochemical Database of Finland Manual. Geological Survey of Finland, Report of Investigation 164, 38 pages.

Säävuori, H., Hänninen, R., 1997. Finnish petrophysical database. In: Korhonen, J. V. (ed.) Petrophysics in potential field interpretation: First Workshop for the Finnish Geophysical Crustal Model Program. Abstracts, Espoo, Finland, 15-16 August, 1997. Geological Survey of Finland, Special Publications 23, 67 pages.

Thomson, G. F., Cornwell, J. D. & Collinson, D. W. 1991. Magnetic characteristics of some pyrrhotite-bearing rocks in the United Kingdom. Geoexploration 28, 23–42.

# The seismic signature of the Kylylahti deposit: Initial results from new petrophysical measurements

T. Luhta[1], S. Mertanen[2], E. Koivisto[1], S. Heinonen[2], T. Törmälehto[3] and I. Kukkonen[4]

[1]Department of Geosciences and Geography, P.O. Box 64, FI-00014 University of Helsinki, Finland
[2]Geological Survey of Finland, P.O. Box 96, 02151 Espoo, Finland.
[3]Boliden Kylylahti, Kaivostie 9, FI-83700 Polvijärvi, Finland
[4]Department of Physics, P.O. Box 64, FI-00014 University of Helsinki, Finland
E-mail: tuija.luhta@helsinki.fi

We report new laboratory measurements on seismic P-wave velocities and densities for 216 rock samples from the Kylylahti mine, with the aim of studying the seismic signature of the Kylylahti deposit. The samples were chosen to represent, as well as possible, all the relevant lithological units and compositional variation in the Kylylahti area. The initial results indicate that the semi-massive to massive sulphide mineralizations cause a strong, reflected signal when in contact with any of the hosting rock types. The measurements were carried out at the Geophysical Laboratory of the GTK as a part of the COGITO-MIN project.

**Keywords:** petrophysics, Kylylahti deposit, mineral exploration

## 1. General

University of Helsinki, Geological Survey of Finland (GTK), Institute of Geophysics, Polish Academy of Sciences, Boliden Kylylahti, Vibrometric and Geopartner, research institutions and industry partners from Finland and Poland, are collaborating on the project COGITO-MIN (COst-effective Geophysical Imaging Techniques for supporting Ongoing MINeral exploration in Europe). COGITO-MIN aims to develop cost-effective, novel, geophysical deep mineral exploration techniques, with particular emphasis on seismic imaging (see for more in Koivisto et al., this volume). The seismic reflection data acquisition stage of the COGITO-MIN project took place from early August to late September 2016 in the vicinity of the Kylylahti Cu-Au-Zn mine in Polvijärvi, eastern Finland. The Kylylahti mine is operated by Boliden and is located at the northeastern side of the famous Outokumpu mining and exploration area containing Outokumpu assemblage rocks – i.e., serpentinite, carbonate, skarn and quartz rocks, usually wrapped in black schist and embedded in mica schist – that host Outokumpu-type Cu–Co–Zn–Ni–Ag–Au ores. The Kylylahti deposit comprises three north-northeast elongated semi-massive to massive sulphide lenses along a contact between the carbonate–skarn–quartz rocks and the black schists. The long history of geological and geophysical studies in the Outokumpu area, also including earlier seismic reflection profiles (e.g., Heinonen et al., 2011; Kukkonen et al., 2012), makes the site ideal for testing new concepts.

Accurate interpretation of the acquired COGITO-MIN seismic data relies upon accurate petrophysical characterization of the targets, in particular, upon understanding the acoustic properties in detail. Earlier borehole measurements on the seismic velocities and densities of the ore-bearing Outokumpu assemblage rocks reported by Heinonen et al. (2011), and theoretical seismic velocity and density estimations by Kukkonen et al. (2012) for the Outokumpu-type ores - as well as recent seismic forward modelling results by Komminaho et al. (2016) - imply that both the Outokumpu assemblage rocks and the ore bodies themselves produce detectable seismic signals. However, these results are based on geophysical logging data from the Outokumpu Deep Drill Hole at the southwestern side of the Outokumpu area, with no representative seismic velocity measurements for the Outokumpu assemblage rocks previously available from elsewhere in the overall Outokumpu area, and in particular, with no seismic velocity measurements available for the Outokumpu-type ores at all. The established variation of other petrophysical properties across the Outokumpu area (e.g., Leväniemi 2016), in particular the density variation, implies that also the reflectivity characteristics of the Outokumpu assemblage rocks and the Outokumpu-type ores may vary. Thus, new seismic velocity and density measurements, as well as measurements of other petrophysical properties, were conducted within the COGITO-MIN project during summer 2016, in order to better understand the acoustic properties of the Kylylahti exploration targets.

**2. Sample sets and measurements**

31 samples of the Outokumpu-type ores from the overall Outokumpu area were provided by Asko Kontinen. These were hand specimen samples and their exact coordinates were not known, only the general area of origin (e.g., Luikonlahti, Vuonos etc.). A total of 216 rock samples were provided by Boliden Kylylahti. The samples were mainly drill core samples from six different boreholes in the Kylylahti mine, but seven hand specimen samples were also collected from the piles of the excavated ore. The samples were chosen to represent, as well as possible, all the relevant lithological units and compositional variation in the Kylylahti area. The measurements were carried out at the Geophysical Laboratory of the GTK.

The samples were prepared to get even-ended and suitably sized pieces of the drill cores (or halves of them; the samples included both full drill cores and halved drill cores) and hand specimens. The parameters determined in the measurements were density, porosity, magnetic susceptibility and the intensity of remanent magnetization, electrical properties, including inductive and galvanic resistivity and chargeability, and P-wave velocity. Measurements were conducted according to the laboratory procedures of the GTK (e.g., Airo et al., 2011). Herein, results from the P-wave velocity and density measurements of the 216 samples provided by Boliden Kylylahti are reported.

P-wave velocities were measured using ultra-sonic transducer in room temperature and pressure. Samples were immersed in water for ten days before the first measurements. Measurements were then repeated twice more, after twenty and thirty days of immersion in water. Time of water immersion may have a considerable effect on the results; longer water immersion time increases the P-wave velocity (Airo et al., 2011; Säävuori, pers. comm. 2016). Velocities measured showed a small increase with the immersion time (less than one percent on average). Velocities shown here are weighted averages of all three measurements, with most weight given for the last measurement.

Density was determined by weighing a sample in air and suspended in water. The dry bulk density can be calculated from these measurements. Measuring accuracy is ±0.1%. Density was measured in the beginning of the measurements and after 30 days of soaking in water. The second density measurement was mainly to get the wet weight for porosity measurements.

**3. Results**

P-wave velocities and densities for the samples provided by Boliden Kylylahti are shown in Figure 1.

Generally, the results shown in Figure 1 indicate strong enough contrasts in acoustic impedances (product of density and seismic velocity) to produce a detectable reflected signal from contacts between the Outokumpu assemblage rocks and the surrounding black schists and mica schists, as well as varying acoustic impedances for the Outokumpu assemblage rocks. However, for example, a contact between mica schists and black schists may not produce a reflection, and the quartz rocks are associated with wide ranges of seismic velocity and density

*1A*

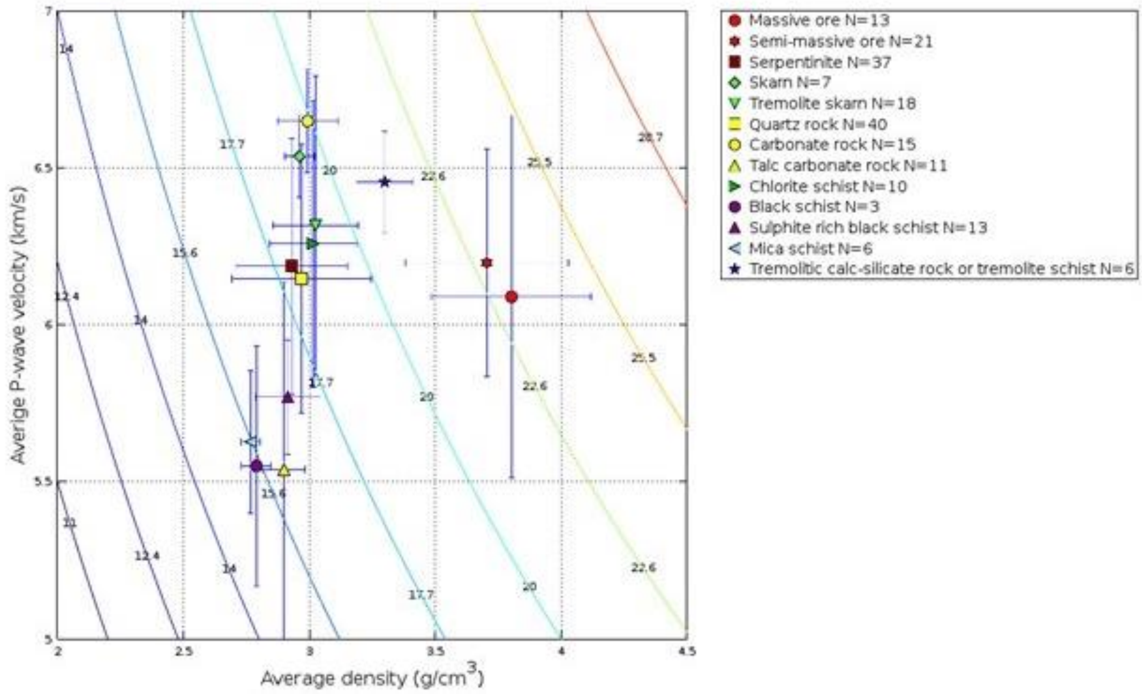


*1B*

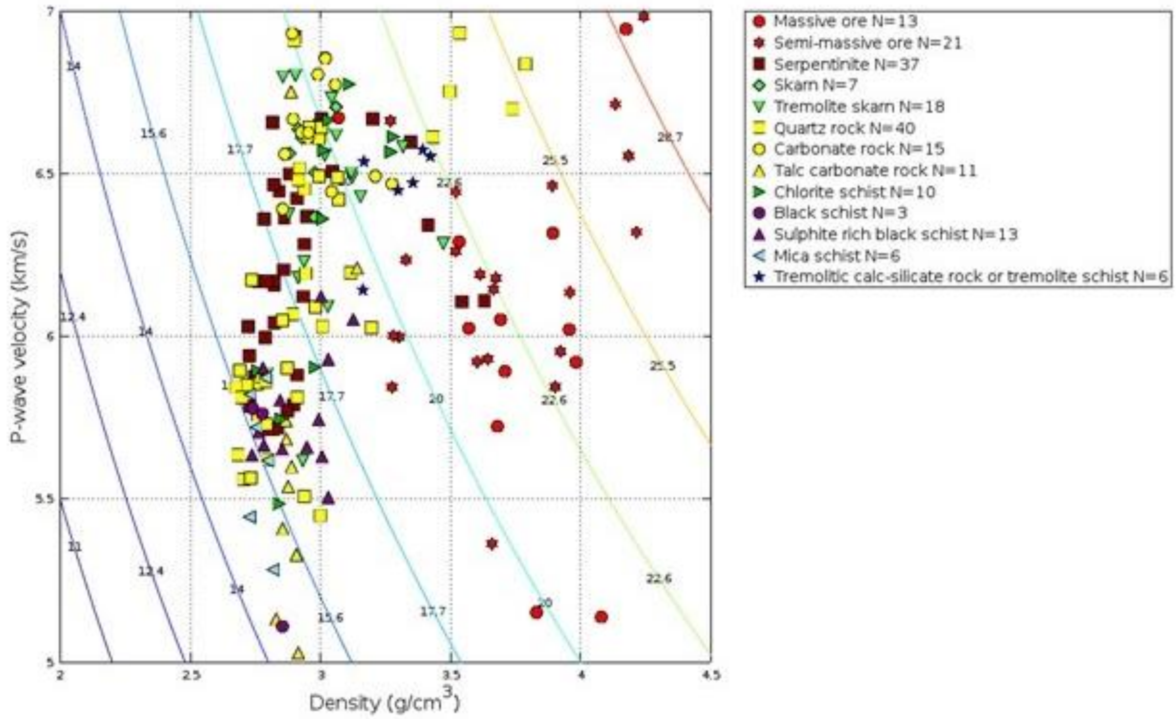


Figure 1. A) Average density and P-wave velocity for the 216 samples provided by Boliden Kylylahti, with standard deviations presented as error bars. B) The actual scatter plot for all the data. Constant acoustic impedance (product of density and seismic velocity) curves in MPa·s/m, with a line spacing corresponding to a reflection coefficient of 0.06 (considered to be enough for a detectable reflection; e.g., Salisbury et al., 1996) between two successive lines, are shown for reference. N in the legend indicates the number of samples.

values (Figure 1B) indicating that systematic reflected signals may not be produced from contacts to quartz rocks. Nevertheless, the semi-massive to massive sulphide mineralizations are characterized with distinctly higher densities, and therefore acoustic impedances, than the other rock types. Thus, the ore bodies should cause a strong, reflected signal when in contact with any of the Outokumpu assemblage rocks or black schists enveloping them.

**4. Conclucions**

These new petrophysical measurements give more insight to the representative acoustic properties of the Outokumpu assemblage rocks and the Outokumpu-type ores in the Kylylahti area. Before this study, no representative P-wave velocity measurements existed for the Outokumpu assemblage rocks at the eastern side of the Outokumpu area, and no P-wave velocity measurements for the Outokumpu-type ores at all. Density values seem to confirm trends found in previous studies (e.g., Leväniemi 2016).

Generally, the results of this study indicate strong enough contrasts in acoustic impedances to produce a detectable reflected signal from contacts between the Outokumpu assemblage rocks and the surrounding black schists and mica schists, as well as varying acoustic impedances for the Outokumpu assemblage rocks. In particular, the results indicate that the semi-massive to massive sulphide mineralizations should cause a strong, reflected signal when in contact with any of the hosting rocks.

Future work includes more detailed analyses of the measurements, with all the other petrophysical parameters measured, as well as available geochemical and geotechnical data on the same rock samples. The 31 hand specimen samples of the Outokumpu-type ores, not reported herein, will also be analysed. The results of the petrophysical analyses will be utilized in the interpretation (including seismic forward modelling) of the seismic reflection data acquired in the Kylylahti area during COGITO_MIN project.

**5. Acknowledgements**

The COGITO-MIN project has been funded through the ERA-MIN network. At the national level, the funding comes from Tekes in Finland and the NCBR in Poland.

**References:**

Airo, M.-L., Säävuori, H. Vuoriainen, S. 2011. Petrophysical properties of the Outokumpu deep drill core and the surrounding bedrock. In: Kukkonen, I. (ed.) Outokumpu Deep Drilling Project 2003-2010, Geological Survey of Finland, Special Paper 51, 63-82.

Heinonen, S., Kukkonen, I., Heikkinen, P., and Schmitt, D. 2011. High resolution reflection Seismics integrated with deep drill hole data in Outokumpu, Finland. In: Kukkonen, I. (ed.) Outokumpu Deep Drilling Project 2003-2010, Geological Survey of Finland, Special Paper 51, 105-118.

Kukkonen, I., T., Heinonen, S., Heikkinen, P. and Sorjonen-Ward, P. 2012. Delineating ophiolite-derived host rocks of massive sulfide Cu-Co-Zn deposits with 2D high-resolution seismic reflection data in Outokumpu, Finland. Geophysics 77, WC213-WC222.

Komminaho, K., Koivisto, E., Heikkinen, P., Tuomi, H., Hellqvist, N. and Kukkonen, I. 2016. Seismic ore exploration in the Outokumpu area, eastern Finland: Constraints from seismic forward modelling and geometrical consideration. Final report of the Tekes Green Mining project "Development Mine Camp Exploration Concepts and Technologies - Brownfield exploration", Special Paper of the Geological Survey of Finland. In print.

Leväniemi, H. 2016. Petrophysical parameters and potential field modelling in the Outokumpu Belt. Final report of the Tekes Green Mining project "Development Mine Camp Exploration Concepts and Technologies - Brownfield exploration", Special Paper of the Geological Survey of Finland. In print.

Salisbury M., Milkereit, B., and Bleeker, W., 1996, Seismic imaging of massive sulfide deposits: Part 1. Rock properties, Economic Geology 91, 821-828.

# Why 3D seismic data are an asset for both exploration and mine planning? Example of Kevitsa Ni-Cu-PGE, Finland

A. Malehmir[1], A. Tryggvason[1], C. Wijns[2], E. Koivisto[3], T. Lindqvist[3], P. Skyttä[4] and M. Montonen[5]

[1]Uppsala University, Uppsala, Sweden
[2]First Quantum Minerals Ltd., Perth, Australia
[3]University of Helsinki, Helsinki, Finland
[4]University of Turku, Turku, Finland
[5]Boliden FinnEx Oy, Kevitsa, Finland

E-mail: alireza.malehmir@geo.uu.se

Kevitsa is a disseminated Ni-Cu-PGE ore body in northern Finland, hosted by an extremely high-velocity (6-8 km/s) mafic-ultramafic intrusion. It is currently being mined at a depth of about 100 m using open-pit mining method. The mine life is expected to be about 20 years, with the final pit depth at around 400-500 m. Based on a series of 2D seismic surveys and given the expected mine life, a high-resolution 3D seismic survey was justified and acquired in winter 2010. Various researchers and teams have exploited these data because of the unique nature of geology, and the data being challenging to interpret but rich in reflectivity. In this study, we present 3D reflection data processing results and complement them with 3D first break tomography work recently carried out. The combined results allow to provide some insights about the nature of some of the reflectors. It for example shows how the tomography results can be used for rock quality studies and further planning of the pit. In particular, we observe a major fracture system, resolved by the tomography results and running in the middle of the planned pit, with the reflection data providing information about its depth extent, estimated to be at least about 500 m. We argue that 3D seismic data should be acquired prior to commencement of mining activities in order to maximize exploration efficiency at depth, but also to optimize mining as it continues towards depth.

**Keywords:** 3D seismic, hard rock, exploration, mining, Kevitsa

## 1. Introduction

Kevitsa 3D seismic survey (~ 9 $km^2$; winter 2010, Figure 1) was motivated by four 2D seismic profiles acquired in 2007 as a part of the HIRE national seismic program of the Geological Survey of Finland (Kukkonen et al., 2009; Koivisto et al., 2012 and 2015), with the primary goals of the 3D survey being open-pit mine planning and deep exploration of massive sulphide occurrences within the resource area (Malehmir et al., 2012; Malehmir et al., 2014). Disseminated Ni-Cu-PGE mineralization is hosted in olivine pyroxenite, Kevitsa intrusion, surrounded by volcano-sedimentary rocks. These various rock units exhibit velocities ranging from 4000 to 8000 m/s in more than 11 deep (> 800 m) boreholes logged using full-waveform sonic and VSP measurements (Malehmir et al., 2012). During the processing of the 3D data, it became obvious from the refraction static model that the bedrock required high velocities on the order of 7500 m/s within the planned open pit. Although the data were high seismic fold, respective receiver and shot line spacing of 70 and 80 m, and receiver and shot point spacing of 15 and 45 m, the high velocity background resulted in poor reflectivity signatures in the first couple of hundred meters of the migrated reflection volume (Malehmir et al., 2012). Pronounced reflectors within the planned open pit and greater Kevitsa intrusion were observed to start from 150-200 m depth and were related to either magmatic layering within the Kevitsa intrusion or faults and fracture systems both of which had implications for the design of the pit and future exploration at the site. A tomography test was conducted to cover the near surface reflectivity gap and, if possible, to be used for rock quality studies to aid mining at the site. No tie with surface geology has been possible until recent advance of mining to almost 100 m depth in certain locations, allowing improved interpretation of the reflection and tomography results, which will be the focus of this study.

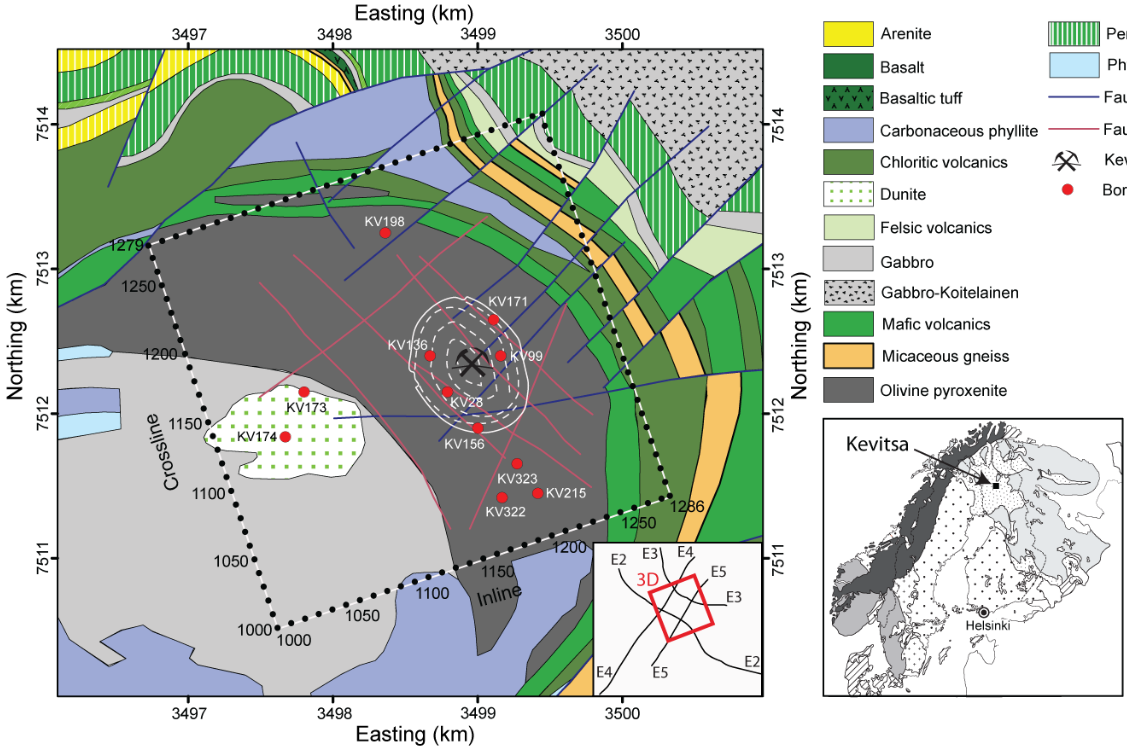


**Figure 1.** Geological map of Kevitsa showing the location of the planned open pit (stage 4), 3D seismic survey area, and 2D seismic profiles E2, E3, E4 and E5 in the inset map. The 3D seismic data and derived tomography results are the focus here.

## 2. 3D first break tomography

Turning-ray 3D traveltime tomography (Tryggvason et al., 2002) was carried out using about 2.5 millions of first breaks after testing various parameters and tuning the inversion parameters, also excluding bad quality picks. Tests were carried out using various cell sizes and various upper and lower velocity bounds. Finally, an inversion cell sizes of 10x10 m horizontally and 5 m vertically for the top of the model were selected. Below 50 m depth, cells of 10x10x10 m were used. The smaller cells on the top of the model were used to better account for the variable bedrock depth and to avoid velocity artefacts in deeper cells due to a large velocity contrast at the bedrock interface. In this case, a large velocity contrast between the glacial sediments and the bedrock was expected. In the end, the inversion was done in several steps, using a subset of the data to derive a coarse model that was later resampled to the final cell sizes. The final seven iterations with all the data were then done using this model as a starting model. This procedure was time consuming, but resulted in better data fit and a more reasonable model than if all the data were inverted in one step starting for example from a 1D starting model. The final 3D tomography model shows a maximum depth penetration of about 200 m with some gaps in the model (no ray coverage) around this depth range.

## 3. Results

Figure 2 shows a series of 3D views from the reflection seismic volume, bedrock surface as surveyed after the removal of overburden and prior to the start of mining, RQD and tomography velocity models. Several bedrock lineaments are notable particularly one running nearly in N-S direction (R8). Kevitsa intrusion is clearly notable in the tomography model as a region of high velocity. Nevertheless, a major low-velocity zone in the same direction as R8 and crossing the planned open pit can be seen in the depth slice of the tomographic model (Figure 2d). There are also indications of low and high velocity regions within the intrusion that may indicate variations in rock competency, probably due to the degree of talc alteration and fracturing. The low-velocity zone loses its definition towards greater depths in the tomography volume. However the reflection volume suggests a pronounced reflector (R8 at about -110 m elevation in Figure 2a) with similar orientation as the low-velocity zone suggesting the same structures. The exposed bedrock (Figure 2b) and drillhole fracture data indicate a brittle fracture and fault system (Lindqvist, 2014) gently WNW-dipping (about 35°). The R8 structure appears to also provide a boundary to the reflectivity pattern within the intrusion and thus may be important in controlling mineralization and its lateral extent in Kevitsa (Koivisto et al., 2015).

One of the objectives of the 3D tomography was to use the velocity model to predict probable blasting and crushing conditions in terms of rock competency. Rock competency can be related to both degree of fracturing, which is important in the near-surface region and close to large structures, and to talc alteration, which has important implications for crushing and processing. Figure 2c shows a 3D visualization of the RQD model derived from existing boreholes (interpolated using a distance weighting method) and can be compared with the tomography results shown in Figure 2d from the same view. A visual comparison between the

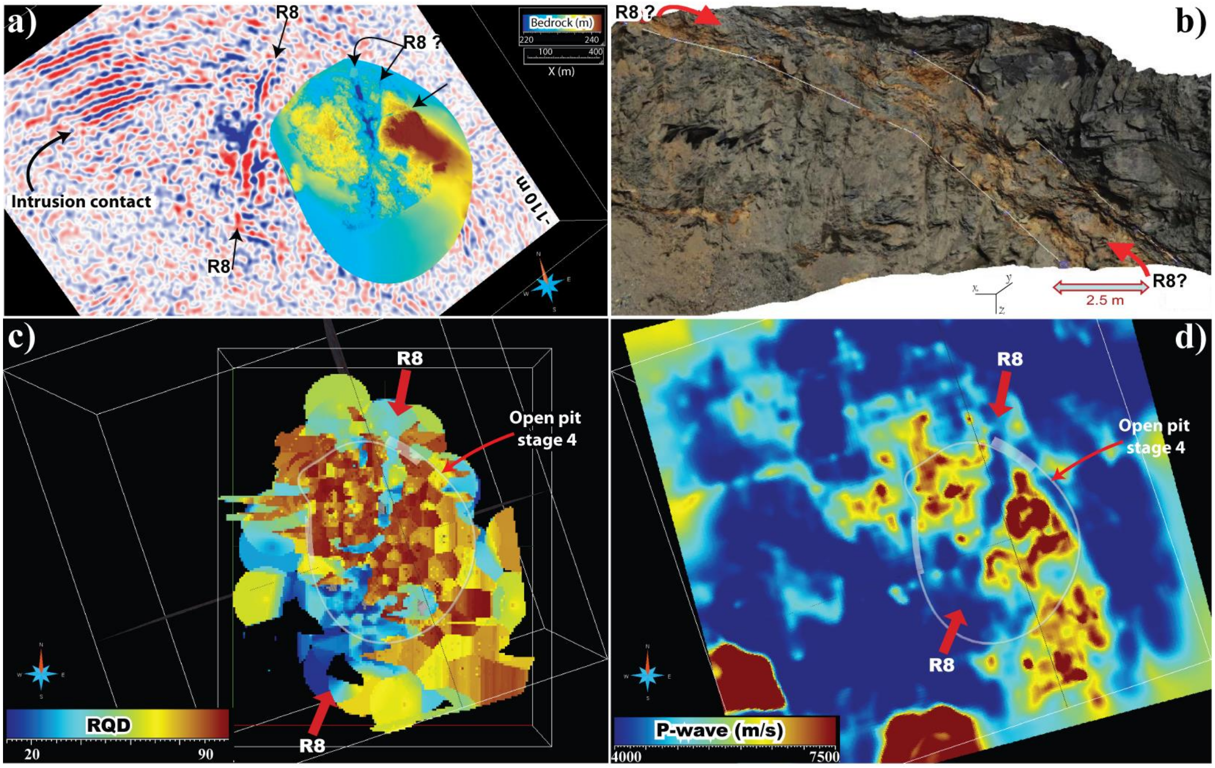


**Figure 2.** 3D views showing (a) a depth slice from the migrated volume at about 110 m below sea level, and bedrock surface (coloured region around 230 m above sea level) and lineaments (black arrows) as surveyed after the removal of the overburden and before mining activities commenced. Note some of the lineaments have similar orientation as the reflector (R8) seen at -110 m level in the reflection volume. (b) R8 is believed to be associated with a gently dipping fracture system as it is now being exposed and mined. (c) RQD versus (d) tomography models showing an excellent correspondence between the two and clear signature of the R8 fracture system in the models.

two models suggests a good correspondence between the low-velocity zones and low RQD regions suggesting that the velocity model can be used to help inform blasting, crushing, and processing behaviours.

## 4. Conclusions

3D tomography was employed to link near-surface geological features with those interpreted from the reflection seismic volume, given that the reflection seismic survey parameters and extremely high velocities caused a major loss of reflectivity near the surface. The tomography revealed a major low-velocity zone in the bedrock associated with a gently dipping reflector observed at about 150 m depth and extending to depths of more than 500 m. Qualitative correspondence between the velocity and RQD models implies that the velocity model can be used for predicting rock competency, and thus material behaviour during blasting, crushing and processing.

## 5. Acknowledgments

We are thankful to numerous people for their contributions to this work. FQM provided the seismic and support data for the interpretation of the results. HiSeis and Uppsala University acquired the 3D seismic data in Kevitsa. A similar version to this presentation was given at the first conference on geophysics for mineral exploration and mining, Barcelona, September 2016.

## References:

Lindqvist, T., 2014. 3D characterization of brittle fracture zones in Kevitsa open pit excavation, northern Finland. MSC thesis, University of Helsinki, Finland, 87 p.

Koivisto, E., Malehmir, A., Hellqvist, N., Voipio, T. and Wijns, C., 2015. Building a 3D model of lithological contacts and near-mine structures in the Kevitsa mining and exploration site, northern Finland: constraints from 2D and 3D reflection seismic data. Geophysical Prospecting, 63, 754-773.

Koivisto, E., Malehmir, A., Heikkinen, P., Heinonen, S. and Kukkonen, I., 2012, 2D reflection seismic investigations in the Kevitsa Ni-Cu-PGE deposit, northern Finland. Geophysics, 77, WC149-WC162.

Kukkonen, I., Lahti, I., Heikkinen, P., and HIRE Working Group of the Geological Survey of Finland, 2009. HIRE Seismic Reflection Survey in the Kevitsa Ni-PGE deposit, North Finland. GTK Report Q23/2008/59, 38 pp.

Malehmir, A., Juhlin, C., Wijns, C., Urosevic, M., Valasti, P. and Koivisto, E., 2012. 3D reflection seismic investigation for open-pit mine planning and exploration in the Kevitsa Ni-Cu-PGE deposit, Northern Finland. Geophysics, 77, WC95-WC108.

Malehmir, A., Koivisto, E., Manzi, M., Cheraghi, S., Durrheim, R., Bellefleur, G., Wijns, C., Hein, K. and King, N., 2014. A review of reflection seismic investigations in three major metallogenic regions: the Kevitsa Ni-Cu-PGE district (Finland), Witwatersrand goldfields (South Africa), and the Bathurst Mining Camp (Canada). Ore Geology Reviews, 56, 423-441.

Tryggvason, A., Rögnvaldsson, S. Th. and Flóvenz, Ó.G., 2002. Three-dimensional imaging of the Pand S-wave velocity structure and earthquake locations beneath Southwest Iceland. Geophys. J. Int., 151, 848-866.

# Digging deeper with LiDAR: Vertical slip profiles of post-glacial faults

J. Mattila[1], A. Ojala[2], R. Sutinen[3], J-P. Palmu[2] and T. Ruskeeniemi[2]
[1]1Posiva Oy, Olkiluoto, 27160, Eurajoki, Finland
[2]Geological Survey of Finland, Betonimiehenkuja 4
02151 Espoo, Finland
[3]Geological Survey of Finland, Lähteentie 2
96101 Rovaniemi, Finland

E-mail: jussi.mattila@posiva.fi

In this article we describe a methodology to extract continuous slip profiles for postglacial faults using LiDAR DEM data. The acquisition of continuous slip profiles provides more complete data for the estimation of earthquake dynamics, which further serves as detailed input data for seismic risk assessment. Slip profiles also contain information of the propagation history of fault segments and can thus be applied in the characterisation of earthquake dynamics.

**Keywords:** postglacial faults, neotectonics, earthquake, LiDAR, slip profile, seismic hazard assessment, Finland

## 1. Introduction

Topographic and recently acquired LiDAR data from northern Finland show prominent fault scarps that can be related to postglacial deformation (e.g. Kujansuu, 1964; Kuivamäki et al., 1998, Palmu et al. 2015) and as such the scarps are also considered as manifestations of past earthquakes associated with the release of horizontal flexural stresses during endglacial phase (e.g. Arvidsson, 1996). From a seismic hazard point of view, it is important to assess the frequency-magnitude relations of such earthquakes and typically the magnitude estimations are carried out by using well known scaling laws linking fault slip values and the lengths of the fault scarps to earthquake magnitudes (e.g. Wells & Coppersmith 1994, Leonard 2010). Frequency-magnitude assessments are important for example in the safety assessment of deep nuclear waste repositories, which need to look at seismic risk for a time period of up to 1 Ma. Typically the slip values for the faults are acquired by measuring fault scarp heights at sporadic locations by making vertical cross sections through the fault scarps and measuring the height difference between the top and bottom of the scarp, but in this paper we present a methodology to measure full slip profiles by the use of LiDAR data. This data can further be used in the assessment of the distribution of slip values, which provides much more efficient tool for assessing earthquake dynamics. LiDAR data also allows constraining of the kinematics of the postglacial faults as the surface ruptures occasionally show evidence of a horizontal slip component aside the prominent reverse faulting. Typical examples of horizontal slip component are shown for example through en echelon array of surface ruptures and restraining bends showing upheaval of glacial sediments with respect to surrounding topography.

## 2. Methodology for measuring fault slip profiles

In our proposed methodology, a polyline is digitized both at the top and bottom of the fault scarps and the polyline is then draped onto the LiDAR DEM in such a way that the polyline honours the true topography of the fault scarp. After this either of the polylines is divided into a set of points, separated by a preset distance of 1 meter, for example. For each of the points, the closest point to the remaining polyline is then searched for and once these two points are joined, this forms a vector that is perpendicular to the latter polyline. The z-component of the resulting vector then represents the vertical height of the fault scarp and the slip profile for the fault scarp is then acquired by collecting the z-components of each vector as a function of the distance from the beginning of the fault segment.

In this paper we use a fault scarp observed at Riikonkumpu area (Ojala et al. 2016, Mattila et al., 2016), located east of Kittilä as a case study. The fault system consists of several fault segments which cover a distance of ca. 15 km in SW-NE orientation (Figure 1). We focus first on segment 2b (Figure 1) as an example of slip profile acquisition. We first manually digitize polylines to the top and bottom of the scarp, drape the polylines onto the 2 meter resolution LiDAR DEM (Figure 2) and then extract vectors in one meter intervals as described in the preceding section (Figure 3). The extracted vertical slip profile of the analysed fault segment is shown in Figure 4. The full slip profile for the Riikonkumpu fault system, including also a cumulative slip profile, is shown in Figure 5.

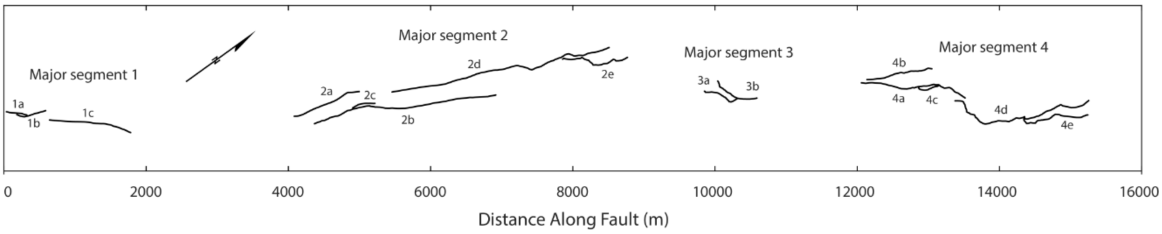


***Figure 7.*** *Geometry and structure of the Riikonkumpu fault system.*

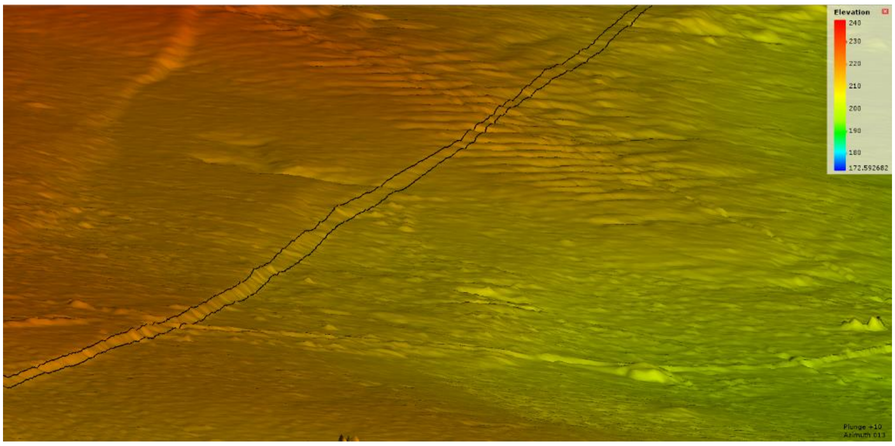


***Figure 8.*** *Polylines digitized onto the top and bottom of the segment 2b scarp of the Riikonkumpu fault system. Screenshot from Leapfrog-software. LiDAR point cloud data by National Land Survey of Finland and DEM processing (from the point cloud data) by Geological Survey of Finland.*

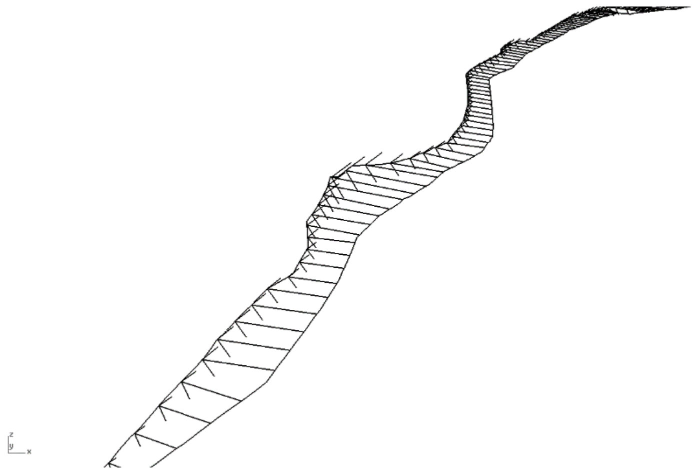

***Figure 9.*** *Vectors perpendicular to the polyline representing the bottom of the fault scarp extracted in set interval. The z-component of the vectors represents the vertical height of the fault scarp at the location of the vector.*

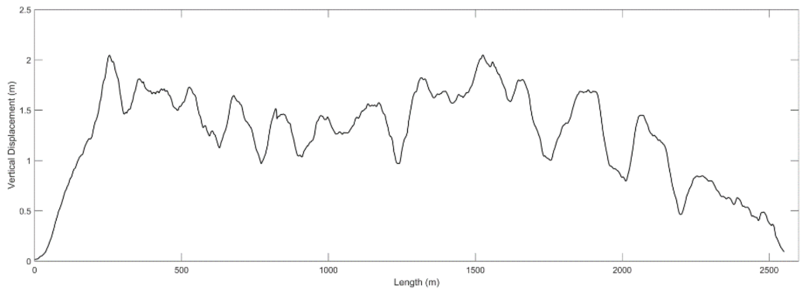


***Figure 10.****Vertical slip profile of the segment 2b of the Riikonkumpu fault system. Not that to reduce noise within the measurements, the data has been smoothed by computing a moving average with a bin size of 50 meters.*

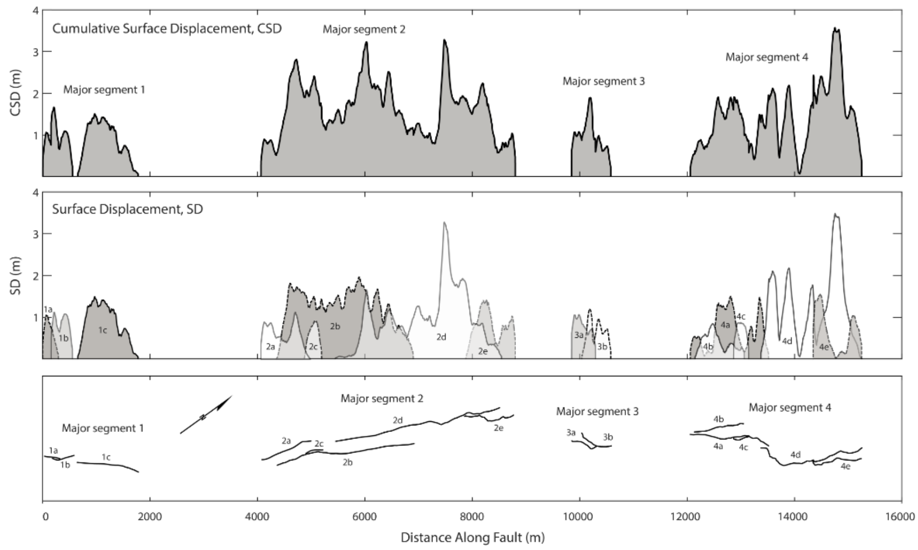


***Figure 11.*** *Vertical slip profile (middle diagram) and cumulative slip profile (upper diagram) for the Riikonkumpu fault system.*

## 3. Conclusions

The methodology proposed in this paper allows the extraction of continuous vertical slip profiles for postglacial faults by using LiDAR DEM data. The use of the continuous slip data allows more comprehensive extraction of slip statistics and as such also serves as detailed input data for the estimation of earthquake magnitudes and seismic risk assessment. Slip profiles may further be used as a tool for the assessment of the propagation direction of earthquake surface ruptures and the evolution of whole fault systems. In light of the known postglacial faults, the application of the methodology with LiDAR DEM allows unprecedented way to characterise the evolution and dynamics of the faults.

## References:

Arvidsson, R., 1996. Fennoscandian earthquakes: whole crustal rupturing related to postglacial rebound. Science 274, 744-746

Kuivamäki, A., Vuorela, P., Paananen, M., 1998. Indication of postglacial and recent bedrock movements in Finland and Russian Karelia. Geological Survey of Finland Report YST-99, 97 p.

Kujansuu, R., 1964. Nuorista siirroksista Lapissa. Summary: Recent faults in Lapland. Geologi 16, 30-36.

Leonard, M., 2010. Earthquake Fault Scaling: Self-Consistent Relating of Rupture Length, Width, Average Displacement, and Moment Release. Bulletin of the Seismological Society of America, Vol. 100, No. 5A, pp. 1971–1988

Mattila, J., Aaltonen, I., Ojala, A.E.K., Palmu, J.-P., Käpyaho, A., Lindberg, A., Ruskeeniemi, T., Hänninen, P., Sutinen, R., Savunen, J. 2016. Structural Geology of the Naamivittikko and Riikonkumpu postglacial fault scarps in Finnish Lapland. Bulletin of the Geological Society of Finland Spec. Vol. Abstracts of The 32nd Nordic Geological Winter Meeting 13th-15th January 2016, Helsinki, Finland, p. 312

Ojala, A.E.K., Palmu, J.-P., Savunen, J., Käpyaho, A., Lindberg, A., Mattila, J., Ruskeeniemi, T., Hänninen, P., Sutinen, R. 2016. Characterization of Riikonkumpu fault scarp in Kittilä. Bulletin of the Geological Society of Finland Spec. Vol. Abstracts of The 32nd Nordic Geological Winter Meeting 13th-15th January 2016, Helsinki, Finland, p. 315.

Palmu, J.-P. Ojala, A.E.K., Ruskeeniemi, T., Sutinen, R., Mattila, J., 2015. LiDAR DEM detection and classification of postglacial faults and seismically-induced landforms in Finland: a paleoseismic database. GFF 137, 344–352.

Wells, D.L., Coppersmith, K.J., 1994. New empirical relationships among magnitude, rupture length, rupture width, rupture area, and surface displacement. Bulletin of the Seismological Society of America 84 (4), 974-1002.

# Supracrustal rocks from the SE border of the Central Finland Granitoid Complex, something new or business as usual?

P. Mikkola[1], K. Mönkäre[2], M. Ahven[3] & H. Huhma[4]

[1]Geological Survey of Finland, P.O. Box 1237, 70211 Kuopio, Finland
[2]Department of Geography and Geology, University of Turku, 20014 Turku, Finland
[3]Savo vocational collage, Metalwork and machinery, P.O. Box 87, 70101 Kuopio, Finland
[4]Geological Survey of Finland, P.O. Box 96, 02151 Espoo, Finland
E-mail: perttu.mikkola@gtk.fi

Based on new geochemical and age data from the supracrustal rocks bordering the Central Finland Granitoid Complex in southeast represent the eastern continuation of the classical Tampere group volcanic rocks and paragneisses of the Pirkanmaa migmatite suite. The volcanic units in the study are represent mainly intermediate calc-alkaline rocks formed in arc setting between 1895 and 1875 Ma. Only small units directly associated with the Pirkanmaa migmatite suite have picritic compositions. Unmigmatized greywackes of the Pirkanmaa migmatite suite have maximum deposition ages of 1.90–1.92 Ga, whereas for the migmatitic sample the corresponding age is 10 to 20 ma younger.

**Keywords:** Paleoproterozoic, Svecofennia, Fennoscandia, volcanism, greywackes, migmatites, age determinations

## 1. General

Our study area is located at the contact between the Central Finland Granitoid Complex (CFGC) (Figure 1) and supracrustal units, both volcanic and sedimentary, flanking it to south-east. Over the last five years significant amount of new data have been accumulated in ore potential estimation project of the Geological Survey of Finland. Here we shortly summarize the results related to the ages and composition of the supracrustal units in the area. The volcanic and metasedimentary units have been regarded as the eastern continuations of the Tampere group volcanic rocks and Pirkanmaa migmatite suite rocks, more intensively studied further west (Kähkönen 2005, Lahtinen et al. 2009).

## 2. Makkola suite

The volcanic rocks in the study area form a discontinuous belt trending northeast. Preservation of the primary structures varies, locally they are well preserved, but often destroyed by deformation and metamorphism, especially near the Leivonmäki Shear Zone running parallel to the volcanic rocks. The primary structures vary from volcanic breccias to massive tuffs and tuffites with clear sedimentary structures. Due to combination of often poor exposure and deformation, stratigraphic approach was not possible, instead the volcanic rocks were divided into lithodemes based on composition and original structures.

Compositionally the rocks forming the Makkola suite are calc-alkaline, mainly intermediate to felsic rocks, with limited amount of basic variants, the latter are mainly subvolcanic dykes and small intrusions. Based on geochemical data all the small separate segments are similar and originally part of the same larger sequence. Effects of chemical alteration are observable, but only in limited cases the alteration has been pervasive.

Based on five age determination samples the age of volcanism in the area varies from 1895 Ma to 1875 Ma, which coincides with plutonic rocks surrounding the volcanic rocks. One of the samples interpreted to represent mainly intraformational sediments also contained detrital Neoarchean zircons.

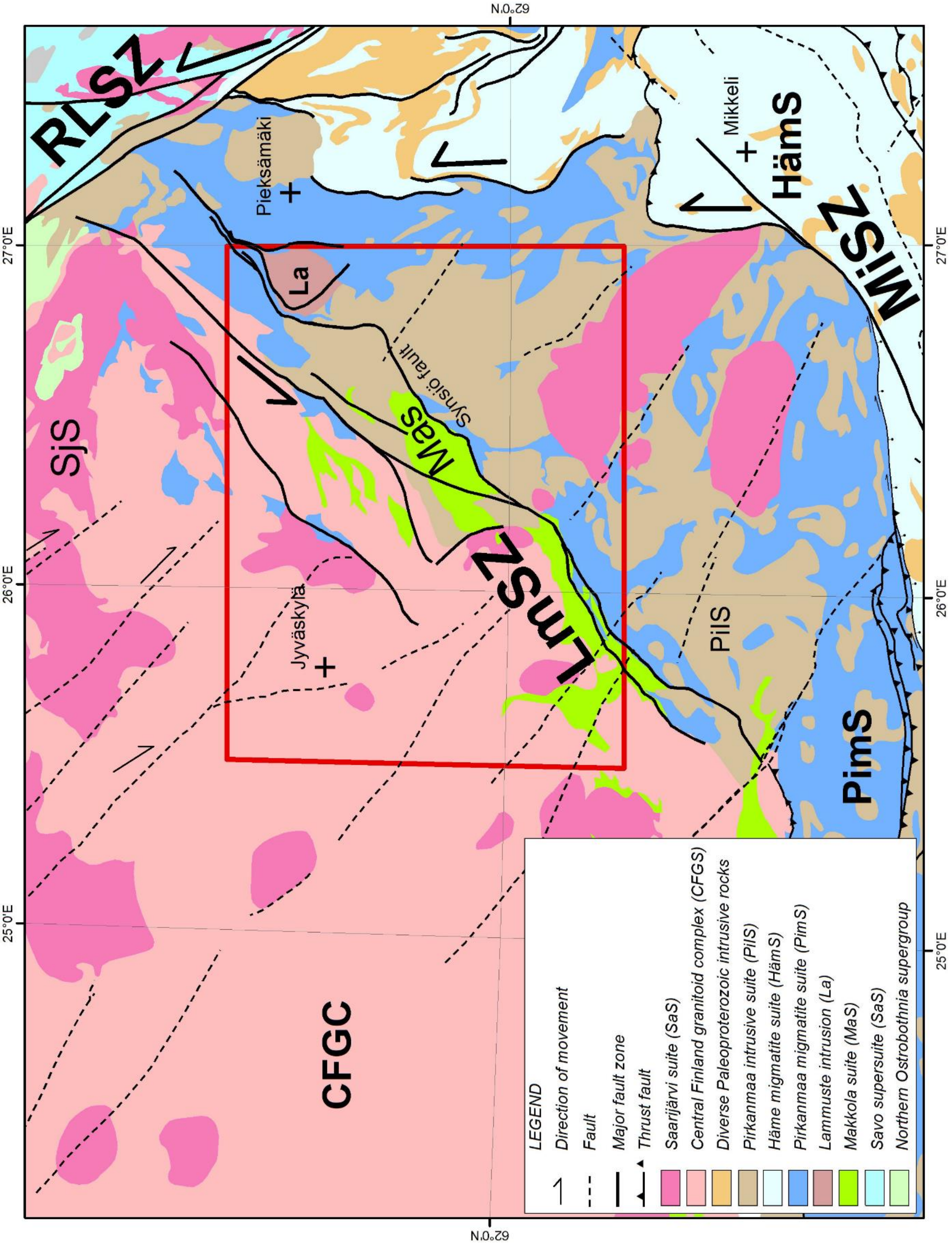


**Figure 1.** General **g**eological map of the study area and its surroundings located southwest from the Raahe-Laatokka shear zone (RLSZ) and transected by Leivonmäki shear zone (LmSZ). The volcanic rocks forming the Makkola suite are located between the Central Finland Granitoid Complex and Pirkanmaa migmatite and intrusive suites. Map modified from DigiKP.

## 3. Pirkanmaa migmatite suite

Contact between the metasedimentary rocks interpreted to belong to the Pirkanmaa migmatite suite in the study area are, based on field observations and geophysical data tectonic with both the Makkola suite and CFGC.

Metasedimentary rocks forming the Pirkanmaa migmatite suite form two major groups: well preserved unmigmatized greywackes and intensively migmatized and folded paragneisses. Small amount of volcanic rocks occur in within the Pirkanmaa migmatite suite, typically in the vicinity of its contacts with the CFGC or Makkola suite. These volcanic rocks are typically intensively altered, but differ from the Makkola suite with their picritic compositions.

All of the three age determination samples from unmigmatized greywackes, with conglomerate and pelite interbeds, contained similar zircon populations: abundant Paleoproterozoic zircons with ages from 1.91 to 2.10 Ga and another Neoarchean peak. The one migmatized sample deviated from the unmigmatized ones as it did not contain Archean zircons and the youngest detrital zircon was ca 1890 Ma in age, albeit defining reliably the age of the youngest detrital zircon in migmatized samples is an ambitious task.

## 4. Results

The age and geochemistry of the Makkola suite are mainly similar to those previously reported for the Tampere group (Kähkönen 2005 and references therein) and also for the smaller volcanic segments within the CFGC (Nikkilä et al. 2016). Major difference is that the equivalent of the Myllyniemi formation, i.e. lower turbiditic sequence of the Tampere group deposited before major volcanic activity, was not found in the study area.

The detrital age results from the Pirkanmaa migmatite suite are similar to those reported earlier (Lahtinen et al. 2009). Three of the samples must have been deposited prior to the volcanic activity of the Makkola suite or as the contact is tectonic, at such a distance or location that the Makkola suite did not form its source. For the fourth sample Makkola suite is a potential source for part of the zircon population.

## References:

Bedrock of Finland - DigiKP. Digital map database [Electronic resource]. Espoo: Geological Survey of Finland [referred 01.09.2016]. Version 2.0.

Lahtinen, R., Huhma, H., Kähkönen, Y., Mänttäri, I., 2009. Paleoproterozoic sediment recycling during multiphase orogenic evolution in Fennoscandia, the Tampere and Pirkanmaa belts, Finland. Precambrian Research 174, 310–336.

Kähkönen, Y., 2005. Svecofennian supracrustal rocks. In: Lehtinen, M., Nurmi, P., Rämö, T. (Eds.), The Precambrian Bedrock of Finland—Key to the evolution of the Fennoscandian Shield. Elsevier Science B.V., pp. 343–406.

Nikkilä, K., Mänttäri, I., Nironen, M., Eklund, O., Korja, A., 2016. Three stages to form a large batholith after terrane accreation – An example from the Svecofennian orogen. Precambrian Research 281, 618–638.

# Shock wave propagation in heterogeneous targets (ordinary chondrites) and in numerical setup of shock recovery experiments

J. Moreau[1], T. Kohout[1,2] and K. Wünnemann[3]

[1]Department of Physics, University of Helsinki (Gustaf Hällströmin katu 2 A, 00560, D331, Helsinki)
[2]Institute of Geology, The Czech Academy of Sciences, Prague, Czech Republic
[3]Museum für Naturkunde, Berlin, Leibniz Institute for Evolution and Biodiversity Science, Berlin, Germany.
E-mail: julien.moreau@helsinki.fi

We give some insight to the shock wave interactions in heterogeneous samples such as ordinary chondrites of type H and into the numerical setup for shock recovery experiments. We used the shock physics code iSALE (Wünnemann et al., 2006) to qualify the interactions of the shock wave due to impedance contrasts between materials of different origins and the shock wave reflections at the materials boundaries. To quantify the results we analysed the reflection index of materials and the enhancement of the pressure in the different setups. This article is in the scope of the shock-darkening study by Kohout et al. (2014) and submitted work from Moreau et al., (2016).

**Keywords:** shock-darkening, shock wave, iSALE, numerical modelling

## 1. Introduction

To study the shock-darkening in ordinary chondrites (process during which metals and iron sulphides melt into a network of veins rendering the chondrites lithology darker) we used the shock physics code iSALE to generate shock waves in an olivine sample containing particles of iron and troilite (mesoscale modelling). Results showed complex shock wave interactions within the heterogeneous medium.

In addition to the shock-darkening study, we used the iSALE code to simulate shock recovery experiments on meteorites (Langenhorst and Deutsch, 1994; Langenhorst and Hornemann, 2005), representing an olivine sample embedded in a steel (iron) container.

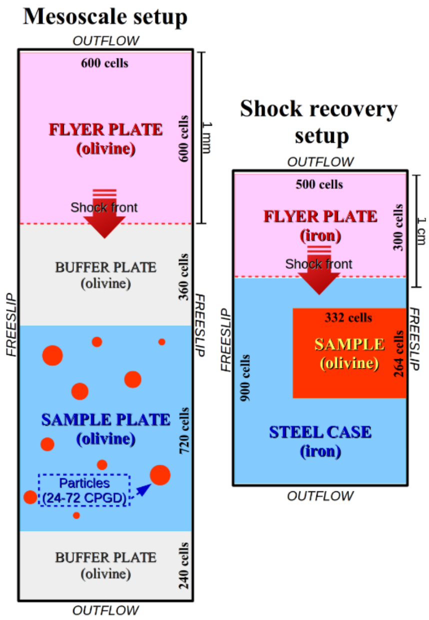


**Figure 1.** Conceptual models for the mesoscale setup (Moreau et al., 2016) and the shock recovery experimental setup.

## 2. Methods

For both numerical setups, we implemented layers of specific materials. One layer was a flyer plate that, given some velocity, generated the planar shock wave to the layers beneath it. Each setup had its own specific strength properties and resolution of the layers (in width and height). In Figure 1 can be seen the conception models for each setup.

To analyse the shock wave interactions within the samples, we used the reflection index that is the amount of time an element (Lagrangian tracer) has encountered a steady pressure for a specific time frame (set to 3 time steps for each setup). In addition, for the mesoscale setup, we calculated the difference between the primary shock wave and the final peak-pressure that tracers have sustained. For the shock recovery experimental setup we represented that amount as the enhancement of the primary shock wave (nominal pressure for each material) in percent.

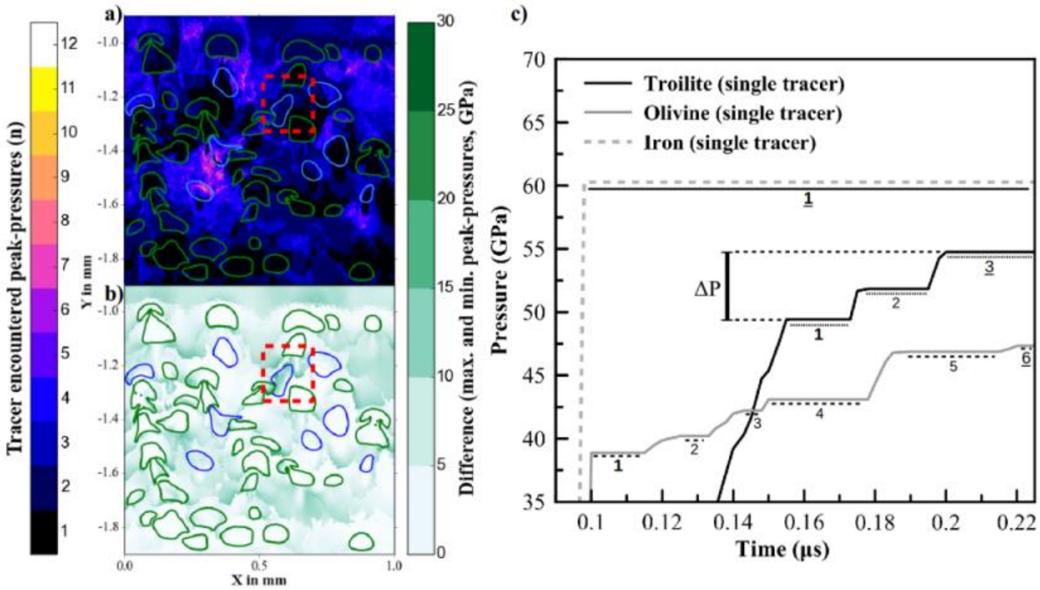


**Figure 2.** Details and complexity of the peak-pressures ramping in the sample plate after release (H ordinary chondrite mesoscale model at 39.22 GPa nominal pressure): a) peak-pressures plateaus frequencies attained by each material unit tracer, b) differences between the lowest and highest peak pressure plateaus (ΔP), c) examples of tracers recorded peak-pressures over time. The dashed lines represent the encountered peak pressure plateaus, bold numbers are the primary shock wave peak-pressures and underlined numbers are the final recorded peak-pressures. The sum of the encountered peak-pressures in a) is the amount of peak pressure plateaus of a minimum three occurrences (0.005 µs in time lapse) in a tracer. The dashed red box indicates an area of interest.

## 3. Results

In Figure 2 are shown the results for a H ordinary chondrite mesoscale model at 39.22 GPa nominal pressure for which particles of iron (green) and troilite (blue) are delineated (Moreau et al. 2016). Details on the method to calculate the reflection index is shown in Figure 2c. In Figure 3 are shown the results for a sample plate hit with a 30 GPa nominal pressure.

## 4. Discussion

In figures 2 and 3 we see how complex are the reflections inside the samples. In Figure 2 the troilite grains and olivine matrix are subject to large amount of reflections. These reflections are due to the reflected shock wave from nearby iron grains or troilite grains. These reflections show large differences in the primary shock wave pressures and the peak-pressures and it is due to the impedance contrasts (Hirose and Lonngren, 1985; Kinslow and Cable, 1970) between iron grains and olivine that enhance the pressure that is reflected. In Figure 3 the enhancement of the pressure inside the sample plate (from <10% to >100% of enhancement on certain zones) is due to complex reflections and impedance contrast at the boundaries between the sample and the steel case (iron). In Figure 4 we see a snapshot of the shock wave traversing the sample in the shock recovery experimental setup that shows the strong reflection from the bottom boundary. Later on, a final reflection will come from the top boundary when the reflection of the bottom boundary has travelled the whole sample, explaining the higher enhancement in the top part of the sample.

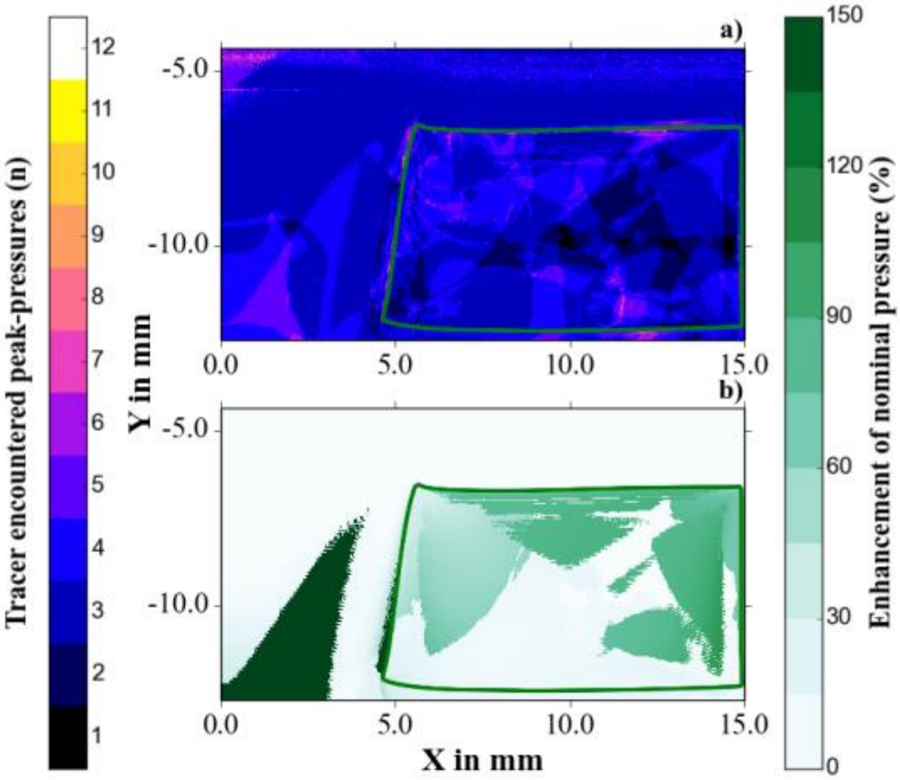


**Figure 3.** Details and complexity of the peak-pressures ramping in the olivine sample (30 GPa nominal pressure): a) peak-pressures plateaus frequencies attained by each material unit tracer, b) enhancement of the nominal pressure (for both olivine and iron). The sample is delineated by the green line.

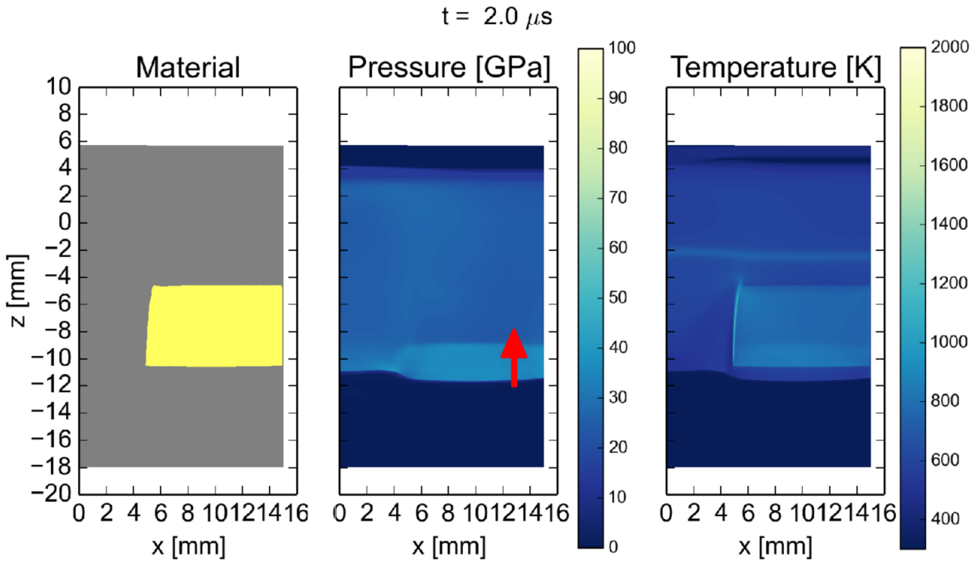


**Figure 4.** Snapshot of the shock recovery experimental setup at 30 GPa of nominal pressure in the sample plate. It shows materials, pressures and temperatures. The red arrow show the reflected shock wave at the boundary between the steel case (iron, grey) and the sample (olivine, yellow). A faint reflection can be seen from the top left corner of the sample.

## 5. Conclusions

We showed that shock wave interactions within an heterogeneous medium are strong and lead to high enhancement of a primary shock wave pressure to a final peak-pressure in most of the cases. We also proved these interactions to be of the same nature in both the mesoscale and the shock recovery experimental setup for which strong reflections from boundaries can enhance the primary shock wave to a final peak-pressure. In both setup, the material that enhanced the pressure in olivine or troilite was iron.

## References:

Hirose A., Lonngren K., 1985. Introduction to Wave Phenomena, J. Willey & Sons, New York.

Kinslow R., Cable A. J., 1970. High-velocity impact phenomena, Academic Press, Michigan University, 579 pp.

Kohout T., Pesonen L. J., Deutsch A., Wünnemann K., Nowka D., Hornemann U., Heikinheimo E., 2012. Shock experiments in range of 10-45 GPa with small multidomain magnetite in porous targets. Meteoritics & Planetary Science 47:10, 1671-1680.

Langenhorst F., Deutsch A., 1994. Shock experiments on pre-heated alpha- and beta-quartz; I, Optical and density data. Earth and Planetary Science Letters 125:407–420.

Langenhorst F., Hornemann U., 2005. Shock experiments on minerals: Basic physics and techniques. EMU Notes in Mineralogy 7:357–388.

Moreau J., Kohout T., Wünnemann K., 2016. Shock-darkening in ordinary chondrites: pressure-temperatures conditions determination by shock physics mesoscale modeling. Meteoritics & Planetary Science, sumitted.

Wünnemann K., Collins G. and Melosh H., 2006. A strain-based porosity model for use in hydrocode simulations of impact and implication for transient crater growth in porous targets. Icarus, 180:514-527.

# Applying double-difference technique to relocate induced microseismic events in Pyhäsalmi mine, Pyhäjärvi.

J. Nevalainen[1], O. Usoltseva[2] and E. Kozlovskaya[3]

[1] Sodankylä Geophysical Observatory, Oulu unit, University of Oulu, Finland
[2] Institute of Geosphere Dynamics, Russian academy of Science, Moscow, Russia
[3] Oulu Mining School, University of Oulu, Finland
[1] E-mail: jouni.nevalainen@oulu.fi

Pyhäsalmi mine, Pyhäjärvi, Finland, is known to have induced seismicity due ore extraction for past decades. In 2002, when Pyhäsalmi mine was expanding operations under the old mine, a microseismic network was installed around deep ore body. The system consist over 20 geophones that are mainly around the excavation site. Since the installation, over 150000 events have been observed. Seismic observations are one of the quickest ways to map mines state-of-health. However the event localization of the microseismic monitoring system is not ideal as average of 20 m accuracy can be achieved at central part of the deep ore body at best. We have applied double-difference technique successfully on microseismic data in order to enhance the accuracy of event positioning.

**Keywords:** Seismics, tomography, induce seismicity, double-difference, Finland, Pyhäsalmi, mine

## 1. General

It is known for centuries that mining causes increased seismicity in vicinity of the mining area (Guha, 2000; Caw, 1956). Although seismicity within mines is related to the mining operation it is not easy task to forecast origin time or hypocentre of seismic event as it is a complex equation of geology, mining method as well production speed. The extraction of ore and host rock in mine environment causes pressure distribution to change within rock. At weak zones, like cracks or existing faults, the rock cannot handle increased pressure and fails, which can lead to hazardous accidents within a mine (Brady, 2004). Therefore it is necessary to monitor seismic phenomena within mines (Guha, 2000). One major task is to track hypocentre of the microseismic event in the mines. The difficulty of localization of microseismic event is that in order to obtain hypocentre and origin time you need to know the seismic velocity structure of the mine. Usually this is not the case and it is necessary to use assumptions to descript the seismic velocity within study area. This leads only to approximate solution for hypocentre and origin time. In this study we present initial results of applying double-difference algorithm on microseismic data of Pyhäsalmi copper mine. Our aim is to study how well double-difference relocating algorithm enhances seismic event positioning. Results are compared the knowledge of mining in Pyhäsalmi mine.

## 2. Microseismic localization

Microseismic event localization is based on observing seismic waves originated from event with geophones that are connected to the main server of the microseismic system. By detecting and picking P- and S-waves (body waves) from every station it is possible to calculate events hypocentre and origin time using assumption of seismic velocity structure of the study area. However this is the main error source for event localization because it is difficult to assess what is the real seismic velocity structure without active measurements. Furthermore when mining operation continues it changes seismic velocity structure constantly. Therefore it is common to use either homogenous or very simple seismic velocity models for the mines. Third option is to use station specific seismic velocity. All of the methods need to define with a-priori knowledge like extensometer information and are unique for individual mines.

### 3. Microseismic data in Pyhäsalmi mine

Microseismic event data from the Pyhäsalmi mine has been measured since 2002, when the microseismic monitoring network was installed to the mine. The networks main target is to locate frequently occurring microseismic events for monitoring changes in rock mass and for safety of mining operations. The Pyhäsalmi mines microseismic monitoring system hardware was acquired from Integrated Seismic System International (ISSI) Company and the software was provided by the Institute of Mine Seismology (IMS). Most of the geophones are one component sensors (vertical), but few 3-component geophones are also installed in key locations of the mine. Geophones have been placed around the Pyhäsalmi deep ore body. The microseismic network is automated by triggering option and system quickly notifies approximate location and magnitude of the event. The microseismic networks event localization accuracy has been determinated by the Pyhäsalmi Mining Ltd and also by Pyy (2007). According to Pyy, the best accuracy of seismic event location corresponds to upper and central part of the deep ore body and the poorer location accuracy is for events outside the microseismic system and in the bottom part of the mine within the production area. The average event location accuracy estimated by Pyy (2007) is 30 m. After this Pyhäsalmi mine Ltd has upgraded the microseismic monitoring system and thus the accuracy of the locating is improved as well.

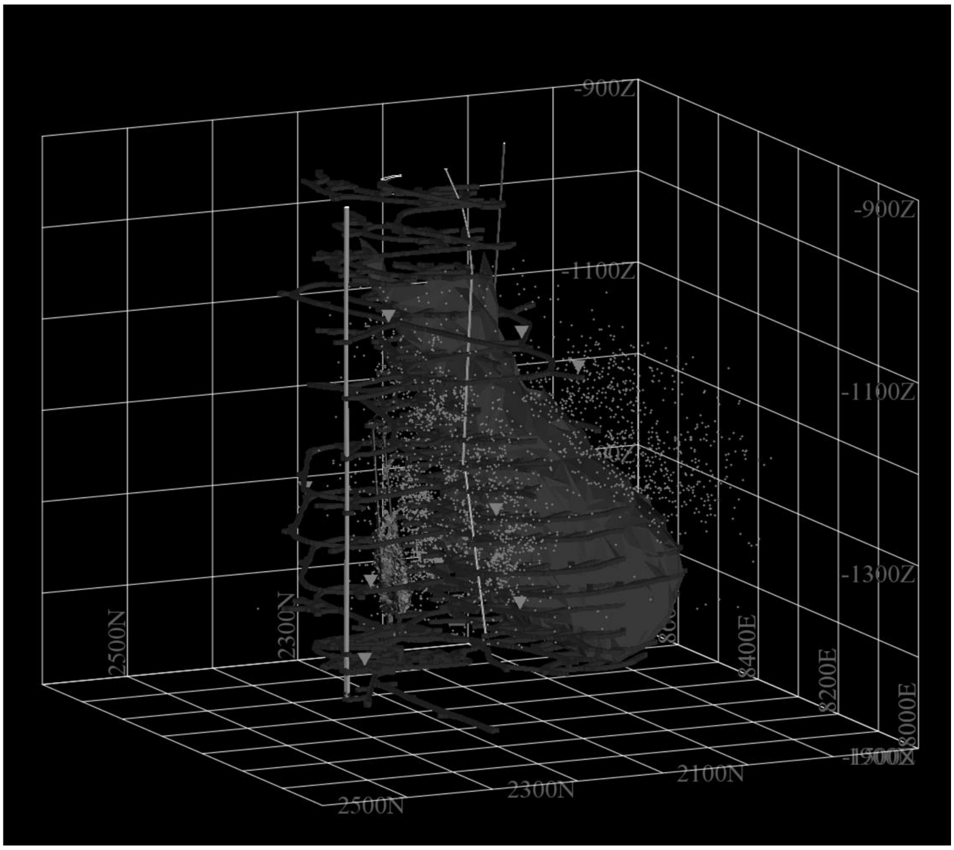


**Figure 1.** The microseismic events around deep ore body in Pyhäsalmi mine. Dots represent seismic events and triangles microseismic networks geophones.

**4. Double-difference method and example results**

We apply double-difference algorithm to Pyhäsalmi mines microseismic data in order to relocate originally calculated event positions (Waldhauser & Ellsworth, 2000; Waldhauser, 2011). Double-difference relocation method exploits the close pairs of events with common receiver. The fundamental equation of this iterative least-squares procedure relates the residual between the observed and predicted phase travel time difference for pairs of earthquakes observed at common stations to changes in the vector connecting their hypocenters through the partial derivatives of the travel times for each event with respect to the unknown. When the earthquake location problem is linearized using the double-difference equations, the common mode errors cancel, principally those related to the receiver-side structure (Waldhauser & Ellsworth, 2000). Because technique needs event pairs with common receiver the method has some limitations especially for isolated events. Due the structural changes in mining environment also time period between two events cannot be too long. As parameters we used maximum distance of 50 meter for event pair and minimum distance to the common station to be 100 meters. In Figure 2 is example of results of applying double-difference technique on two week microseismic data from January of year 2011. In the figure is presented a 50 meter slice in horizontal plane from depth of 1175 meter to 1225 meter from the ground surface.

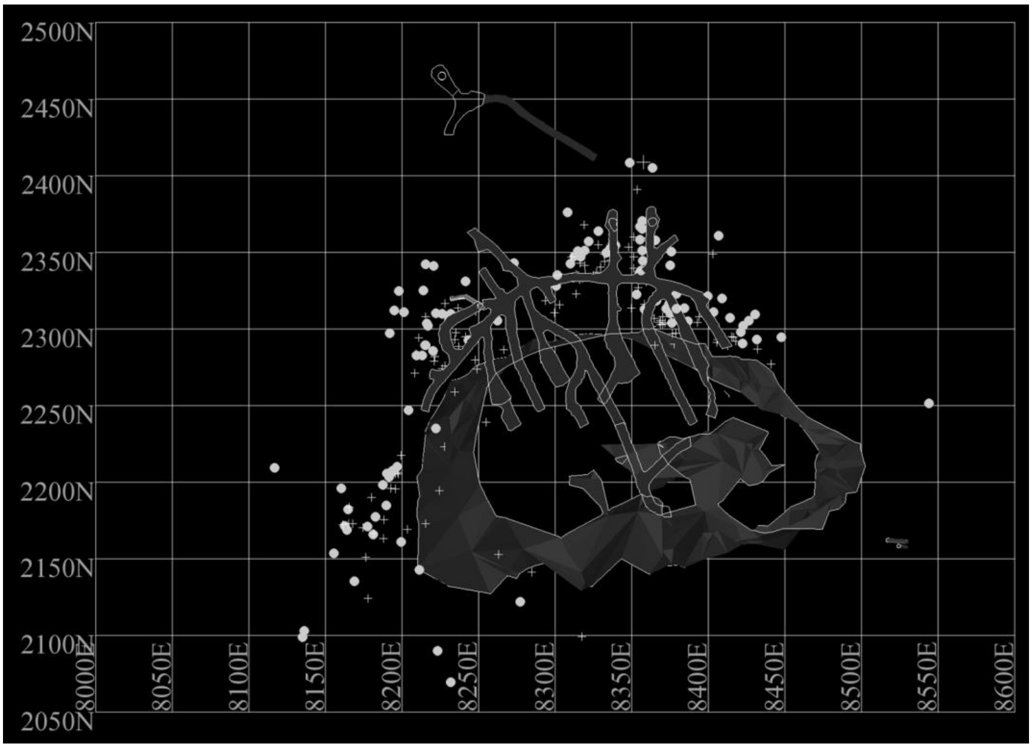


**Figure 2.** Results of applying double difference technique on two weeks microseismic data from Pyhäsalmi mine. Data is from January 2011. Dots represent original location of the Pyhäsalmi data and crosses relocated events.

From the results it can be seen that relocated events are closer to the deep ore body than original event positioning and thus nearer to the contact zone between ore body and host rock. The average correction is around 10 meters. The relocation with double-difference did not work well at bottom part of the mine due too long distance between original event pairs for studied data period. The best areas for the analysis in this example were mid and upper regions around deep ore body.

## 5. Conclusion

Double-difference technique algorithm was applied to microseismic data of microseismic monitoring network in Pyhäsalmi mine. The results showed that using double-difference technique it is possible relocate seismic sources with better accuracy. The method is most useful at regions with dense seismicity.

## References:

Brady, B. H. G. & Brown, E. T., 2004. Rock mechanics for underground mining. Third edition. Kluwer Academic Publishers, Netherlands, 628 pp.

Caw, J.M., 1956. The Kolar gold field, Mine and quarry engineering, 22, 258, and 306.

Guha, S.K., 2000. Induced Earthquakes. Kluwer Academic Publishers, Dordrecht, Netherlands. pp. 314.

Pyy, A., 2007. Tutkimus Pyhäsalmen kaivoksen mikroseismisen havaintoverkon paikannustarkkuudesta (A study for localization accuracy of Microseismic networks at Pyhäsalmi mine). Master’s thesis, Department of physics, University of Oulu.

Waldhauser F. & Ellsworth, W.L., 2000. A Double-Difference Earthquake Location Algorithm: Method and Application to the Northern Hayward Fault, California.

Waldhauser, F., 2001. hypoDD: A computer program to compute double-difference earthquake locations, USGS Open File Rep., 01-113.

# Effect of crustal scale shear zones to the crustal deformation during extension

K. Nikkilä[1]

[1]Geology and Mineralogy, Akademigatan 1, Åbo Akademi University
E-mail: knikkila@abo.fi

Many inherited structures and mechanical components affect to the post-collisional evolution in orogens. Here I present the effect of the crustal scale shear zones in a weak vs. a rigid crustal blocks during a post-collisional lateral spreading. The results are based on two analog modelings and discussion in a dissertation (Nikkilä et al., 2009; 2015; Nikkilä, 2016).

**Keywords:** pre-existing weakness zones, middle crust, lateral spreading, shear zones, extension

## 1. Inherited features in an orogen

Orogeny can increase volume and thickness of the orogenic crust (Cawood et al., 2009; Tetreault and Buiter, 2014). Accretionary and collisional orogens have been important in terms of the production of continental crust. In the formation of a continental crust, where large plates, and one or more microplates, or arcs, have been involved there tend to be complicated geological structures in the orogens. Hence, the orogen can be composed of heterogeneous crustal components which have different mechanical properties as well as inherited tectonic boundaries and large scale shear zones.

When the orogeny leads to over-thickening of a crust, the crust may undergo syn- to post-collisional extension, caused by the differences in gravitational potential energy between the thickened crust and its thinner surroundings (England and Thompson, 1986; Vanderhaeghe et al., 1999; Rey et al., 2001). The gravitational potential energy difference will cause crustal scale lateral spreading towards the thinner areas. In a thickened crust radioactive heating will initiate partial melting in the middle and lower crusts (England and Thompson, 1986). If there is enough partial melts in the crust, the spreading will accommodate in that layer.

Post- and syncollisional middle to lower crustal spreading driven by gravitational instabilities (gravitational collapse) have been studied by conceptual and geodynamic models (e.g. Rey et al., 2001; Vanderhaeghe and Teyssier, 2001; Beaumont et al., 2001; Nikkilä et al., 2009; 2015; Harris et al., 2012). The crustal architecture is outlined with two to three layers with different mechanical properties, and in the models, the inherited components and structures, such as mechanically heterogeneous crust or tectonic boundaries, are often lacking. Nevertheless, modeling the differences in the mechanical properties is more common in geodynamic models than modeling the reactivation of pre-existing large-scale shear zones.

## 2. Reactivation of the shear zones in an extension

In literature it has often been concluded that the pre-existing structures such as faults and shear zones have an effect in the style of deformation during extension (and in collision) (e.g. Fuegenschuh et al., 1997; Whitney et al. 2004; Corti et al., 2005; Jamieson and Beaumont, 2011; Tetreault and Buiter, 2014).

In geodynamic models by e.g. Koyi and Skelton (2001) and Rey et al (2009) the reactivation of the pre-existing shear zones have been modeled in extensional regime, however, in the models the shear zones are located mainly in the upper crust. Nikkilä et al (2015) studied the reactivation of the tectonic boundaries and crustal scale shear zone in a mechanically heterogeneous crust during post-collisional extension. Here I present and compare the results of two sets of analog modeling experiments, thermomechanical (Nikkilä et al., 2009) and centrifuge (Nikkilä et al., 2015), which simulated the lateral spreading of a thick crust after formation of the partial molten crustal layer. I have concentrated on the formation and the deformation of the large scale shear zones in the lateral spreading of a thick crust.

### 3. Effect of the pre-existing crustal scale shear zones

The results indicate that in a thick, three-layer crust, with a weak middle crustal layer:

- crustal scale shear zones do not develop;
- the pre-existing tectonic boundaries and the crustal scale shear zones will increase the extension rate;
- deeper sequences of the crust will exhume in the presence of the shear zones;
- in a rigid crust many minor core complexes will develop if the crustal scale pre-existing shear zones are not present;
- in a weak crust, without the crustal scale shear zones, the core complexes extend in a wider area but less deep sequences are uplifted, in comparison to a weak crust with shear zones.

The results suggest that studying the crustal evolution of post-collisional lateral spreading/extension, the inherited weakness zones are important to take account. The end results and duration may vary depending on the existence and/or lack of the tectonic boundaries and the crustal scale shear zones. Even thought the results are highly applicable in the post-collisional lateral spreading of a thick, three-layer crust, the results also suggest that these features need to take account also in any extensional environment.

### References:


Beaumont, C., Jamieson, R.A., Nguyen, M.H., Lee, B., 2001. Himalayan tectonics explained by extrusion of a low-viscosity crustal channel coupled to focused surface denudation. Nature 414 (6865), 738-742.

Cawood, P.A., Kröner, A., Collins, W.J., Kusky, T.M., Mooney, W.D., Windley, B.F., 2009. Accretionary orogens through Earth history. Geological Society, London, Special Publications 318 (1), 1-36.

Corti, G., Moratti, G., Sani, F., 2005. Relations between surface faulting and granite intrusions in analogue models of strike-slip deformation. J. Struct. Geol. 27, 1547-1562.

England, P.C., Thompson, A., 1986. Some thermal and tectonic models for crustal melting in continental collision zones. Geological Society, London, Special Publications 19 (1), 83-94.

Fuegenschuh, B., Seward, D., Mancktelow, N., 1997. Exhumation in a convergent orogen: the western Tauern window. Terra Nova 9 (5-6), 213-217.

Harris, L.B., Godin, L., Yakymchuk, C., 2012. Regional shortening followed by channel flow induced collapse: A new mechanism for "dome and keel" geometries in Neoarchaean granite-greenstone terrains. Precambrian Res. 212-213, 139-154.

Jamieson, R.A., Beaumont, C., 2011. Coeval thrusting and extension during lower crustal ductile flow? implications for exhumation of high-grade metamorphic rocks. J. Metamorph. Geol. 29 (1), 33-51.

Koyi, H.A., Skelton, A., 2001. Centrifuge modelling of the evolution of low-angle detachment faults from high-angle normal faults. J. Struct. Geol. 23 (8), 1179-1185.

Nikkilä, K., Roy Chowdhury, B.S., Dietl, C., Korja, A., Eklund, O., Zanella, F., 2009. Thermomechanical analogue modelling of the extensional collapse of a collisional orogeny the Svecofennian orogen, Finland. Geotectonic Research 96, 21-38.

Nikkilä, K., Korja, A., Koyi, H., Eklund, O., 2015. Analog modeling of one-way gravitational spreading of hot orogens – A case study from the Svecofennian orogen, Fennoscandian Shield. Precambrian Res. 268, 135-152.

Rey, P., Vanderhaeghe, O., Teyssier, C., 2001. Gravitational collapse of the continental crust: definition, regimes and modes. Tectonophysics 342 (3–4), 435-449.

Rey, P.F., Teyssier, C., Whitney, D.L., 2009. Extension rates, crustal melting, and core complex dynamics. Geology 37 (5), 391–394,

Tetreault, J.L., Buiter, S.J.H., 2014. Future accreted terranes: a compilation of island arcs, oceanic plateaus, submarine ridges, seamounts, and continental fragments. Solid Earth 5, 1243-1275.

Vanderhaeghe, O., Burg, J., Teyssier, C., 1999. Exhumation of migmatites in two collapsed orogens: Canadian Cordillera and French Variscides. Geological Society, London, Special Publications 154 (1), 181-204.

Vanderhaeghe, O., Teyssier, C., 2001. Partial melting and flow of orogens. Tectonophysics 342 (3-4), 451-472.

Whitney, D.L., Teyssier, C., Vanderhaeghe, O., 2004. Gneiss domes and crustal flow. Geological Society of America Special Papers 380, 15-33.

# Logging and lithology of the Kumpula Campus drill hole

K. Penttilä[1], I. Kukkonen[2], J.S. Heinonen[1], M. Räisänen[1] and R. Valtonen[1]

[1]Department of Geosciences and Geography, P.O. Box 64, 00014 University of Helsinki, Finland
[2]Department of Physics, P.O. Box 64, 00014 University of Helsinki, Finland

E-mail: Kalle.Penttila@helsinki.fi

In this study, we describe the general lithological characteristics of the Kumpula Campus drill hole. The main purpose of the drill hole will be undergraduate education in geological logging, petrophysics, and borehole geophysics. The purpose of this study is to perform a detailed logging of the core, identify rock types, and find out how the drill core correlates with the bedrock outcrops of the area. Detailed thin section studies have not been performed yet, but are currently being planned.

**Keywords:** petrology, lithology, Kumpula, Geology, drill hole, Helsinki

## 1. Introduction

A 370 m deep drill hole with continuous coring was drilled in the southern part of the Kumpula campus of University of Helsinki in late 2015 (Kukkonen et al., this volume; Figure 1). In addition to the present study, two other ongoing MSc thesis projects are discussed in posters of the Lithosphere 2016 symposium (Räisänen et al., this volume; Valtonen et al., this volume).

This study aims to perform a detailed logging of the drill core using the newly built logging facilities at the Department of Geosciences and Geography. In addition, rock types will be identified and inspected in detail with a petrographic microscope. The results and the rock types will be compared with the local geology of the area.


**Figure 1.** Location of the drill site and direction of the drilling.

## 2. Geological setting

According to the modern view, the bedrock of southern Finland was formed mainly during the Svecofennian orogeny at 1.9–1.8 Ga ago. The oldest rocks of the study area are the highly metamorphosed ~1.9 Ga hornblende gneisses and mica schists. These rocks are crosscut by only slightly younger (~1.88–1.87 Ga) tonalites and ~1.8 Ga late-orogenic granites that were formed by partial melting of the Proterozoic metasedimentary rocks in the middle crust (e.g., Nurmi and Haapala 1986, Lahtinen 1994).

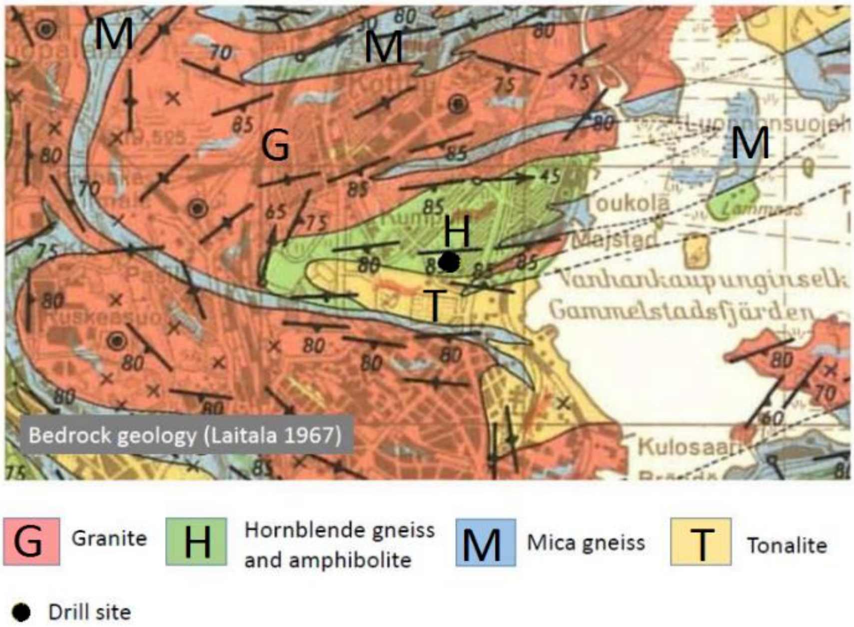


**Figure 2.** Geology of the Kumpula area with the location of the drill hole (after Laitala, 1991).

The geology of the Kumpula Campus area is typical to southern Finland (Figure 2). The Precambrian rocks of the area steadily dip south at approximately 80° angle. The hole was drilled into the hornblende gneiss. There are six major outcrops close to the hole in Kumpula and in these the rock types are gneiss, hornblende gneiss, granite and tonalite (Laitala 1991).

## 3. Current situation of the project and future

Most of the core has now been logged in detail and thin section samples are being selected. Preliminary mapping in the nearby areas has also been performed. Example of the variation of the rock type in the drill core is shown for the first 100 meters in Table 1. We have already discovered from the drill hole that the rock type changes a lot (as seen in these borehole images) between (hornblende)gneiss, granites, granite gneiss and migmatites (vein gneiss) (Table 1.). We also encountered very dark fine-grained veins, which are probably amphibolite. In some parts, there are lots of chlorite, which has probably formed by hydrothermal processes.

## References:

Kukkonen, I.T., Koivisto, E. and Whipp, D. (this volume). Helsinki University Kumpula campus drill hole project. In: *Kukkonen et al. (Eds.),* Lithosphere 2016 – Ninth Symposium on the Structure, Composition and Evolution of the Lithosphere in Finland. Programme and Extended Abstracts, Espoo, Finland, November 9-11, 2016. Institute of Seismology, University of Helsinki, Report S-65, 166 pages.

Lahtinen, R., 1994. Crustal evolution of the Svecofennian and Karelian domains during 2.1-1.79 Ga, with special emphasis on the geochemistry and origin of 1.93-1.91 Ga gneissic tonalites and associated supracrustal rocks in Rautalampi area, central Finland. Geological Survey of Finalnd, Bulleting 378, 128 s.

Laitala, M., 1991. Helsingin kartta-alueen kalliperä. Summary: Pre-Quaternary rocks of the Helsinki map-sheet area. Suomen geologinen kartta 1:100 000, kallioperäkarttojen selitykset, lehti 2034, Geologian tutkimuskeskus, Espoo. 47s.

Nurmi, P.A. and Haapala, I., 1986. The Proterozoic granitoids of Finland: Granite types, metallogeny and relation to crustal evolution. Bulleting of the Geological Society of Finland, 58, s.203-233.

Räisänen, M., Kukkonen, I., Heinonen, J.S., Valtonen, R. and Penttilä, K. (this volume). Geochemical characteristics of the Kumpula campus area: drill core and outcrop data. In: *Kukkonen et al. (Eds.),* Lithosphere 2016 – Ninth Symposium on the Structure, Composition and Evolution of the Lithosphere in Finland. Programme and Extended Abstracts, Espoo, Finland, November 9-11, 2016. Institute of Seismology, University of Helsinki, Report S-65, 166 pages.

Valtonen, R., Kukkonen, I., Heinonen, J.S., Räisänen, M. and Penttilä, K. (this volume). Kumpula campus drill hole: Fracture mapping and 3D-modeling. *Kukkonen et al. (Eds.),* Lithosphere 2016 – Ninth Symposium on the Structure, Composition and Evolution of the Lithosphere in Finland. Programme and Extended Abstracts, Espoo, Finland, November 9-11, 2016. Institute of Seismology, University of Helsinki, Report S-65, 166 pages.

**Table 1.** Lithology for the first 100m of the Kumpula drill hole.

| Begin, m | End, m | Rock type |
|---|---|---|
| 0 | 0.20 | overburden |
| 0.20 | 7.75 | hornblende gneiss |
| 7.75 | 14.00 | granite gneiss |
| 14.00 | 15.13 | granite gneiss |
| 15.13 | 17.75 | gneiss |
| 17.75 | 23.08 | hornblende gneiss |
| 23.08 | 25.24 | granite gneiss |
| 25.24 | 28.79 | hornblende gneiss |
| 28.79 | 30.16 | granite gneiss |
| 30.16 | 33.00 | chlorite gneiss |
| 33.00 | 34.70 | granite gneiss |
| 34.70 | 35.52 | chlorite |
| 35.52 | 47.66 | hornblende gneiss |
| 47.66 | 50.82 | granite |
| 50.82 | 53.82 | hornblende gneiss |
| 53.82 | 56.30 | granite |
| 56.30 | 64.52 | hornblende gneiss |
| 64.52 | 68.80 | granite migmatite |
| 68.80 | 79.00 | migmatite |
| 79.00 | 81.36 | granite |
| 81.36 | 82.71 | hornblende gneiss |
| 82.71 | 83.43 | granite |
| 83.43 | 84.49 | hornblende gneiss |
| 84.49 | 86.97 | granite |
| 86.97 | 93.71 | hornblende gneiss |
| 93.71 | 100.00 | granite gneiss |

# Modelling an Enhanced Geothermal System doublet in crystalline rock

Katerina Piipponen[1]
[1]Department of Physics, P.O. Box 68, FI-00014 University of Helsinki, Finland
E-mail: katja.piipponen@helsinki.fi

Geothermal energy has a great potential and nowadays possible to build a geothermal plant in crystalline rock, and areas away from high heat flow. Permeability of the rock must be enhanced for feasible fluid flow through hot subsurface at depths as deep as 7 kilometres. Analytical and numerical models have been developed to estimate fluid flow and heat transfer at this depth. Numerical modelling is done with Finite Element Analysis tool COMSOL Multiphysics.

**Keywords:** Enhanced Geothermal System, geothermal modelling, heat transport, fluid flow, rock permeability, finite element analysis

## 1. Introduction

New technologies make utilization of geothermal energy possible at areas with low heat flow and permeabilities. Building a geothermal plant in crystalline rock is much more demanding: it requires drilling deeper in order to achieve feasible temperatures and overcoming difficulties caused by pressure. The concept of Enhanced Geothermal System (EGS) is similar to hydrothermal geothermal plants: drill holes for injection and production are drilled to the desired depth and water is circulated through the reservoir, as illustrated in Figure 1. During circulation water is heated up to the temperature of the reservoir and hot water is then pumped up and used for heating. The difference between EGS and conventional hydrothermal plants is that in EGS existing fractures must be engineered to increase permeability to feasible levels.

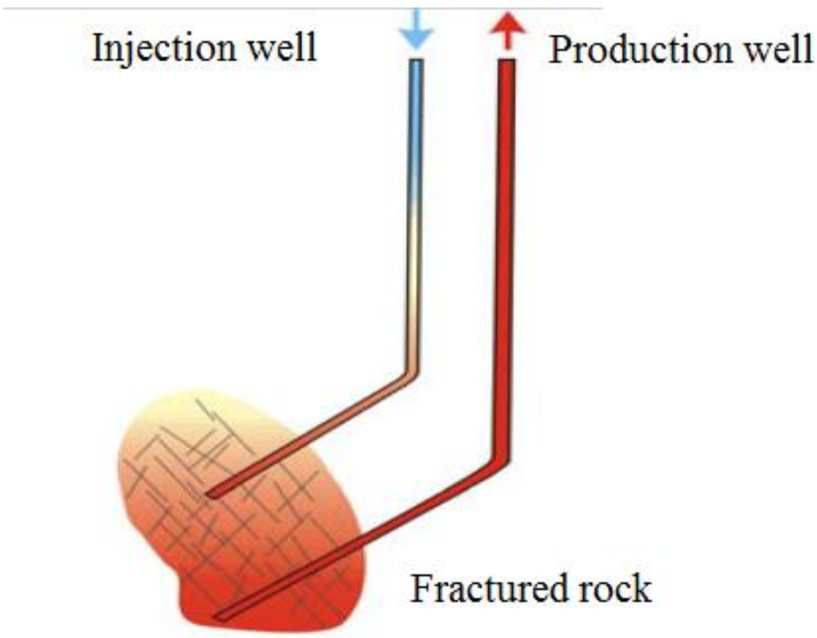


**Figure 1**. Conceptual drawing of an EGS: two wells from the surface are drilled to the depth and rock permeability is stimulated to be able to circulate water from one well to another.

**2. Physical background**

For water to heat up sufficiently it must be circulated in temperatures as high as possible. Heat transfer mechanisms are advection with the fluid flow and conduction in the "recharge area" or the rock. In Southern Finland, where geothermal gradient is around 16K/km, achieving temperature of over 100°C requires drilling to as deep as 7 km. At such depth pressure closes fractures and therefore decreases permeability, the crucial parameter for fluid flow.

Permeability is a complex parameter that can be considered spatially correlated and lognormally distributed. This means that during stimulation permeability becomes increasingly channelized. Such permeability distribution can be modelled and applied to the fluid flow model in order to achieve channelized flow pattern. An example of permeability pattern is presented in Figure 2.

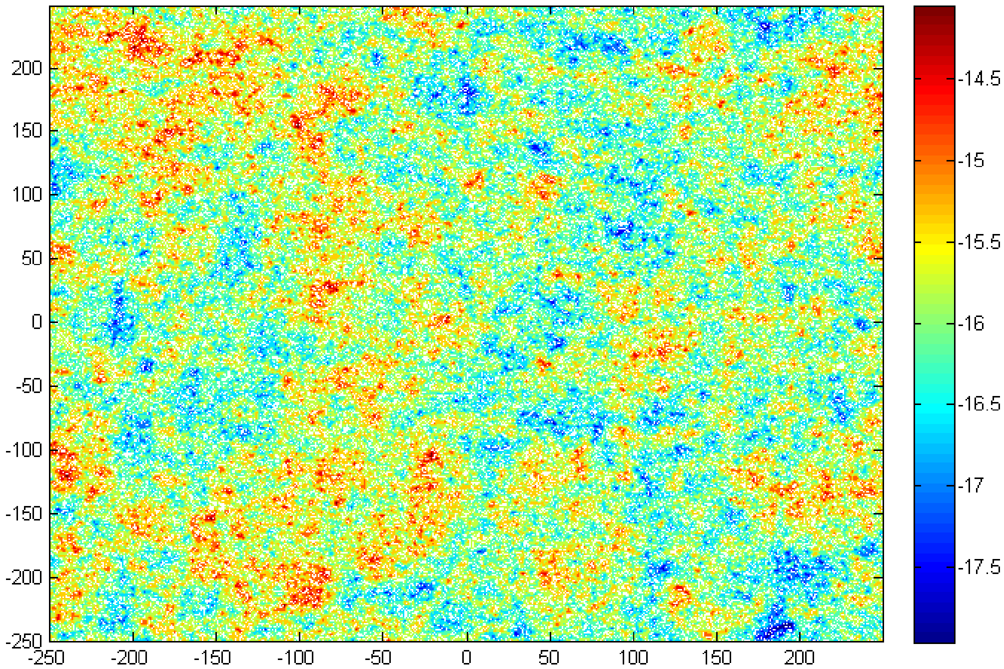


**Figure 2:** Example of permeability distribution.

**3. The models**

Analytical model used in the study include heat and fluid transport models by Rodemann (1979). This model an idealized model for heat transport with fluid flow in single fracture.
Numerical model is built with COMSOL Multiphysics finite element analysis software. The permeability distribution is to be implemented in the numerical model so the effect of heterogenous permeability can be studied.

Analytical model is used to order to verify the numerical results. Preliminary results are similar for both models.

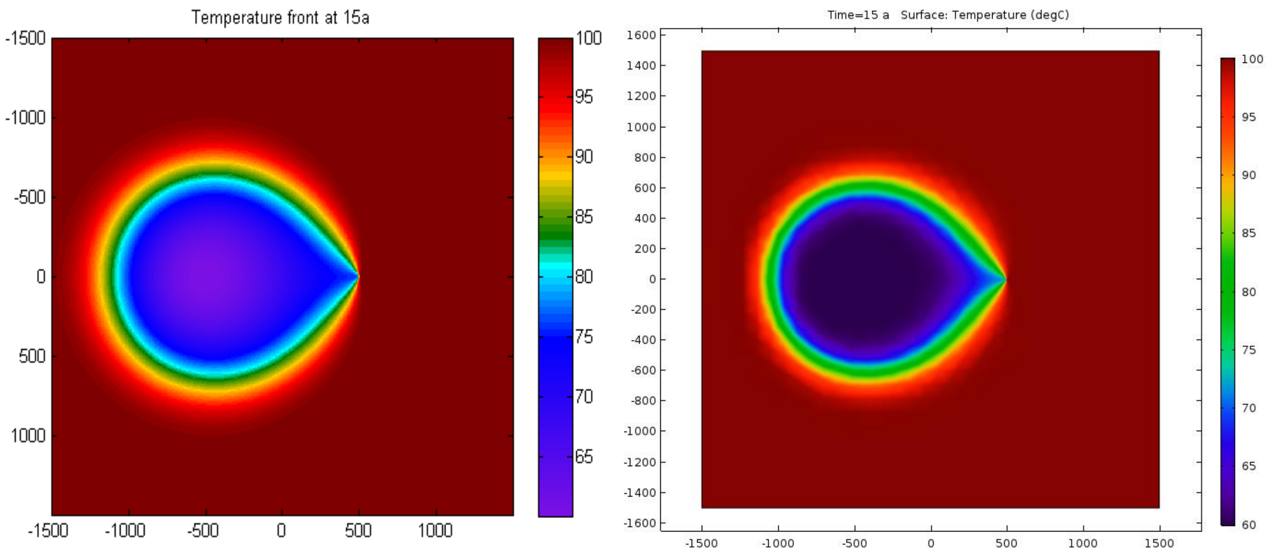


**Figure 4:** Temperature front after 15 years of cold water input at steady rate. Similar results of analytical model (left) and numerical model (right).

## References:

Leary, P., Malin, P., Pogacnik, J., Valles, B., Geiser, P., 2014. Lognormality, δκ ~ κ δφ, EGS, and All That, Proceedings, Thirty-Ninth Workshop on Geothermal Reservoir Engineering

Rodemann, H., 1979. Niedersächsisches Landesamt für Bodenforschung Hannover, Geowissenschaftliche Gemeinschaftsaufgaben

USGS: http://www1.eere.energy.gov/geothermal/pdfs/evaluation_egs_tech_2008.pdf

Tester, J., Anderson, B., Batchelor, A., Blackwell, D., DiPippo, R., Drake, E., Granish, J., Livesay, B., Moore, M., Nichols, K., Petty, S., Toksöz, M., Veatch, R. 2006. The future of geothermal energy: Impact of Enchanced Geothermal Systems (EGS) on the United States in the 21st century, An assessment by an MIT-led interdisciplinary panel, edited by Kubik, M.

# Geodynamical research with superconducting gravimeters at the Metsähovi Geodetic Research Station

A. Raja-Halli and H. Virtanen

Finnish Geospatial Research Institute, National Land Survey

E-mail: arttu.raja-halli@nls.fi

Superconducting gravimeters (SG) are the most sensitive relative gravimeters and hence are very well suited for studying geodynamical phenomena of various time scales. Finnish Geospatial Research Institute, (FGI, former Finnish Geodetic Institute) has operated an SG continuously since 1994 at the Metsähovi Geodetic Research Station. The instrument has been used to study e.g., solid earth tides, crustal loading due to ocean tides and non-tidal mass changes in the Baltic Sea and atmosphere, as well as seismic normal modes of the Earth. In 2014 FGI received a new SG with even lower noise level at sub-seismic periods. With the new instrument we attempt to detect the translational motion of the solid inner core i.e., the Slichter mode. Here we present the current research and status of the FGI's SG's.

**Keywords:** geodynamics, gravity, Metsähovi

## 1. Introduction

FGI's Metsähovi Geodetic Research Station is a global geodetic "Core Station" and is equipped with all space geodetic techniques: Satellite Laser Ranging (SLR), Global Navigation Satellite Systems (GNSS), geodetic Very Long Baseline Interferometry (VLBI) and a DORIS (Doppler Orbitography and Radiopositioning Integrated by Satellite) beacon. In addition there is a dedicated gravity laboratory equipped with two superconducting gravimeters and an absolute gravimeter for geodynamical research. SG together with GNSS is crucial for studying loading effects which affect also observations made with the other instruments. Loading is mainly caused by the mass changes in the Gulf of Finland and atmosphere. Studies have shown that 1 meter sea level rise in the Gulf of Finland weighs Southern Finland down 11mm (e.g., Virtanen & Mäkinen 2003, Virtanen 2006, Nordman *et al.* 2015). Observations made with the SG have been used also to study the free oscillations of the Earth (Figure 2.) (Virtanen 2006). Recently we have studied the effect of local hydrology on gravity (Mäkinen *et al.* 2014).

## 2. Superconducting gravimeters of FGI

A superconducting gravimeter is a relative gravity instrument based on the levitation of a superconducting sphere in a stable magnetic field created by a current in superconducting coils (e.g., Goodkind, 1999). An SG can detect periodical changes in gravity as small as $10^{-11}$ms$^{-2}$ (nGal, 1 microgal = 1 μGal = 10mm s$^{-2}$, 1 nanogal = 1nGal = 0.01nm s$^{-2}$). For a single event, the detection threshold is higher, conservatively about $10^{-9}$ ms$^{-2}$. Due to its high sensitivity and low drift rate, the SG is very good for the study of geodynamical phenomena through their gravity signatures (Hinderer and Crossley, 2000). Currently there is approximately 35 SG's operated globally.

Superconducting gravimeter GWR T020 operated at the Metsähovi Geodetic Research Station continuously from August 1994 till September 2016 – second longest continuous SG time series in the World. In 2014 a new modern dual sensor OSG-073 SG was installed in Metsähovi to the same gravity laboratory as T020 (Figure 1.). During 2016 the OSG-073 went through several improvements and is now divided into two separate SG's: a portable SG iGrav-013 and stationary OSG-022. The former offers portability and very low drift and the latter is one of the world's most sensitive instruments in the sub-seismic bands (<1mHz). Metsähovi

T020 was part of the Global Geodynamics Project (since 2015 IGETS - "International Geodynamics and Earth Tide Service") which was an international research effort to combine and gather the data from all SG's in the World. The scientific objectives of the GGP were e.g., normal modes, mantle rheology, tides, solid earth-oceans-atmosphere interactions, hydrology and Earth rotation (e.g., Hinderer 2004). The iGrav-013 and OSG-022 will continue in the IGETS service. All gravity data from participating SG's is freely available through the IGETS service (*http://isdc.gfz-potsdam.de/igets-data-base*).

**Figure 1.** Superconducting gravimeters at Metsähovi. The old T020 on the left and the new OSG-073 on the right.

**3. Geodynamical Research**

SG's have proven to be very valuable in the geodynamical research. It can measure effects with varying periods from seconds to years. Largest signal in the time varying gravity is the solid earth tides with amplitudes of several hundreds of $nm/s^2$ in periods from hours up to 18.6 years. Tidal analyses are used to obtain information about elastic properties of the Earth and to study and validate ocean tide models. Because of the low drift and high sensitivity, SG's have brought new insight also to other long period phenomena such as Free Core Nutation (FCN), Chandler Wobble (CW) and nonlinear ocean tides (e.g. Virtanen 2006).

SG together with GNSS gives indispensable information on the crustal loading at Metsähovi. In addition to solid earth tides and loading caused by ocean tides, Metsähovi has vertical deformations of over a cm due to changes in the mass of atmosphere and the Baltic Sea. It is important to correct for these deformations on the other geodetic measurements. With SG we can also monitor microseisms with strongest spectral peaks at around 12 and 6 seconds created by storm surges in the northern Atlantic (Virtanen 1998). This microseism is causing noise in other gravity measurements (absolute and relative). Depending on the frequency of the microseism we can distinguish the source area for the microseism e.g., Norvegian coast or northern Atlantic (Virtanen 1998).

SG's have also proven to be very good instrument for studying the inner structure of the Earth from the normal mode spectrum of the Earth. SG's have lower noise than seismometers at sub-seismic frequencies (<1mHz) hence providing a better tool for observing the gravest normal modes of the Earth (Figure 2.)(Rosat 2004). By studying the frequencies of these normal modes we can test the suitability of different Earth models such as 1066a, PREM or CORE11. With the new very low noise instrument OSG-022 together with similar instruments in France and Germany we aim to detect the translational oscillation of the solid inner core i.e., Slicther mode (Slichter 1961, Rosat 2011). By determining the frequency of this mode we could give an estimate on the density contrast at the inner core boundary (ICB) as well as give an estimation on the viscosity of the fluid at the ICB.

To study these different geophysical signals we need to first correct the gravity signal for other known effects. Hence we are currently developing a more sophisticated hydrogeological model of Metsähovi area to study and model the gravitational effect of the local hydrology on the observed SG signal. The attraction of the local hydrology is the biggest unclear signal in the gravity time series with peak-to-peak of several μGal's. The hydrological signal has a distinct seasonal period but also shows periods within few hours due to strong precipitation and complex runoff. In addition to a basic meteorological station with temperature, humidity, pressure and wind sensors, we have also installed a comprehensive hydrological sensor network to Metsähovi: with 3 deep groundwater boreholes in the bedrock; 11 boreholes on the soil above the bedrock; soil moisture sensors; snow height and water equivalence sensors; rain gauge and two global radiation sensors. With the hydrological observations we can model the evapotranspiration and runoff of the water at Metsähovi. By carefully correcting the gravity time series for the hydrological effect we are able to study tidal signals as well as the normal modes with a better accuracy (Mäkinen *et al.* 2014).

Due to small linear drift of the SG it is not directly compatible for postglacial rebound studies. However, the absolute gravity measurements that are used for PGR research could benefit from the high resolution time varying gravity signal for correcting e.g., local hydrology (e.g., Ekman&Mäkinen 1996, Mäkinen *et al.* 2005, Virtanen *et al.* 2014).

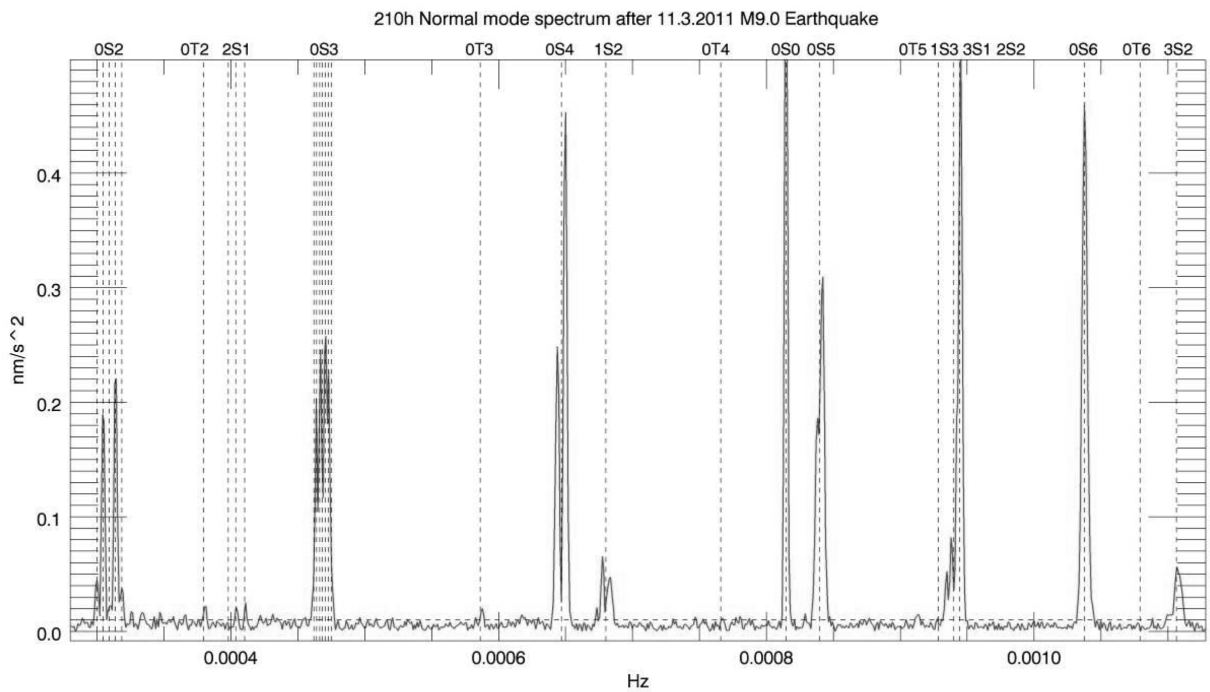


**Figure 2.** Earth's normal mode spectrum observed with the SG T020 after the Tohoku M9.0 earthquake on 11.3.2011. The gravest spherical and toroidal normal modes are clearly visible. Modes are splitted to several overtones due to the rotation and ellipticity of the Earth.

## 3. Conclusions and future work

The superconducting gravimeter of the FGI has contributed on several geophysical studies. The studied phenomena range from 18.6 year solid earth tide to seismic normal modes and microseism due to high swells on the Atlantic with periods of only 6 seconds.

With the new low noise OSG-022 and by utilising improved models for the local hydrology we will search for the Slichter mode and improve the measurements of the gravest normal modes. In addition the SG's will provide important observations on the crustal loading at Metsähovi that cause error and biases in the space geodetic observations.

## References:


Ekman M. and Mäkinen J., 1996. Recent postglacial rebound, gravity change and mantle flow in Fennoscandia. Geophysical Journal International, vol. 126, no. 1, pp. 229–234.

Goodkind, J., 1999. The superconducting gravimeter, Review of Scientific Instruments 70 (11), 4131-4152.

Hinderer, J., Crossley, D., 2000. Time variations in gravity and inferences on the Earth's structure and dynamics. Surveys in Geophysics 21, 1–45.

Hinderer, J., Crossley, D., 2004. Scientific achievements from the first phase (1997-2003) of the Global Geodynamics Project using a worlwide network of supeconducting gravimeters. J. Geodyn. 38 (3-5), 237-262.

Mäkinen J., Engfeldt A., Harsson B.G.., et al., 2005. The Fennoscandian land uplift gravity lines 1966–2003. In Gravity, Geoid and Space Missions, C. Jekeli, L. Bastos, and J. Fernandes, Eds., IAG Symposium 129, pp. 328–332, Springer, Berlin, Germany.

Mäkinen J., Hokkanen T., Virtanen H., Raja-Halli A., Mäkinen R.P., 2014. Local hydrological effects on gravity at Metsähovi, Finland: implications for comparing observations by the superconducting gravimeter with global hydrological models and with GRACE.
In: Proceedings of the International Symposium on Gravity, Geoid and Height Systems GGHS 2012, October 9–12, 2012, Venice, IAG Symposia 141.

Nordman, M., Virtanen, H., Nyberg, S., Mäkinen, J., 2015. Non-tidal loading by the Baltic Sea: comparison of modelled deformation with GNSS time series. GeoResJ, 40 pp.14-21.

Rosat, S., Hinderer, J., Crossley, D., and J. P. Boy, 2004. Performance of superconducting gravimeters from long period seismology to tides. J. Geodyn. 38 (3-5), 461-476.

Rosat, S., 2011. A review of the Slichter modes: An observational challenge. Jon M. Phillips. *The Earth's Core: Structure, Properties and Dynamics*, Nova Science Publishers, Inc, pp. 63-77.

Slichter, L.B.,(1961),The fundamental free mode of the Earth's inner core. Proc. Nat. Acad. Sci. USA 47, 186-190.

Virtanen, H., 1998. On superconducting gravimeter observations above 8 mHz at the Metsähovi station, Finland. Rep. Finn. Geod. Inst. 98:5.

Virtanen H. and Mäkinen J., 2003. The effect of the Baltic Sea level on gravity at the Metsähovi station. Journal of Geodynamics, 35, 4–5: 553–565.

Virtanen H. 2006. Studies of earth dynamics with the superconducting gravimeter [PhD dissertation]. University of Helsinki.

Virtanen, H., Bilker-Koivula, M., Mäkinen, J., Näränen, J., Ruotsalainen, H., 2014. Comparison between measurements with the superconducting gravimeter T020 and the absolute gravimeter FG5-221 at Metsähovi, Finland in 2003-2012. Bull. Inf. Marées Terrestres 148 ,11923-11928

# Geochemical charasteristics of the Kumpula campus area: Drill core and outcrop data

M. Räisänen, I. Kukkonen, J.S. Heinonen, R. Valtonen and K. Penttilä
Dept. of Geosciences and Geography, University of Helsinki, FI-00014, Finland
E-mail: milja.raisanen@helsinki.fi

The Kumpula Campus Drill Hole Project provides educational environment and data for future drill hole related courses and research in geology and geophysics. Current geological studies of the drill hole concern petrology, fracture mapping and geochemistry. This study is about geochemical examination of the Kumpula campus drill core and outcrops and also a comparison between a PXRF-analyzer and a WD-XRF-analyzer. The comparison leads to usefulness evaluation of the PXRF-analyzer.

**Keywords:** geochemistry, XRF, Helsinki, Svecofennian

## 1. Introduction

The diamond core drilling of the Kumpula campus drill hole was performed in December 2015 by Suomen Malmi Oy. The drill hole is 370m deep, 76mm in diameter and in an angle of 70 degrees NE. The core is 56mm in diameter (Kukkonen et al., this volume).

The aim of the Kumpula Campus Drill Hole Project is to provide environment and data for research and undergraduate education in geosciences at the University of Helsinki. In addition to the department's scientific equipment investments of 2015, the campus drill hole provides now a teaching and testing environment for the new geophysical and geological analyzers. The intention is to keep the drill hole open and available for scientific analyses as long as possible, hopefully for decades. (Kukkonen and Koivisto 2015).

## 2. Geological setting

The bedrock in Helsinki area has formed during the Svecofennian orogeny, in Paleoproterozoic era about 1.9 billion years ago. Originally sedimentary and volcanic rocks went through metamorphosis during the Svecofennian orogeny and formed for example mica-gneisses, acidic gneisses, amphibolites, hornblende-gneisses and migmatites. Later during the orogeny, igneous rocks like granite, granodiorite and tonalite formed own sections conforming the bedrock structures. (Laitala 1991, Kähkönen 1998).

The Kumpula campus area is mainly hornblende-gneiss with granite veins that have formed later during the orogeny and migmatitic mixtures of these both. The amphibolites and hornblende-gneisses in Helsinki area show hardly any structures related to formation because of the relatively strong deformation during the metamorphosis. (Laitala 1991).

## 3. XRF-analyses

This study concentrates on the geochemical aspect of the drill core and outcrops. The aim is to do a comparison between the portable x-ray fluorescence spectrometer (PXRF): NITON Thermo Scientific XL3t GOLDD+ and wavelength dispersive x-ray fluorescence spectrometer (WD-XRF): PANalytical Axios mAX 4kW, which uses Omnian method. Comparing the geochemical results of the PXRF-analyzer with the results of the quantitative WD-XRF, the usefulness of the PXRF is discovered.

The examining of the drill core started with taking XRF analyses with the portable device roughly on every rock unit. This led to about 150 analyses of the whole core. Based on visual features and different oxide percentages, four frequent rock types were defined. Along with hornblende-gneiss, the drill core includes granite, amphibolite and calc-silicate rock. Also about

15 sample pieces of hornblende-gneiss sections have been sawed, on every 30 meters. Those sample pieces are going to be analyzed with both of the XRF-analyzers and so the possible geochemical changes compared to depth are discovered. Thin section works are also going to be carried out for the sample pieces, one for each of the four rock types.

Field work in the surroundings of the campus was done during the summer of 2016. About 115 on-site PXRF analyses were taken on 11 selected outcrops and road cuttings and the intention is to compare those results with the results of the core. Also under examination is what kind of effects does the coarseness of the weathered surface or surface that is covered with lichen or traffic pollution, have on the results.

**4. First conclusions and future work**

When examining the results of the PXRF-analyzer, the primary interest is seeing if the ”total” –value actually represents the success of the analysis, since the value is highly dependent on the surface features (Figure 1). It will be interesting to see, if the relative percentages of the elements stay the same also in cases of low total caused by for example uneven surface.

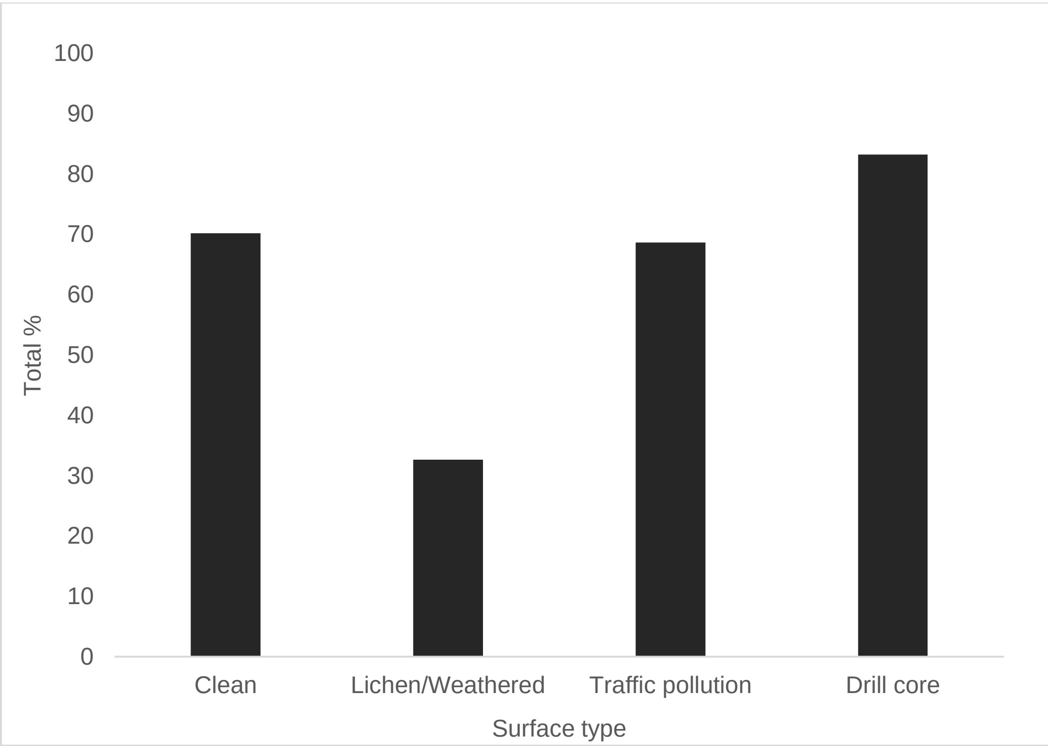


**Figure 1.** Average total values for different kinds of surfaces.

The first comparison was done for $TiO_2$ / FeO ratio compared to total with different kinds of symbols representing different surface conditions (Figure 2). The diagram shows how most of the $TiO_2$/FeO –values stay roughly between 0 – 0,4. However clean surfaces and drill core give values that are a bit more scattered, where weathered/lichen covered surfaces and especially traffic polluted surfaces give quite constant ratios for $TiO_2$/FeO. The diagram shows also how traffic polluted and weathered/lichen covered surfaces have total values that are noticeably more scattered than clean surfaces and drill core. Yet based on this diagram, it is still too early to make definite conclusions and further examination needs to be done.

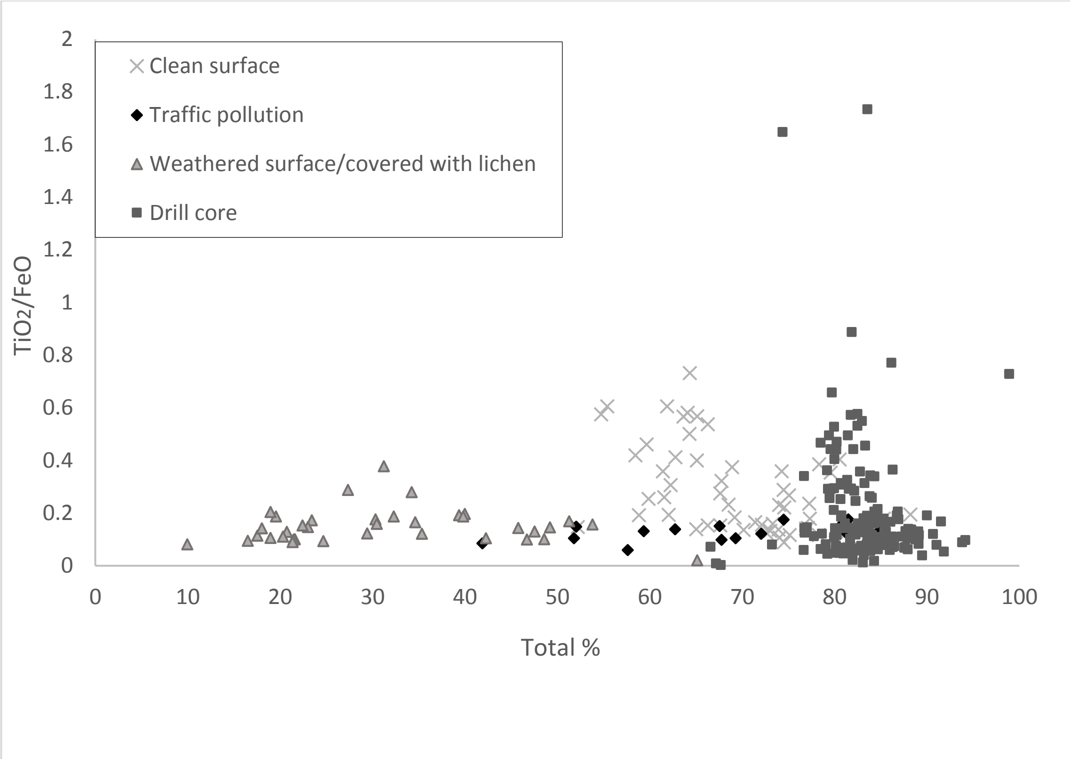


**Figure 2.** $TiO_2$ /FeO ratio compared to total in different kinds of surfaces. All of the values are measured with PXRF-analyzer.

The final conclusions of the usefulness of the PXRF-analyzer are going to be important information for the future field courses and research in our department.

Together with Kalle Penttilä's petrographic work and Riikka Valtonen's fracture mapping, we are going to have an insight of what lays beneath our campus and which might be interesting topics to still work with in the future.

## References:

Kukkonen, I. and Koivisto, E. 2015. Matemaattis-luonnontieteellinen tiedekunta. Kumpulan kampuksella kaivetaan reikää. Page visited 2.10.2016. http://www.helsinki.fi/ml/ajankohtaista/2015/2015kairaus.html

Kukkonen, I.T., Koivisto, E. and Whipp, D. (this volume). Helsinki University Kumpula campus drill hole project. In: *Kukkonen et al. (Eds.),* Lithosphere 2016 – Ninth Symposium on the Structure, Composition and Evolution of the Lithosphere in Finland. Programme and Extended Abstracts, Espoo, Finland, November 9-11, 2016. Institute of Seismology, University of Helsinki, Report S-65, 166 pages.

Kähkönen, Y. 1998. Svekofenniset liuskealueet – merestä peruskallioksi. In Lehtinen, M., Nurmi, P. and Rämö, T. (edit.). Suomen kallioperä: 3000 vuosimiljoonaa. Suomen Geologinen Seura ry, Helsinki, 200–227.

Laitala, M. 1991. Helsingin kartta-alueen kallioperä. Geological Map of Finland 1 : 100 000 . Explanation to the Maps of Pre-Quaternary rocks, sheet 2034. Geological Survey of Finland, Espoo, 47 p.

# Mid-Proterozoic evolution of southern Laurentian lithosphere; crustal domains and potassic/ultrapotassic magmatic suites in Mojavia and Mazatzal provinces

O.T. Rämö[1], J.P. Calzia[2], V.T. McLemore[3] and P. Heikkilä[1]

[1]Geosciences, University of Helsinki
[2]U.S. Geological Survey, Menlo Park, California
[3]New Mexico Tech, Socorro, New Mexico
E-mail: tapani.ramo@helsinki.fi

Paleoproterozoic cratonic rocks and Mesoproterozoic potassic/ultrapotassic alkaline suites from the southern margin of Laurentia have Nd isotopic and elemental geochemical compositions that help to refine evolutionary traits of Laurentian lithosphere. Two Proterozoic crustal provinces examined (Mojavia, Mazatzal) (a) bear evidence for substantial involvement of pre-existing crust (old and more juvenile, respectively) in making these terranes, (b) reveal two distinct subcontinental lithospheric mantle domains attached to them, and (c) imply that the Mesoproterozoic Mountain Pass carbonatite (1375 Ma) was derived from enriched mantle lithosphere.

**Keywords:** shonkinite, carbonatite, minette, granite, Sm-Nd isotopes, Laurentia, USA

## 1. Introduction

The Proterozoic North American lithosphere serves as a model for Precambrian crustal growth around an Archean nuclei. In southern Laurentia, Proterozoic crustal domains (Mojavia, Yavapai, Mazatzal) were accreted onto the pre-existing Archean lithosphere (Wyoming province) to form a secular growth pattern from the northwest to the southeast (e.g., Whitmeyer and Karlstrom, 2008). Three principal crustal provinces have been distinguished by Sm-Nd isotope geochemistry (Bennett and DePaolo, 1987), and they have been delineated on the basis of $T_{DM}$ model ages (DePaolo, 1981). In province 1 (Mojavia), $T_{DM}$ range from ≥ 2.5 to 2.0 Ga, in province 2 (Yavapai) from 2.0 to 1.8 Ga, and in province 3 (Mazatzal) from 1.8 to 1.7 Ga (Bennett and DePaolo, 1987; Rämö and Calzia, 1998). We have compiled a comprehensive data set based on whole-rock Sm-Nd isotope compositions (published and unpublished) of cratonic rocks from Mojavia and Mazatzal and present some new ideas regarding the time-integrated evolution of these two Precambrian terranes. We elaborate on the significance of two Mesoproterozoic potassic/ultrapotassic suites in Mojavia (the 1410-1375 Ma Mountain Pass shonkinite and carbonatite) and Mazatzal (the 1460 Ma Burro Mountains minette and potassic granite) and discuss their bearing to the assembly and subsequent evolution of southern Laurentian lithosphere.

## 2. Sm-Nd isotope geochemistry of Mojavia and Mazatzal

The crustal structure of southern Laurentia (Fig. 1A) displays an amalgamate of crustal domains assembled in collisional events at 1.75-1.70 Ga (Ivanpah orogeny) and 1.65-1.63 Ga (Mazatzal orogeny) (Whitmeyer and Karlstrom, 2008). South of the Archean Wyoming province, these Proterozoic crustal domains show a consistent pattern of initial Nd isotopic compositions becoming more radiogenic from Mojavia through Yavapai to Mazatzal (Bennett and DePaolo, 1987; Rämö and Calzia, 1998). Figure 2 shows the Nd isotopic composition of cratonic rocks from Mazatzal in SW New Mexico and SE Arizona ($\varepsilon_{Nd}$ at 1460 Ma) and Mojavia in SE California ($\varepsilon_{Nd}$ at 1400 Ma). For all granitoids and metamorphic rocks, the Mojavia samples have more negative $\varepsilon_{Nd}$ (-9 to -3) than those from Mazatzal ($\varepsilon_{Nd}$ -1 to +4).

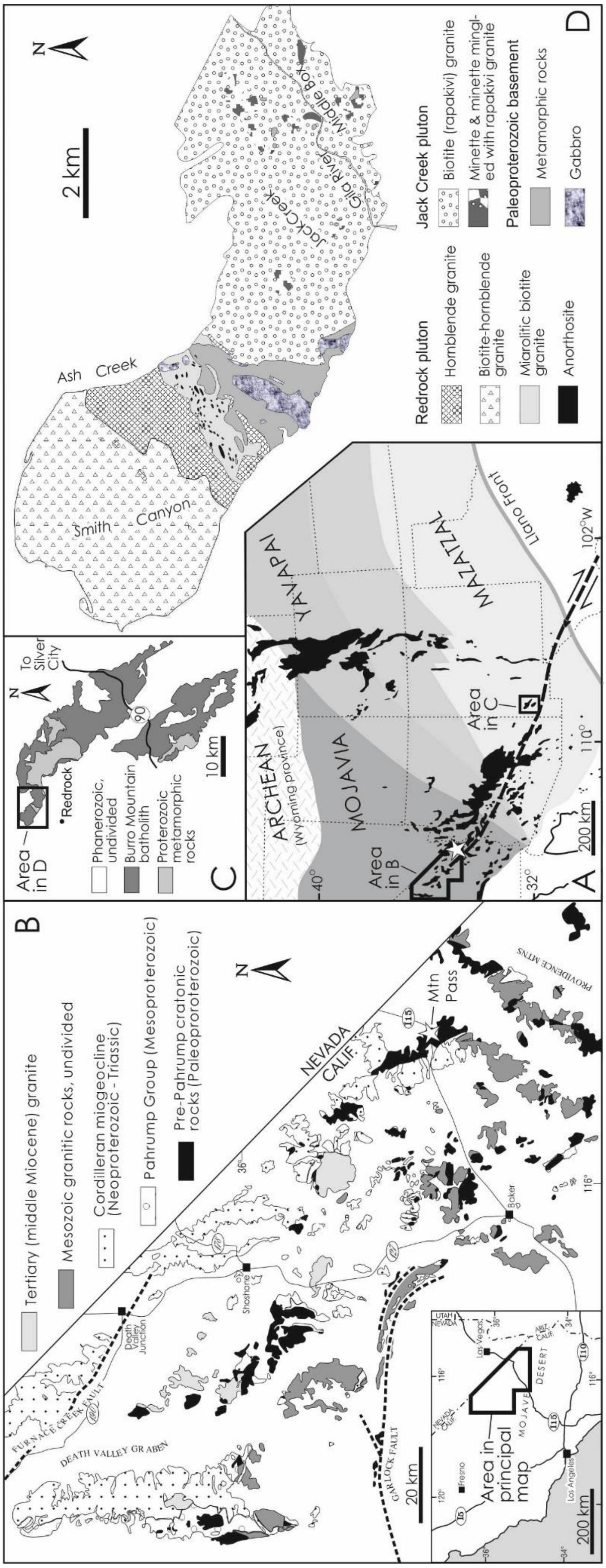


**Figure 1.** (A) Division of Proterozoic crustal domains south of the Archean Wyoming province in southern Laurentia. Black denotes areas of exposed cratonic (Precambrian) rocks. Star marks location of the Mountain Pass alkaline suite (1410-Ma shonkinite, syenite, and granite; 1375-Ma carbonatite). Llano Front marks the northwestern margin of the Grenville orogeny at 30º-34º N latitude. Heavy dashed line denotes a Proterozoic transcurrent zone along the southern margin of Laurentia, extending from west Texas to southeastern California (Bickford et al., 2000). (B) Geological map of the southern Death Valley region, Mojavia province, southeastern California showing the distribution of Proterozoic and Phanerozoic lithologic units exposed in a grossly extended terrain. Inset shows location of the southern Death Valley region relative to southern California (modified from Rämö and Calzia, 1998). (C) General geological map of the Burro Mountains, Mazatzal province, southwestern New Mexico (modified from Rämö et al., 2003). (D) Geological map of the northwestern part of the Burro Mountains. This terrane is dominated by two Mesoproterozoic granite plutons, Redrock (1220 Ma; associated with massif-type anorthosite) in the west and Jack Creek (1460 Ma; intermingled potassic granite and minette) in the east, with a sliver of metamorphic Mazazal crust in between (modified from Rämö et al., 2003).

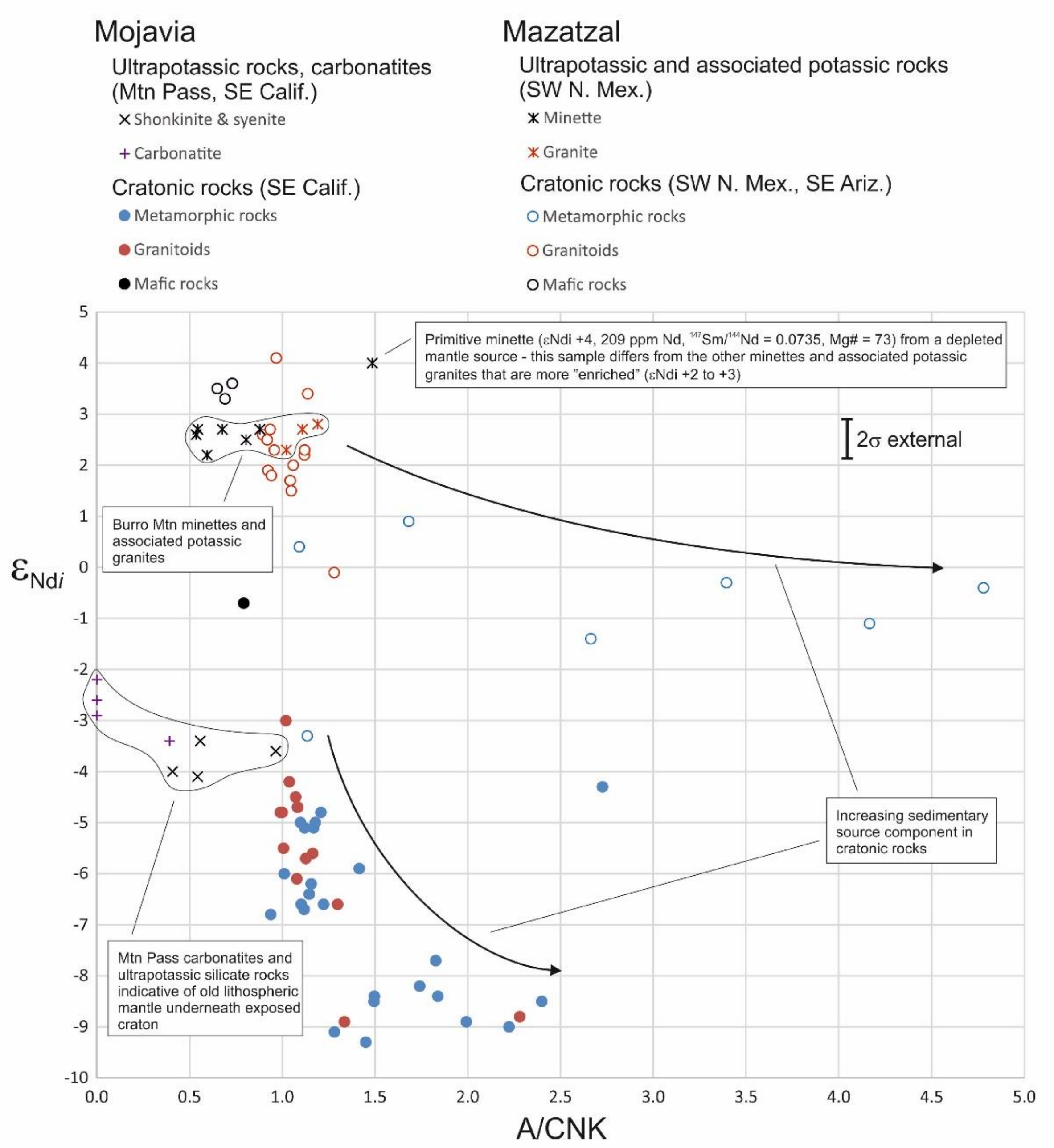


**Figure 2.** A/CNK (molar $Al_2O_3/(CaO+Na_2O+K_2O)$) vs. $\varepsilon_{Ndi}$ diagram showing the composition of cratonic samples from Mojavia and Mazatzal and associated potassic/ultrapotassic igneous suites. Initial values calculated at 1400 Ma for Mojavia and at 1460 Ma for Mazatzal. Data from Rämö and Calzia (1998), Amato et al. (2008), McLemore et al. (2012), and the authors (unpublished).

## 3. Potassic/ultrapotassic suites

The two potassic/ultrapotassic suites examined from Mojavia and Mazatzal were emplaced at ~1400 Ma and ~1460 Ma, respectively, and comprise alkaline silicate rocks (shonkinite, syenite, minette, alkali granite) and carbonatite (Mojavia). LREE values of these rocks are very high (up to 300 ppm Nd in the silicate rocks and up to 4600 ppm Nd in carbonatite). The initial Nd isotope composition of these samples (Fig. 2) falls into two categories: shonkinites, syenites, and carbonatite from Mountain Pass have $\varepsilon_{Ndi}$ of -4 to -2; minettes and granites from the Burro Mountains have $\varepsilon_{Ndi}$ of +2 and +3, save for one minette sample with an $\varepsilon_{Ndi}$ of +4.

## 4. Lithospheric evolution

Our new compilation of Nd isotope compositions of cratonic rocks from Mojavia and Mazatzal provinces show some probably important patterns. Both suites show clear patterns of increasing aluminium saturation index with decreasing $\varepsilon_{Nd}$ values (Fig. 2). This points to incorporation of pre-existing crustal material in the form of sedimentary detritus from varying provenances into the nascent Mojavia and Mazatzal crustal provinces (cf. Rämö and Calzia, 1998). Obviously, these provenances were quite different age-wise (Archean vs. Paleoproterozoic).

The Mountain Pass carbonatite is exceptional in having clearly negative $\varepsilon_{Nd}$ values (cf. Bell and Simonetti, 2010). Moreover, the initial Nd isotope compositions of the alkaline silicate rocks and the Mountain Pass carbonatite are all negative and almost identical, and a common source for them in the sublithospheric mantle is viable. These rocks thus probably register an ancient (Paleoproterozoic) subcontinental mantle domain that was formed while the Mojavia province was assembled. The Burro Mountains minettes, on the other hand, probably tapped a more juvenile, depleted mantle lithosphere attached to the Mazatzal crustal province.

## 5. Concluding remarks

The Nd isotope composition of cratonic rocks and Mesoproterozoic alkaline suites from the Mojavia and Mazatzal provinces sheds new light on the assembly of southern Laurentia in terms of crustal processes (e.g., interplay of different provenances) and crust-mantle dynamics. The Mesoproterozoic potassic/ultrapotassic alkaline suites of Mountain Pass (southeastern California) and Burro Mountains (southwestern New Mexico) provide a useful proxy in pursuit of the age and time-integrated Sm-Nd isotope evolution of the subcontinental lithospheric mantle in the two areas examined.

## References:

Amato, J.M., Boullion, A.O., Serna, A.M., Sanders, A.E., Farmer, G.L., Gehlers, G.E., Wooden, J.L., 2008. Evolution of the Mazatzal province and the timing of the Mazatzal orogeny: Insights from U-Pb geochronology and geochemistry of igneous and metasedimentary rocks in southern New Mexico. Geological Society of America Bulletin 120, 328-346.

Bell, K., Simonetti, A., 2010. Source of parental melts to carbonatites – critical isotopic constraints. Mineralogy and Petrology 98, 77-89.

Bennett, V.C., DePaolo, D.J., 1987. Proterozoic crustal history of the western United States as determined by neodymium isotopic mapping: Geological Society of America Bulletin 99, 674-685.

Bickford, M.E., Soegaard, K., Nielsen, K.C., McLelland, J.M., 2000. Geology and geochronology of Grenville-age rocks in the Van Horn and Franklin Mountains area, west Texas: Implications for the tectonic evolution of Laurentia during the Grenville: Geological Society of America Bulletin 112, 1134-1148.

DePaolo, D.J., 1981. Neodymium isotopes in the Colorado Front range and crust-mantle evolution in the Proterozoic. Nature 291, 193-196.

McLemore, V.T., Rämö, O.T., Heizler, M.T., Heinonen, A.P., 2012. Intermittent Proterozoic plutonic magmatism and Neoproterozoic cooling history in the Caballo Mountains, Sierra County, New Mexico; Preliminary Results. In: Lucas, S.G., McLemore, V.T., Lueth, V.W., Spielmann, J.A., Krainer, K. (Eds.) Geology of the Warm Springs Region: New Mexico Geological Society 63rd Annual Field Conference, Guidebook, 235-248.

Rämö, O.T., Calzia, J.P., 1998. Nd isotopic composition of cratonic rocks in the southern Death Valley region: Evidence for a substantial Archean source component in Mojavia. Geology 26 (10), 891-894.

Rämö, O.T., McLemore, V.T., Hamilton, M.A., Kosunen, P.J., Heizler, M., Haapala, I., 2003. Intermittent 1630-1220 Ma magmatism in central Mazatzal province: New geochronologic piercing points and some tectonic implications. Geology 31 (4), 335-338.

Whitmeyer, S.J., Karlstrom, K.E., 2007. Tectonic model for the Proterozoic growth of North America. Geosphere 3 (4), 220-259

# Mesoproterozoic Nuna supercontinent and the geomagnetic field in light of recent paleomagnetic and geochronological data from diabase dykes of Finland

J M. Salminen[1], R Klein[1], T Veikkolainen[1], L J. Pesonen[1], S Mertanen[2]

[1]Department of Physics, 00014 University of Helsinki, Finland
[2]Geological Survey of Finland, 02151 Espoo, Finland
E-mail: Johanna.m.salminen@helsinki.fi

**Keywords:** Baltica, paleomagnetism, geochronology, Nuna, Columbia, NENA, geocentric axial dipole

**Abstract**

The number of good quality paleomagnetic data of the Mesoproterozoic supercontinent Nuna (e.g. Columbia, Hudsonland) has increased in recent years enabling more reliable global continental reconstructions (e.g Hoffman 1997; Evans and Mitchell 2011; Zhang et al. 2012; Pisarevsky et al. 2014). Supercontinent Nuna included Baltica, Laurentia, Siberia, proto-Australia and Antarctica, Amazonia and West Africa, Congo-São Francisco, North China, Kalahari and India cratons. Baltica and Laurentia are thought to represent two of the most important building blocks of this supercontinent in a single geologically valid NENA (North Europe- North America) juxtaposition between ca. 1.75-1.27 Ga forming the core of Nuna with Siberia (e.g. Gower et al. 1990; Evans and Mitchell 2011).

Recent high quality, precisely dated Mesoproterozoic paleomagnetic poles of Baltica support the NENA connection. These include the pole from Åland (1575.9 ± 3.0 Ma; U-Pb) diabase dykes (Salminen et al. 2015) and coeval pole from Satakunta diabase dykes (Salminen et al. 2014) in Finland; a pole for the Mesoproterozoic Satakunta sandstones in Finland (Klein et al. 2014); and poles for Lake Ladoga basalts and intrusives (1459 ± 3, 1457 ± 2 Ma; U-Pb) in Russia (Salminen and Pesonen 2007; Lubnina et al. 2010).

One striking feature of the 1.576 Ga high quality paleomagnetic data for Åland and Satakunta is the asymmetry of polarity, i.e. the mean directions of normal (N) and reversed (R) polarities are not antiparallel at 95% confidence level and do not pass the reversal test (McFadden and McElhinny 1990). One possible reason for such an asymmetry could be an unusual behaviour of the geomagnetic field at the Mesoproterozoic, which would hamper the paleomagnetic reconstructions. Antipodality of N and R directions is expected in the case where the geomagnetic field is represented by the geocentric axial dipole (GAD), whereas steepening or shallowing of inclinations can result from the contamination of GAD by zonal multipolar fields. We used 26 global dual-polarity paleomagnetic results from PALEOMAGIA database (Veikkolainen et al. 2014a) to detect possible deviations from the GAD hypothesis (Hospers 1954) applying the quantity called inclination asymmetry (Veikkolainen et al. 2014b). The asymmetry tests indicate that GAD is a relatively good fit at the Mesoproterozoic (1.7-1.4 Ga) and therefore zonal multipolar fields do not explain the observed asymmetry.

One other possible reason for asymmetry is an unremoved secondary component, which could explain the asymmetry for Åland and Satakunta data. Additional support for component mixing comes from the secondary component distribution, which is streaked in part toward the N-polarity direction. A third reason can be a small but significant age difference between N and R magnetized dykes which could explain the asymmetry. However, the actual age span for the Mesoproterozoic dykes for Baltica awaits further precise age dating.

In addition to results from Åland, Satakunta and Lake Ladoga we present here new high quality Mesoproterozoic paleomagnetic and geochronological results from the Häme dykes (1642 ± 2 Ma, 1647 ± 14 Ma; U-Pb) in Finland that do not show asymmetry. These results also support the NENA connection placing Baltica on equatorial latitudes at 1.64 Ga.

## References

Evans, D.A.D., and Mitchell, R.N., 2011. Assembly and breakup of teh core of Paleoproterozoic-Mesoproterozoic supercontinent Nuna. Geology 39, 443-446.

Gower, C.F., Ryan, A.B., Rivers, T. (1990). Mid-Proterozoic Laurentia-Baltica: an overview of its geological evolution and a summary of the contributions made by this volume. In: Mid-Proterozoic Laurentia-Baltica, ed. C.F. Gower, T. Rivers and B. Ryan, Geological Association of Canada Special Paper 38, 1-20.

Hoffman, P.F. 1997. Tectonic genealogy of North America. In: Van der Pluijm, B.A., Marshak, S. (Eds.), Earth Structure: An Introduction to Structural Geology and Tectonics. McGraw-Hill, New York, 459–464.

Hospers, J., 1954. Rock magnetism and polar wandering. Nature 173, 1183-1184.

Klein, R.S., Pesonen, L.J., Salminen, J., and Mertanen, S., 2014. Paleomagnetic study of Mesoproterozoic Satakunta sandstone, Western Finland. Precambrian Research 244, 156-169.

Lubnina, N., Mertanen, S., Söderlund, U., Bogdanova, S., Vasilieva, T., and Frank-Kamenetsky, D., 2010. A new key pole for the East European Craton at 1452 Ma: Palaeomagnetic and geochronological constraints from mafic rocks in the Lake Ladoga region (Russian Karelia). Precambrian Research 183, 442-462.

McFadden, P.L. and McElhinny, M.W. 1990. Classification of the reversal test in palaeomagnetism. Geophysical Journal International 103, 725-729.

Pisarevsky, S.A., Elming, S., Pesonen, L.J., and Li, Z-X. 2014. Mesoproterozoic paleogeography: Supercontinent and beyond. Precambrian Research, 244, 207–225.

Salminen, J., and Pesonen, L.J., 2007. Paleomagnetic and rock magnetic study of the Mesoproterozoic sill, Valaam island, Russian Karelia. Precambrian Research 159, 212-230.

Salminen, J., Mertanen, S., Evans, D.A.D., and Wang, Z., 2014. Paleomagnetic and geochemical studies of the Mesoproterozoic Satakunta dyke swarms, Finland, with implications for a Northern Europe – North America (NENA) connection within Nuna supercontinent. Precambrian Research 244, 170-191.

Salminen, J.M., Klein, R., Mertanen, S., Pesonen, L.J., Fröjdö, S., Mänttäri, I., Eklund, O, 2015. Palaeomagnetism and U-Pb geochronology of ca. 1570 Ma intrusives from Åland archipelago, SW Finland – implications for Nuna. In Li, Z. X, Evans, D.A.D. and Murphy, J.B. (eds.): Supercontinent Cycles Through Earth History. Geological Society, London Special Publications 424. http://doi.org/10.1144/SP424.3

Veikkolainen, T., Pesonen, L.J., and Evans, D.A.D., 2014a. PALEOMAGIA – A PHP/MYSQL database of the Precambrian paleomagnetic data. Studia Geophysica et Geodaetica 58, 425-441.

Veikkolainen, T., Pesonen, L.J., and Korhonen, K., 2014b. An analysis of geomagnetic field reversals supports the validity of the Geocentric Axial Dipole (GAD) hypothesis in the Precambrian. Precambrian Research 244, 33-41.

Zhang, S., Li, Z.-X., Evans, D.A.D., Wu, H., Li, H., and Dong, J. 2012. Pre-Rodinia supercontinent Nuna shaping up: A global synthesis with new paleomagnetic results from North China. Earth and Planetary Science Letters 353-354, 145-155.

# Comparison of the upper mantle structures beneath northern and southern Finland based on the teleseismic tomography results of POLENET/LAPNET and SVEKALAPKO seismic arrays

H. Silvennoinen[1] and E. Kozlovskaya[2]

[1]Sodankylä geophysical observatory, PL3000, 90014 University of Oulu, Finland
[2]Oulu mining school, PL3000, 90014 University of Oulu, Finland
E-mail: hanna.silvennoinen@oulu.fi

We used teleseismic travel time tomography method to study the 3D velocity structure of the upper mantle beneath the POLENET/LAPNET passive seismic array in northern Finland. The mantle structures revealed differ significantly from the structures found earlier beneath the SVEKALAPKO array located in southern and central Finland and overlapping with the southernmost extent of POLENET/LAPNET array.

**Keywords:** lithosphere, upper mantle, seismic, tomography, Fennoscandia

## 1. Introduction

The passive seismic POLENET/LAPNET array recorded continuous seismic waveforms in northern Fennoscandia from May 2007 to September 2009 (Kozlovskaya et al., 2007) (Fig. 1). The experiment was a part of the Polar Year 2007-2008. The array was centred in northern Finland and extended to the surrounding area in Sweden, Norway and Russia. It consisted of 58 seismic stations with the average distance between stations 70 km. 37 of the stations were temporary installations and 21 were permanent seismic stations of Finland, Sweden and Norway. All of the station sites except two temporary stations had broadband instruments deployed at least for a part of the recording period. The primary target of the experiment was to increase the knowledge of the structure of the crust and upper mantle beneath northern Fennoscandia and to estimate the depth of the lithosphere-asthenosphere boundary, if possible.

The SVEKALAPKO array (Hjelt et al., 1996) can be considered the predecessor of the POLENET/LAPNET in southern and central Finland with a slight overlap in the study areas in the southern part of the POLENET/LAPNET study area (Fig. 1). The SVEKALAPKO array was operational 1998-1999. The array consisted of 55 broadband and 88 short period instruments with the average distance between stations 50 km.

Together POLENET/LAPNET and SVEKALAPKO arrays cover Finland and partially the surrounding areas in Sweden, Norway and Russia with a relatively dense array of seismic recordings.

## 2. Teleseismic traveltime tomography method

In seismic tomography method, the 3D structure of the Earth is studied by estimating the travel times of seismic waves originating from distant. The method is analogous to the methods used for example in X-ray tomography. The method optimises relative travel times, the differences between observed and theoretical travel times, through a 3D velocity model beneath the selected study area.

The method assumes that the seismic velocities outside the study volume follow a selected, typically 1D, reference model and that any lateral velocity perturbations are located inside the study volume. As a consequence, the method does not resolve the vertical velocity variation well but only the horizontal variations at the depths defined by the selected starting model. Despite this limitation, the method is widely used and well established in constraining the 3D structure within the lithosphere and the uppermost asthenosphere.

Both our study of POLENET/LAPNET data (Silvennoinen et al., 2016) and an earlier study of SVEKALAPKO data (Sandoval et al., 2004) used the same basic inversion code Telinv based on the original code of Evans and Achauer (1993), though the code has been modified and improved by multiple authors during the intervening decade (see Karousová (2013) for details).

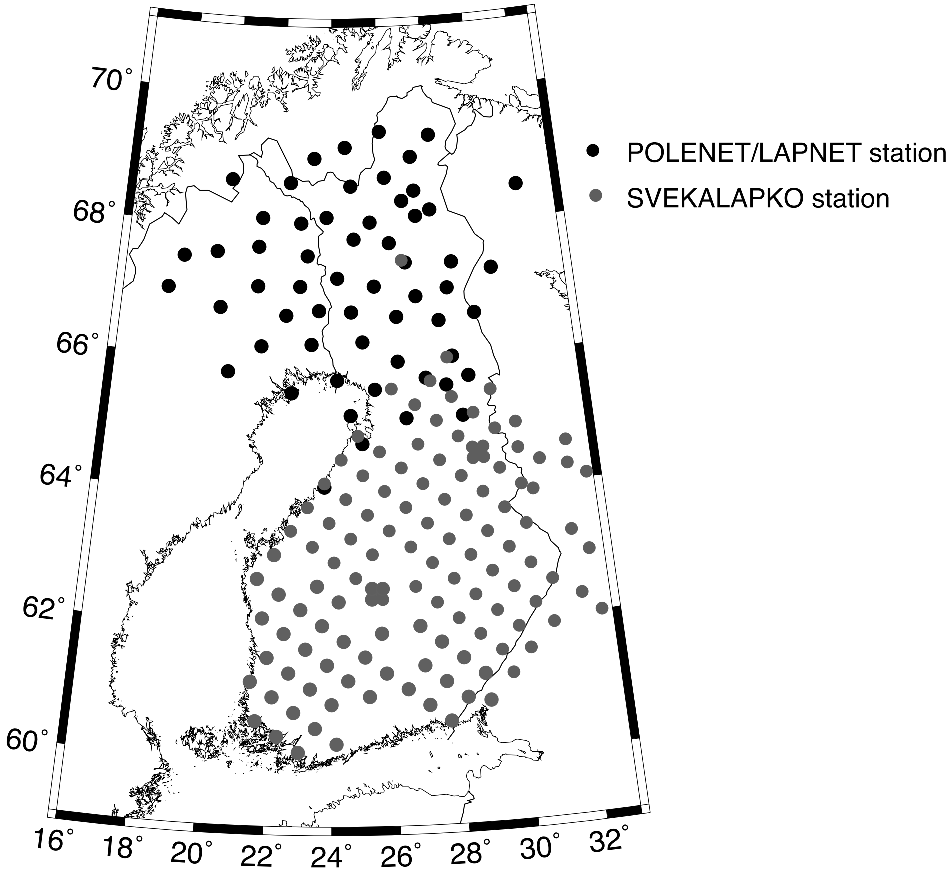


**Figure 1.** A map of the seismic stations of POLENET/LAPNET and SVEKALAPKO arrays.

**3. Results and conclusions**

The teleseismic P-wave traveltime tomography results of the SVEKALAPKO array (Fig. 1) beneath southern and central Finland (Sandoval et al., 2004) revealed a deep high-velocity cratonic root below the central Finland. This feature is the major characteristic of the model, for example, the main tectonic feature; the boundary between Archaean and Proterozoic terranes is not visible in the tomography results.

On the contrary, the teleseismic tomography results of the POLENET/LAPNET study area in northern Finland (Fig. 1) revealed a very different mantle. The mantle is characterised by a slow velocity anomaly beneath central Finnish Lapland and higher velocities in the northeastern, southeastern and western corners (Silvennoinen et al., 2016). We interpreted the higher velocities in the corners to represent Archaean cratonic lithosphere similar to the one interpreted below southern and central Finland.

## 4. References

Evans, J. and Achauer, U., 1993. Teleseismic velocity tomography using the AHC method: theory and application to continental scale studies. In H.M. Iyer and K. Hirahara, editors, Seismic Tomography, pages 319{360. Chapman and Hall, London, 1993.

Hjelt, S.-E., Daly, S., and SVEKALAPKO colleagues, 1996. SVEKALAPKO, Evolution of Palaeoproterozoic and Archaean Lithosphere, 56–67. In: Gee, D. and Zeyen, H. (Eds.). EUROPROBE 1996 – Lithosphere Dynamics: Origin and Evolution of Continents, EUROPROBE Secretariate, Uppsala University.

Karousová, H., 2013. User's Guide for tomographic code TELINV2012. http://www.ig.cas.cz/en/research-teaching/software-download

Kozlovskaya, E. and POLENET/LAPNET Working Group, 2007. POLENET/LAPNET, RESIF – Réseau Sismologique et géodésique Français, Seismic Network, doi:10.15778/RESIF.YV2011, http://data.datacite.org/10. 15778/RECIF.XK2007.

Sandoval, S., Kissling, E., Ansorge, J., and SVEKALAPKO STWG, 2004. Highresolution body wave tomography beneath the SVEKALAPKO array: II. Anomalous upper mantle structure beneath the central Baltic Shield. Geophys. J. Int., 157:200-214.

Silvennoinen, H., Kozlovskaya, E., and Kissling, E., 2016. POLENET/LAPNET teleseismic P wave travel time tomography model of the upper mantle beneath northern Fennoscandia, Solid Earth, 7, 425-439, doi:10.5194/se-7-425-2016.

# A new geological map of the SE Fennoscandian Shield as a tool for the Early Precambrian Crustal Evolution study (exemplified by the Archean)

A.I. Slabunov[1], S.A. Svetov[1], V.S. Kulikov[1] and A.K. Polin[1]

[1]Institute of Geology, Karelian Research Centre, Russian Academy of Sciences, Petrozavodsk, Pushkinskaya St., 185910, Russia
E-mail: slabunov@krc.karelia.ru

A 1:750 000 scale geological map of SE Fennoscandia (Fig. 1), which includes the Karelian craton, Belomorian mobile belt and SE Svecofennian orogen, was compiled in the Institute of Geology, KarRC, RAS (Kulikov et al., 2016; Svetov et al., 2016). Its legend is based on the International Stratigraphic Scale. The geological structure of the territory consists of the geological units of three eons: the Archaean, the Proterozoic and the Phanerozoic.

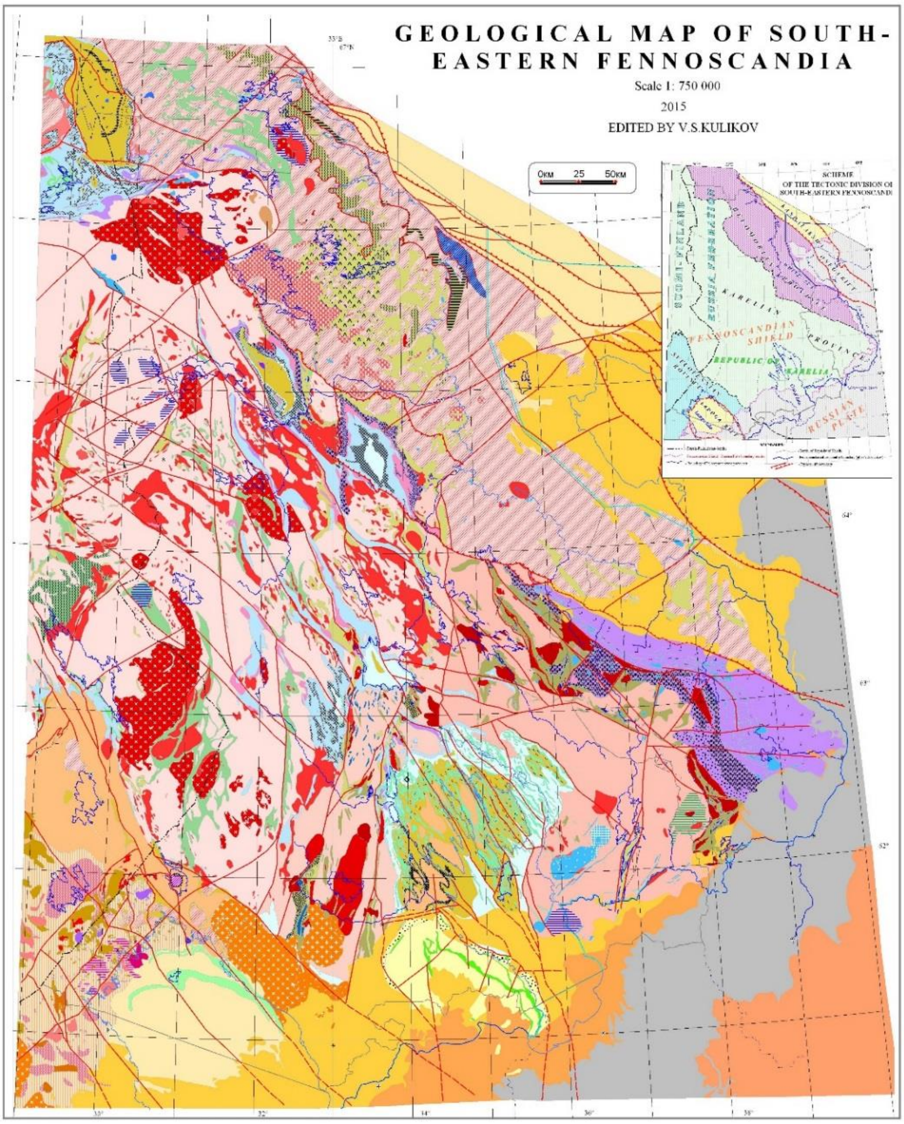


**Figure 1**. Geological Map of SE Fennoscandia (Kulikov et al., 2016; Svetov et al., 2016)

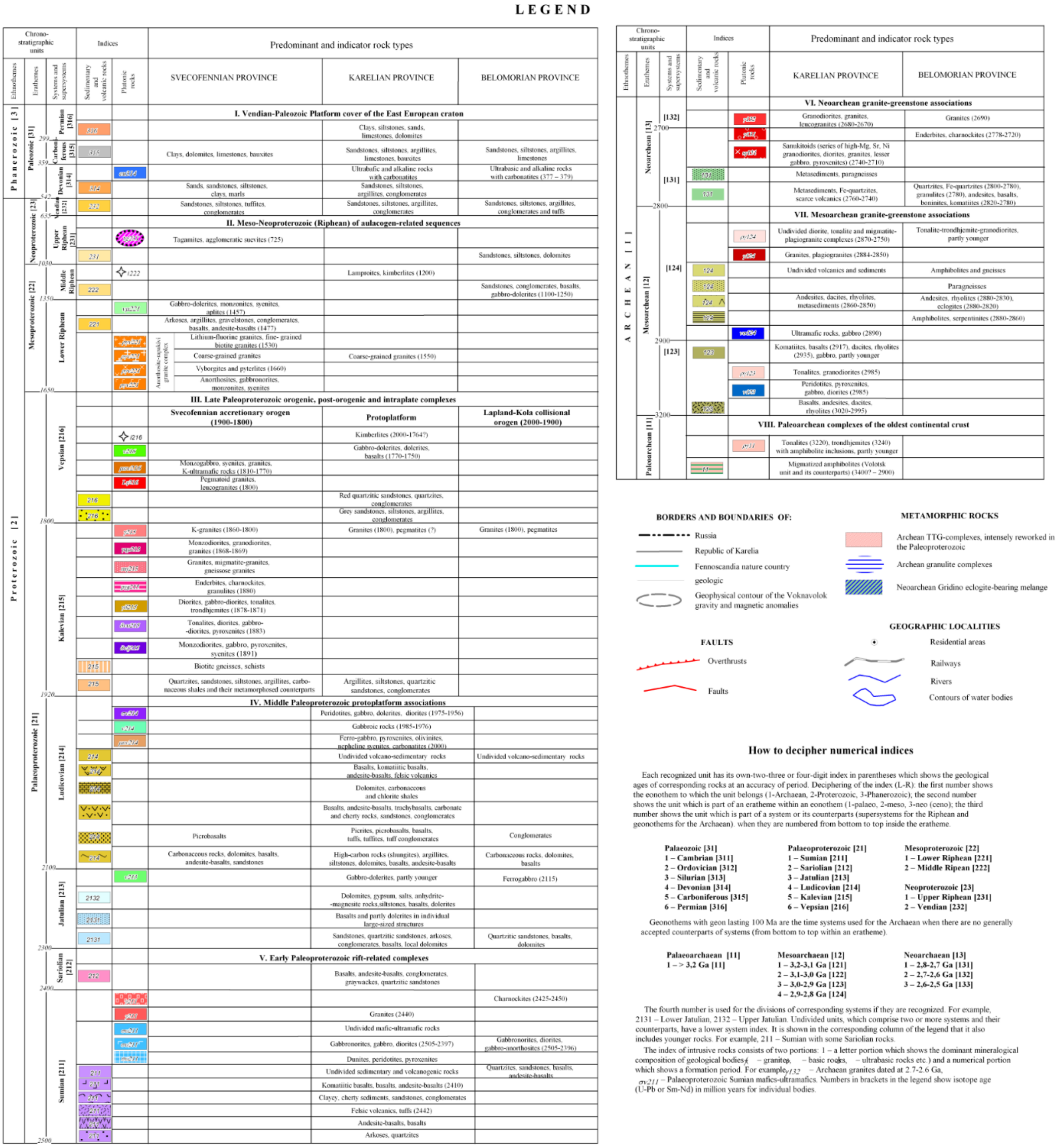


**Figure 2.** Geological Map of SE Fennoscandia (Kulikov et al., 2016; Svetov et al., 2016)

In the Proterozoic eon, magmatism of varying intensity took place in three eras. In the Palaeoproterozoic, igneous complexes are recognized in all six periods, but the Sumian (2.5-2.4 Ga) formation with layered mafic-ultramafic intrusions and associated volcanics, the Jatulian (2.3-2.1 Ga) trapp formation with volcanic and subvolcanic facies and the Ludicovian (2.1-1.92 Ga) formation with picritic-basaltic volcanism and gabbroic rock and peridotite intrusions are the most significant (Glushanin et al., 2011 and references therein). Alkaline-ultramafic and carbonatitic intrusive units, as well as kimberlites, were formed in the Palaeoproterozoic.

Palaeoproterozoic metamorphism in the Svecofennian (1.89–1.81 Ga) and Belomorian (1.94–1.85 Ga) provinces was quite intense.

An anorthosite-rapakivi granite formation was common in the southeastern part of the region in the Mesoproterozoic. Rifting events with a trapp formation in the eastern White Sea region (Baluev et al., 2012) and those with a kimberlite-lamproite formation in West Karelia took place in the Middle Riphean superperiod. The Palaeozoic is known as an amagmatic era, except for the Devonian, when events in the Kola alkaline-ultramafic LIP occurred in the northern part of the territory.

The main methods used for the construction of a crustal evolution model are correlation of geological processes (Slabunov et al., 2006) and, if possible, palaeomagnetic data (Lubnina, Slabunov, 2011).

The Fennoscandian Shield is split up into three fragments of the Palaeoarchean (3.5-3.2 Ga) continental crust that presumably existed as one microcontinent (Hölttä P et al., 2014). About 3.1 Ga ago it broke up.

Ca.3.05 Ga ago a new growth cycle of the continental crust began. During the 3.05-2.95 Ga period the crust was forming by subduction and subsequent accretion to the largest old Vodlozero block (Svetov, 2005). Mantle-plume magmatism manifests itself in the central part of the block and within the surrounding ocean. The bulk of the Archaean continental crust of the Fennoscandian Shield was formed during the 2.95-2.82 Ga period. Fragments of island-arc volcanics, ophiolites and eclogites (Slabunov et al., 2006) have been encountered in the Fennoscandian Shield. Moreover, ca 2.88□2.82 Ga oceanic formation of Seriak-type, island-arc volcanics of the Keret greenstone belt (GB), metagraywacke (front-arc basin sediments) of the Chupa paragneiss belt, Salma eclogites were formed in the Belomorian province. They mark the subduction boundary of the lithospheric plates. The main continental crust-forming geodynamics is provided by subduction-accretion processes. These processes also dominated over the 2.78-2.72 Ga period, when island-arc volcanics, eclogites and suprasubduction ophiolites were also produced. It should be stressed that island-arc volcanics (Kichany GB) and granulites were derived in the suprasubduction zone in the Belomorian province simultaneously with the Neoarchaean eclogites formed in the subducting slab. Thus, a set of complexes that mark the subduction persists here, and a short continental subduction episode stands out.

During the 2.71-2.58 Ga period collision and postcollision processes took place. The Belomorian province is the core of the collisional orogen, where nappe-fold tectonics, kyanite-subfacies metamorphism, partial rock melting and granitic magmatism occurred. This process in the western Karelian Province seems to be reflected by alkali-enriched gabbro and diorite intrusions (Mikkola et al., 2016).

This collisional even took place not only in the Fennoscandian Shield but also in Kaapvaal (2.7-2.67 Ga processes in the Limpopo complex), the Superior Province (2.68 Ga Minnesotan orogeny ). It was probably the final event upon the formation of the first Neoarchean Supercontinent (Slabunov & Lubnina, 2015).

This is a contribution to RFBR Project 15-05-09288.

**References:**

Baluev, A. S., Zhuravlev, V. A., Terehov, E. N., Przhijalgovskij, E. S. Tectonics of the White Sea and adjacent territories (Explanatory notes to the “Tectonic map of the White sea and adjacent territories” on a scale 1 : 1500000)]. Proceedings of the Geological Institute RAS. Vol. 597. Moscow: GEOS, 2012. 104 p.

Glushanin, L. V., Sharov, N. V., Shhipcov, V. V. Eds. 2011. Palaeoproterozoic Onega Structure (geology, tectonics,deep structure and mineralogeny). Petrozavodsk: KarRC of RAS, 431 p.

Hölttä, P., Heilimo, E., Huhma, H., Kontinen, A., Mertanen, S., Mikkola, P., Paavola, J., Peltonen, P., Semprich, J., Slabunov, A. and Sorjonen-Ward, P., 2014. The Archaean Karelia and Belomorian Provinces, Fennoscandian Shield. In: Evolution of Archean Crust and Early Life. Modern Approaches in Solid Earth Sciences (eds Dilek, Y. and Furnes, H.), Springer, pp. 55-102.

Kulikov, V. S., Svetov, S. A., Slabunov, A. I., Kulikova, V. V., Polin, A. K., Golubev, A. I., Gorkovets, V. Ya., Ivashchenko, V. I., Gogolev, M. A. 2016. Geological map of Southeastern Fennoscandia (scale 1:750 000): a new approach to map compilation. Proceedings of the Karelian Research Centre RAS. Precambrian Geology Series 9. DOI: 10.17076/geo444

Lubnina, N. and Slabunov, A. 2011. Reconstruction of the Kenorland Supercontinent in the Neoarchean Based on Paleomagnetic and Geological Data. Moscow University Geology Bulletin, 2011, Vol. 66, No. 4, pp. 242–249.

Mikkola, P., Heilimo, E., Halkoaho, T., Käpyaho, A. 2016. The tectonomagmatic significance of Neoarchaean variably alkali-enriched gabbro and diorite intrusions of the western Karelia Province. figshare. Geological Society, London, Special Publications, 449

Slabunov, A.I., Lobach-Zhuchenko, S.B., Bibikova, E.V. Sorjonen-Ward, P., Balagansky, V.V., Volodichev, O.I., Shchipansky, A.A., Svetov, S.A., Chekulaev, V.P., Arestova, N.A., Stepanov, V.S. 2006. The Archaean nucleus of the Fennoscandian (Baltic) Shield In: European Lithosphere Dynamics: Geol Soc London 32, pp. 627-644.

Slabunov, A & Lubnina, N. 2015. Neoarchean Kenorland Supercontinent: geological and paleomagnetic arguments. In 2015 IAGR Annual Convention &12th International Conference on Gondwana to Asia, Tsukuba, Japan. Abstract Volume IAGR Conference Series No. 21, pp. 102-103.

Svetov, S.A. 2005. Magmatic systems in the ocean-continent transition zone in the Archean of the eastern Fennoscandian Shield. Karelian Research Centre (KRC), Russian Academy of Sciences (RAS), Petrozavodsk, 230 p.

Svetov, S. A., Slabunov, A. I, Kulikov, V. S. 2016. A new geological map of the SE Fennoscandian Shield as a basis for the study of the evolution of the early earth crust. 35 IGC. Geoscience Data and Information Systems. Cape Town, South Africa.

# Metasomatic alkali-feldspar syenites within the Suomenniemi rapakivi granite complex, SE Finland

E. Suikkanen and O.T. Rämö

Department of Geosciences and Geography, P.O. Box 64, 00014 University of Helsinki, Finland
E-mail: einari.suikkanen@helsinki.fi

The ca. 1645 Ma Suomenniemi rapakivi granite complex in SE Finland mostly comprises metaluminous to peraluminous amphibole and biotite granites. Numerous bodies of peralkaline alkali-feldspar syenite are present in the SE part of the complex. Petrographic analysis and isotope geochemistry indicate that the alkali-feldspar syenites formed via fluid-induced brecciation, dequartzification and sodic alteration of the Suomenniemi granites. The metasomatism led up to complete replacement of the original granite mineralogy by oxidized, sodic assemblages, dominated by alkali feldspar and aegirine-augite. The process resembles fenitization of granitic rocks around carbonatite or ijolite intrusions. Whether the fluids originated from a hidden alkaline intrusion, or were related to the evolution of the subalkaline rapakivi magmas, is not known.

**Keywords:** Finland, rapakivi, alkali-feldspar syenite, episyenite, fenite, metasomatism

## 1. Introduction and description of the alkali-feldspar syenites

The ca. 1645 Ma Suomenniemi complex is located at the northern margin of the Wiborg rapakivi batholith (Figure 1). The complex comprises metaluminous amphibole granites that grade to metaluminous or slightly peraluminous biotite granites. Minor topaz granite bodies are also found. NW-oriented quartz-feldspar porphyry (ca. 1635 Ma) and diabase dykes intrude the complex and the surrounding Svecofennian basement. Peralkaline alkali-feldspar syenites form a distinct group of rocks within the Suomenniemi complex. Their origin have been investigated via petrographic, geochemical and isotope geochemical analyses.

The alkali-feldspar syenites are pink to deep purple, coarse-grained, NW-oriented dyke-like bodies or small (<10 m in diameter) patches whose contacts with the granites are in many cases obscured by similar colour and texture. They are peralkaline rocks with high $Na_2O/K_2O$ and $Fe_2O_3/FeO$ ratios and corresponding sodic mineral assemblages, and can be divided into

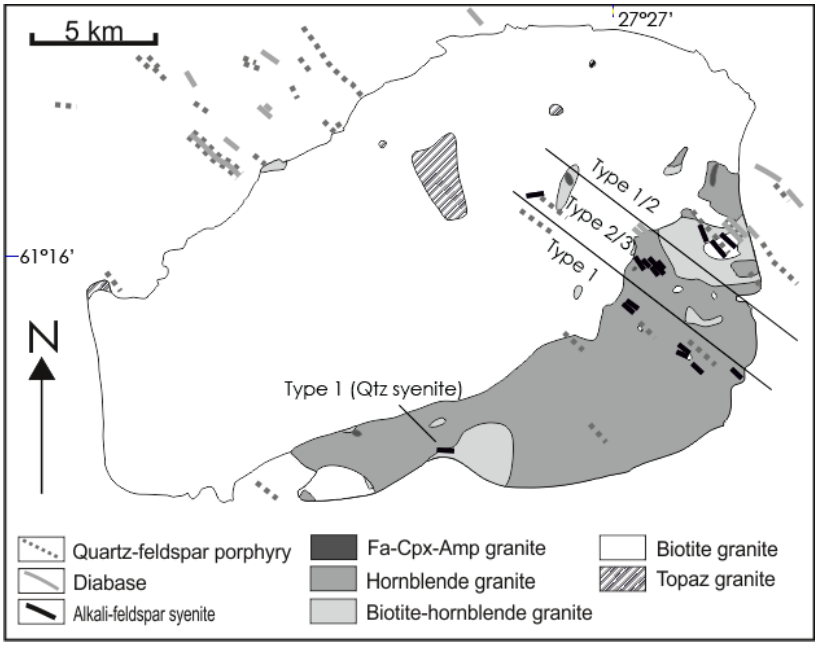



**Figure 12**. Geological map of the Suomenniemi complex after Rämö and Mänttäri (2015). The alkali-feldspar syenites are divided into three distinct groups by their mineralogy (see text) and delineate NW-trending zones.

three groups by their *dominant* mineralogy and texture:

(1) Orthoclase perthite and sodic-calcic amphibole ± aegirine. Primary minerals are strained and fractured, and secondary amphibole and feldspar fill interstitial spaces. Perthite is usually highly turbid and replaced by albite to a variable degree. Oligoclase and quartz are rare. The change from this type is more or less gradual to type (2), below.

(2) Mesoperthite and aegirine-augite ± sodic amphibole. Submillimeter mesoperthite grains form a granoblastic (polygonal) matrix between larger grains of perthite. Aegirine-augite forms inclusion-rich sheets or granular clusters. Alkali feldspar microtextures and possibly bulk compositions are variable. Swapped albite rims form between feldspar grains.

(3) Albite and aegirine-augite. Albite is present as small grains that fill spaces between larger grains of albitic feldspar. Aegirine-augite is as in (2).

Accessory minerals invariably include euhedral apatite and zircon, and subhedral to anhedral titanite and magnetite/hematite. Minor amounts of secondary quartz and epidote are common and andradite may replace aegirine-augite in (2).

The alkali-feldspar syenites are indistinguishable from the Suomenniemi granites by their *in situ* zircon ages (ca. 1645 Ma; Rämö and Mänttäri 2015; Suikkanen et al. 2016) and $\delta^{18}O_{VSMOW}$-values (ca. +8 ‰; Elliott et al. 2005; Suikkanen et al. 2016), as well as their εNd(t) values (ca. -1.5 at 1640 Ma; Rämö 1991; unpublished data by the authors).

## 2. Discussion and conclusions

These data imply that the alkali-feldspar syenites formed from the subalkaline granites via sodic metasomatism and associated dequartzification. The texture and mineralogy of the metasomatites were influenced by system temperatures and compositions, fluid-rock ratios, and the extent of brecciation and mobilization of the material. The zoned placement of the different types of alkali-feldspar syenites (Figure 1) implies spatial control on the strength of metasomatism. The most notable geochemical changes were decrease in $SiO_2$, FeO, CaO, Sr, and F and increase in $Na_2O$, $Fe_2O_3$, and $Al_2O_3$. $K_2O$, Rb, and Ba decreased along with progressive albitization of potassic feldspar. Nd-isotopic data reveal that the metasomatizing fluids did not introduce measurable amounts of isotopically different Nd into the system.

The alkali-feldspar syenites of the Suomenniemi complex greatly resemble fenitized granites around alkaline and carbonatite intrusions, such as those in Fen, Norway (Kresten and Morogan 1986). They probably formed by fault-controlled metasomatism similar to the vein fenites of Kresten (1988). Because no alkaline rocks (including peralkaline granites) or carbonatites have been found within the Finnish rapakivi granite terrain and the source of the metasomatizing fluids is obscure, these alkali-feldspar syenites may not be fenites in the strict sense.

## References:


Elliott, B.A., Peck, W.H., Rämö, O.T., Vaasjoki, M., Nironen, M., 2005. Magmatic zircon oxygen isotopes of 1.88-1.87 Ga orogenic and 1.65-1.54 Ga anorogenic magmatism in Finland. Min Pet 85, 223-241

Kresten, P., 1988. The chemistry of fenitization: Examples from Fen, Norway. Chem Geol 68, 329-349.

Kresten, P. and Morogan, V., 1986. Fenitization at the Fen complex, southern Norway, Lithos 19, 27-42.

Rämö, O.T., 1991. Petrogenesis of the Proterozoic rapakivi granites and related basic rocks of southeastern Fennoscandia: Nd and Pb isotopic and general geochemical constraints. Geol Surv Finland Bull 355, 161p.

Rämö, O.T. and Mänttäri, I., 2015. Geochronology of the Suomenniemi rapakivi granite complex revisited: Implications of point-specific errors on zircon U-Pb and refined $\lambda_{87}$ on whole-rock Rb-Sr. Bull Geol Soc Finland 87, 25-45.

Suikkanen, E., Rämö, O.T., Mänttäri, I. 2016. *In situ* zircon U-Pb ages and $\delta^{18}O_{VSMOW}$ values of alkali feldspar syenites and topaz granites from the Suomenniemi batholith. Bull Geol Soc Finland Special Volume 1, 229.

# Defining mantle sources of large igneous provinces: insights from pristine picrites in Karoo LIP, Luenha River, Mozambique

S.T. Turunen[1], A.V. Luttinen[2] and J.S. Heinonen[1]

[1]Department of Geosciences and Geography, P. O. Box 64, 00014 University of Helsinki
[2]Finnish Museum of Natural History, P. O. Box 44, 00014 University of Helsinki
E-mail: sanni.turunen@helsinki.fi

A subaerial picrite lava series exposed at the Luenha River, Mozambique, shows a unique geochemical fingerprint within the 180 Ma Karoo large igneous province. The available chemical and Nd and Sr isotopic data indicate derivation of the Luenha picrites from a primitive mantle-like source, whereas previous studies have revealed a depleted mantle source for other Karoo picrites. Comparison between the different Karoo picrites and basalts suggests that the depleted mantle source was predominant within the Karoo triple rift, whereas the primitive mantle-like source identified for the Luenha picrites may well have been the main source of voluminous flood basalts in southern Africa. Involvement of two contrasting mantle reservoirs has significant implications for the origin of the Karoo LIP and its environmental influences.

**Keywords:** large igneous province, Karoo, flood basalt, picrite, mantle plume

## 1. Mantle sources of the Karoo large igneous province

During the Mid-Jurassic breakup of Gondwana supercontinent, voluminous flood basalts and related mafic dyke swarms were emplaced in southern Africa and Dronning Maud Land, Antarctica (Fig. 1). The principal mantle sources of the geochemically diverse and widespread volcanism in the Karoo large igneous province (LIP) have been frequently debated during the past few decades (e.g. Ellam and Cox, 1989, 1991; Riley et al., 2005; Heinonen and Luttinen, 2008; Wang et al., 2015). Crustal contamination has probably overprinted the primary characteristics of all but few Karoo flood basalt magmas, which has hampered identification of the mantle sources.

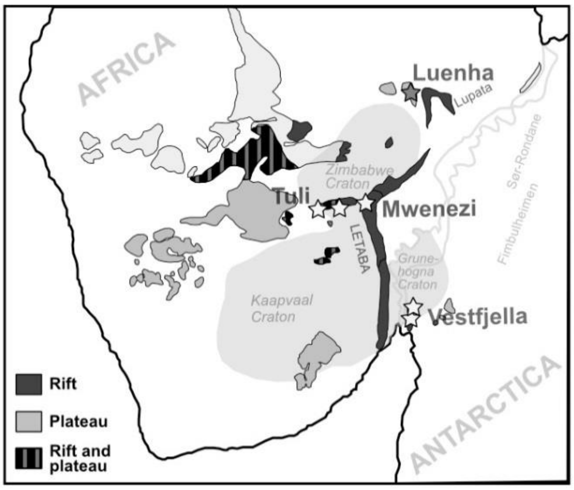


**Figure 1.** Karoo large igneous province reconstructed at 180 Ma. The occurrences of flood basalts associated with the Karoo triple rift (black) and the remnants of an enclosing lava plateau (grey) and picrite localities are indicated (white stars –rift-related, grey star.– Luenha picrites). Modified after Jourdan et al. (2007), Ellam and Cox (1989, 1991), Duncan et al. (1990), Luttinen et al. (2010) and Heinonen and Luttinen (2008).

Karoo high-Mg (picritic) rock types are common in the Mwenezi-Tuli area (Fig. 1), but these picrites probably represent contaminated magmas (Ellam and Cox, 1991). On the other hand, rare examples of uncontaminated picrites from Antarctica (Vestfjella; Fig. 1) have revealed a mantle source that is isotopically indistinguishable from the depleted upper mantle (Heinonen et al., 2010; Heinonen and Kurz, 2015). Many of the different Karoo flood basalt types may have been derived from depleted mantle-sourced primary magmas by contamination with incompatible element-enriched crustal and lithospheric mantle materials (Ellam and Cox, 1991). In fact, geochemical modelling has suggested that depleted mantle may be the principal mantle source of magmatism within the Karoo triple rift (Fig. 1; Luttinen et al., 2015; Heinonen et al., 2016). In this study, we report a suite of picritic lavas from the Luenha River, Mozambique (Fig. 1). We show the Luenha picrites to represent a new compositional type of Karoo magmatism and suggest they may be record a significant, previously unknown mantle reservoir of the Karoo LIP.

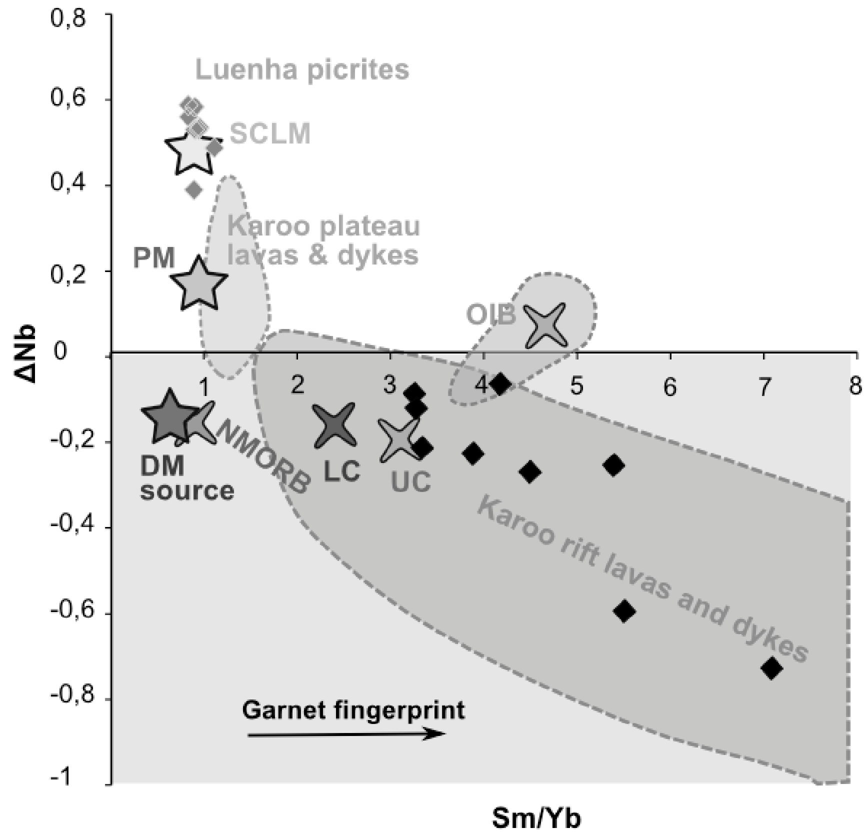


**Figure 2.** ΔNb values vs. Sm/Yb ratios in the Luenha picrites (grey diamonds) and Karoo rift picrites (black diamonds). Compositional fields of Karoo flood basalt lavas and dykes in the Karoo triple rift and those of the enclosing lava plateau are indicated (see Fig. 1). Average compositions of normal MORB and OIB are shown for comparison. Possible depleted (DM), primitive (PM), and subcontinental lithospheric (SCLM) mantle sources and upper (UC) and lower crustal (LC) contaminants are shown for comparison. The compositional effect of decreasing amount of partial melting in the presence of residual garnet is illustrated (garnet fingerprint). Reference data from Salters and Stracke (2004), Jourdan et al. (2007), Smith et al. (2009), Sun and McDonough (1989), McDonough (1990), Wedepohl (1995), Luttinen and Siivola (1997), Ellam and Cox (1989, 1991), Duncan et al. (1990), Heinonen and Luttinen (2008). ΔNb values have been calculated according to Fitton et al. (1997).

**2. Geochemistry of the Luenha picrites**

The Luenha picrites contain unaltered, euhedral high-Mg olivine ($Fo_{86}$–$Fo_{89}$) phenocrysts, and their whole-rock MgO contents (9.4–24.7 wt. %) are high even after taking into account the effect of olivine accumulation. Compared to the picrites previously described from the Karoo LIP (Ellam and Cox, 1989, 1991; Riley et al., 2005; Heinonen and Luttinen, 2008), the Luenha picrites show notably low $TiO_2$ (0.3–1.0 wt. %) contents. The Luenha picrites are further distinguished from the other Karoo picrites by their nearly unfractionated heavy REE ratios (Sm/Yb ~1) and by their undepleted Nb contents relative to other high-field-strength elements, such as Zr and Y (Fig. 2).

The enrichment or depletion of Nb relative to Zr and Y can be quantified using the so-called ΔNb parameter ($\Delta Nb = 1.74 + \log [Nb/Y] - 1.92 \log [Zr/Y]$; Fitton et al. 1997): The Luenha picrites are typified by notably high, positive ΔNb (0.4–0.6), whereas the previously studied depleted mantle-sourced picrites and flood basalts in Antarctica and the Karoo rift zone have negative ΔNb (Fig. 2). It is petrologically important to notice that the high ΔNb values of the Luenha picrites are not readily explained by contamination of depleted mantle-derived magmas, and thus indicate a Nb-undepleted mantle source (cf. Fitton et al., 1997). Furthermore, ratios of highly incompatible elements indicate that the Luenha picrites include uncontaminated or very mildly contaminated types. The least-contaminated Luenha picrites show trace element and isotopic affinities to primitive mantle ($^{87}Sr/^{86}Sr_{(180Ma)} = 0.7041$, $\varepsilon_{Nd\,(180\,Ma)} = +0.1$). The relatively more LREE-enriched samples exhibit chemical and isotopic indications of crustal contamination (e.g. $^{87}Sr/^{86}Sr_{(180Ma)}$ up to 0.7076).

**2. Conclusions**

Overall, geochemical comparison indicates that the Luenha picrites represent a previously unknown high-Mg magma type in the Karoo LIP. They are typified by low-$TiO_2$ and high-ΔNb compositions and primitive mantle-like incompatible element and isotopic ratios. Unfractionated heavy REE ratios (low Sm/Yb) suggest the primary melts were segregated from a garnet-free mantle source, which points to relatively low pressure conditions or notably high degree of partial melting, or both (Fig. 2). In contrast, previously reported Karoo picrites have relatively high $TiO_2$, low ΔNb and relatively high Sm/Yb values. Based on these features and the isotopic ratios of the uncontaminated samples ($\varepsilon_{Nd\,(180\,Ma)}$ up to +8; Heinonen and Luttinen, 2008; Heinonen et al., 2010), these picrites represent low degrees of melting of depleted mantle at relatively high pressure.

Judging from geochemical similarities, for example low Sm/Yb and high ΔNb (Fig. 2), the Karoo plateau lavas and dykes may have originated from the same or similar mantle sources as the Luenha picrites. This correlation suggests that magmatism in the Karoo LIP was sourced by at least two different kinds of principal mantle reservoirs: A depleted mantle source has been associated with the rift zone (Luttinen et al., 2015; Heinonen et al., 2016), whereas the primitive mantle-like source of the Luenha picrites is a plausible source for the voluminous plateau flood basalts. Whether the primitive mantle-like source of the Luenha picrites was part of sublithospheric mantle or lithospheric mantle is currently unclear, although a sublithospheric source would be a thermodynamically more viable source for voluminous flood basalt magmas (e.g. Arndt and Christensen, 1992). Involvement of two contrasting mantle reservoirs has significant implications for the magma generation and emplacement processes and the environmental influences of Karoo LIP magmatism.

## References:


Arndt, N.T. and Christensen, U. 1992. The role of lithospheric mantle in continental flood volcanism: Thermal and geochemical constraints. Journal of Geophysical Research, 97, No B7, 10967–10981.

Duncan, A.R., Armstrong, R.A., Erlank, A.J., Marsh, J.S. and Watkins, R.T. 1990. MORB-related dolerites associated with the final phases of Karoo flood basalt volcanism in Southern Africa. Published in Mafic Dykes and Emplacement Mechanisms, edited by Parker, A.J., Rickwood, P.C. and Tucker, D.H. Rotterdam: Balkema, 119–129.

Ellam, R.M. and Cox, K.G. 1989. A Proterozoic lithospheric source for Karoo magmatism: evidence from the Nuanetsi picrites. Earth and Planetary Science Letters, 92, 207–218.

Ellam, R.M. and Cox, K.G. 1991. An interpretation of Karoo picrite basalts in terms of interaction between astenospheric magmas and the mantle lithosphere. Earth and Planetary Science Letters, 330–342.

Fitton, J.G., Saunders, A.D., Norry, M.J., Hardarson, B.S. and Taylor, R.N. 1997. Thermal and chemical structure of the Iceland plume. Earth and Planetary Science Letters, 153, 197–208.

Heinonen, J.S. ja Kurz, M.D. 2015. Low-$^{3}He/^{4}He$ sublithospheric mantle source for the most magnesian magmas of the Karoo large igneous province. Earth and Planetary Science Letters, 426, 305–315.

Heinonen, J.S. and Luttinen, A.V. 2008. Jurassic dikes of Vestfjella, wester Dronning Maud Land, Antarctica: geochemical tracing of ferropicrite sources. Lithos, 105, 347–364.

Heinonen, J.S., Carlson, R.W. and Luttinen, A.V. 2010. Isotopic (Sr, Nd, Pb and Os) composition of highly magnesian dikes of Vestfjella, western Dronning Maud Land, Antarctica: A Key to the origins of the Jurassic Karoo large igneous province? Chemical Geology, 277, 227–244.

Heinonen, J.S., Luttinen, A.V. and Bohrson, W.A. 2016. Enriched continental flood basalts from depleted mantle melts: modeling the lithospheric contamination of Karoo lavas from Antarctica. Contributions to Mineralogy and Petrology, 171:9, doi:10.1007/s00410-015-1214-8.

Jourdan, F., Bertrand, H., Schärer, U., Blichert-Toft, J., Féraud, G. and Kampunzu, A.B. 2007. Major and trace element and Sr, Nd, Hf, and Pb isotope compositions of the Karoo large igneous province, Botswana-Zimbabwe: Lithosphere vs. mantle plume contribution. Journal of Petrology, 48, No 6, 1043–1077.

McDonough, W.F. 1990. Constraints on the composition of the continental lithospheric mantle. Earth and Planetary Science Letters, 101, 1–18.

Luttinen, A.V. and Siivola, J.U. 1997. Geochemical characteristics of Mesozoic lavas and dikes from Vestfjella, Dronning Maud Land: recognition of thee distinct chemical types. The Antarctic Region: Geological Evolution and Processes, 495–503.

Luttinen, A.V., Leat, P.T., Furnes, H. 2010. Björnnutane and Sembberget basalt lavas and the geochemical provinciality of Karoo magmatism in western Dronning Maud Land. Antarctica. Journal of Volcanology and Geothermal Research, 198, 1–18.

Luttinen, A.V., Heinonen, J., Kurhila, M., Jourdan, F., Mänttäri, I., Vuori, S. and Huhma, H. 2015. Depleted mantle-sourced CFB magmatism in the Jurassic Africa-Antarctica rift: Petrology and $^{40}Ar/^{39}Ar$ and U/Pb chronology of the Vestfjella dyke swarm, Dronning Maud land, Antarctica. Journal of Petrology, doi:10.1093/petrology/egv022.

Riley, T.R., Leat, P.T., Curtis, M.L., Millar, I.L., Duncan, R.A. and Fazel, A. 2005. Early–middle Jurassic dolerite dykes from Western Dronning Maud land (Antarctica): Identifying mantle sources in the Karoo large igneous province. Journal of Petrology, 46, 1489–1524.

Salters, V.J.M. and Stracke, A. 2005. Composition of the depleted mantle. Geochemistry, Geophysics, Geosystems, Vol 5, Issue 5, DOI: 10.1029/2003GC000597.

Smith, C.B., Pearson, D.G., Bulanowa, B.G., Beard, A.D., Carlson, R.W., Wittig, N., Sims, K., Chimuka, L., Muchemwa, E. 2009. Extremely depleted lithospheric mantle and diamonds beneath the Southern Zimbabwe Craton. Lithos, 112 S, 1120–1132.

Sun, S.-s. and McDonough, W.F. 1989. Chemical and isotopic systematics of oceanic basalts: implications for mantle compositions and processes. Geological Society, London, Special Publication, 42, 313–345.

Wedepohl, K.H. 1995. The composition of the continental crust. Geochimica et Cosmochimica Acta, 59, No 7, 1217–1232.

Wang, X.-C. et al. 2015. Continental flood basalts derived from the hydrous mantle transition zone. Nature Communications 6:7700 doi: 10.1038/ncomms8700.

# Aijala mine tailings area as an example of a source of secondary raw materials

T. Valjus [1], M. Markovaara-Koivisto[1] and T. Tarvainen[1]

[1]Geological Survey of Finland, P.O.Box 96, 02151 Espoo, Finland
E-mail: Tuire.Valjus@gtk.fi

In this article we describe the Aijala tailings ponds' potential to be a source of secondary raw minerals. The tailings pond was targeted as a study site because the mines, Aijala and Metsämonttu, from which the tailings are from, have been shut several decades ago, and therefore the tailings might contain significant amounts of minerals which could be utilised with the modern processes. The amount of Cu, Zn, Ag and Pb has been estimated within the tailings layers. Aijala tailings pond is one of the Finnish pilot areas of EU funded SMART GROUND project.

**Keywords:** secondary raw materials, mine tailings, Aijala, Finland, SMART GROUND

## 1. Smart ground project

Raw material are becoming a more important for the EU economy. The recycling and recovery of these materials becomes more relevant as they become scarser and their prices raise. According to an estimation, there are in the EU area between 150 000 and 500 000 highly variable landfills, and they could contain a significant potential of secondary raw materials. However, there is no standardised inventory available of the secondary raw materials in these landfills, nor are the present reporting standards sufficient.

The SMART GROUND project funded by the EU's Horizon 2020 program intends to improve availability and accessibility of information of the secondary raw material in the EU. The consortium will create a single EU database (SmartGround database) that integrates all the data from existing sources and new information retrieved with time progress. Such database will enable the exchange of contacts and information among the relevant stakeholders (e.g. companies), which are interested in providing or obtaining secondary raw materials. The project produces detailed information of secondary raw materials from three pilot landfills of each partner countries. Aijala tailings pond is one of the Finnish pilots.

## 2. Aijala tailings pond

The Aijala copper mine was active in the community of Kisko, which is part of Salo today, in years 1945 – 1958. The enrichment plant worked in Ailaja till 1974, as the ore was brought from the nearby Metsämonttu Zn-Pb mine between years 1952 – 1958 and 1964 – 1974. Also ore from Telkkälä Ni-Cu mine was enriched in Aijala in 1970. (Sipilä, 1994)

The composition of Aijala tailings pond has been studied already in 1982 by Kokkola. The Aijala tailings pond contains around 2 million tons of waste which average metal content is as follows: 0.12 % copper, 0.5 % lead, 0.11 % silver and 0.69 ppm gold. Thickness of the tailings layer is on average 8.7 m and the deepest part is 12 m thick. (Sipilä, 1994, Kokkola, 1982)

**3. Soil drilling and geochemistry**

In summer 2016 Geological Survey of Finland took additional samples of the Aijala tailings pond. Five additional drill holes were made and the tailings samples were analysed in 1 m intervals, 48 samples in total. A vast geochemical analysis was carried out, but in this article only copper, zinc, lead and silver are referred to.

Even if the tailings material looked the same from top to bottom, the geochemical assays of the samples taken from the drill holes revealed the interface of the tailings material from Metsämonttu and Aijala mines. The top part which contained tailings from Metsämonttu mine was rich in lead and the bottom part containing tailings from Aijala, was rich in copper (Figure 1).

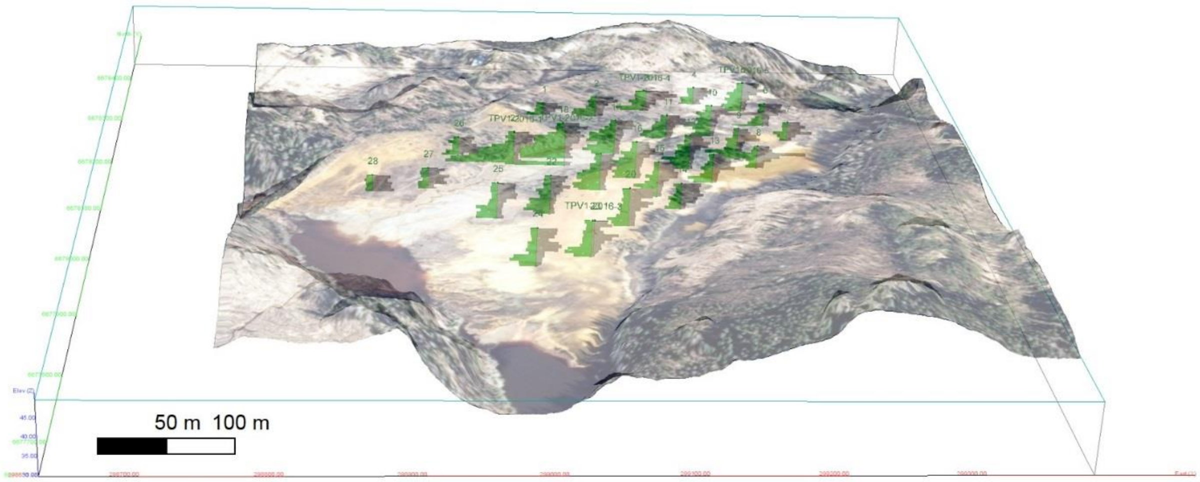


**Figure 1.** Topography of the Aijala tailings pond with an aerial photo draped onto the surface. The copper and lead content in the tailings are marked with green and grey bars next to the old and new drill holes.

**4. Geophysical studies**

Geophysics was utilised to study the inner structure and dimensions of the tailings pond. Gravimetric, magnetic and electromagnetic GEM-2, and electrical resistivity tomography (ERT) surveys were carried out. Results of the gravimetric survey were used to interpret the thickness of the tailings pond and depth of the bedrock surface. The drill holes were used as reference points in the interpretations, as they were drilled to the hard soil material underneath the tailings pond. Magnetic survey gave a general picture of the iron content in different parts of the tailings pond. GEM-2 method was utilised to map electrical conductivity of the tailings ponds surface layers from 1 up to 10 m depth. Electrical resistivity tomography was used to study changes in the electrical conductivity of the tailings material up to 30 meters depth. The results of the geophysical interpretations helped in defining the inner structures of the pond and they also gave more information of the variation of the tailings ponds bottom and bedrock surface. The results were utilised in 3D modelling of the structure of the tailings pond (Figure 2).

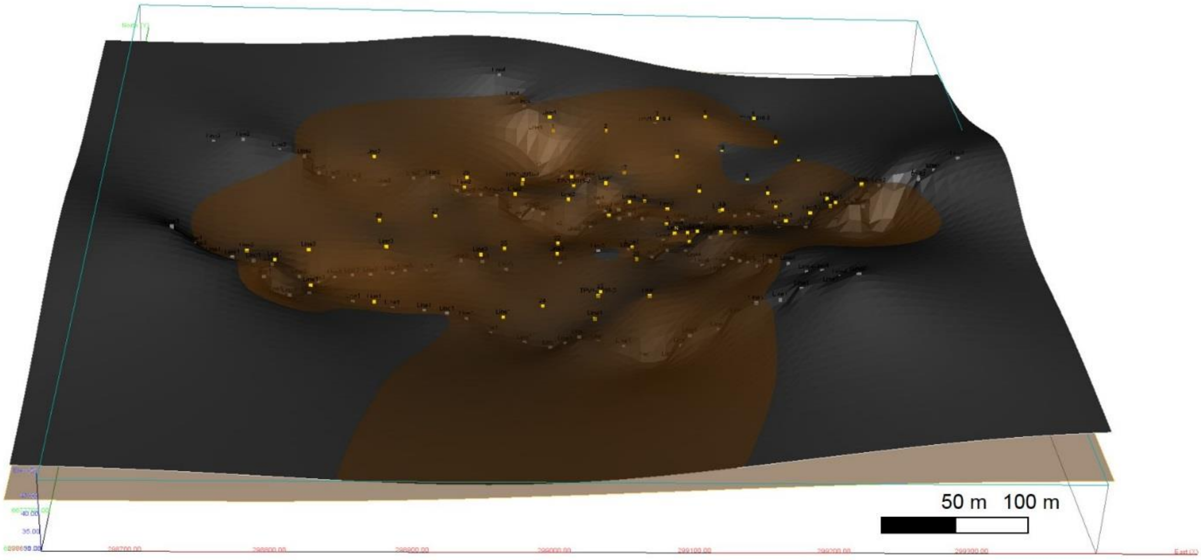


**Figure 2.** Bedrock (grey) and tailings bottom (brown) layers were generated according to the gravity interpolations of the bedrock depth (grey points) and tailings bottom (yellow points).

## 5. Mineral resources estimation

The mineral resources in the Aijala tailings pond were estimated by interpolating the metal contents in the old and new drill cores into a 1 $m^3$ resolution block model. Because the geochemical composition of the tailings pond is not continuous, the interpolation was carried out separately to the Metsämonttu mine tailings layer and the Aijala mine tailings layer.

The blocks belonging to the different layers were determined by the layers generated according to the gravimetric interpretations of the bedrock surface and the tailings bottom (Figure 2). The blocks belonging to the two different tailings layers were separated by a layer generated to the approximate middle of the change in geochemical content seen in the drill cores (Figure 1).

We used Kriging method to interpolate the metals contents in the block model. The used search ellipsoid was horizontal and 200 m in length and in width and 2 m in depth. This is because the metal content of the layers is assumed to be rather continuous in horizontal direction, and the changes in metal content are more likely to be in vertical direction.

Figure 3 shows as an example the interpolated copper content in the Metsämonttu mine tailings layers. The total volume of the layer is 852 399 $m^3$, and it contains approximately 678 tons of copper.

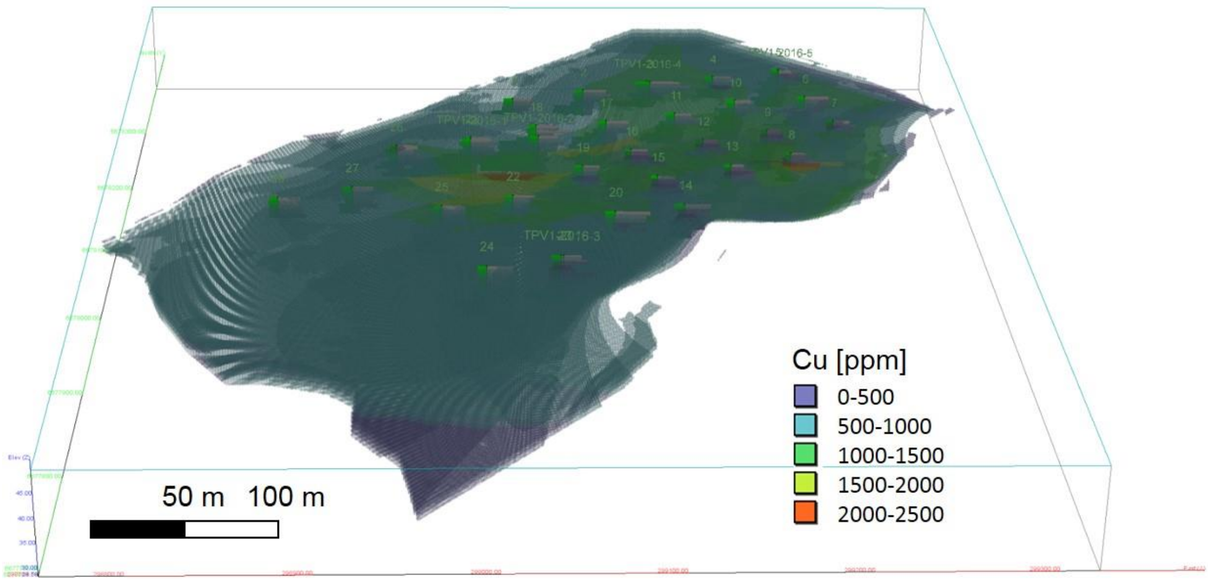


**Figure 3.** Block model showing the interpolated copper content in Metsämonttu mine tailings layer. The drill holes show copper (green) and lead (grey) contents in the analyzed samples.

## 6. Conclusions

The Aijala tailings pond example of a landfill as a source of secondary raw materials in EU is a detailed study with 3D model of the structure of the landfill. The information concerning the landfill can be found later in the standardised EU landfill database, and it can be utilised by the possible re-user of the raw material to make feasibility study and planning the operations.

## References:

Sipilä, P., 1994. Aijalan, Pyhäsalmen ja Makolan sulfidimalmikaivosten rikastamoiden jätealueiden ympäristövaikutukset. Osa II – Aijala. Geologian tutkimuskeskus, Arkistoraportti KA 33/94/1.2, 26 pages.

Kokkola, M., 1982. Jätealueen soijatutkimus Kisko, Aijala. Outokumpu OY Report 067/2014 03/MK/1982. 5 pages + 3 appendices.

Salminen, R. (ed.), 2005. Geochemical Atlas of Europe. Part 1: Background information, Methodology and Maps. Geological Survey of Finland, Espoo. 525 pages.

# Kumpula campus drill hole: Fracture mapping and 3D-modeling

R. Valtonen[1], I. Kukkonen[2], J.S. Heinonen[1], M. Räisänen[1], K. Penttilä[1]

[1]Department of Geosciences and Geography, P.O. Box 64, 00014 University of Helsinki, Finland
[2]Department of Physics, P.O. Box 64, 00014 University of Helsinki, Finland

E-mail:riikka.valtonen@helsinki.fi

In this study, we describe the fracture mapping project in at the Kumpula campus area, University of Helsinki. Central part of the project is the recently completed Kumpula campus drill hole, which gives us a possibility to study the areal geology in three dimensions. The aim is to map fractures of the drill core and fracturing of the Kumpula hill area, and make a 3D-model based on this data. Also the plan is to make XRD-tests from minerals in the fracture fillings and to achieve preliminary understanding of the age relationships of the different sets of fractures in the Kumpula area.

**Keywords**: fracture mapping, Kumpula, 3D-model, core logging, Helsinki

## 1. Introduction

The Kumpula hill is situated in the southern part of Helsinki. In November-Dcember 2015 a continuously cored drill hole was drilled there, the hole being 370 m deep. With this drill core it is possible to make a more accurate study of the bedrock in Kumpula. There currently are three master thesis projects ongoing using the results of the drill core, which are related to the petrology, geochemistry and fracture mapping of Kumpula.

## 2. Geological setting

The bedrock of Helsinki formed about 1.9–1.8 billion years ago in Proterozoic era, during the Svecofennian orogeny (e.g., Laitala 1991). Presently, the bedrock Helsinki represents the roots of this orogenic belt, eroded to the present level before 590 Ma (Laitala 1991).

Several fracture zones can be found within Helsinki area (Laitala 1991). They were formed during and after the Svecofennian orogeny and they reflect how stress fields in the area have changed with time (Elminen et al. 2008). Fracture zones can cause problems, when, for example, construction support structures are built on top or through one (Elminen et al. 2008).

## 3. Structural mapping and logging

The aim of this study is to map fractures from the drill core and compare these results to the fractures mapped in the field and finally make a 3D-model of the Kumpula campus area. The project started in January 2016, first by photographing the drill core and by getting an overall understanding of it. After this, more detailed logging was performed and the fractures were labelled. They were divided into fractures without filling, with filling and to smooth fractures. Also the roughness of the fracture plane and cutting angle were estimated.

In addition to drill core logging, field work was carried out in the Kumpula campus area. There are six major outcrops around the Kumpula campus and along Kustaa Vaasa road there are road cuts as well. At the outcrops, the fractures were measured for their dip, strike, roughness of the fracture plane, length of the fracture, and aperture of the fracture. Possible fracture fillings were also inspected.

In order to help detect fractures accurately and achieving correct RQD-measurements and fracture orienations, there are oriented optical and acoustic data available from the drill hole as well. These data have been processed with a program called WellCad (Figure 1). By using WellCAD it is possible to calculate the accurate angle of every fracture and also observe fractures which are not clearly visible in the drill core. Our aim is also to make XRD analyses on the fracture fillings, in order to identify the fracture minerals and to achieve a better understanding of the age relationship of the fractures.

Finally, the ultimate goal of this project is to create a 3D model of the Kumpula area fracturing using MOVE software and to compare it to existing data from the Helsinki area.

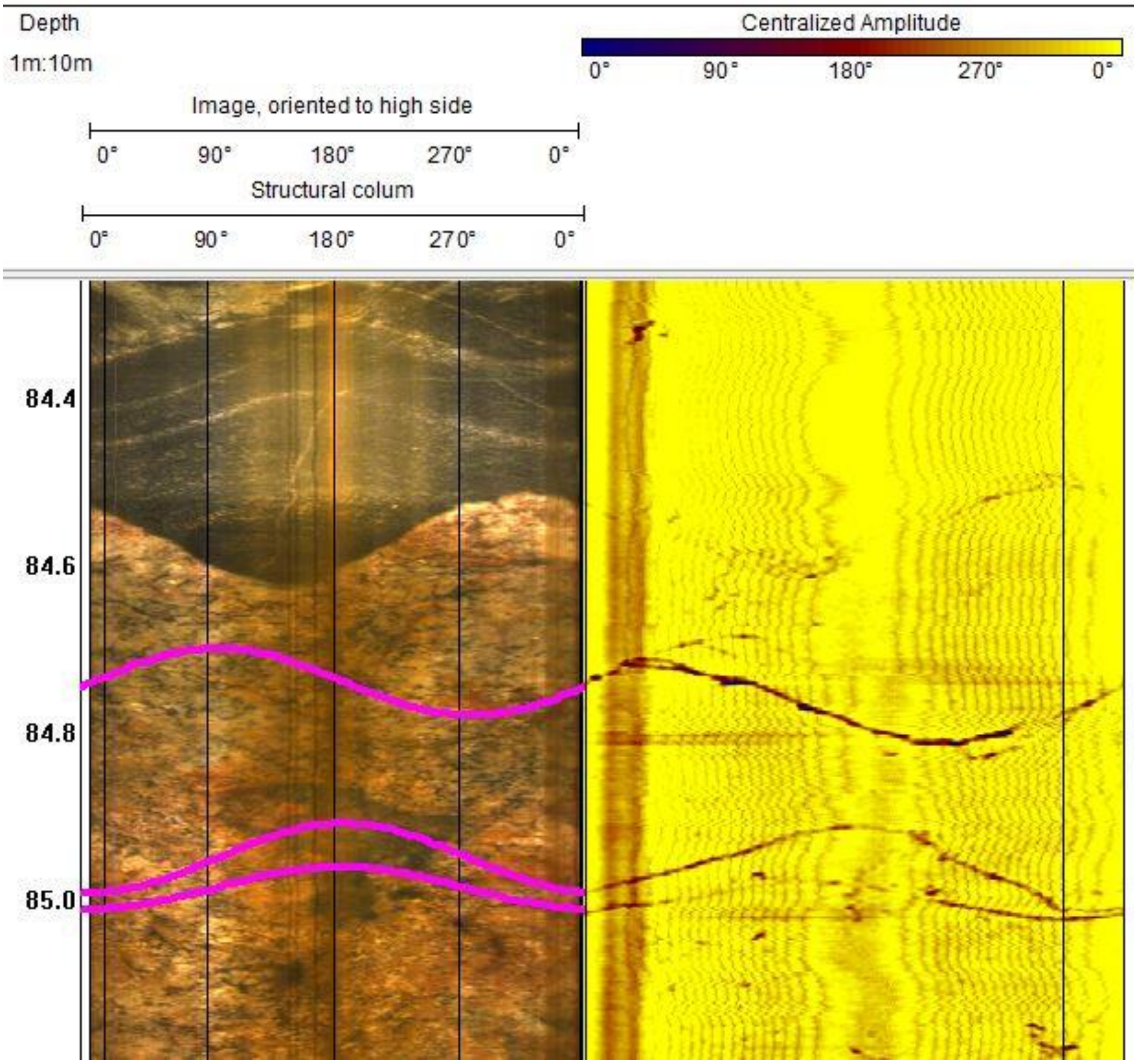


**Figure 1.** WellCad-processed image from the drill hole at the depth of between 84.2 m and 85.2 m. Image on the left shows optical data and image on the right shows acoustic data. Three fractures are clearly visible in the acoustic photo. They are at the depth of 84.74 m, 84.95 m and 84.99 m. Contacts between different rock types are clearly visible in the optical image.

## 4. Preliminary results and future studies

Compilation of the fracture data is still ongoing, but some results are already available. There are about 800 fractures in the drill core in total and two minor fracture zones. The fracture zones are at depth of 108.78 to 109.21 m and 294.40 to 295.14 m. These fracture zones had to be cemented during drilling and their orientations are not yet clear.

There at least two distinctly different fracture fillings: one has a red color and the other is green. Fracture fillings are usually found separately, but sometimes also together in the same fracture. Fracture orientations are still being measured and they have not yet been adjusted to correct geographical orientation. .

Concerning the field measurements, overall it seems that there are two major directions of fractures: NE/E-SW/W and NW/N-SE/S. This is consistent with the previous results from the area (e.g., Wennertsröm et al. 2008).

In the future, the plan is to perform XRD analyses on the fracture fillings so that it is possible to get a better idea on the composition and thermal conditions of fluids which have passed through the fractures. Then it is possible to make some conclusions about which of the two fracture directions is older. However, the main focus of the study is to create a 3D-model for the fractures of the area using MOVE software, in the hopes that this model then helps the future planning of construction activities at Kumpula.

## References

Elminen T., et al. Fault structures in the Helsinki Area, southern Finland. Teoksessa: Airo M-L., Elminen T., Hopgood A., Huhma H., Koistinen T., Mänttäri I., Mertanen S., Niemelä R., Pajunen M., Salmelainen J., Vaarma M., Wasenius P., Wennerström M. 2008. Tectonic evolution of the Svecofennian crust in southern Finland –a basis for characterizing bedrock technical properties. Geological Survey of Finland, Special Paper 47, Espoo. 185– 215 s.

Kukkonen, I.T., Koivisto, E. and Whipp, D. (this volume). Helsinki University Kumpula campus drill hole project. In: *Kukkonen et al. (Eds.),* Lithosphere 2016 – Ninth Symposium on the Structure, Composition and Evolution of the Lithosphere in Finland. Programme and Extended Abstracts, Espoo, Finland, November 9-11, 2016. Institute of Seismology, University of Helsinki, Report S-65, 166 pages.

Laitala M.,1991. Helsingin kartta-alueen kallioperä. Summary: Pre-Quarternary rocks of the Helsinki map-sheet area. Suomen geologinen kartta 1:100 000, Kallioperäkarttojen selitykset, lehti 2034. Geologian tutkimuskeskus, Espoo. 47s.

Penttilä, K., Kukkonen, I., Heinonen, J.S., Räisänen, M. and Valtonen, R. (this volume). Logging and lithology of the Kumpula Campus drill hole. In: *Kukkonen et al. (Eds.),* Lithosphere 2016 – Ninth Symposium on the Structure, Composition and Evolution of the Lithosphere in Finland. Programme and Extended Abstracts, Espoo, Finland, November 9-11, 2016. Institute of Seismology, University of Helsinki, Report S-65, 166 pages.

Räisänen, M., Kukkonen, I., Heinonen, J.S., Valtonen, R. and Penttilä, K. (this volume). Geochemical characteristics of the Kumpula campus area: drill core and outcrop data. In: *Kukkonen et al. (Eds.),* Lithosphere 2016 – Ninth Symposium on the Structure, Composition and Evolution of the Lithosphere in Finland. Programme and Extended Abstracts, Espoo, Finland, November 9-11, 2016. Institute of Seismology, University of Helsinki, Report S-65, 166 pages.

Valtonen, R., Kukkonen, I., Heinonen, J.S., Räisänen, M. and Penttilä, K. (this volume). Kumpula campus drill hole: Fracture mapping and 3D-modeling. *Kukkonen et al. (Eds.),* Lithosphere 2016 – Ninth Symposium on the Structure, Composition and Evolution of the Lithosphere in Finland. Programme and Extended Abstracts, Espoo, Finland, November 9-11, 2016. Institute of Seismology, University of Helsinki, Report S-65, 166 page

Wennerström M., et al. Orientation and properties of jointing in Helsinki area, southern Finland. Teoksessa: Airo M-L., Elminen T., Hopgood A., Huhma H., Koistinen T., Mänttäri I., Mertanen S., Niemelä R., Pajunen M., Salmelainen J., Vaarma M., Wasenius P., Wennerström M. 2008. Tectonic evolution of the Svecofennian crust in southern Finland –a basis for characterizing bedrock technical properties. Geological Survey of Finland, Special Paper 47, Espoo. 253– 283 s.

# Applying seismic cutoff depth in thermal modelling of the Fennoscandian Shield

T. Veikkolainen[1], I.T. Kukkonen[1] and T. Tiira[2]

[1]Department of Physics, University of Helsinki, Gustaf Hällströmin katu 2a, 00560 Helsinki
[2]Institute of Seismology, University of Helsinki, Gustaf Hällströmin katu 2b, 00560 Helsinki
E-mail: toni.veikkolainen@helsinki.fi

This study presents an analysis of seismic cutoff depth and heat flow field of the Fennoscandian Shield. Altogether 4190 earthquake events from years 2000-2015 in Finnish and Swedish national catalogues have been applied for this purpose. To model the heat flow field, 223 values from both countries and their neighbouring areas were used to find out if any correlation between the maximum earthquake focal depth (cutoff depth) and surface heat flow exists. Because heat flow and cutoff depth appear unrelated, it seems evident that regional variations of heat flow are caused by shallow lying variations (i.e., in upper crust) in heat production instead of deeper sources. Therefore one-dimensional layer models with temperature-dependent thermal conductivity are functional for the shield area.

**Keywords:** seismology, seismic cutoff depth, heat flow, temperature, Finland, Sweden

## 1. Introduction

The maximum focal depth (i.e. cutoff depth) of earthquakes is one of the main tectonothermal parameters of the lithosphere, frequently used to approximate the boundary between brittle and ductile transformation. In Fennoscandia, the large proportion of felsic rocks in the upper and middle crust indicates that this boundary roughly represents the temperature of 350 °C (Blanpied et al. 2001; Moisio, 2005). Several areas in the world have featured a negative correlation between the cutoff depth and terrestrial heat flow density (e.g. Wong and Chapman, 1990), yet no study of this kind has been done using Fennoscandian data.

The spatial distribution of earthquakes in Fennoscandia has obvious concentrations on intraplate faults, which result from postglacial isostatic adjustment, ridge-push from distant plate boundaries, and changes in the gravitational potential field (Korja et al. 2015). Heat flow field in the area varies between 35.3 ± 6.3 mWm$^{-2}$ in Archean areas to 81.6 ± 13.9 mWm$^{-2}$ in post-Sveconorwegian granites (Slagstad et al. 2009).

## 2. Heat flow and seismic data

For our study, we gathered heat flow data mainly from Finland and Sweden. Norwegian, Danish, Estonian and Russian data from the proximity were also taken into account because we needed to interpolate a heat flow surface which is reasonably constrained also in Finnish and Swedish border regions. For interpolation, we applied the radial basis function method in Scientific Python (SciPy). The size of our interpolation grid was 0.05 degrees in both latitude and longitude dimensions, fine enough to allow a subsequent correlation with latitude-longitude coordinates of earthquakes. The paleoclimatic corrections to heat flow values were mainly those reported in the literature, yet for Russian data, an estimated bulk correction of 10 mWm$^{-2}$ was used, because detailed data were unattainable. The resulting map (Figure 1, left) shows a westward- and southward-increasing trend.

Our earthquake information was gathered from the Finnish and Swedish national catalogues and covered years 2000-2015. Data with magnitudes less than 0.1, and a few events with locations far outside both Swedish and Finnish territory were excluded. Obvious duplicates (N=66) were also removed.

For analysis, we took latitude, longitude, focal depth and local magnitude ($M_L$) of events (N=4190) into consideration, 801 from the Finnish and 3389 from the Swedish catalogue. There appeared no obvious relation between focal depth and magnitude.

To compare thermal and earthquake data, values from our interpolated surface heat flow grid were calculated at all epicentres. Five areas of notable seismic activity were investigated in separate subset analyses: the southern Gulf of Bothnia coast of Sweden (area 1), the northern Gulf of Bothnia coast of Sweden (area 2), the Swedish Norrbotten and western Finnish Lapland (area 3), the Kuusamo region of Finland (area 4) and the southernmost Sweden (area 5). The total count of events in these subsets was 3619 (Figure 2).

The paleoclimatically corrected mean heat flow at earthquake epicenters turned out to be 49.8 $mWm^{-2}$, virtually same as the steady-state value of 49.7 ± 0.4 $mWm^{-2}$ obtained by Kukkonen & Jõeleht (2003) for Fennoscandian Shield and East European Platform. Therefore it is unlikely that earthquake epicenters are strongly biased towards certain lithologies, but they represent the average Fennoscandian crust reasonably well for modelling purposes, and our interpolation works adequately.

Seismic cutoff depths in data of our regional subsets and the main dataset are shown in Table 1. As calculated from all events (Figure 1, right), the arithmetic mean cutoff depth was 28.0 km (averaged from 90th, 95th and 99th) percentiles, with a standard deviation of 4.3 km. As long as the cutoff depth is assumed to be an isotherm, no hypothesis of spatially varying deep-seated heat sources is needed, despite differences in surface heat flow.

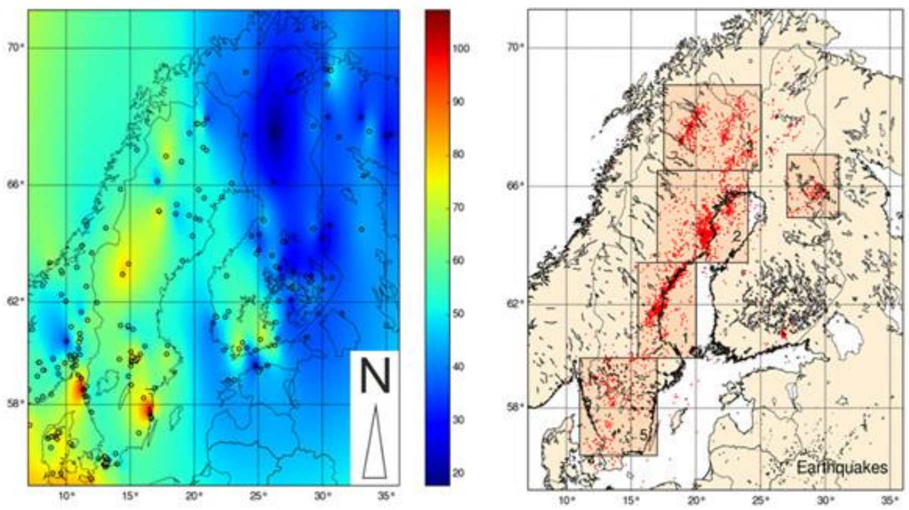


**Figure 1.** Left: Palaeoclimatically corrected heat flow map of Finland, Sweden and adjacent areas. Scale is in $mWm^{-2}$. The total count of data is 223. Right: Spatial distribution of our earthquake data. Rectangles, numbered by “1”, “2”, “3”, “4” and “5” show regions where the heat flow field and earthquakes were taken into more detailed investigations.

## 3. Thermal modelling and conclusions

Solving the cutoff depth gave us a parameter suitable for one-dimensional thermal models of lithosphere, such as a model with three layers (Kukkonen et al. 1999). In our one-dimensional models, parameters were set as follows: paleoclimatically corrected surface heat flow 49.8 $mWm^{-2}$, surface mean temperature 3 ºC (estimated from meteorological records), temperature at the seismic cutoff depth 350 ºC, heat flow at Moho 9-15 $mWm^{-2}$ (Kukkonen and Peltonen, 1999; Kukkonen and Lahtinen, 2001), and depth of Moho 46 km (Grad et al. 2009). Thermal conductivity $\lambda$ was dependent on temperature T by $\lambda = \lambda_0(1+CT)$ where $\lambda_0$ is the surface value (3.1 $Wm^{-1}K^{-1}$) and C (0.0008) is an empirical factor.

Depending on seismic cutoff depth (28 ± 4 km), three separate models were constructed. All models had an upper layer of 10 km thickness, yet depths of middle and lower layers were changed. Distinct values of heat production [$\mu Wm^{-3}$] were used as follows: in layer 1 1.48, 1.19 or 2.43 (model 1, 2 or 3), in layer 2 1.00, 0.78 or 0.55 (model 1, 2 or 3) and in layer 3 0.50, 0.55 or 0.36. Heat production is actually one of the most poorly known thermal parameters, yet it is typically largest in granitoids and smallest in mafic and ultramafic rocks which dominate the lower part of the crust. Other parameters were adjusted step-by-step until reasonable boundary conditions were met (Table 2).

Because the obtained mean Moho temperature (516 ± 110 ºC) is smaller than the Curie constraint of 580 °C for magnetite, lithospheric mantle of Fennoscandia may have magnetic sources. To fine-tune thermal constraints of the upper crust, a larger number of heat flow determinations from deep boreholes (over 2 km) are important. If sufficient heat flow and earthquake data are available, our analysis could be repeated in other shield areas as well.

**Table 1.** Earthquake cutoff depths (km) corresponding to the 90th, 95th and 99th percentiles of data in our five subsets and mean values weighted using the number of data in each subset as a weight. Parentheses indicate that less than five events with a greater focal depth than the cutoff depth have been registered in the area. Values for the entire study area are also given.

| | **1 (N=804)** | **2 (N=1489)** | **3 (N=864)** | **4 (N=139)** | **5 (N=323)** | **Entire area** |
|---|---|---|---|---|---|---|
| **90th** | 22.4 | 25.1 | 21.9 | 24.0 | 22.8 | 23.4 |
| **95th** | 26.6 | 27.5 | 27.8 | 26.3 | 27.1 | 26.9 |
| **99th** | 30.4 | 34.7 | 35.6 | (31.1) | (31.1) | 33.7 |

**Table 2.** Temperature and heat flow at layer boundaries in our models. Heat production parameters are listed in Table 1 and other parameters explained in the text. Three values indicate models 1, 2 and 3, respectively.

| | **Temperature [ºC]** | **Heat flow [$mWm^{-2}$]** | **Thermal conductivity [$Wm^{-1}K^{-1}$]** |
|---|---|---|---|
| **Surface (0 km)** | 3.0 (all models) | 49.8 (all models) | 3.10 (all models) |
| **Boundary 1 (10 km)** | 148, 153 or 131 | 35.0, 37.9 or 25.5 | 2.77, 2.76 or 2.81 |
| **Boundary 2 (28 km, 24 km or 32 km)** | 350 (all models) | 17.0, 27.1 or 14.1 | 2.42 (all models) |
| **Moho (46 km)** | 494, 616 or 438 | 12.0, 14.9 or 9.0 | 2.22, 2.07 or 2.29 |

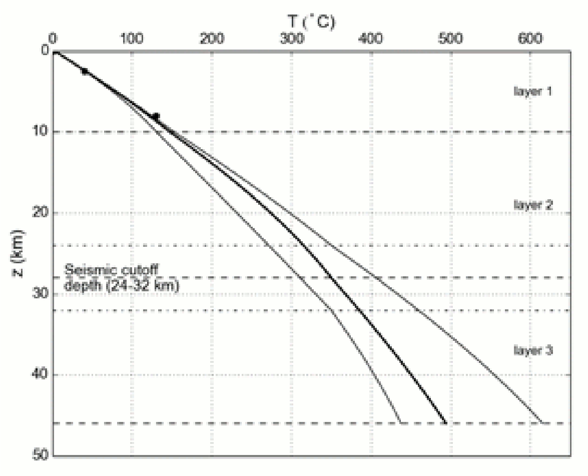


**Figure 2.** Thermal models of the Fennoscandian crust, featuring temperature-dependent thermal conductivity and fixed heat production constraints for layers 1, 2 and 3 in cases with seismic cutoff depths of 24, 28 and 32 km. Solid symbols indicate the temperature (130 °C) of Kola superdeep borehole at 8 km (Popov et al. 1999) and that (40 °C) of Outokumpu borehole at 2.5 km depth (Kukkonen et al. 2011). For other numeric values, see Table 1.

## References:


Blanpied, M.L., Lockner, D.A., Byerlee, J.D., 1991. Fault stability inferred from granite sliding experiments at hydrothermal conditions, Geophys. Res. Lett., 18, 609-612.

Grad, M., Tiira, T., ESC Working Group, 2009. The Moho depth map of the European plate. Geophys. J. Int. 176, 279-292.

Korja, A., Uski, M., Koskinen, P., Lund, B., Grigull, S., Nironen, M., Kosonen, E., Högdahl, K., 2015. Observations on Intraplate Seismicity in Central Fennoscandia, Geophys. Res. Abstr., 17, EGU2015-10344.

Kukkonen, I.T., Peltonen, P., 1999. Xenolith-controlled geotherm for the central Fennoscandian Shield: implications for lithosphere–asthenosphere relations, Tectonophysics, 304, 301--315.

Kukkonen, I.T., Lahtinen, R., 2001. Variation of radiogenic heat production rate in 2.8–1.8 Ga old rocks in the central Fennoscandian shield, Phys. Earth Planet. Inter., 126, 279--294.

Kukkonen, I.T., Jõeleht, A., 2003. Weichselian temperatures from geothermal heat flow data, J. Geophys. Res. Solid Earth, 108, 2163.

Kukkonen, I.T., Jokinen, J., Seipold, U., 1999. Temperature and pressure dependencies of thermal transport properties of rocks: Implications for uncertainties in thermal lithosphere models and new laboratory measurements of high grade rocks in the central Fennoscandian shield, Surv. Geophys., 20, 33-59.

Kukkonen, I.T., Rath, V., Kivekäs, L., Šafanda, J., Čermak, V., 2011. Geothermal studies of the Outokumpu Deep Drill Hole, Finland: Vertical variation in heat flow and paleoclimatic implications. Phys. Earth Planet. Inter., 188, 9-25.

Moisio, K., 2005. Numerical lithospheric modelling: Rheology, stress and deformation in the central Fennoscandian Shield, PhD thesis, University of Oulu, Oulu, Finland.

Popov, Y.A., Pevzner, S.C., Pimenov, V.P., Romushkevich, R.A., 1999. New geothermal data from the Kola Superdeep well SG-3, Tectonophysics, 306, 345-366.

Slagstad, T., Balling, N., Elvebakk, H., Midttømme, K., Olesen, O., Olsen, L., Pascal, C., 2009. Heat-flow measurements in Late Palaeoproterozoic to Permian geological provinces in south and central Norway and a new heat-flow map of Fennoscandia and the Norwegian-Greenland Sea, Tectonophysics, 473, 341-361.

Wong, I.G., Chapman, D.S., 1990. Deep intraplate earthquakes in the western United States and their relationship to lithospheric temperature. Bull. Seism. Soc. Am., 80, 589-599.

# Two geochemically A-type intrusions in Central Finland Granitoid Complex: evidence of coeval mafic and felsic magmatism

V. Virtanen[1] and E. Heilimo[2]

[1]University of Helsinki, P.O. Box 64, 00014, Helsinki, Finland
[2]Geological survey of Finland, P.O. Box 1237, 70211, Kuopio, Finland
E-mail: [1]ville.z.virtanen@helsinki.fi, [2]esa.heilimo@gtk.fi

We have studied Riitalampi and Viininperä intrusions; belonging mineralogically, geochemically, and temporally to the Type 3a postkinematic suite of the Central Finland Granitoid Complex. Generally, the biotite-hornblende bearing quartz monzonites have A-type geochemical affinity, e.g. high contents of total alkalis and high field strength elements (HFSE), and high FeO*/MgO ratio. Field observations together with numerical modelling of a mingling of the mafic enclaves suggest that synplutonic mafic dykes intruded to the partly crystalline intrusions, particularly in the case of Riitalampi intrusion.

**Keywords:** Central Finland Granitoid Complex, A-type, bimodal magmatism, mingling

## 1. Introduction

Mainly compressional Svecofennian orogeny ~1.91–1.77 Ga consists of amalgamation of Paleoproterozoic crustal material to the Archean Karelia Province (e.g. Lahtinen, 1994, Nironen, 1997). Voluminous granitoid magmatism is related to the compressional stage leading to the formation of the large 40000 km$^2$ Central Finland Granitoid Complex (CFGC). Bulk of the CFGC is composed of ca. 1.89–1.88 Ga granitoids that are considered synkinematic with respect to the orogeny (Vaasjoki, 1996, Nironen 2005).

A volumetrically minor suite of ca. 1.88–1.87 Ga weakly to undeformed and unfoliated porphyritic granitoids have also been described in the CFGC. These granitoids are often referred as postkinematic granitoids (Elliott et al., 1998), they generally exhibit A-type geochemical affinity, e.g. high total alkalis, high FeO*/MgO ratio, as well as high Ba and Zr concentrations (Nironen et al., 2000). Based on mineralogical and geochemical differences postkinematic granitoids can be divided into four subgroups (Elliott et al., 1998; Nironen et al., 2000). Mainly monzogranitic and granodioritic Type 1 differs from mineralogically similar Type 2 by e.g. lower total alkali concentrations. Type 3a consists of mainly quartz monzonites and monzogranites with pyroxene-bearing marginal assemblage, whereas Type 3b has pyroxene throughout. In addition to the felsic magma, a mafic magma component have been described from some of the intrusions (Nironen et al., 2000). A petrogenetic model, proposed for the postkinematic suite, is litospheric delamination at the later stage of the main crust forming event followed by mantle-derived mafic underplating and intraplating, which provided heat to partially melt granulitic lower crust (Nironen et al., 2000; Elliott, 2003).

## 2. Intrusion descriptions

The 1879 ± 4 Ma (Hannu Huhma written communication, 2015) Riitalampi intrusion is 10 x 5 km in dimensions (Fig. 1). The northern boundary of the intrusion is located 4 km south from the village of Toivakka in the southern CFGC. The intrusion consists mostly of unfoliated alkali feldspar porphyritic biotite-hornblende bearing quartz monzonite. Subhedral to ovoidal alkali feldspar phenocrysts are regularly mantled by < 1 mm thick layers of re-crystallized, often myrmekitic fine grained plagioclase and quartz. As typical accessory minerals zircon, apatite, allanite, ilmenite, and titanite can be observed. Abundant mafic and intermediate enclaves and intruding dykes can be found throughout the intrusion. The enclaves are elongated and generally 5–20 cm in diameter, but the largest ones exceed 1 m in diameter. Some of the enclaves are rimmed by < 5 mm thick reaction rims of amphibole and biotite, and internal alkali feldspar xenocrysts are a typical feature, evidencing synplutonic mingling (Fig. 2).

Ca. 4 km southeast from the Riitalampi intrusion lies the circular (3.5 x 3.5 km) Viininperä intrusion (Fig. 1). Majority of Viininperä intrusion is composed of alkali feldspar porphyritic biotite-hornblende quartz monzonite with medium-grained groundmass. Phenocrysts are similar with alkali feldspar phenocrysts of the Riitalampi intrusion. Northern margin, however, consists of texturally similar biotite-hornblende syenogranite with several mafic to intermediate enclaves showing similar mingling structures as described in Riitalampi. In addition, a monzogabbro has been found at one outcrop near the center of the intrusion.

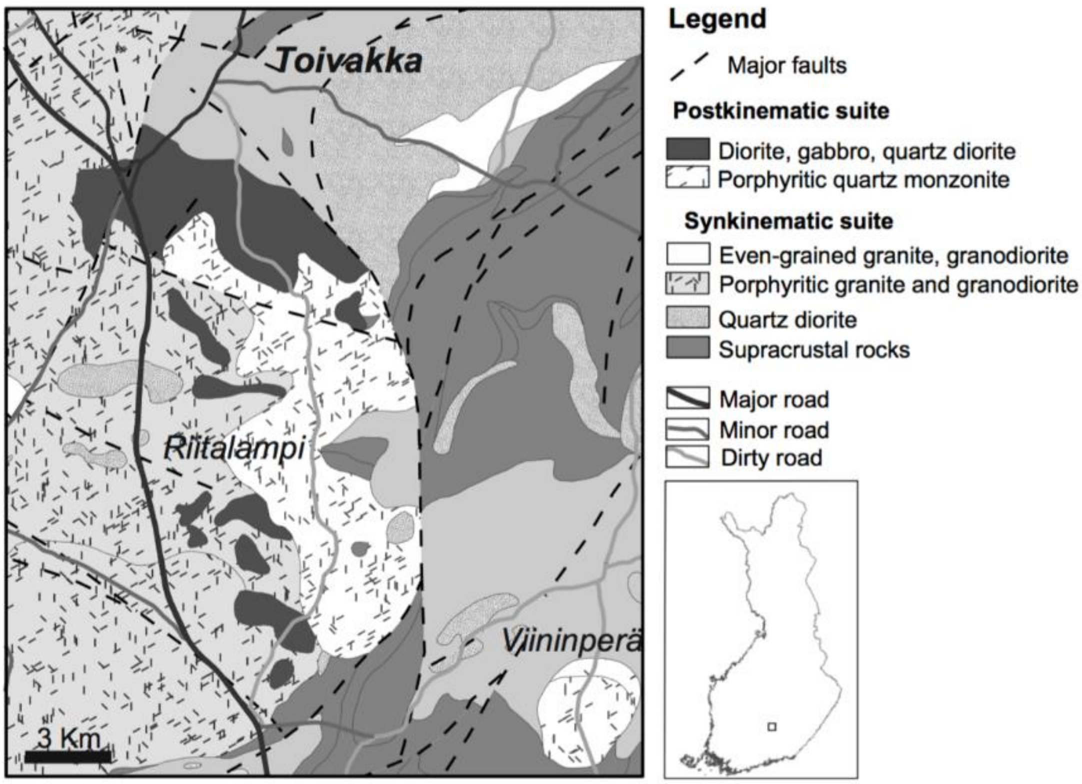


Figure 1. Geological map of the Riitalampi and Viininperä intrusions (Mikkola et al., in review).

**3. Geochemistry and geochronology**

Whole-rock geochemical analyses were performed with X-ray fluorescence (XRF) and inductively coupled plasma mass spectrometry (ICP-MS) by Labtium Ltd.. Both of the studied intrusions show high concentrations in alkalis ($K_2O$+$Na_2O$ = 7.85–9.14 wt.%) and HFSE, especially Zr (455–844 ppm), and high FeO*/MgO ratio (5.28–12.45) (Fig. 3) what makes them compositionally similar with A-type granitoids. These geochemical features separate studied intrusions from the synkinematic suite, which is characterized by lower total alkali, Ba, and HFSE concentrations, and lower FeO*/MgO ratio at similar $SiO_2$ contents (Fig. 3).

The Viininperä intrusion was dated by in-situ U-Pb analysis of zircons. The analysis was performed at the Finnish Isotope Geology Laboratory with laser ablation inductively coupled plasma mass spectrometer (LA-ICPMS) equipped with single collector. A total of 25 spots were analysed of which 4 were discarded because of high concentrations of common lead. The 21 selected spots gave the Viininperä intrusion an emplacement age of 1882 ± 3 Ma (Hannu Huhma, written communication, 2016).

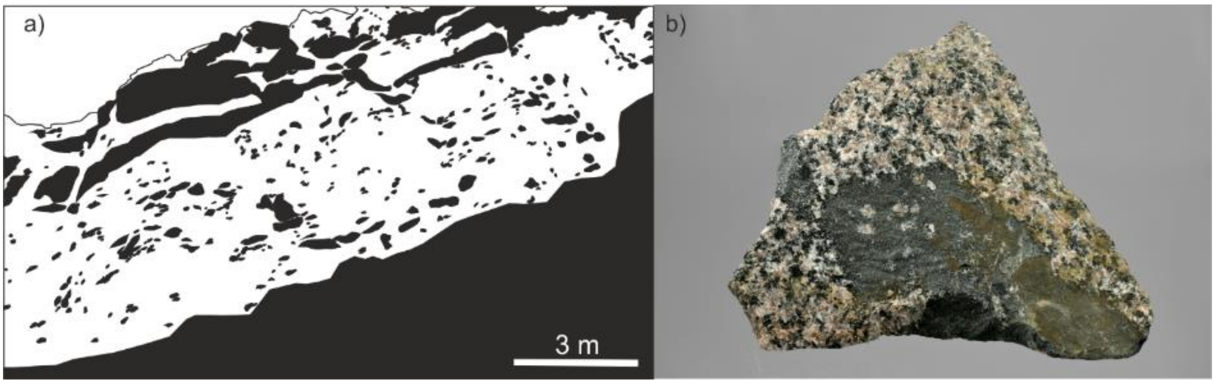


**Figure 2.** a) A sketch of a synplutonic dioritic dyke (black) intruding into the Riitalampi quartz monzonite (white) on a vertical wall of a quarry (outcrop ASM$-2013-224). b) Sample ASM$-2013-224.1 showing dioritic enclave with alkali feldspar xenocrysts inside the host quartz monzonite. A thin biotite-hornblende-bearing reaction rim can be observed around the enclave. Photo taken by Jouko Ranua. Length of the sample is ca. 20 cm.

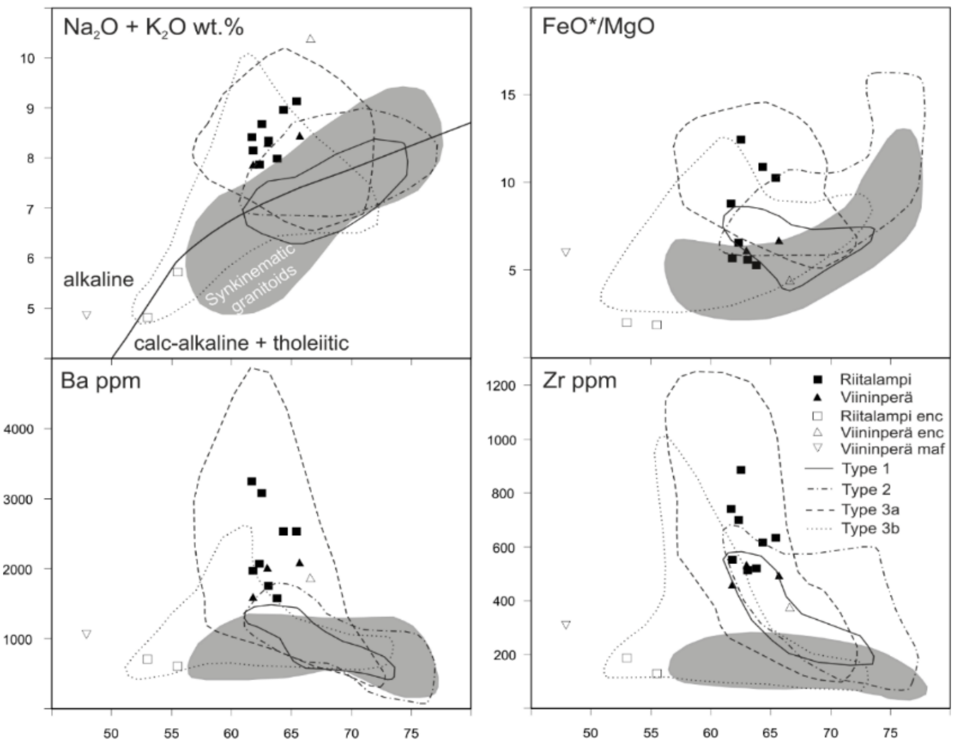


**Figure 3.** Selected bivariate diagrams of Riitalampi and Viininperä intrusions, associated enclaves (enc), and Viininperä monzogabbro (maf). The different types of postkinematic intrusions (Type 1, 2, 3a and 3b) and synkinematic rocks (the grey area) are added for comparison (Nironen et al. 2000).

## 4. Mingling model of mafic and felsic components

We have used an unsophisticated model, to identify the observed mingling between mafic and felsic components, with MAGFRAC, a program based on least-squares approximation (Morris, 1984). Whole-rock composition of a dioritic enclave (PIM$-2012-88.2) was mixed with mineral major element oxide compositions of Riitalampi quartz monzonite sample ASM$-2013-224.1 that were analysed with electron probe microanalyzer (EPMA) equipped with four wavelength dispersive detectors (WDS) at the University of Helsinki. The aim was to produce a mixture that would be geochemically equivalent to an intermediate enclave containing alkali feldspar xenocrysts inside quartz diorite (ASM$-2013-224.2) associated with the sample ASM$-2013-224.1.

The mingling model, presented here, includes mixture of the dioritic enclave with alkali feldspar, plagioclase, quartz, biotite, and hornblende of the quartz monzonite. The mineral compositions used are averages of five analysis in the case of feldspars, and six analysis in the case of biotite and hornblende. The best fit was obtained by mixing of 84.5% diorite with 7.7% alkali feldspar, 7.7% plagioclase, 1.77% quartz, -1.8% biotite and -0.6% hornblende (sum $r^2$ = 0.007; the closer to zero the better the fit). The modelled relative abundances of alkali feldspar, plagioclase and quartz are similar with the abundances observed in the sample ASM$-2013-224.1.

## 5. Discussion

Clear geochemical resemblance between the studied intrusions and Type 3a postkinematic suite is evident by high total alkali, Ba, and Zr concentrations. The ages of the intrusions 1879 ± 4 Ma and 1882 ± 3 Ma support the interpretation of the postkinematic suite.The mixing model provide new evidence related to the suggested bimodal nature of the postkinematic magmatism. Synplutonic mafic dykes and small intrusions intruded to the quartz monzonitic magma that was already partly crystallized, as evidenced by the alkali feldspar xenocrysts inside the enclaves. The model suggests that alkali feldspar, plagioclase, and quartz participated in the mingling process of the magmas. The role of biotite and hornblende is somewhat ambiguous, as the best fit for the model was achieved by removal of these phases from the dioritic component. The biotite-hornblende-rich reaction rims around the enclaves supports removal of biotite and hornblende from dioritic component.

## References:

Elliott, B.A., Rämö, O.T., and Nironen, M., 1998. Mineral chemistry constraints on the evolution of the 1.88–1.87 Ga post-kinematic granite plutons in the Central Finland Granitoid Complex. Lithos, 45, 109–129.

Elliott, B.A., 2003. Petrogenesis of the Post-kinematic Magmatism of the Central Finland Granitoid Complex II; Sources and Magmatic Evolution. Journal of Petrology, 44, 1681–1701.

Lahtinen, R. Crustal evolution of the Svecofennian and Karelian domains during 2.1–1.79 Ga, with special emphasis on the geochemistry and origin of 1.93–1.91 Ga gneissic tonalites and associated supracrustal rocks in the Rautalampi area, central Finland. Geological Survey of Finland, Bulletin 378, 128 p.

Mikkola, P., Heilimo, E., Aatos, S., Ahven, M., Eskelinen, J., Halonen, S., Hartikainen, A., Kallio, V., Kousa, J., Luukas, J., Makkonen, H., Mönkäre, K., Niemi, S., Romu, I. and Solismaa, S. (in review) Jyväskylän seudun kallioperä. Geologian tutkimuskeskus tutkimusraportti.

Morris, P. A., 1984. MAGFRAC: a basic program for least-squares approximation of fractional crystallization. Computers and Geosciences, 10, 437–444.

Nironen, M., 1997. The Svecofennian Orogen: a tectonic model. Precambrian Research, 86, 21–44.

Nironen, M., 2005. Proterozoic orogenic granitoid rocks. In: Lehtinen, M., Nurmi, P. A. and Rämö, O. T. (Eds.), Precambrian Geology of Finland – Key to the Evolution of the Fennoscandian Shield. Elsevier, Amsterdam, 443–480.

Nironen, M., Elliott, B.A, and Rämö, O.T., 2000. 1.88–1.87 Ga post-kinematic intrusions of the Central Finland Granitoid Complex: a shift from C-type to A-type magmatism during litospheric convergence. Lithos, 53, 37–58.

Vaasjoki, M., 1996. Explanation to the geochronological map of southern Finland: The development of the continental crust with special reference to the Svecofennian orogeny. Geological Survey of Finland, Report of Investigation 135, 30p.

**ISSN 0357-3060**
**ISBN 978-952-10-9588-7 (Paperback)**
**Helsinki University Print**
**Helsinki 2016**
**ISBN 978-952-10-9589-4 (PDF)**